Title

Investigating the role of P-glycoprotein on drugs exhibiting enhanced renal clearance in cystic fibrosis patients

Author

Susanto, Miki,

Publication Date

2002

Peer reviewed|Thesis/dissertation

Investigating the Role of P-glycoprotein on Drugs Exhibiting Enhanced Renal Clearance in Cystic Fibrosis Patients

by
Miki Susanto
B.Sc. Biochemistry, University of Texas at Austin, Austin, TX

DISSERTATION

Submitted in partial satisfaction of the requirements for the degree of

DOCTOR OF PHILOSOPHY

in

PHARMACEUTICAL CHEMISTRY

in the

GRADUATE DIVISION

of the

UNIVERSITY OF CALIFORNIA, SAN FRANCISCO

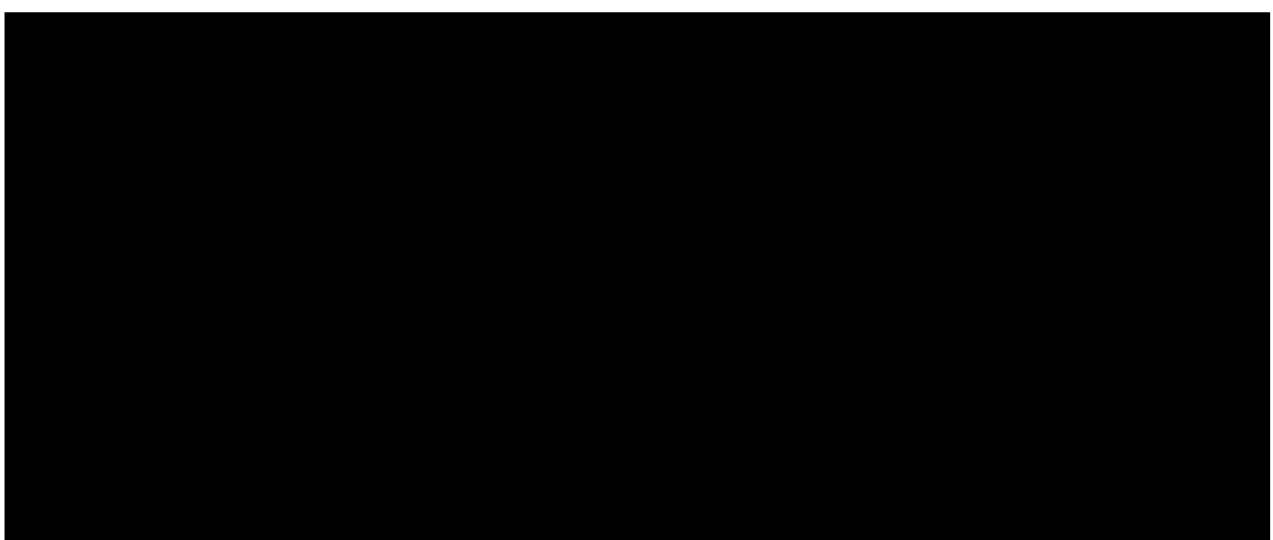

Date University Librarian

Degree Conferred:.....

To my family and friends

with thanks and love

ACKNOWLEDGEMENTS

I have been very fortunate to have the help and support of many people to make my graduate studies a truly rewarding and memorable experience. First, I would like to express my sincere gratitude to my research advisor, Dr. Les Benet. Les has been an amazing mentor. He provided a tremendous amount of support and guidance throughout my graduate school years, especially during the oral qualifying exam and the thesis writing process. He also helped me grow as a better scientist by allowing me freedom to pursue my ideas and to think independently. I have been blessed to have the opportunity to learn under his mentorship.

Dr. Hideaki Okochi, a post-doctoral fellow in our lab, provided a tremendous amount of help for the *in vivo* experiments in mice and rats. Dr. Emil Lin from the Drug Studies Unit kindly provided the support for the LC/MS/MS analysis of mice and rat plasma samples and his post-doctoral fellow, Dr. Yong Huang, was very helpful in developing the LC/MS/MS methods and running the plasma samples. Dr. Phillip Smith and his students, Melanie Tallman and Brendan Bender, at the University of North Carolina, Chapel Hill, kindly taught me the bleeding technique in mice. Jennifer Monahan assisted me with the task of breeding and genotyping CF mice. Sumiko Hirai helped with the preparation of a number of experiments. I am truly indebted to these people for generously sharing their time and effort to help me.

My warmest gratitude to my thesis committee members, Drs. Les Benet, Deanna Kroetz and Carol Basbaum for sacrificing their precious time during the Christmas holiday season to read my thesis and providing me with prompt and valuable

suggestions. A note of thanks is also in order to my orals committee, Drs. Kathy Giacomini, Deanna Kroetz, Carol Basbaum and Nancy Sambol for their time and a surprisingly pleasant qualifying examination. I would also like to thank Dr. Betty-ann Hoener for making the TA-ing a worthwhile learning process.

My colleagues in the Benet lab, Drs. Wolfgang Jacobsen, Andrea Soldner, Noboru Okamura, Taiji Sawamoto, Michael Reid and Mark Grillo assisted me by sharing their expertise with me and providing many helpful discussions. My special thanks to my classmates, Carolyn Cummins and Wendy Putnam, and other fellow students, Chi-Yuan Wu, Jae Chang, Winnie Kim, Chunze Li, Justine Lu and Yvonne Lau, for making lab a fun place to do research.

I also want to extend my gratitude to Zhigang Yu and Tan Nguyen, for assisting me with molecular biology techniques, Dr. David Ginzinger from the UCSF Cancer Center for designing primers for real-time RT-PCR, Dr. Xiaohui Fang from the Mathias lab for providing the CF mice breeders and Dr. Ray Frizzell from the University of Pennsylvania for providing the CFPAC-1 pLJ CFTR cell line.

My family and friends deserve a special praise for their tremendous support and encouragement throughout my Ph.D. program at UCSF. My parents and my sister, Lany, and my brothers, Agus, Aman and Ali, encouraged and inspired me all along the way. I would also like to thank my former professor, Dr. Ira Levine, for his continuous guidance and support. Finally, my deepest thanks to Sean, for believing in me in everything that I do, for encouraging me to realize my potential and for his patience and understanding.

Miki Susanto December, 2002

ABSTRACT

Investigating the Role of P-glycoprotein on Drugs Exhibiting Enhanced Renal Clearance in Cystic Fibrosis Patients

Miki Susanto

The goal of the research was to determine if P-glycoprotein (P-gp) plays a role in enhancing the renal clearance (CLr) of drugs in cystic fibrosis (CF) patients. We hypothesized that the enhanced CLr of drugs observed in CF patients was due to increased P-gp expression in those patients, which would caused increased CLr of drugs that are substrates of P-gp. Bidirectional transport and inhibition study results in control (MDCK1) and P-gp overexpressing (MDCK1-MDR1) cell lines showed that antibiotics that have a higher active CLr in CF patients (dicloxacillin, trimethoprim and ciprofloxacin) are substrates of P-gp while those that do not (sulfamethoxazole, iothalamate and cefsulodin), are not substrates of P-gp. Ciprofloxacin, besides being a substrate of P-gp, is also a substrate of an unidentified absorptive transporter. *In vivo* pharmacokinetic studies showed no correlation between P-gp expression and the CLr of trimethoprim and ciprofloxacin in mice. GG918, a P-gp inhibitor, had no effect on the disposition of trimethoprim and ciprofloxacin in rats. There was 3-fold higher *mdr1a* and 14-fold higher *mdr1b* expression in the kidneys of female than male wild type mice. P-gp expression was similar between male and female ΔF508 CF mice. However, there was a difference in P-gp expression between wild type and ΔF508 CF mice. Both *mdr1a* and *mdr1b* expressions were decreased by approximately 60% and 70%, respectively, in female ΔF508 CF compared to female CF wild type mice. On the other hand, both the *mdr1a* and *mdr1b* expressions were increased by approximately 50% and 360%, respectively, in male ΔF508 CF compared to male CF wild type mice. The combined overall effect in the kidneys of male and female ΔF508 CF mice was a two-fold increase in *mdr1b* expression. This agrees with our hypothesis that P-gp expression might be increased in the kidneys of CF patients. There was no difference in the expression of *cftr* between the kidneys of P-gp wild type and P-gp

knockout mice, regardless of the sex of the mice. We also compared the expression of *MDR1* between CFPAC-1 and CFPAC-1 pLJ CFTR cells. In the presence of wild type *CFTR* gene, *MDR1* expression was significantly decreased while the expressions of MRP1, 2 and 3 and OATP-C, D, E and 8 were not changed. This result agrees with the hypothesis that P-gp expression might be upregulated in the kidneys of CF patients due to defects in their *CFTR* gene. In conclusion, the cause of the enhanced CLr of drugs in CF patients remains unknown. More research will need to be performed to answer the question and in determining whether P-gp could be responsible for the observed enhanced CLr in CF patients.

TABLE OF CONTENTS

Chapter 2

In Vitro Bidirectional Transport Studies

Chapter 3

Mice Breeding and Genotyping

Chapter 4

In Vivo Pharmacokinetic Studies in Mice

Chapter 5

In Vivo Pharmacokinetic Studies in Rats

Chapter 6

P-glycoprotein and CFTR Expression in Various Mouse Models

LIST OF TABLES

LIST OF FIGURES

Chapter 1

Introduction

1.1 Statement of Purpose

The overall goal of my thesis research is to determine if P-glycoprotein (P-gp) plays a role in enhancing the renal clearance (CLr) of several drugs in cystic fibrosis (CF) patients. To treat their persistent lung infections, CF patients take many antibiotics and due to the observation that some antibiotics are eliminated faster in CF patients, they are usually prescribed with higher dosage of antibiotics. However, not all antibiotics exhibit higher clearance in CF patients. Therefore, it might not be appropriate or it could be dangerous to prescribe higher dosages for all drugs in CF patients. Most antibiotics are cleared renally, therefore by knowing the cause(s) of the enhanced renal clearance of drugs in CF patients, we will be able to design a better dosage regimen to treat CF patients. We hypothesize that the enhanced renal clearance of drugs observed in CF patients is due to increased P-gp expression in those patients, which in turn will cause increased renal clearance of drugs that are substrates of P-gp. If this hypothesis is proven correct, we may adjust the dose given to CF patients based on whether or not the drug is a substrate of P-gp.

In order to understand the thought processes or supporting literature evidence that led to this hypothesis, we need to understand more about cystic fibrosis, CFTR, P-glycoprotein and the renal system, which will be presented below.

1.2 Cystic Fibrosis

1.2.1 A brief history

Cystic fibrosis (CF) is one of the most common lethal genetic disorders affecting primarily Caucasian populations. It is an autosomal recessive disorder, which occurs in approximately 1 in 2500 live births. Currently there are more than 30,000 people in the US who have this

disease and more than 10 million people (1 in 22 to 28 Caucasians) who are symptom-less carriers of the defective gene (1). The earliest accurate medical description of a CF case was given in 1595 by Dr. Pieter Pauw in an autopsy report of an 11-year-old girl believed to have CF (2). The girl was described as being meager with a swollen, hardened and gleaming white pancreas (2). In 1936 Fanconi *et al.* (3) recognized the disease as separate from celiac disease and was probably the first to refer to it as "cystic fibromatosis with bronchiectasis" (4). In 1938 the first comprehensive description of the disease was provided by Dr. Dorothea Anderson and to emphasize the pancreatic lesion, she coined the term "cystic fibrosis of the pancreas" (5). This nomenclature was challenged by Farber in 1945 (6) and he introduced the term mucoviscidosis to describe the disease and this term is still widely used outside the English speaking world (4). In 1946 the genetic etiology and autosomal recessive pattern of inheritance of CF was understood (7). The significant discovery of high salt concentration in the sweat of CF patients, which is the gold standard CF diagnosis tool used today, was made in 1948 by Dr. Paul di Sant' Agnese and his colleagues (8).

It took about five decades from the time the disease was described by Fanconi *et al.* (3) to the discovery of the genetic defect that caused CF. In 1985, the position of the CF gene was localized to chromosome 7 and ultimately in 1989 the gene was successfully identified to position 7q31.2 by positional cloning techniques (9-11). The gene product was called CFTR, which stands for Cystic Fibrosis Transmembrane Conductance Regulator (9-11). Recently the gene was given a new name by the Human Gene Nomenclature Committee (HGNC). The approved name for the gene is "ABC-binding cassette, subfamily C, member 7" with the approved gene symbol, *ABCC7* (see Table 1.7)(12).

Even though it is widely accepted that defects in CFTR are responsible for CF, how the loss of CFTR causes CF remains incompletely understood and there is still no cure for the disease (1).

1.2.2 Clinical features of CF

CFTR is expressed on the apical membrane of epithelial cells, it functions as a cAMP-regulated chloride channel and a regulator of other transport proteins (13-29).

The absence of the channel causes abnormal electrolyte transport in the epithelial cells of several organ systems that lead to to the clinical manifestations of the disease. The organ systems affected in CF include lung and upper respiratory tract, pancreas, the gastrointestinal tract, hepatobiliary system, sweat glands and genitourinary tract (1, 4).

1.2.2.1 Lung and upper respiratory tract

The manifestation in the lung is the major cause of morbidity and mortality in CF patients. They have persistent chronic pulmonary infection coupled with an abnormal inflammatory defense mechanism that leads to persistent coughing, chronic sputum production, airway obstruction by mucus, nasal polyps (in 15% of patients), sinusitis and intense pulmonary inflammation, which slowly progresses to bronchiectasis and lung destruction (1). The onset of respiratory symptoms is variable among patients with some patients not displaying any symptoms until adulthood while others showing the symptoms early in infancy. It is still not clear how the CFTR defect in the airway causes the lung to become susceptible to bacterial infection (30). One theory hypothesizes that due to the defect in CFTR, there is a lack of fluid secretion that is followed by excessive fluid absorption that then leads to thickening of the airway mucus and impaired mucociliary clearance. Impaired mucociliary clearance leads to bacterial infection and inflammation that signals the immune system to destroy the bacteria and lung cells. This process releases DNAs into the airway, causing an already thick mucus to be even thicker and the vicious cycle continues until ultimately the whole lung is destroyed (30,31). Another theory proposes that the loss of CFTR alters the airway surface liquid salt composition, which then changes the ability of airway defense mechanisms to eliminate bacteria, ultimately resulting in bacterial colonization and lung destruction by the immune system (32).

Several strains of bacteria are frequently found in CF patients. *Staphylococcus aureus* and *Haemophilus influenza* are commonly encountered in infants and toddlers while *Pseudomonas aeruginosa* takes over as the disease progresses (33, 34). *Burkholderia cepacia, Stenotrophomonas maltophilia, Alcaligenes xylosoxidans, Aspergillus fumigatus* and nontuberculous bacteria are also isolated from the airway of CF patients (33, 34). With proper

antibiotic treatments and prophylaxis the median survival and quality of life of CF patients has improved from death in early childhood to over 30 years of age (1, 35, 36). Table 1.1 lists some of the oral antibiotics commonly used in CF patients. Besides oral antibiotics, CF patients are also treated with intravenous antibiotic therapy.

Table 1.1 Some of the oral antibiotics commonly used to suppress respiratory pathogens in CF patients. Adapted from Welsh *et al.* (1)

Pathogen	**Antibiotics**	**Dose**	
		Child	**Adult**
S. aureus	Dicloxacillin	6.25 mg/kg q. 6 hr	250-500 mg q. 6 hr
	Cephalexin	12.5 mg/kg q. 6 hr	500 mg q. 6 hr
	Amoxicillin-clavulanate	12.5-22.5 mg/kg q. 12 hr	400-875 mg q. 12 hr
	Erythromycin	15 mg/kg q. 8 hr	250 mg q. 8 hr
	Clarithromycin	7.5 mg/kg q. 12 hr	500 mg q. 12 hr
H. influenza	Cefaclor	10-15 mg/kg q. 8 hr	250-500 mg q. 8 hr
	Amoxicillin	20-40 mg/kg q. 8 hr	500 mg q. 8 hr
S. aureus	Cefixime	8 g/kg q. 24hr	400 mg q. 24 hr
and	Amoxicillin-clavulanate	12.5-22.5 mg/kg q. 12 hr	400-875 mg q. 12 hr
H. influenza	Trimethoprim-sulfamethoxazole	4 mg/kg q. 12 hr (TMP), 20 mg/kg q. 12 hr (SMZ)	160 mg q. 12 hr (TMP), 800 mg q. 12 hr (SMZ)
	Cefpodoxime	5 mg/kg q. 12 hr	200 mg q. 12 hr
	Cefuroxime	20 mg/kg q. 12 hr	250-500 mg q. 12 hr
P. aeruginosa	Ciprofloxacin	Not approved	500-750 mg q. 12 hr
	Ofloxacin	Not approved	400 mg q. 12 hr
B. cepacia	Trimethoprim-sulfamethoxazole	4 mg/kg q. 12 hr (TMP), 20 mg/kg q. 12 hr (SMZ)	160 mg q. 12 hr (TMP), 800 mg q. 12 hr (SMZ)
	Doxycycline	5 mg/kg initial dose + 2.5 mg/kg q. 12 hr	200 mg initial dose + 100 mg q. 12 hr
	Minocycline	4 mg/kg initial dose + 2 mg/kg q. 12 hr	200 mg initial dose + 100 mg q. 12 hr

q. = every

1.2.2.2 Pancreas

Besides pulmonary symptoms, the majority of CF patients also exhibit clinical manifestation in the pancreas (1). The pancreatic symptoms are the second most common presenting symptoms in infants with CF. Unlike pulmonary function, there is a good correlation for genotype-phenotype with pancreatic function in CF (37). About 85% of CF patients are classified as pancreatic insufficient (PI) while the remaining 15% are pancreatic sufficient (PS). This classification is based upon whether or not the patient exhibits steatorrhea secondary to fat maldigestion and malabsorption (1). Most patients homozygous for ΔF508 are PI while those with at least one copy of partially functional mutations (e.g., R177H, R334W, A455E and 3849+10kb C to T) are PS (38, 39).

The onset of pancreatic insufficiency varies from patient to patient. In some patients it develops *in utero* while in others pancreatic insufficiency progresses over the years (40). Obvious symptoms of pancreatic insufficiency occur when more than 85% of the pancreas is lost (41). PI patients have a pancreatic enzyme deficiency that leads to fat and protein maldigestion and malabsorption that then results in distended abdomen, poor weight gain, stunted linear growth, deficiency in fat-soluble vitamins (A, D, E, K) and frequent, bulky and greasy stools (42, 43). To correct these abnormalities, CF patients take enzyme replacement therapy and nutritional supplementation (1, 44, 45). Also, as patients today with CF live longer, both glucose intolerance and CF related diabetes mellitus (CFRDM) are becoming common complications (46-50). CFRDM has a clinical presentation that is distinct from class I and II diabetis mellitus. Due to the increasing incidence of CFDRM, the Cystic Fibrosis Foundation recommends annual screening of all patients with a casual glucose level greater than 126 mg/dl (1).

1.2.2.3 Gastrointestinal tract

About 10-20% of CF patients present meconium ileus (MI) at birth. It is highly associated with PI and the ΔF508 mutation (51). Throughout their lives, CF patients may repeatedly experience distal intestinal obstruction syndrome (DIOS), an obstruction of the small bowel

(52). About 20% of CF patients at the age of 12-30 months experience rectal prolapse that can be corrected in almost all cases by manual reduction with gentle pressure (1, 53).

1.2.2.4 Hepatobiliary system

Because CFTR is expressed in the apical surface of the biliary tract epithelia and not in the hepatocytes, hepatobiliary disease in CF only affects the biliary duct and not the hepatocytes (1). A large percentage of patients at autopsy show focal biliary cirrhosis where "focal zones of numerous bile ducts and tubules contain distinctly eosiniphilic, granular secretions that appeared to form plugs that caused ductal dilation" (4). About 20% of CF patients have gallstones, probably due to depletion of the bile acid pool caused by decreased digestive enzymes and increased stools (4).

1.2.2.5 Sweat glands

CF patients have elevated concentrations of chloride, sodium and potassium ions in their sweat. They suffer from excessive water and electrolyte losses (1). However, their sweat glands appear to have normal micro-and macroscopic morphology (54).

1.2.2.6 Genitourinary tract

Approximately 97% of CF males are infertile due to azoospermia that is attributed to congenital bilateral absence of the vas deferens (CBAVD). They usually have normal prostates and normal or slightly decreased size testes (1). CF females have reduced fertility due to thick dehydrated mucus in the cervix. The ovaries, fallopian tubes and uterus appear to be normal by gross anatomic and microscopic examination (1).

1.2.3 Diagnosis of CF

Due to the vast number of mutations affecting the CFTR gene, genetic screening is very difficult and diagnoses of a patient with CF is based on two criteria: the presence of at least one clinical feature and evidence that there is CFTR dysfunction (1).

CFTR dysfunction is categorized by these criteria (1):

- elevated chloride concentration in sweat (higher than 60 mM). This is the gold standard and can be measured as early as 2 days after birth. The sweat is collected by pilocarpine iontophoresis and chloride concentration is measured chemically (55).
- the presence of two known disease-causing alleles in the *CFTR* gene.
- abnormal ion transport across the nasal epithelium (CF patients have a higher nasal potential difference).

The clinical features of CF are (1):

- chronic pulmonary disease manifested by chronic cough and sputum production along with persistent infections especially by *Pseudomonas aeruginosa, Staphylococcus aureus, Haemophilus influenzae* or *Burkholderia cepacia*
- high salt concentration in the sweat
- gastrointestinal and nutritional symptoms such as meconium ileus, pancreatic insufficiency, focal biliary cirrhosis and failure to thrive
- infertility in the male due to obstructive azoospermia
- a history of CF in the family

According to the Cystic Fibrosis Foundation, as of 1998, most CF patients are diagnosed because of the presence of persistent respiratory symptoms and failure to thrive (Table 1.2)

Table 1.2 The frequency of clinical symptoms in CF patients. Adapted from Welsh *et al.* (1)

Symptoms	**Frequency (%)**
persistent respiratory symptoms	51.2
steatorrhea	35.1
positive family history	17.0
liver disease	1.0
failure to thrive	43.0
meconium ileus	18.6
sinus disease	2.4
electrolyte imbalance	5.3

1.2.4 CF modifier genes

CF is a very complex disease and it affects many organ systems: lung and upper respiratory airways, gastrointestinal tract, liver, genitourinary tract, pancreas and sweat glands. The clinical manifestation of the disease is variable among patients. For example, exocrine pancreatic insufficiency only occurs in approximately 85% of CF patients, meconium ileus is present in approximately 10-20% of patients and there is a considerable variation in the severity and onset of the airway pathology (1). Most patients exhibit respiratory symptoms and signs by infancy but some may not present any symptoms until adulthood. Part of this variability can be explained by the vast number of *CFTR* mutations. The severity of pancreatic insufficiency is correlated with the genotype. However, the genotype-phenotype correlation for pulmonary phenotype is less than perfect (37). It is thought that polymorphisms, modifier genes and environmental factors, differences in therapy or patient compliance could be the cause.

Genetic "modifier" loci that influence the severity of intestinal disease have been found in CF mice in chromosome 7, which is orthologous to human chromosome 19 (56) and found in CF patients in the region of chromosome 19D19S112 (57). Currently several genes are being studied as potential modifiers of CF and most of these genes are involved in the control of infection, inflammation and immunity (58). Some of these genes are HLA class II antigens, mannose-binding lectin, antiproteases (α1-antitrypsin and α1-antichymotrypsin), glutathione-S-transferase, nitric oxide synthase type I, TNF-α, TGF-β, IL-1β and IL-1Ra (58). Table 1.3 lists the locus and the phenotypic effects of these genes on CF.

1.3 CFTR

CFTR, the gene that is defective in CF patients, was cloned in 1989 utilizing positional cloning techniques (9-11). It is located on the long arm of chromosome 7 (7q31.2). The gene contains 27 exons spanning approximately 250 kb of DNA (9-11) that is transcribed into a mature mRNA of 6.5 kb which then produces a 1480 amino acid, glycosylated membrane glycoprotein with a molecular mass of approximately 168 kDa (10).

Table 1.3 Potential modifier genes of CF. Adapted from Acton and Wilmott (58)

Gene Product	Allele	Locus	Genotype effect	Phenotype effect in CF
Human leukocyte antigen, class II	CFM1	19q13	modification of Ca^{2+}-regulated Cl- channel	incidence of meconium ileus
	DR4	6p21.3	unknown	↓ risk of *P. aeruginosa* infection, ↑ risk of ABPA
	DR7	6p21.3	unknown	↑ risk of *P. aeruginosa* infection, ↑ risk of ABPA, higher serum IgE
	DR2, 5	6p21.3		↑ risk of ABPA
	DQ2	6p21.3		↓ risk of ABPA
	B7, DR15, DQ6	6p21.3		↑ risk of liver disease and portal hypertension in males
Mannose-binding lectin (MBL)	MBL-Null	10q11.2-q21	↓ MBL production	more severe lung disease in CF patients chronically colonized with *P. aeruginosa*
α1-antitrypsin	S	14q32.1	↑ intracellular degradation	less severe lung disease
	Z		abnormal translocation to the golgi	less severe lung disease
α1-antichymotrypsin	$^{(-15)}$Ala	14q31-q32.3	unknown	less severe lung disease and ↓ risk of *P. aeruginosa* infection
Glutathione-S-transferase	GSTM1-Null	1p13.3	absence of protein product	earlier diagnosis, more severe lung disease, ↓ survival
Nitric oxide synthase I	NOS1	12q24.2-q24.31	unknown	↑ risk of colonization with *P. aeruginosa*
Tumor necrosis factor-α	TNF2	6p21.3	↑ concentrations of TNF-α	more severe lung disease, lower weight z-scores
Transforming growth factor-β	TGFβ1	19q13.1	↓ concentrations of TGF-β	more severe lung disease
Interleukin-1β	IL-1β+3953A1+	2q14	↑ IL-1β	
Interleukin-1 receptor antagonist	IL- 1 RA A2+	2q12.1	↑ IL-1 Ra	

* ABPA = allergic bronchopulmonary aspergillosis

1.3.1 CFTR structure

Based on its amino acid sequence, CFTR is a member of a transport protein superfamily called ATP-binding casette (ABC)-transporters (see Table 1.7). It has twelve transmembrane domains that is divided into two membrane-spanning domains (MSD1 and MSD2), with Walker A and B, as well as the ABC "signature" sequence, LSGGQ motifs, in nucleotide-binding domains (NBD1 and NBD2) that interact with ATP (Table 1.4) (59). These motifs are the defining characteristics of ABC transporters.

Table 1.4 Conserved motifs in NBDs of CFTR. Adapted from Sheppard and Welsh (59)

Motif	Sequence	No. of Last Residue
Walker A	G X X G X G K S/T	
CFTR NBD1	G S T G A G K T	465
CFTR NBD2	G R T G S G K S	1251
LSGGQ	L S G G Q	
CFTR NBD1	L S G G Q	552
CFTR NBD2	L S H G H	1350
Walker B	R X_7 h h h h D	
CFTR NBD1	R X_7 L Y L L D	572
CFTR NBD2	R X_7 I L L L D	1370

X = any amino acid residue, h = hydrophobic residue

Besides two MSDs and two NBDs, CFTR also has an R domain that contains multiple consensus sequences for phosphorylation by cAMP-dependent protein kinase (PKA) (Fig. 1.1) (59). The MSDs are involved in the formation of the chloride selective pore, the NBDs are responsible for hydrolyzing ATP to regulate channel gating while the R domain phosphorylation controls channel activity (59).

1.3.2 CFTR function

CF epithelia display a defective Cl^- conductance that is dependent upon cAMP agonists. After the *CFTR* gene was discovered in 1989, it was not clear whether CFTR itself is a cAMP-dependent chloride channel or a regulator of such chloride channels (59). The facts that CFTR is a member of ABC transporters and the primary sequence of CFTR does not resemble that of

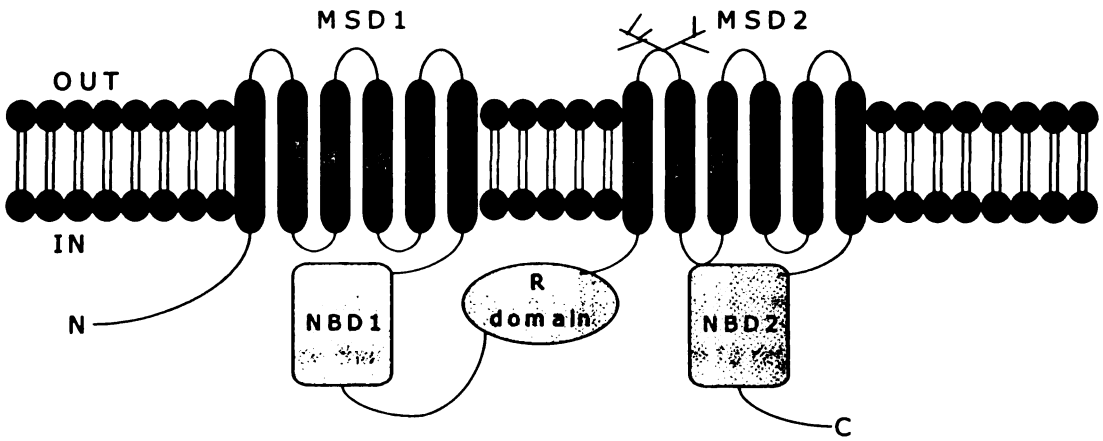

Figure 1.1 A model of CFTR structure. Adapted from Sheppard and Welsh (59)

any other known ion channels suggest that CFTR is a regulator of chloride channels. However, based on numerous studies it is now known that CFTR is itself a cAMP-dependent chloride channel and it is also a regulator of numerous ion channels (13-29).

Several lines of evidence demonstrated that CFTR is a chloride channel (59). First, heterologous expression studies with recombinant CFTR generate a unique Cl^- current that is activated by cAMP agonists (13-18). Second, there is no difference in the biophysical properties and regulation of Cl^- current between cells that express recombinant CFTR and cells that have endogenous CFTR (60). Third, mutations of some specific amino acids in CFTR altered the anion selectivity of the CFTR channel (13). Fourth, planar lipid bilayers containing reconstituted purified recombinant CFTR display Cl^- conductance similar to normal epithelia (15).

Heterologous expression studies in cells that do not normally express CFTR and cAMP-dependent chloride channels such as Xenopus oocytes, Chinese hamster ovary, HeLa, NIH-3T3 fibroblasts and Sf9 insect cells showed that overexpression of recombinant CFTR led to a cAMP-dependent Cl^- current with the following properties:

- acute activity regulated by cAMP (PKA-dependent CFTR phosphorylation) (18, 61)
- no strong rectification, unlike other Cl^- channels, (62)

- linear current-voltage relationship (59)
- time- and voltage-independent gating behavior (59)
- selective for anions over cations with conductance and permeability selectivity of $Br^- \geq Cl^- > I^- > F^-$ (13, 59, 62)
- the single channel conductance is 4-12 pS (13, 59, 62)

Besides acting as a chloride channel, CFTR has been shown to regulate other ion channels as well, such as amiloride-sensitive epithelial Na^+ channel (ENaC), outwardly-rectifying chloride channel, a water channel (AQP3), voltage-gated (KvLQT-1) and ROMK-potassium channels (19-29).

1.3.3 CFTR mutations

Currently more than 1000 mutations have been discovered in the gene and reported to the CF Genetic Analysis Consortium (CFGAC) database (63). Of these mutations, only about 83% are associated with CF disease while the rest are classified as polymorphisms (Table 1.5). A mutation is classified as a disease-associated mutation because it causes CF disease while a mutation identified on the non-CF chromosome of a healthy CF heterozygote is classified as a polymorphic mutation because it does not cause CF (1). Currently there are about 190 polymorphisms in the *CFTR* gene reported to CFGAC. Fifty-five percent of those polymorphisms are in the coding region with half of these resulting in amino acid substitutions (1, 63). Polymorphic mutations are assumed to be benign but it has been discovered that certain polymorphisms, even though they do not cause CF, are associated with male infertility (e.g., F508C, intron 8 5T) and altered CFTR function (e.g., M470V) (64, 65).

Most of the mutations are uncommon worldwide, although they may occur in higher frequency in selected populations such as W1282X in Ashkenazi Jews due to the founder effect (66, 67). The most common mutation, deletion of phenylalanine at position 508 (ΔF508), accounts for nearly 70% of mutations in the European-descent Caucasian population. Besides ΔF508, only four other mutations (G542X, G551D, W1282X, N1303K) individually account for more than

Table 1.5 Type and frequency of mutations that cause CF. Adapted from Welsh *et al.* (1)

Mutation	Frequency (%)	Examples
missense (amino acid substitutions)	44	R117E, R334W, R347P, N1303K, G551D
frameshift	22	3569delC, 1078delT
splice site	16	621 +1G →T; 711 + 1G→T
nonsense	14	G542X, R553X, W1282X
in-frame deletions	2	ΔF508
promoter mutations	1	
genomic rearrangements	1	

1% of CF alleles worldwide (1, 63). Currently what causes the high frequency of ΔF508 mutation in the Caucasian population is not known. The ΔF508 mutation results in a temperature-sensitive defect in protein processing; at 37°C little or no mature protein is detected at the plasma membrane (68), however at 27°C some ΔF508 CFTR protein reaches the cell membrane where it forms a partially functioning chloride channel (69-71).

Based on the mechanism by which the function of the CFTR is disrupted, the mutations in the CFTR gene can also be divided into four categories according to the effects of the mutation (Table 1.6).

Table 1.6 Classification of CFTR gene mutations. Adapted from Geddes *et al.* (72)

Mutation	CFTR defect	Example
Class I	defective or reduced CFTR protein production	G542X, R553X, Q493X, W1282X
Class II	abnormal or defective processing of the CFTR protein	ΔF508
Class III	disruption of activation and regulation of CFTR protein	G551D
Class IV	altered conductance of the CFTR protein	R117H, R347P, R334W

1.3.4 Expression of CFTR

CFTR is expressed in the apical membrane of epithelia of many organs such as sweat glands, pancreas, gastrointestinal tract, lung, uterus, placenta, testis, brain and kidney (10, 73, 74).

In sweat glands, CFTR is expressed in the epithelia lining the ducts of the glands (73). In the pancreas, CFTR is restricted to epithelia lining the small secretory ducts (exocrine canniculi) and it is not expressed in the acinar cells or islets of Langerhans (73). In the intestine, decreased CFTR expression is observed along the crypt-villus and the proximal-distal axes (75). CFTR expression is high in Brunner's gland, crypt cells and a subpopulation of primarily villus epithelia called CFTR high expresser (CHE) cells (75-79). CFTR expression is higher in duodenal crypts and decreases towards the distal colon (75). In the lung, CFTR is expressed at low levels in both the surface epithelia and the underlying lamina propria of the bronchi and bronchioles (74). In the uterus, CFTR is expressed in the epithelial lining of the endometrium and not in the endometrial stroma, the myometrium or the perimetrium (75). In the placenta, CFTR is expressed in the highly differentiated cytotrophoblast cells and not in the JAr cell line (80). In the testis, CFTR expression is regulated during the cycle of the seminiferous epithelium. It is highly expressed in the round spermatids of stages VII and VIII but not in germ cells at other stages of maturation (75). It is not expressed in the somatic cells of the testis, the Sertoli and Leydig cells (75). CFTR is expressed in multiple areas of the brain, cerebral cortex, medial preoptic area and anterior hypothalamus (81-84). In the kidney, CFTR is expressed abundantly in kidney cortex and medulla (85). It is expressed at the apical epithelia of both proximal and distal renal tubules, with highest expression in S1-segment of proximal tubule (10, 73, 86). It is not expressed in the glomerulus (73).

The level of CFTR expression in various tissues has not necessarily correlated well with disease pathology. CFTR expression is low in lung yet it is the organ that is affected the most in CF. It is also somewhat surprising to find abundant CFTR in the kidneys since there is no major renal dysfunction associated with CF although CF kidneys exhibit reduced renal excretion of NaCl, a decreased capacity to dilute and concentrate urine and increased renal clearance of several drugs (87, 88). Perhaps the pathopysiology of CF varies with the capacity of different epithelia to express alternate ion channel pathways that can overcome the functional defect of CFTR. A possible candidate is P-glycoprotein (P-gp), a protein that is also involved in chloride transport since it is a regulator of cell-swelling activated chloride channels (89-91). There is

evidence in the literature that CFTR expression is inversely-regulated with P-gp expression (92-94), Like CFTR, P-gp is also a member of the ABC superfamily.

1.3.5 ABC superfamily

As we mentioned earlier, both CFTR (*ABCC7*) and P-glycoprotein (*ABCB1*) are members of the ABC superfamily. The ABC superfamily is comprised of proteins containing the ABC unit, a 200-250 stretch of amino acids that have conserved Walker A and B motifs and a signature ABC sequence (see Table 1.4). These conserved sequences are located in the nucleotide-binding domains (NBDs). They also have membrane-spanning domains (MSDs). ABC proteins are involved in the transport of various compounds, from small inorganic ions to large polypeptides, across biological membranes (95). These proteins are present in organisms ranging from procaryotes to mammals. Currently 55 human ABC proteins are known (12). Based on their sequence similarity scores they are further divided into seven subfamilies: ABC-A to ABC-G (Table 1.7) (12, 95). Defects in ABC proteins are associated with many diseases (96): CF with CFTR (*ABCC7*), PFIC-3 (progressive familial intrahepatic cholestasis) with MDR2 (*ABCB4*), Dubin-Johnson syndrome with MRP2 (*ABCC2*), persistent hypoglycemia of infancy with SUR1 (*ABCC8*) and Stargardt disease and age-related macular degeneration with ABCR (*ABCA4*).

1.4 P-glycoprotein

P-glycoprotein, or P-gp, is an energy-dependent efflux pump that extrudes a wide range of structurally unrelated drugs from cells. It was first discovered due to its ability to contribute multidrug resistance to tumor cells (97). It was discovered in 1976 by Juliano and and Ling in Chinese Hamster ovary cells that overexpress a cell surface phosphoglycoprotein, termed P-glycoprotein, where the P stands for permeability (97). P-gp is encoded by *MDR1* gene (98-102), located on the long arm of chromosome 7 (7q21.1) (103-105). The gene contains 28 exons spanning over 100 kb of DNA (106) that is transcribed into a mature mRNA of 4.5 kb which then produces a 1280 amino acid, glycosylated membrane glycoprotein with a molecular mass of approximately 170 kDa (107-110).

Table 1.7 Members of ABC superfamily (http://www.gene.ucl.ac.uk/cgi-bin/nomenclature/searchgenes.pl)

Approved Gene Symbol	Approved Gene Name	Location	Previous Symbols	Aliases	Tissue
			ABC1 (subfamily A)		
ABCA1	ATP-binding cassette, sub-family A (ABC1), member 1	9q31	ABC1, HDLDT1	TGD, Tangier disease	many tissues
ABCA2	ATP-binding cassette, sub-family A (ABC1), member 2	9q34	ABC2		brain, kidney, lung, heart
ABCA3	ATP-binding cassette, sub-family A (ABC1), member 3	16p13.3	ABC3	ABC-C, EST111653	lung+other tissues
ABCA4	ATP-binding cassette, sub-family A (ABC1), member 4	1p22	STGD1, ABCR, RP19, STGD	FFM, Stargardt disease	retina
ABCA5	ATP-binding cassette, sub-family A (ABC1), member 5	17q21-q25		EST90625	muscle, heart, testes
ABCA6	ATP-binding cassette, sub-family A (ABC1), member 6	17q21		EST155051	liver
ABCA7	ATP-binding cassette, sub-family A (ABC1), member 7	19p13.3		ABCX	peripheral leukocytes, thymus, spleen, bone marrow
ABCA8	ATP-binding cassette, sub-family A (ABC1), member 8	17q24		KIAA0822	ovary
ABCA9	ATP-binding cassette, sub-family A (ABC1), member 9	17q24		EST640918	heart
ABCA10	ATP-binding cassette, sub-family A (ABC1), member 10	17q24		EST698739	muscle, heart
ABCA11	ATP-binding cassette, sub-family A (ABC1), member 11			EST1133530	
ABCA12	ATP-binding cassette, sub-family A (ABC1), member 12	2q35		DKFZP434G232	stomach
			MDR (subfamily B)		
ABCB1	**ATP-binding cassette, sub-family B (MDR/TAP), member 1**	**7q21**	**PGY1, MDR1**	**P-gp**	**many tissues**

ABCB2	transporter 1, ATP-binding cassette, sub-family B (MDR/TAP)	6p21.3	TAP1	PSF1, RING4, D6S114E	most cells, ER
ABCB3	transporter 2, ATP-binding cassette, sub-family B (MDR/TAP)	6p21.3	TAP2	PSF2, RING11, D6S217E	most cells, ER
ABCB4	ATP-binding cassette, sub-family B (MDR/TAP), member 4	7q21	PGY3, MDR3	MDR2/3, PFIC-3	hepatocyte
ABCB5	ATP-binding cassette, sub-family B (MDR/TAP), member 5	7p14		EST422562	ubiquitous
ABCB6	ATP-binding cassette, sub-family B (MDR/TAP), member 6	2q33-q36		EST45597, umat	mitochondria
ABCB7	ATP-binding cassette, sub-family B (MDR/TAP), member 7	Xq12-q13	ABC7	EST140535, Atm1p	mitochondria
ABCB8	ATP-binding cassette, sub-family B (MDR/TAP), member 8	7q35-q36		EST328128, M-ABC1	mitochondria
ABCB9	ATP-binding cassette, sub-family B (MDR/TAP), member 9	12q24		EST122234	heart, brain, lysosomes
ABCB10	ATP-binding cassette, sub-family B (MDR/TAP), member 10	1q32		EST20237	mitochondria
ABCB11	ATP-binding cassette, sub-family B (MDR/TAP), member 11	2q24	BSEP, PFIC2	ABC16, SPGP, PFIC-2, PFIC2, PGY4	hepatocyte
ABCB10P	ATP-binding cassette, sub-family B (MDR/TAP), member 10 pseudogene	15q13-q14		M-ABC2, MABC2	

MRP/CFTR (subfamily C)

ABCC1	ATP-binding cassette, sub-family C (CFTR/MRP), member 1	16p13.1	MRP, MRP1	GS-X	many tissues
ABCC2	ATP-binding cassette, sub-family C (CFTR/MRP), member 2	10q24	cMOAT	DJS, MRP2, cMRP	liver, intestine, kidney
ABCC3	ATP-binding cassette, sub-family C (CFTR/MRP), member 3	17q21		MRP3, cMOAT2, EST90757, MLP2, MOAT-D	intestine, kidney
ABCC4	ATP-binding cassette, sub-family C (CFTR/MRP), member 4	13q31		MRP4, EST170205, MOAT-B	many tissues
ABCC5	ATP-binding cassette, sub-family C (CFTR/MRP), member 5	3q25-q27		MRP5, SMRP, EST277145, MOAT-C	many tissues

ABCC6	ATP-binding cassette, sub-family C (CFTR/MRP), member 6	16p13.1	ARA	MRP6, EST349056, MLP1	kidney, hepatocyte
ABCC7	**cystic fibrosis transmembrane conductance regulator, ATP-binding cassette (sub-family C, member 7)**	**7q31-q32**	**CF, CFTR**	**MRP7**	**lung, intestine, cholangiocytes, kidney**
ABCC8	ATP-binding cassette, sub-family C (CFTR/MRP), member 8	11p15.1	SUR, HRINS	HI, PHHI, SUR1, MRP8	pancreas
ABCC9	ATP-binding cassette, sub-family C (CFTR/MRP), member 9	12p12.1		SUR2	heart and skeletal muscle, lower levels in other tissues
ABCC10	ATP-binding cassette, sub-family C (CFTR/MRP), member 10	6p21		EST182763, MRP7	low in all tissues
ABCC11	ATP-binding cassette, sub-family C (CFTR/MRP), member 11	16q12		MRP8	low in all tissues
ABCC12	ATP-binding cassette, sub-family C (CFTR/MRP), member 12	16-16q12		MRP9	low in all tissues
	ALD (subfamily D)				
ABCD1	ATP-binding cassette, sub-family D (ALD), member 1	Xq28	ALD	AMN, ALDP, adrenoleukodystrophy	peroxisomes
ABCD2	ATP-binding cassette, sub-family D (ALD), member 2	12q11-q12	ALDL1	ALDR, ALDRP	peroxisomes
ABCD3	ATP-binding cassette, sub-family D (ALD), member 3	1p22-p21	PXMP1	PMP70	peroxisomes
ABCD4	ATP-binding cassette, sub-family D (ALD), member 4	14q24	PXMP1L	PMP69, P70R, EST352188	peroxisomes
ABCD1P1	ATP-binding cassette, sub-family D (ALD), member 1, pseudogene 1	2p11			
ABCD1P2	ATP-binding cassette, sub-family D (ALD), member 1, pseudogene 2	10p11			
ABCD1P3	ATP-binding cassette, sub-family D (ALD), member 1, pseudogene 3	16p11			
ABCD1P4	ATP-binding cassette, sub-family D (ALD), member 1, pseudogene 4	22q11			

OABP (subfamily E)					
ABCE1	ATP-binding cassette, sub-family E (OABP), member 1	4q31	RNASEL1, RNASELI, RNS4I	RLI, OABP	ovary, testes, spleen
GC N20 (subfamily F)					
ABCF1	ATP-binding cassette, sub-family F (GCN20), member 1	6p21.33	ABC50	EST123147	all
ABCF2	ATP-binding cassette, sub-family F (GCN20), member 2	7q35-q36		EST133090	all
ABCF3	ATP-binding cassette, sub-family F (GCN20), member 3	3q25.1-q25.2		EST201864	all
White (subfamily G)					
ABCG1	ATP-binding cassette, sub-family G (WHITE), member 1	21q22.3		ABC8	brain, spleen, lung
ABCG2	ATP-binding cassette, sub-family G (WHITE), member 2	4q22-q23		EST157481, MXR, BCRP, ABCP	placenta, breast, liver, intestine
ABCG3	ATP-binding cassette, sub-family G (WHITE), member 3	8p12-8p12		Abcp2, Mxr2	
ABCG4	ATP-binding cassette, sub-family G (WHITE), member 4	11q23		WHITE2	liver
ABCG5	ATP-binding cassette, sub-family G (WHITE), member 5 (sterolin 1)	2p21			liver, small intestine
ABCG8	ATP-binding cassette, sub-family G (WHITE), member 8 (sterolin 2)	2p21			liver, small intestine

MDR1 is part of the *MDR* gene family, containing two genes in human and three genes in rodents (111, 112). *MDR* genes are further classified into two classes based on their sequence identities and functions. Class I genes code for the drug transporter associated with multidrug resistance while class II genes code for a phospholipid transporter (Table 1.8). *MDR1* and *MDR2* genes share 76%, while *mdr1a* and *MDR1* share 88% of sequence homology (113).

Table 1.8 Nomenclature of multidrug-resistance gene family. Adapted from Silverman (111) and Borst and Schinkel (112)

Species	Class I genes	Class II genes
Human	*MDR1/ABCB1*	*MDR2/MDR3/ABCB4*
Mouse	*mdr1a/mdr3, mdr1b/mdr1*	*mdr2*
Rat	*mdr1a, mdr1b*	*mdr2*
Hamster	*p-gp1, p-gp2*	*p-gp3*

The *MDR* gene family is part of a larger gene superfamily, ATP-binding cassette (ABC) transporter superfamily (see Table 1.7).

1.4.1 P-glycoprotein expression

P-gp expression is ubiquitous. P-gp is expressed on the apical membrane of epithelial cells of many organs. The level of expression is highly variable among subjects, suggesting genetic or environmental factors (114-116). It is expressed at very high levels in human adrenal cortical cells, at high levels in the brush border of renal proximal tubule epithelium, the canalicular membrane of biliary hepatocytes, apical surface of pancreatic ductules and the mucosal surface of jejunum, ileum and colon, (117-119). It is also expressed on the capillary endothelial cells of the brain and testes (117-119), in placenta (120), in secretory glands of the pregnant endometrium (121, 122), in peripheral lymphocytes (123) and in CD34 positive bone marrow cells (124). Respiratory epithelia also express P-gp at low levels (125). T-cells and macrophages also appear to express P-gp (126-128)

1.4.2 P-glycoprotein structure

P-gp is an integral membrane glycoprotein comprised of 1280 amino acids with a molecular mass of approximately 170 kDa (107-110). Because it is a member of the ABC transporter family just like CFTR, it has twelve transmembrane domains that are divided into two membrane-spanning domains (MSD1 and MSD2), with Walker A and B and ABC-"signature"

sequence motifs in nucleotide-binding domains (NBD1 and NBD2) that interact with ATP. However, unlike CFTR, it does not have the R domain (Figure 1.2) (129, 130).

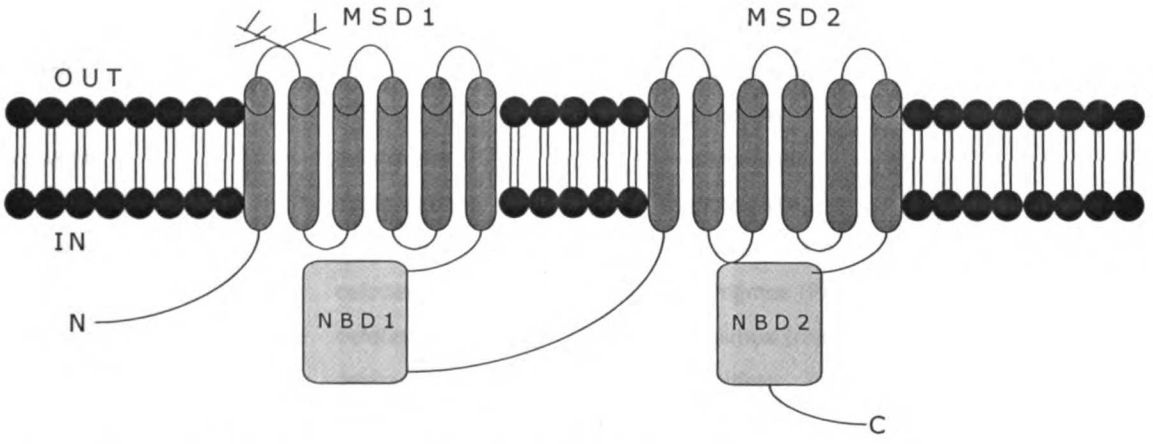

Figure 1.2 A model of P-glycoprotein structure. Adapted from Higgins *et al.* (131)

1.4.3 P-glycoprotein function

P-gp contributes to multidrug resistance in tumor cells, which is characterized by cross-resistance to multiple structurally and mechanistically unrelated cytotoxic drugs to which cells have never been exposed (102, 110, 132-136). This multidrug resistance is due to increased expression of P-gp in tumor cells upon exposure to a single cytotoxic drug. P-gp is an ATP-dependent efflux pump that can recognize a wide variety of compounds, such as vinca alkaloids, anthracyclines, epipodophyllotoxins, immunosuppressants and HIV-protease inhibitors (Table 1.9). (100, 137, 138). Increased P-gp expression leads to decreased accumulation of various drugs inside the cells (139-144). To overcome multidrug resistance phenomena, much research has been undertaken to find pharmacologic agents that can reverse or sensititize multidrug-resistant cells and tumors. These agents are known as P-gp modulators, chemosensitizers or reversers. (Table 1.9) (145-160).

Currently the physiologic role of P-gp is unknown but due to the location of its expression and function, it is hypothesized that the putative physiologic role of P-gp is a protective mechanism against xenobiotics and endogenous metabolites. Therefore, besides contributing

Table 1.9 A partial list of P-gp substrates and inhibitors. Adapted and expanded from Ambudkar *et al.* (178), Silverman (111), Wacher *et al.* (137) and Seelig (179, 180).

P-gp substrates		P-gp inhibitors
vincristine	aldosterone	verapamil
vinblastine	azidopine	vinblastine
vindesine	bepredil	ketoconazole
doxorubicin	BIBW22 BS	itraconazole
verapamil	bisantrene	clotrimazole
daunorubicin	catharantine	miconazole
epirubicin	cefazolin	cyclosporine A
actinomycin D	cefoperazone	tacrolimus (FK506)
mithramycin	cefotetan	sirolimus (rapamycin)
mitomycin C	cepharanthine	quinidine
mitoxanthrone	cinchonidine	PSC833
puromycin	CP 100356	VX-710
gramicidin D	dexniguldipine	LY335979
valinomycin	dibucaine	BIBW22
erythromycin	dipyridamole	GF120918 (GG918)
ivermectin	domperidone	amiodarone
paclitaxel (taxol)	gallopamil	hydrocortisone
docetaxel	methadone HCl	progesterone
etoposide	monensin	testosterone
teniposide	morphine	tamoxifen
topotecan	morphine-6-glucuronide	mifopristone (RU486)
colchicine	ondansentron	reserpine
emetine	phenoxazine	staurosporine
ethidium bromide	prazosin	quercetin
Hoechst 33342	phenytoin	trifluoroperizine
rhodamine 123	S 9788	felodipine
calcein AM	SDB-ethylenediamine	nifedipine
ritonavir	spiperone	nitrendipine
saquinavir	thioridazine	nicardipine
indinavir	valinomycin	terfenadine
nelfinavir	vindoline	diltiazem
cerivastatin	yohimbine	lidocaine
simvastatin	losartan	erythromycin
lovastatin	amprenavir	troleandomycin
atorvastatin	losartan	

fluvastatin
digitoxin
digoxin
terfenadine
morphine
loperamide
diltiazem
nicardipine
nifedipine
celiprolol
rifampicin
diltiazem
estradiol
estrogen glucuronide
hydrocortisone
cyclosporine
tacrolimus (FK506)
sirolimus (rapamycin)
cimetidine
dexamethasone
S-farnesyl cysteinmethylester
cis-flupenthixol
fluphenazine
methylbenzoylreserpate
methylreserpate
perphenazine
trifluoperazine
triflupromazine
triton X-100
tetraphenylphosphonium bromide
N-acetyl-leucyl-leucyl-norleucine
yeast α-factor pheromone

to multidrug resistance, P-gp is also involved in absorption and disposition of drugs and metabolites. P-gp plays a large role in affecting the pharmacokinetics of drugs (bioavailabilty, clearance, half life and volume of distribution) and contributes to drug-drug interactions (161-169).

P-gp is expressed at high levels on the mucosal surface of the jejunum, ileum and colon (117, 119). It pumps drugs out from the gastrointestinal tract into the gut lumen, thereby reducing drug absorption/bioavailability. P-gp on the canalicular membrane of hepatocytes and the brush border membrane of renal proximal tubule cells enhances drug elimination into the bile and urine, thereby increasing drug clearance and reducing drug half life. P-gp in the endothelial cells of the blood-brain barrier prevents drug entry into the central nervous system, which also reduces the volume of distribution. P-gp in the placenta is thought to protect the fetus against toxic xenobiotics (120); P-gp in the adrenal may be involved in steroid secretion or in protecting the plasma membrane of steroid secreting cells from the toxic effects of high steroid concentration (170, 171).

In addition to contributing to multidrug resistance and drug disposition, P-gp is also involved in regulating the activity of an unidentified chloride channel (172). It was first speculated that since P-gp showed a structural similarity to CFTR, which functions as a cAMP-dependent chloride channel, it was thought that P-gp might also function as an ion channel (173-175). It is now known that P-gp itself does not have intrinsic channel activity but instead can regulate an unidentified endogenous cell-swelling activated-chloride channel (89-91). P-gp phosphorylation by protein kinase A and C modulates the cell-swelling activated chloride currents and the two pathways act by distinct mechanisms (91, 172, 175). Currently the physiological importance of P-gp regulated chloride channels remains controversial.

1.5 Renal System

The kidney is a major excretory organ, and thus has been studied extensively. Unless indicated otherwise, most of the information presented here are from books written by Arthur Vander (176) and Christopher Lote (177). The kidney performs many critical functions:

electrolyte and water homeostasis, excretion of metabolic wastes and drugs in urine, control of arterial blood pressure, secretion of erythropoietin, production of 1,25-dihydroxyvitamin D_3 and gluconeogenesis. We will describe each of these kidney functions in more details.

1. Electrolyte and water homeostasis

To maintain a stable concentration of the body's water and inorganic ions, the kidney regulates the excretion of water, sodium, potassium, chloride, calcium, magnesium, sulfate, phosphate, bicarbonate and hydrogen ion into the urine. The kidney also plays a small role in maintaining the concentration of some organic nutrients and trace elements such as zinc and iron.

2. Excretion of metabolic wastes

There are many end products of the chemical reactions in the body that serve no known biological functions hence they are called waste products. For example, urea is the end product of protein catabolism, uric acid is the end product of purine catabolism, creatinine is the end product of muscle activities and bilirubin is the end product of hemoglobin breakdown. Some of these metabolic wastes are harmless but others could be toxic if they accumulate in the body. The kidney functions to eliminate these wastes from the body. The identity of many of these wastes have been documented but there are many others that are unknown and cause toxicity in renal failure patients.

3. Control of arterial blood pressure

There are several mechanisms by which the kidney regulates arterial blood pressure. As stated above, the kidney regulates sodium balance, and sodium concentration is critical for maintenance of blood volume and pressure. The kidney also produces renin, a proteolytic enzyme responsible for the generation of angiotensin, a vasocontrictor. The kidney is also thought to synthesize other vasoactive compounds that regulate arterial blood pressure.

4. Secretion of erythropoietin

Hypoxia in the kidney induces mesangial and tubular cells of the renal cortex to produce erythropoietin via prostaglandin synthesis. Erythropoietin is a glycoprotein hormone with a MW of ~34 kDa and 161 amino acids that stimulates erythrocyte production by the bone marrow.

5. Production of 1,25-dihydroxyvitamin D_3

Vitamin D consists of a group of closely related sterols. One member of this family, vitamin D_3, also called cholecalciferol, is synthesized in the skin by the ultraviolet radiation of 7-dehydrocholesterol. It is also available from plant food. Vitamin D_3 is inactive and it is hydroxylated in the 25 position by the liver followed by hydroxylation in the 1 position by the kidney. The product, 1,25-dihydroxyvitamin D_3, is the active form of vitamin D and it enhances bone resorption, stimulates active absorption of calcium and phosphate in the intestine and reabsorption of calcium and phosphate in the kidney tubular cells. The concentration of 1,25-dihydroxyvitamin D_3 is controlled by the second hydroxylation step, which occurs in the kidney. Therefore, the kidney plays an important role in calcium and phosphate homeostasis.

6. Gluconeogenesis

Like the liver, during prolonged fasting, the kidney synthesizes glucose from amino acids and other precursors and releases it into the bloodstream.

7. Excretion of drugs/xenobiotics into urine

Besides the liver, the kidney is the most important organ involved in eliminating xenobiotics from the body. Most drugs that are not metabolized are eliminated by the kidney and for drugs that do get metabolized by phase I and phase II reactions, the metabolites usually are also excreted renally. Renal elimination is comprised of three basic processes: glomerular filtration, tubular secretion and tubular reabsorption.

1.5.1 Glomerular filtration

The kidney is a paired organ located outside the peritoneal cavity in the posteriol abdominal wall. A single functioning unit of the kidney is called a nephron and there are approximately 1-1.5 million of these in each human kidney. A nephron consists of two parts: a filtering component called the renal corpuscle and a tubule extending out from the corpuscle. The renal corpuscle in turn is made up of a glomerulus (a tuft of highly convoluted capillaries) and a Bowman's capsule. The glomerulus protrudes into the Bowman's capsule and fluids filtered from the glomerulus flows into the lumen of Bowman's capsule, which is called Bowman's space. The capsule is connected on the other side to the first portion of the renal tubule, into which the filtered fluid flows. This is the first step of urine production and the process is called glomerular filtration where certain plasma components (water and solutes) are filtered from glomerular capillaries into the Bowman's space.

The blood supply of the glomerulus comes from the afferent arterioles and only about 20% of the plasma (no erythrocytes) is filtered from the glomerulus, while the remaining unfiltered portion drains into the efferent arteriole. The volume of filtration from the glomerulus into Bowman's space per unit of time is defined as glomerular filtration rate (GFR). In a young, healthy 70-kg person, the GFR is 125 ml/min. It is a very high capacity system designed to remove huge quantities of unwanted waste products and foreign compounds from the body. Small solutes with a MW <7,000 daltons are freely filtered but large molecules such as plasma proteins and cells cannot be filtered. For compounds that bind to protein, only the unbound component can be filtered by the glomerulus. GFR is governed by several factors: hydraulic permeability, surface area and net filtration pressure (NFP).

$$\text{GFR} = \text{hydraulic permeability} \times \text{surface area} \times \text{net filtration pressure}$$

Net filtration pressure is determined by the difference in the forces that induce and oppose filtration across the glomerulus. Factors that change any of these parameters will change GFR.

$$NFP = P_{GC} - P_{BC} - \pi_{GC}$$

P_{GC} = glomerular-capillary hydraulic pressure

P_{BC} = Bowman's capsule hydraulic pressure

π_{GC} = oncotic pressure of glomerular-capillary plasma

1.5.2 Tubular reabsorption and secretion

As we mentioned above, the glomerular filtrate flows from the Bowman's space into the kidney tubule. As it flows through the different portions of the tubule, two processes can cause changes of the composition of the glomerular filtrate: tubular reabsorption and tubular secretion. The tubule is closely associated with the peritubular capillaries that permit transfer of compounds between the kidney lumen and the blood. If a compound crosses from the lumen to the capillaries, the process is called tubular reabsorption while the opposite scenario is called tubular secretion, where the compound goes from the capillaries to the kidney lumen.

The tubule is made up of a single layer of epithelial cells resting on a basement membrane with a tight junction between adjacent cells. The part of the tubule that connects with the Bowman's capsule is called proximal tubule which is then followed by these segments: descending thin limb of Henle's loop, ascending thin limb of Henle's loop, thick ascending limb of Henle's loop, distal convoluted tubule, connecting tubule, cortical collecting duct, outer medullary collecting ducts and inner medullary collecting ducts. The fluid from the collecting ducts empties into a calyx of the renal pelvis that then empties into the urinary bladder via the ureter. Many secretion and reabsorption processes occur along the tubules but once the fluid enters a calyx, it is no longer altered and it has the same composition as the urine. Therefore urine composition is a reflection of the three renal processes: glomerular filtration, tubular reabsorption and secretion.

As we mentioned earlier, the tubule is made up of a single layer of epithelial cells resting on a basement membrane with a tight junction between adjacent cells. Along the tubule, there are two routes for reabsorption and secretion: paracellular and transcellular. The paracellular route involves diffusion across a tight junction down an electrochemical gradient while the transcellular route involves crossing luminal (apical) and contraluminal (basolateral)

membranes by either a passive or an active process: diffusion, facilitated diffusion, primary active transport, secondary active transport, tertiary active transport and endocytosis.

The driving force for diffusion is the electrochemical gradient. Small lipophilic compounds can diffuse across cell membranes while ionic compounds cross through specific ion channels/pores in the membranes. Facilitated diffusion also occurs because of an electrochemical gradient but this process requires the help of carrier/membrane proteins for compounds to get across the cell membranes. Because it involves carrier proteins, facilitated diffusion displays saturability, specificity and inhibition.

Primary active transport also requires carrier proteins and displays saturability, specificity and inhibition but unlike facilitated diffusion, the direction of transport is against an electrochemical gradient. The driving force for this process comes from ATP hydrolysis. An example of a primary active transport is Na-K ATPase that is located on the basolateral membrane. Secondary active transport involves carrier proteins that can transport two compounds simultaneously, either in the same direction (cotransport) or in the opposite direction (antiport). One compound is moving down its electrochemical gradient and the energy released from this process drives the movement of the second compound against its electrochemical gradient. For example, glucose is reabsorbed from the proximal tubule by secondary active cotransport with Na^+.

Endocytosis is the invagination of a portion of the plasma membrane until it is pinched off and becomes an isolated vesicle filled with extracellular fluid. This process requires ATP hydrolysis and is a mechanism for macromolecule uptake.

Prior to the 1870s, glomerular filtration was thought to be the sole process involved in the renal elimination of compounds. Heidenhain and Neisser (181) were the first to demonstrate in 1874 using canine tubular cells that tubular secretion was involved in renal excretion; in 1923 Marshall and Vickers (182) showed the excretion of an organic anion dye phenol red in the marine teleost fish that lacked a glomerulus. Twenty three years later Rennick *et al.* (183)

showed the existence of a transport system for organic cations as well. Since then, it has been established that there are specific and selective transporters for organic cations and organic anions at the luminal and basolateral membranes of the kidney tubule (184-186).

Many of the transporters involved in xenobiotic elimination are located at the kidney proximal tubule cells. They are separated into two groups based on the type of drugs that they carry: organic anion or organic cation transporters. Organic anion transporters belong to either the *OAT* or *OAT-K/OATP* gene family while organic cation transporters belong to either the *OCT* or *OCTN* gene family (187). There are also other transporters that are neither organic anion nor organic cation transporters and they belong to either P-glycoprotein (*MDR*) or multidrug-resistance associated protein (*MRP*) gene families. (187, 188). OATP1, OAT-K1, P-gp, MRP2 and OAT-K2 have been shown to localize to brush border membranes while OCT1, OAT1 and MRP1 are located in basolateral membranes (187). Currently the location of OAT3, OATP3, OCT3, OCTN1, OCTN2 are unknown (187).

As mentioned earlier, P-gp is located at the apical/luminal/brush-border membrane of renal proximal tubule cells and it is thought that P-gp contributes to renal clearance of drugs by extruding drugs out from the cells into the kidney lumen.

1.6 Altered Pharmacokinetic of Drugs in CF Patients

As stated earlier, CF patients suffer from recurrent and chronic respiratory tract infections and to treat the infections, these patients take many antibiotics (see Table 1.1); it was observed as early as 1975 that disposition of many drugs is altered in CF patients (189-194). Surprisingly, the plasma concentrations of many drugs are lower in CF than non-CF patients (189-194). The lower concentrations are thought to be due to larger apparent volume of distribution (V_d) and higher metabolic (CL_{NR}) and renal clearances (CL_r) of drugs in CF patients (189-194). The organs involved in drug elimination, the gastrointestinal tract, the liver and the kidney, all have some degree of dysfunction in CF patients but usually defects in these organs led to higher plasma concentrations due to decreased clearances (191). Currently the precise mechanisms of the altered drug disposition in CF patients remain unknown.

Many studies have been done to compare the pharmacokinetics of drugs between CF and non-CF populations. Even though there are a few conflicting studies in the literature, an increase in volume of distribution, a decrease in half-life and an enhanced metabolic and renal clearance of many (but not all) antibiotics in CF patients have become a recognized pattern and many review articles have been written on this topic (189-194).

Table 1.10 shows that the protein binding of most drugs (e.g., dicloxacillin, trimethoprim, sulfamethoxazole, cefsulodin, (R)-warfarin) is not different between controls and CF patients, with the exception of theophylline and (S)-warfarin.

Table 1.10 Comparison of protein binding of several drugs in CF patients. Adapted and expanded from Rey *et al.* (189) and Touw (190)

Drugs	CF patients		Controls		References
	N	fu (%)	N	fu (%)	
dicloxacillin	10	11.6 ± 7.7	8	5.6 ± 1.9	195
cefsulodin	3	83	3	85	196
cloxacillin	7	5.2 ± 5.1	8	3.8 ± 2.1	197
ceftazidime	10	96.9 ± 6.1	10	98 ± 5.6	198
gentamicin	12	85.7 ± 2.6	8	82.6 ± 3.8	199
theophylline	11	42 ± 41	15	36 ± 35	200
sulfamethoxazole	7	53 ± 4	8	53 ± 5	201
trimethoprim	7	61 ± 5	8	63 ± 5	201
(R)-warfarin	6	0.45 ± 0.11	6	0.37 ± 0.06	202
theophylline[a]	10	46 ± 9	10	36 ± 6	203
(S)-warfarin[a]	6	0.43 ± 0.09	8	0.55 ± 0.09	204

a = statistically significant difference from controls, $P < 0.05$.
N = number of subjects.
fu = fraction unbound.

Table 1.11 shows that the renal function is not altered in CF patients, except in studies done by the Karolinska group, where the glomerular filtration rate is slightly higher in CF patients, supposedly due to the essential fatty-acid status of their patients (205). Table 1.12 shows that the volume of distribution of some drugs (e.g., ceftazidime, cloxacillin, gentamicin) is increased in CF patients, while other drugs (e.g., trimethoprim, sulfamethoxazole, cefsulodin) exhibit no change. Table 1.13 shows that the half-life of some drugs (e.g., cloxacillin,

Table 1.11 Comparison of renal function clearances in CF patients. Adapted and expanded from Prandota *et al.* (192)

Drugs	CF patients		Controls		References
	N	CL	N	CL	
endogenous creatinine	9	83.8 ± 17.4 mL/min/1.73m^2	9	93.3 ± 19.3 mL/min/1.73m^2	208
endogenous creatinine	12	133.8 ± 24.6 mL/min/1.73m^2	6	145.8 ± 23.4 mL/min/1.73m^2	199
creatinine	7	163 ± 38 mL/min/1.73m^2	6	171 ± 52 mL/min/1.73m^2	209
creatinine	11	73.5 ± 18.2 mL/min/m^2	11	68.4 ± 1.65 mL/min/m^2	210
creatinine	11	77.7 ± 25.8 mL/min	12	88.1 ± 25.9 mL/min	211
creatinine	10	196 mL/min/1.73m^2	8	127 mL/min/1.73m^2	195
iothalamate	12	147.5 ± 29.2 mL/min/1.73m^2	6	142.9 ± 33.3 mL/min/1.73m^2	199
^{99m}Tc-DTPA	8	95.8 ± 20.0 mL/min/1.73m^2	10	98.9 ± 12.9 mL/min/1.73m^2	212
^{125}I-orthohippurate[b]	8	496 ± 102 mL/min/1.73m^2	10	499 ± 60 mL/min/1.73m^2	212
PAH[b]	16	616 ± 78 mL/min/1.73m^2	10	601 ± 61 mL/min/1.73m^2	213
inulin[a]	16	136 ± 8 mL/min/1.73m^2	10	108 ± 12 mL/min/1.73m^2	206
inulin[a]	16	131 ± 8 mL/min/1.73m^2	10	100 ± 20 mL/min/1.73m^2	206
inulin[a]	5	121 ± 33 mL/min/1.73m^2	6	104 ± 13 mL/min/1.73m^2	207
inulin[a]	16	127 ± 18 mL/min/1.73m^2	10	112 ± 10 mL/min/1.73m^2	213
inulin[a]	5	142 ± 38 mL/min/1.73m^2	5	102 ± 15 mL/min/1.73m^2	196
inulin	-	142 ± 40 mL/min/1.73m^2	-	137 ± 28 mL/min/1.73m^2	214

a = statistically significant difference from controls, $P < 0.05$.
b = renal blood flow marker
N = number of subjects
CL= total clearance.
PAH = para-amino hippurate
DTPA = diethylenetriamine pentaacetic acid

Table 1.12 Comparison of volume of distribution of several drugs in CF patients. Adapted and expanded from Rey *et al.* (189) and Touw (190)

Drugs	CF patients		Controls		References
	N	V_d	N	V_d	
ceftazidime[a]	10	0.237 ± 0.033 L/kg	10	0.197 ± 0.033 L/kg	198
cloxacillin[a]	12	0.1365 ± 0.0527 L/kg	12	0.099 ± 0.0168 L/kg	197
gentamicin[a]	19	0.339 ± 0.03 L/kg	17	0.236 ± 0.016 L/kg	215
gentamicin[a]	19	9.51 ± 0.91 L/m^2	17	7.47 ± 0.81 L/m^2	215
theophylline[a]	10	0.59 ± 0.1 L/kg	10	0.44 ± 0.05 L/kg	203
tobramycin[a]	12	0.31 ± 0.08 L/kg	8	0.23 ± 0.07 L/kg	199
ciprofloxacin[a]	11	2.1 ± 0.8 L/kg	12	3.8 ± 0.9 L/kg	216
ciprofloxacin	12	2.21 ± 0.89 L/kg	12	2.25 ± 0.48 L/kg	217
ciprofloxacin	6	2.8 ± 0.5 L/kg	6	3.2 ± 0.6 L/kg	218
ticarcillin	11	7.24 ± 1.75 L/m^2	11	6.22 ± 1.25 L/m^2	210
fleroxacin[b,c]	13	1.6 ± 0.5 L/50kg	12	1.8 ± 0.3 L/50kg	219
methicillin	7	41.1 ± 17.4 L/1.73m^2	6	30.3 ± 7.2 L/1.73m^2	209
tobramycin	12	15.5 ± 4.0 L/1.73m^2	8	14.4 ± 5.2 L/1.73m^2	199
(S)-warfarin	6	0.153 ± 0.018 L/kg	5	0.138 ± 0.022 L/kg	204
sulfamethoxazole	7	0.26 ± 0.02 L/kg	9	0.26 ± 0.04 L/kg	201
trimethoprim	7	1.5 ± 0.2 L/kg	9	1.7 ± 0.2 L/kg	201
netilmicin	8	0.31 ± 0.11 L/kg	8	0.36 ± 0.16 L/kg	220
amikacin	9	0.26 ± 0.06 L/kg	4	0.26 ± 0.03 L/kg	221
aztreonam	8	0.20 ± 0.02 L/kg	8	0.18 ± 0.04 L/kg	222
amikacin	11	16.0 ± 4.7 L/1.73m^2	9	14.9 ±3.8 L/1.73m^2	223
cefsulodin	7	16 ± 13 L/1.73m^2	5	25 ± 5 L/1.73m^2	196

a = statistically significant difference from controls, $P < 0.05$.
b = V_d at steady state.
c = lean body mass.
N = number of subjects.
V_d = apparent volume of distribution.

Table 1.13 Comparison of half-life of several drugs in CF patients. Adapted and expanded from Rey *et al.* (189) and Touw (190)

Drugs	CF patients		Controls		References
	N	$t_{1/2}$	N	$t_{1/2}$	
cloxacillin[a]	16	46.1 ± 11.3 min	12	57.1 ± 17.3 min	197
theophylline[a]	10	361 ± 123 min	10	568 ± 188 min	203
theophylline[a]	11	5.6 ± 0.7 h	15	6.9 ± 1.5 h	200
ceftazidime[a]	10	90 ± 11.1 min	10	105.3 ± 12.4 min	198
sulfamethoxazole[a]	14	6.04 ± 2.08 h	?	11 ± 3 h	224
trimethoprim[a]	14	5.68 ± 1.78 h	?	14.7 ± 7.5 h	224
sulfamethoxazole[a]	7	7.72 ± 2.05 h	8	10.1 ± 2.55 h	201
trimethoprim[a]	7	5.36 ± 0.87 h	8	10.1 ± 1.63 h	201
fleroxacin[a]	13	10.5 ± 2.6 h	12	13.5 ± 2.9 h	219
fleroxacin	13	12.1 ± 2.3 h	12	15.6 ± 3.2 h	219
ciprofloxacin[a]	11	2.62 ± 1.04 h	12	3.93 ± 1.12 h	216
ciprofloxacin	12	4.5 ± 1.9 h	12	5.1 ± 1.0 h	217
ciprofloxacin	6	4.5 ± 1.0 h	6	4.8 ± 0.8 h	218
ciprofloxacin	7	5.1 ± 1.9 h	11	4.4 ± 0.8 h	225
dicloxacillin	10	1.4 ± 0.5 h	8	1.2 ± 0.2 h	195
methicillin	7	1.05 ± 0.53 h	6	0.85 ± 0.24 h	209
cefsulodin	7	1.33 ± 0.22 h	5	1.5 ± 0.31 h	196
ticarcillin	11	53.1 min	11	70.8 min	210
amikacin	11	1.5 ± 0.5 h	9	1.6 ± 0.4 h	223
gentamicin	17	1.62 ± 0.15 h	17	1.98 ± 0.27 h	226
tobramycin	12	1.73 ± 0.42 h	8	1.85 ± 0.38 h	199
netilmicin	8	1.37 ± 0.27 h	8	2.29 ± 0.86 h	220
cefepime	11	2.28 ± 0.49 h	12	2.41 ± 0.62 h	211
cefepime	7	1.71 ± 0.53 h	7	1.96 ± 0.44 h	227
aztreonam	8	1.54 ± 0.17 h	8	1.81 ± 0.33 h	222
amikacin	9	1.10 ± 0.26 h	4	0.83 ± 0.15 h	221
(S)-warfarin	6	29.5 ± 4.2 h	8	25.9 ± 5.4 h	204
(R)-warfarin	6	34.7 ± 9.6 h	6	40.6 ± 8.2 h	202
furosemide	6	0.73 ± 0.17 h	6	0.80 ± 0.11 h	228
ibuprofen	13	92 ± 27 min	4	86 ± 17 min	229

a = statistically significant difference than controls, $P < 0.05$.
$t_{1/2}$ = half-life of drugs.
N = number of subjects.

theophylline, ceftazidime, sulfamethoxazole, trimethoprim) is decreased in CF patients, while other drugs (e.g., dicloxacillin, cefsulodin, methicillin, amikacin) display no change. Table 1.14 shows that the total clearance of many drugs is increased in CF patients (e.g., cloxacillin, methicillin, ticarcillin, sulfamethoxazole, trimethoprim, furosemide, ibuprofen) while some drugs (e.g., cefepime, netilmicin, antipyrine) show no change. Table 1.15 shows that the renal clearance of some drugs (e.g., dicloxacillin, trimethoprim, ticarcillin, methicillin) is increased in CF patients and some drugs (e.g., sulfamethoxazole, cloxacillin, cefepime) exhibit no change.

1.7 Hypothesis

Because most antibiotics are eliminated renally (Table 1.16) and many antibiotics exhibit enhanced renal clearance in patients with CF (Table 1.15), the goal of our studies was to determine the mechanism(s) responsible for those enhanced renal clearances.

Renal clearance is the volume of plasma from which a substance is completely removed by the kidneys per unit time. To determine what causes the enhanced renal clearance of drugs in CF, we need to examine the components of renal clearance. As we stated earlier, three factors govern renal clearance: filtration, tubular secretion and tubular reabsorption. Enhanced renal clearance could be due to an increase in filtration rate, an increase in tubular secretion or a decrease in tubular reabsorption. Filtration rate is governed by glomerular filtration rate (GFR) and protein binding and is equal to fu x GFR (fu = fraction unbound). There is no difference in protein binding of most drugs between controls and CF patients (Table 1.10). GFR in CF patients has been studied with conflicting results, but most studies have shown that it is not altered in CF patients (Table 1.11). The Karolinska group has reported slightly increased GFR in their CF patients and it is thought to be due to the essential fatty acid status of their patients (206, 207,205). Thus, in most cases enhanced renal clearance is not due to an increase in filtration rate but is due to either an increase in tubular secretion or a decrease in tubular reabsorption or both.

Table 1.14 Comparison of total clearance of several drugs in CF patients. Adapted and expanded from Rey *et al.* (189), Touw (190) and Prandota (192)

Drugs	Dose (mg/kg)	CF patients		Controls		References
		N	CL	N	CL	
dicloxacillin[a]	6.25 po	10	0.47 ± 0.325 L/h/kg	8	0.185 ± 0.069 L/h/kg	195
cloxacillin[a]	25 IV	16	261 ± 103 mL/min/1.73m^2 CL_{NR} = 132.2 ± 129.6 mL/min/1.73m^2	12	147 ± 30 mL/min/1.73m^2 CL_{NR} = 54.1 ± 27.2 mL/min/1.73m^2	197
methicillin[a]	15 IV	7	512 ± 62 mL/min/1.73m^2	6	424 ± 90 mL/min/1.73m^2	209
ticarcillin[a]	120 CF, 75 C IV	11	0.16 L/h/kg	11	0.096 L/h/kg	210
sulfamethoxazole	800 mg po	14	24.1 ± 13.0 ml/min	?	13.4 ± 4.4 ml/min	224
sulfamethoxazole[a]	10 IV	7	0.0262 ± 0.0064 L/h/kg CL_{NR} = 0.024 ±0.0062 L/h/kg	8	0.0188 ± 0.0043 L/h/kg CL_{NR} = 0.016 ±0.0034 L/h/kg	201
N4-acetyl-sulfamethoxazole[a]		7	CL_f = 0.00903 ± 0.00247 L/h/kg CL_{fu} = 0.0172 ± 0.0047 L/h/kg	8	CL_f = 0.00355 ± 0.0049 L/h/kg CL_{fu} = = 0.00705 ± 0.00166 L/h/kg	201
trimethoprim[a]	2 IV	7	0.181 ± 0.044 L/h/kg	8	0.114 ± 0.019 L/h/kg	201
theophylline[a]	5.7 ± 0.7 IV	10	4.3 ± 1.5 L/h/1.73m^2	10	2.2 ± 0.7 L/h/1.73m^2	203
theophylline[a]	5.5 IV	11	73.02 ± 18.4 mL/min/1.73m^2 CL_{NR} = 64.27 ± 19.3 mL/min/1.73m^2	15	49.84 ± 9.63 mL/min/1.73m^2 CL_{NR} = 45.52 ± 9.31 mL/min/1.73m^2	200
acetaminophen[a]		5	0.362± 0.081 L/h/kg	5	0.247± 0.0022 L/h/kg	201
acetaminophen sulfate[a]			0.08 ± 0.023 L/h/kg		0.045 ± 0.008 L/h/kg	201
acetaminophen glucuronide[a]			0.189 ± 0.051 L/h/kg		0.114 ± 0.017 L/h/kg	201

furosemide[a]	0.48-0.55 IV	6	CL_{NR} = 139.5 ± 55 ml/min	6	CL_{NR} = 61 ± 25 ml/min	228
ibuprofen[a]	13.4-13.9 IV	13	99 ± 26 mL/min/1.73m^2	4	67 ± 9 mL/min/1.73m^2	229
ceftazidime[a]	50 IV	10	0.147 ± 0.02 L/h/kg	10	0.089 ± 0.012 L/h/kg	198
lorazepam[a]	0.03 IV	14	1.8 ± 0.2 ml/min/kg	9	0.80 ± 0.08 ml/min/kg	230
lorazepam[a]	0.03 IV	15	1.66 ± 0.44 ml/min/kg	15	1.16 ± 0.50 ml/min/kg	231
tobramycin[a]	75.5 ± 10.2 mg/m^2 CF 55.7 ± 14.7 mg/m^2 C IV	12	121.2 ± 14.9 mL/min/1.73m^2	8	102.2 ± 18.9 mL/min/1.73m^2	199
cefsulodin[a]	Css=2 mg/L	6	134 ± 32 mL/min/1.73m^2	8	107 ±14 mL/min/1.73m^2	206
cefsulodin[a]	Css=30 mg/L	6	137 ± 25 mL/min/1.73m^2	8	114 ± 7 mL/min/1.73m^2	206
cefsulodin	50 mg/kg IV	7	178 ± 81 mL/min/1.73m^2	5	189 ± 43 mL/min/1.73m^2	196
aztreonam[a]	2000 mg IV	8	108 ± 18 mL/min/1.73m^2	8	79 ± 7 mL/min/1.73m^2	222
ciprofloxacin	500 mg po	11	49.7 ± 17.2 L/h	12	54.5 ± 14.6 L/h	216
ciprofloxacin	200 mg IV	12	29.4 ± 6.4 L/h	12	32 ± 4.8 L/h	217
ciprofloxacin	750 mg po	12	43.7 ± 16.3 L/h	12	51.9 ± 28.4 L/h	217
ciprofloxacin	750 mg po	6	27.3 ± 2.5 L/h	6	30.5 ± 4.5 L/h	218
ciprofloxacin[a]	6 mg/kg CF, 4 mg/kg C IV	14	721 ± 113 mL/min/1.73m^2	5	493 ± 45.1 mL/min/1.73m^2	232
cyclosporine[a]	16.7 ± 7.2 CF, 8.2 ± 1.9 C IV	11	95.5 ± 37.5 ml/min/ m^2	11	52.7 ± 16.5 ml/min/ m^2	233

cyclosporine[a]	5 IV	6	0.28 ± 0.07 L/h/kg	5	0.16 ± 0.03 L/h/kg	233
cyclosporine	2 IV	7	5.8 ± 0.9 mL/min/kg	3	5.7 ± 0.9 mL/min/kg	234
fleroxacin	800 mg po	13	CL_{NR} = 46.2 ± 15.3 ml/min/50kg LBM	12	CL_{NR} = 45.4 ± 14.7 ml/min/50kg LBM	219
fleroxacin	800 mg po X 5 days	13	CL_{NR} = 32 ± 12.5 ml/min/50kg LBM	12	CL_{NR} = 33.8 ± 7.8 ml/min/50kg LBM	219
N-demethyl-fleroxacin[a]	single dose	13	CL_f = 429.5 ± 95.0 ml/min/50kg LBM	12	CL_f = 283.1 ± 64.8 ml/min/50kg LBM	219
N-demethyl-fleroxacin[a]	steady state	13	CL_f = 610.0 ± 187.7 ml/min/50kg LBM	12	CL_f = 372.5 ± 120.6 ml/min/50kg LBM	219
N-oxide-fleroxacin[a]	single dose	13	CL_f = 6.94 ± 3.07 ml/min/50kg LBM	12	CL_f = 4.88 ± 1.1 ml/min/50kg LBM	219
N-oxide-fleroxacin[a]	steady state	13	CL_f = 12.4 ± 5.68 ml/min/50kg LBM	12	CL_f = 5.09 ± 1.22 ml/min/50kg LBM	219
cefepime	50 IV	7	127.26 ± 45.52 ml/min	7	121.19 ± 67.19 ml/min	227
cefepime	2000 mg IV	11	119.7 ± 20.1 mL/min	12	103.5 ± 19.8 mL/min	211
amikacin[a]	420 mg/m^2 IV	11	130.8 ± 27.7 mL/min/1.73m^2	9	107.1 ± 17.8 mL/min/1.73m^2	223
amikacin	15-30 CF, 15 C IV	9	131 ± 32 mL/min/1.73m^2	4	157 ± 33 mL/min/1.73m^2	221
antipyrine	10 IV	14	0.9 ± 0.1 ml/min/kg	9	0.70 ± 0.09 ml/min/kg	230
antipyrine		15	1.03 ± 0.69 ml/min/kg	15	0.76 ± 0.28 ml/min/kg	231
3-hydroxymethyl-antipyrin[a]			CL_f = 0.18 ± 0.11 ml/min/kg		CL_f = 0.08 ± 0.05 ml/min/kg	231
R-warfarin[a]	0.375 IV	6	4.06 ± 1.01 ml/h/kg CL_{ffu} = = 997s ± 483 ml/h/kg	6	2.8 ± 0.51 ml/h/kg CL_{ffu} = = 788 ± 219 ml/h/kg	202
R-6-hydroxy warfarin			CL_{ffu} = = 124.2 ± 72.8 ml/h/kg		CL_{ffu} = = 99.4 ± 37.3 ml/h/kg	202

R-7-hydroxy warfarin			CL_{fu} = = 43.8 ± 32.2 ml/h/kg		CL_{fu} = = 34.5 ± 10.6 ml/h/kg	202
R-8-hydroxy warfarin			CL_{f4} = 80.4 ± 85.4 ml/h/kg		CL_{fu} = = 69.5 ± 39.5 ml/h/kg	202
R-10-hydroxy warfarin			CL_{fu} = = 4.38 ± 2.72 ml/h/kg		CL_{fu} = = 16.28 ± 13.71 ml/h/kg	202
S-warfarin	0.375 IV	6	3.6 ± 0.48 ml/h/kg	8	3.82 ± 0.73 ml/h/kg	204
S-6-hydroxy warfarin			CL_f = 0.332 ± 0.108 ml/h/kg		CL_f = 0.407 ± 0.097 ml/h/kg	204
S-7-hydroxy warfarin			CL_f = 1.34 ± 0.49 ml/h/kg		CL_f = 1.8 ± 0.45 ml/h/kg	204
netilmicin	3 IV	8	110.3 ± 39.3 mL/min/1.73m^2	8	87.7 ± 42.8 mL/min/1.73m^2	220
PABA	5 po	18	3.27 ± 1.02 mL/min/kg	6	2.99 ± 1.21 mL/min/kg	235

a = statistically significant difference from controls, $P < 0.05$.
N = number of subjects.
CL = total plasma clearance.
CL_{NR} = non-renal clearance.
CL_f = formation clearance.
CL_{fu} = unbound formation clearance.
PABA = para-amino benzoic acid.
IV= intravenous.
po = orally.
CF = patients with CF.
C = controls.
LBM = lean body weight.

Table 1.15 Comparison of renal clearance of several drugs in CF patients. Adapted and expanded from Rey *et al.* (189) and Prandota (192).

Drug	Dose (mg/kg)	CF patients		Controls		Reference
		N	CLr	N	CLr	
amikacin[a]	420 mg/m^2 IV	11	105.3 ± 21.9 mL/min/1.73m^2	9	86.6 ± 13.2 mL/min/1.73m^2	223
dicloxacillin[a]	6.25 po suspension	10	282 ± 135 mL/min/1.73m^2	8	95 ± 28 mL/min/1.73m^2	195
methicillin[a]	15 IV	7	425 ± 38 mL/min/1.73m^2	6	362 ± 43 mL/min/1.73m^2	209
ticarcillin[a]	15 IV	11	65.6 ± 22 mL/min/m^2	11	46.2 ± 10.9 mL/min/m^2	210
ciprofloxacin[a]	15 IV	14	434 ±135.8 mL/min/1.73m^2	5	232 ± 92.1 mL/min/1.73m^2	232
ciprofloxacin	200 mg IV	12	17.9 ± 6.93 L/h	12	20.8 ± 3.67 L/h	217
trimethoprim[a]	2 mg/kg IV	7	0.124 ± 0.0299 L/h/kg	8	0.072 ± 0.0166 L/h/kg	201
sulfamethoxazole	10 mg/kg IV	7	0.00216 ± 0.00169 L/h/kg	8	0.00273 ± 0.00118 L/h/kg	201
ceftazidime[a]	50 IV	10	130.1 ± 11.4 mL/min/1.73m^2	10	92.7 ± 11.6 mL/min/1.73m^2	198
ceftazidime[a]	50 IV	8	125 ± 20 mL/min/1.73m^2	10	100 ± 9 mL/min/1.73m^2	206
cefsulodin	50 IV	7	140 ± 34 mL/min/1.73m^2	5	141 ± 36 mL/min/1.73m^2	196
cefsulodin[a]	0.25 mg/min/3h infusion	6	122 ± 19 mL/min/1.73m^2	8	92 ± 18 mL/min/1.73m^2	206
cefsulodin[a]	4 mg/min/3h infusion	6	118 ± 16 mL/min/1.73m^2	8	89 ± 5 mL/min/1.73m^2	206
cloxacillin	25 IV	16	123 ± 47 mL/min/1.73m^2	12	94 ± 26 mL/min/1.73m^2	197
cloxacillin	25 po	6	104.8 ± 33.5 mL/min/1.73m^2	7	103.8 ± 22.2 mL/min/1.73m^2	197
tobramycin	75.5 ± 10.2 mg/m^2 CF, 55.7 ± 14.7 mg/m^2 C IV	12	89.5 ± 17.9 mL/min/1.73m^2	8	81 ± 15.8 mL/min/1.73m^2	199
cefepime	50 IV infusion	11	102.86 ± 41.61 mL/min	12	106.87 ± 6.07 mL/min	227
cefepime	2000 mg IV infusion	11	95.1 ± 12.4 mL/min	12	85.1 ± 12 mL/min	211

a = statistically significant difference than controls, $P < 0.05$.
N = number of subjects, CLr = renal clearance, CF = patients with CF, C = control groups without CF.
IV= intravenous, po = orally.

Table 1.16 Fractional urinary excretion of several antibiotics. Adapted from Benet *et al.* (236)

Drugs	**Urinary excretion (%)**
amikacin	98
amoxicillin	86 ± 8
ampicillin	82 ± 10
aztreonam	68 ± 8
bleomycin	68 ± 9
capreomycin	57 ± 19
carbenicillin	82 ± 9
cefazolin	80 ± 16
cefmetazole	80 ± 13
ceftazidime	84 ± 4
cephalexin	91 ± 18
cinoxacin	60-85
ciprofloxacin	65 ± 12
cloxacillin	75 ± 14
dicloxacillin	60 ± 7
doxycycline	41 ± 19
enoxacin	45 ± 11
erythromycin	12 ± 7
gentamicin	> 90
kanamycin	90
lomefloxacin	65 ± 9
methicillin	88 ± 17
mezlocillin	45 ± 6
minocycline	11 ± 2
moxalactam	76 ± 12
nafcillin	27 ± 5
netilmicin	80-90
norfloxacin	26-32
ofloxacin	64 ± 16
oxacillin	46 ± 4
piperacillin	71 ± 14
rifampin	7 ± 3
streptomycin	50 ± 60
sulfamethoxazole	14 ± 2
tetracycline	58 ± 8
ticarcillin	77 ± 12
tobramycin	90
trimethoprim	63 ± 10
vancomycin	79 ± 11

Presently it is not possible to determine the exact contribution of tubular secretion or tubular reabsorption to renal clearance; one can only determine the net tubular secretion or reabsorption. If the renal clearance is greater than fu x GFR then there is a net secretion while if it is less than fu x GFR then there is a net reabsorption. Tubular secretion is an active process that involves transporters such as P-glycoprotein, organic anion and organic cation transporters. Tubular reabsorption is composed of an active process involving transporters and a passive diffusion process that is dependent upon the molecular weight, lipophilicity and the pKa of the drug, urine flow rate and urine pH. Hutabarat *et al.* (201) did not find a significant difference in the urine pH between normal and CF patients.

For most drugs, the actual mechanisms involved in their renal elimination are often unknown. For example, a drug that shows renal clearance equal to GFR could suggest that tubular secretion and reabsorption are not involved or it could also be a result of secretion and reabsorption occurring to the same extent. As a general rule, elimination of most aminoglycosides is thought to involve tubular reabsorption. For cephalosporins both tubular reabsorption and tubular secretion are present while elimination of penicillin derivatives is thought to involve tubular secretion (189). Dicloxacillin, ticarcillin (penicillin derivatives) and trimethoprim (a weak base) are thought to have net tubular secretion and based on their data, Jusko *et al.* (195), de Groot *et al.* (210), Hutabarat *et al.* (201) and Wang *et al.* (237) hypothesized that enhanced tubular secretion is responsible for the enhanced renal clearance of their test drugs. However, the exact mechanisms that cause the enhanced CL_r of those drugs have not been elucidated.

We hypothesize that the enhanced CL_r of some drugs in CF patients is due to an increase in tubular secretion, which is caused by increased P-gp expression in those patients that occurs due to a defect in CFTR. P-gp is a known transporter that can eliminate drugs from the body. In the kidney, P-gp is located in the apical membrane of proximal tubules and it effluxes drugs from the blood to the lumen. Increased P-gp expression could increase the tubular secretion of drugs that are substrates of P-gp hence increasing their renal clearance.

Some evidence in the literature supports the hypothesis that P-gp expression might be upregulated in CF patients. A case history of a CF patient with improved lung function after cancer therapy has been reported (238). This male patient was born in 1968 with ΔF508 on one allele and a stop mutation (G673X) on the other allele, which correspond to two allelic forms of *CFTR* that cause the CF disease. The patient exhibited symptoms since birth, including an infection by *Pseudomonas aeruginosa*. In April 1993 the patient developed fibrosarcoma on his left bicep which was treated by surgery, radiotherapy and chemotherapy with cyclophosphamide and epirubicin. After chemotherapy, it was discovered that his lung function improved (forced vital capacity of 89%) and he no longer needed physiotherapy. His *Pseudomonas aeruginosa* infection was also cleared. Normally once a patient is colonized with *Pseudomonas aeruginosa*, it is never cleared. However, the sweat test performed in January 1997 was still positive for CF. An RT-PCR study was performed to compare the mRNA expression of *MDR* and *MRP* in the nasal epithelial cells of this patient (patient A) versus another CF patient (patient B) that had never been exposed to chemotherapy drugs. The results showed that patient A definitely expressed *MDR* and *MRP* mRNAs in his nasal epithelial cells, while patient B did not express detectable levels. This suggests that *MDR* or *MRP* proteins might complement the defective CFTR function. Since P-gp has been shown to be a regulator of cell-swelling activated chloride channels (89-91), we propose that P-gp might complement the function of CFTR and that its expression is upregulated in the kidney of CF patients since CF kidneys do not exhibit major pathology.

There is evidence in the literature that CFTR expression is inversely-regulated with P-gp expression (92-94). CFTR and P-gp have been shown to have inverse patterns of epithelial expression in certain tissues both *in vitro* and *in vivo*. Breuer *et al.* (94) have shown in the human colon epithelial cell line HT-29 that increased protein expression of P-gp is associated with a corresponding decrease in CFTR protein expression and vice versa (Figure 1.3). Trezise *et al.* (92) have shown in mouse cells (e.g., intestine, uterus, pancreas) expressing *cftr* that *mdr1* mRNA expression cannot be detected and vice versa. They also observed a switch from *cftr* to *mdr1* mRNA expression in the rat uterine epithelium upon pregnancy. Trezise *et*

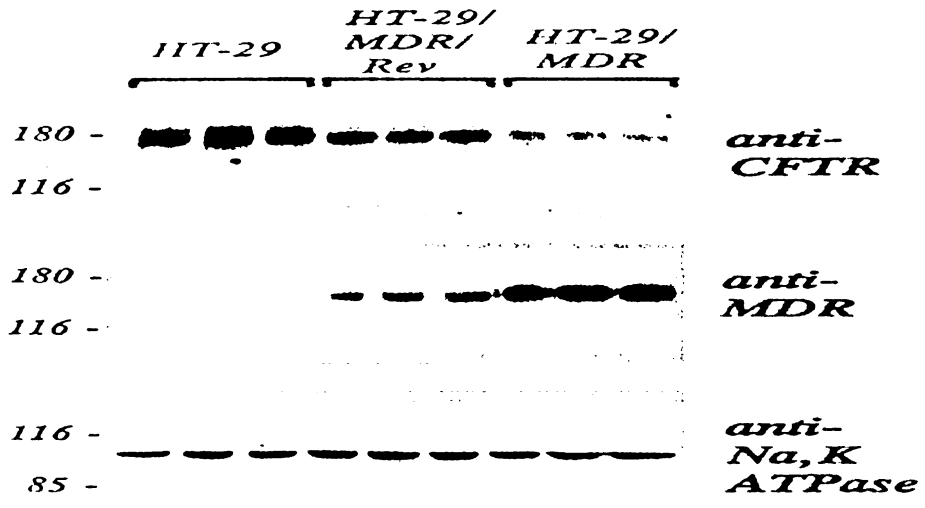

Figure 1.3 Inverse regulation of CFTR and P-gp expression in HT-29 cells. HT-29/MDR cells were grown in the presence of 300 ng/ml colchicine to induce P-gp expression. HT-29/MDR/Rev cells were HT-29/MDR cells that were maintained for 6-weeks in the absence of colchicine. Data from Breuer *et al.* (94).

al. (93) have also shown that in *cftr* neonatal and 3-4 week old knockout mice, *cftr* mRNA expression in the intestines was reduced 4-fold (it is not completely abolished due to a small read-through) while there is a corresponding 4-fold increase in *mdr1* mRNA expression and an intermediate level of *mdr1* mRNA in heterozygous mice (Figure 1.4).

The structural and functional similarities between CFTR and P-gp further support the hypothesis that P-gp expression might be upregulated in CF patients. Both CFTR and P-gp are members of the ABC transporter superfamily, they have similar structures and molecular weights and both proteins are located in the apical membrane of epithelial cells. The genes that encode the proteins are located in chromosome 7q (*CFTR* 7q.31, *MDR1* 7q.21) and have similar promoters (125). CFTR is a chloride channel while P-gp, besides acting as an efflux pump for xenobiotics, is also involved in modulating the function of cell-swelling activated chloride channels (89-91). Thus CFTR and P-gp are functionally related.

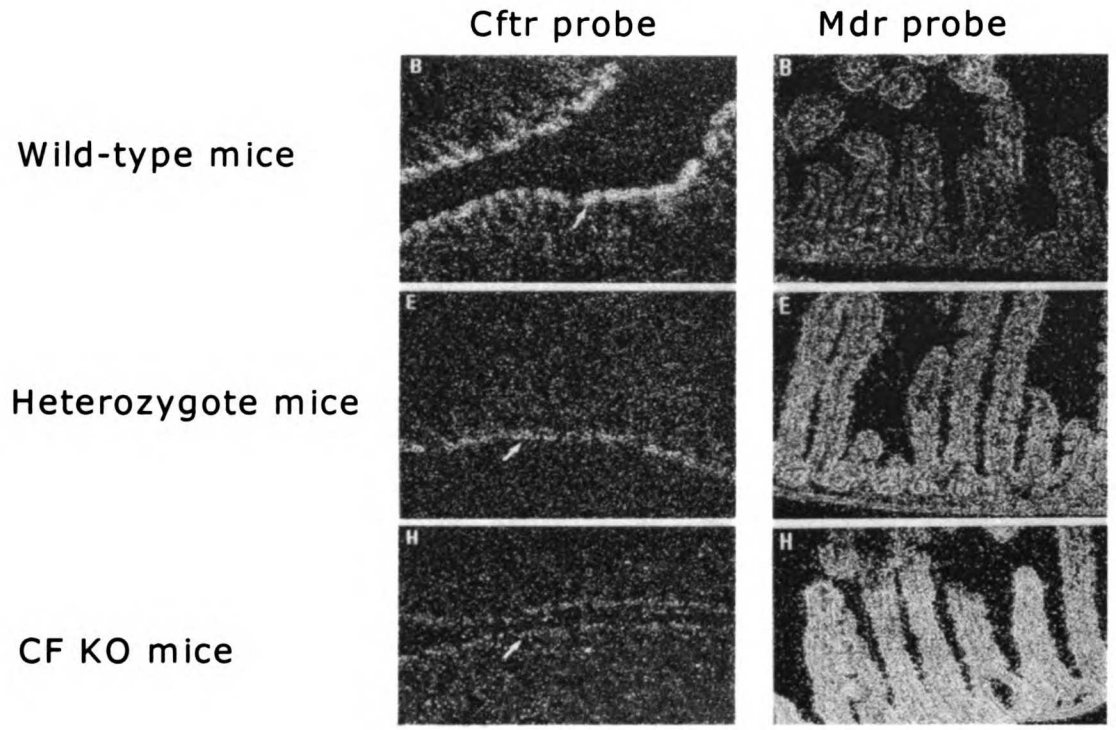

Figure 1.4 Inverse regulation of *cftr* and *mdr1* in the intestine of wild type, heterozygote and CF knockout mice. Data from Trezise *et al.* (93).

The coordinate regulation of P-gp and CFTR, the many similarities between the two proteins and their similar roles as regulators of chloride transport provide circumstantial evidence that these two proteins might have complementary roles. We hypothesize that the absence of CFTR in CF patients might be compensated for by upregulation of P-gp that in turn causes the enhanced renal clearance of drugs that are substrates of P-gp.

1.8 Specific Aims

The hypothesis that we are testing is whether enhanced renal clearance of several drugs observed in CF patients is due to increased expression of P-gp in those patients. To test this hypothesis, there are three specific aims:

1. To determine whether
    a) antibiotics that exhibit enhanced renal clearance in CF patients are substrates of P-gp (Chapter 2).
    b) To determine whether antibiotics that do not exhibit enhanced renal clearance in CF patients are not substrates of P-gp (Chapter 2).
2. To determine and compare the renal clearance of P-gp and non-P-gp substrates in wild type, P-gp and CF knockout mice and examine if there is a correlation between P-gp expression level and renal clearance values (Chapter 4).
3. To compare the amount of P-gp and CFTR expression in the kidney of wild type, P-gp and CF knockout mice and analyze if there is a correlation between P-gp and CFTR expression (Chapter 6).

Ideally, we would also like to compare P-gp expression levels in the CF *vs.* non-CF kidneys. However, that is not feasible since it requires biopsy samples from kidneys, which is a very invasive procedure. An alternative approach is to determine the expression level using kidneys from cadavers, but unfortunately we do not have access to CF kidneys. We hope that the hypothesis and works presented in this thesis will allow others with access to human kidney tissue to investigate differences in P-gp and CFTR expression between CF and normal patients, and aid in predicting whether or not a drug will have altered renal clearance in CF.

Chapter 2

In Vitro Bidirectional Transport Studies

2.1 Overview

Our hypothesis stated that enhanced renal clearance of some antibiotics observed in cystic fibrosis patients is due to elevated P-gp expression in those patients. Accordingly, antibiotics that show enhanced renal clearance in CF patients should be substrates of P-gp while those that do not should not be substrates of P-gp. Therefore we determined if antibiotics that have higher renal clearance in CF patients are indeed substrates of P-gp and whether those that do not, are not substrates of P-gp. This can be achieved by running a bidirectional transport study using control and P-gp overexpressing cell lines grown in a monolayer. *In vitro* bidirectional transport studies with P-gp overexpressing cell lines have been validated and accepted by many as a method to test if a compound is a substrate of P-gp. Utilizing this method, we will determine if several antibiotics that have a higher renal clearance value in CF patients are substrates of P-gp and those that do not have a higher renal clearance value are not substrates of P-gp.

2.2 *In Vitro* Cell Culture Model

2.2.1 Introduction

Cell culture is the growing of cells *in vitro*. Unlike the *in vivo* situation, they are no longer organized into tissues (239). Chambers and Kempton (240) were the pioneers of studying transport by epithelia using culture systems. They demonstrated secretion of phenol red into the lumen of tubules of chick embryo mesonephros in organ culture. Since then, there has been much evidence from studies with a number of epithelial cell lines, such as MDCK, LLC-PK1, Caco-2 and many other cell lines, that transepithelial transport occurs and can be studied in the cell culture systems (135, 241-251).

Epithelial cells form coherent cell sheets called epithelia, which line the inner and outer surfaces of the body. One of the most important functions of epithelia is to serve as the selective permeability barriers separating fluids (252). There are several ways a compound can get across epithelia. It can cross epithelia either by paracellular (between cells) or transcellular (across cell) routes. Passage by the paracellular route is minimized due to the presence of tight junctions. Tight junctions are located at the junction of apical and basolateral membranes. Only small hydrophilic molecules can pass between cells, unless a modulator of the tight junction is present. Transcellular passage can take place either by passive mechanisms or by specific carrier systems, which could be either passive or active. In order for a molecule to be able to passively cross both the apical and basolateral membranes (which are lipophilic) and diffuse through the cytoplasm, an aqueous solution separating the two membranes, the molecule must have the correct physiological properties such as size, charge, lipophilicity, hydrogen bonding potential and solution conformation (253). For molecules that do not possess such characteristics, there are carrier proteins or transporters that can help them get across. On both the apical and basolateral membranes, uptake transporters (e.g., OATs, OATPs, OCTs, OCTNs) are present that function to bring a molecule into cells or efflux transporters (e.g., P-gp, MRP1, MRP2, MRP3) that pump molecules out of cells.

For epithelial cells to perform their characteristic directional transport, epithelia in cultures must form membranes composed of similarly oriented cells (239). MDCK, LLC-PK1, Caco-2 and many other cell lines of diverse origin were shown to display just such characteristics. They all form a basolateral membrane that uniformly faces the supporting structure to which the cells are attached and grow upon, and they have an apical membrane that uniformly faces the medium (239). Physiologically the basolateral membrane is the side that is in contact with the blood vessels and the apical membrane is the side that is facing the lumen. Because the growth of most epithelial cells is attachment dependent, they need to attach to a surface to divide and grow. There are many types of materials upon which cells can grow: petri dish, collagen-coated petri dish, millipore filters, polycarbonate membrane, polyester membrane,

etc. The surface to which the cells are attached can affect the structure, function and expression of transporters and enzymes in those cells (239, 254-256). Cell culture conditions like the media, the number of times the cells have been passaged, the initial density of the cells on the growth surface and the stage of cellular differentiation could also have effects on the expression of transporters and enzymes (253, 257). Therefore, it is important to minimize the variations in the cell culture conditions.

2.2.2 Bidirectional transport study

In order to study the transport properties of epithelial cells, they should be grown on porous supports in a plate system, so that the solution on both the apical and basolateral side can be sampled and transepithelial electrical resistance (TEER) can be measured (258-260). Figure 2.1 shows the system we use for studying bidirectional transport. Epithelial cells are grown on top of the inserts and they formed polarized cells with the basolateral membrane facing down and the apical membrane facing up. The inserts are placed in a six-well plate. During the growth period, cell culture media is placed on both the wells of the six-well plate (referred to as the basolateral side) and on top of the insert (referred to as the apical side). During transport experiments, the solution containing the drug is put in either the basolateral (to measure B to A transport) or apical side (A to B transport) and a sample is taken from the opposite side at different time points. Drug concentrations in the samples are measured to determine drug flux in the B to A and A to B directions.

2.2.3 Transport study design

The objective of our studies is to determine whether or not the drugs of interest are substrates of P-gp, an efflux transporter that is located on the apical membrane of epithelial cells. It pumps compounds from the cells out into the apical solution. P-gp is located on the apical membrane of epithelial cells that line the gut lumen, bile ducts and kidney tubules and endothelial cells that line the blood-brain barrier (118). Physiologically P-gp functions to eliminate xenobiotics from the body since it pumps drugs out into the gut lumen, away from

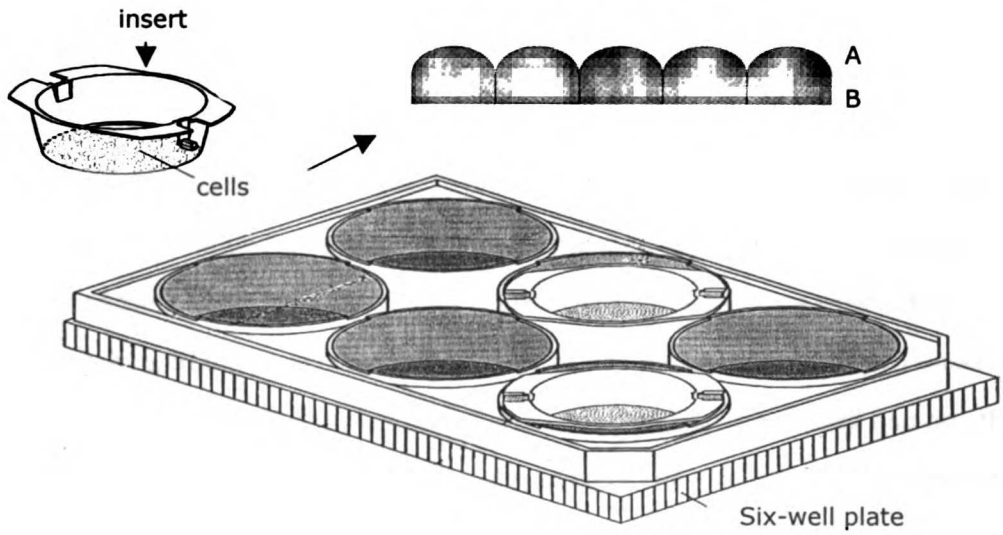

Figure 2.1 Cartoon representation of a cell culture transport study system. Adapted from the information sheet of Falcon Cell Culture Insert System (Becton-Dickinson, Franklin Lakes, NJ)

brain, into the bile and into the kidney lumen. In this project we focus on P-gp function in kidney tubules. It has been postulated that P-gp contributes to the renal clearance of some compounds that are substrates of P-gp by pumping the drugs from the cells out into the kidney lumen. We hypothesize that the enhanced renal clearance observed for some drugs in CF patients is due to enhanced P-gp expression in these patients. To test this hypothesis, we will determine if those drugs that show enhanced renal clearance are substrates of P-gp and if those that do not are not substrates of P-gp.

To determine if a drug is a substrate of P-gp or not, we utilize the *in vitro* cell culture model described above. A bidirectional transport study is performed with control and P-gp overexpressing cell lines. We measure and compare the flux of the drug in the B to A and in the A to B directions in both the control and the P-gp (or MDR1) overexpressing cell lines. Because P-gp is an efflux transporter that pumps drugs out from cells into the apical solution, for a P-gp substrate, the B to A flux should be greater than the A to B flux in both types of cell lines, with the difference more pronounced in the P-gp overexpressing cell line. The B to A

flux in the P-gp overexpressing cell line will be greater than the B to A flux in the control cell line and the A to B flux in the P-gp overexpressing cell line will be smaller than the A to B flux in the control cell line. If the test drug exhibits this pattern, we also conduct inhibition studies to further test if the drug is a substrate of P-gp. A P-gp inhibitor is dosed along with the drug and the drug flux in both directions is measured and compared with the drug flux in the absence of the inhbitor. P-gp inhibitors impede drug efflux from the cells out into the apical side, therefore, in the presence of P-gp inhibitors, the B to A flux will be decreased and the A to B will be increased. If complete inhibition of P-gp function is achieved and no other transporters are involved, the B to A flux should equal the A to B flux. The effect of P-gp inhibitors will be more pronounced on P-gp overexpressing than control cell lines since the P-gp overexpressing cell line has a greater flux difference between the B to A and A to B directions. Figure 2.2 shows a graphical representation of a typical bidirectional and inhibition study with a P-gp substrate.

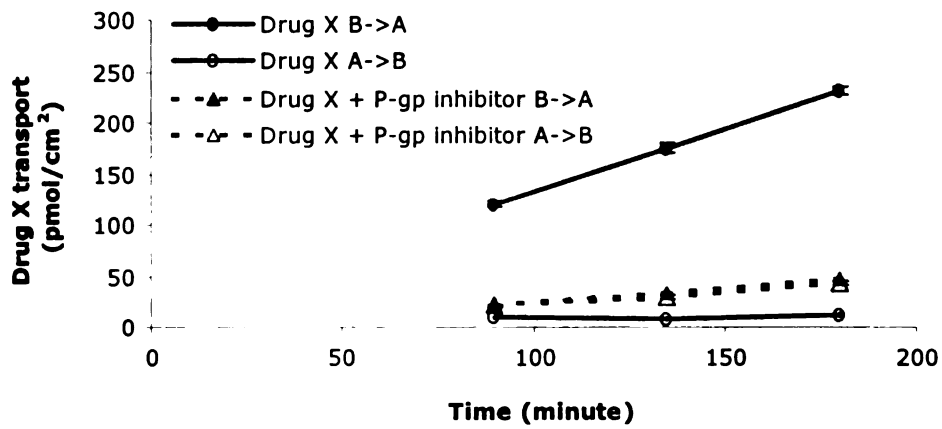

Figure 2.2 Graphical representation of the expected transport and inhibition study results with a P-gp substrate. Drug X = a hypothetical P-gp substrate. ●,▲= B→A and ○,△= A→B

Besides determining if a drug is a substrate of P-gp, we will also test if they are substrates of other multidrug resistance transporters that are closely related to P-gp, such as MRP1 and MRP2. Both MRP1 and MRP2 are efflux transporters like P-gp with the exception that MRP1 is located on the basolateral instead of the apical membrane (261). Therefore, the bidirectional transport profile of MRP2 substrates in control and MRP2 overexpressing cell lines will look just

like Figure 2.2 with the opposite results for MRP1 substrates. An MRP1 substrate will have a higher A to B flux compared to the B to A flux in both the control and the MRP1 overexpressing cell lines. The A to B flux in the MRP1 overexpressing cell line will be higher than the A to B flux in the control cell line and vice versa for the B to A flux.

2.2.4 MDR1, MRP1 and MRP2 overexpressing cell lines

Several P-gp overexpressing cell lines have been constructed: MDCK1-MDR1, MDCK2-MDR1, L-MDR1 and LLC-GA5-COL150 cells. These cell lines were created by transfecting the control cells: MDCK1, MDCK2, LLC-PK1 and LLC-PK1, with human *MDR1* cDNA. The MDCK1-MDR1 cell line was created by Drs. Ira Pastan and Michael Gottesman of the National Institutes of Health (135). MDCK2-MDR1 and L-MDR1 cell lines were created in the laboratory of Prof. Dr. Piet Borst of the Dutch Cancer Institute (262, 263) and LLC-GA5-COL150 cell line was created in the laboratory of Dr. Tanigawara from Kyoto University (264).

Several MRP1 and MRP2 overexpressing cell lines were constructed. MDCK2-MRP1 and L-MRP1 cell lines were created by transfecting the MDCK2 (262) and LLC-PK1 (265) cells, respectively, with human *MRP1* cDNA. MDCK2-MRP2 and L-MRP2 cell lines were created by transfecting the MDCK2 (266, 267) and LLC-PK1 (268) cells, respectively, with human *MRP2* cDNA.

All the control cell lines used for creating the overexpressing cell lines originated from the kidney. The LLC-PK1 cell line was originally derived in 1958 from an unknown site in the kidney of a normal male Hampshire pig (269). The MDCK (Madin-Darby Canine Kidney) cell line was originally derived in 1958 from a normal adult female cocker spaniel kidney by S.H. Madin and N.B. Darby (270). There are two strains of MDCK cells: strain I referred to as MDCK1 and strain II referred to as MDCK2. MDCK1 cells were from a lower passage number (60-70) while MDCK2 cells were from a higher passage number (>100). MDCK1 cells form tighter epithelia monolayers with high electrical resistance (4 $k\Omega cm^2$) while MDCK2 cells form leakier monolayers with low electrical resistance (70 Ωcm^2) (258, 259, 271-273).

2.2.5 Compounds chosen for transport studies

We chose several compounds to determine if they are substrates of P-gp. The criterias employed in choosing the compounds were whether or not they show enhanced renal clearance in CF patients and whether the pure compounds were obtainable. Table 2.1 lists the compounds tested in our studies and Figure 2.3 shows their structures. In 1975, dicloxacillin was the first drug observed to have enhanced renal clearance in CF patients (195). Later Hutabarat *et al.* (201) showed that the renal clearance of trimethoprim was increased in CF patients while no change was observed for sulfamethoxazole. N4-acetylsulfamethoxazole is a metabolite of sulfamethoxazole catalyzed by N-acetyltransferase. The formation clearance of N4-acetylsulfamethoxazole was increased in CF patients. Arvidsson *et al.* (196) showed that the renal clearance of cefsulodin was not different between controls and CF patients. However, Hedman *et al.* (206) observed a difference in cefsulodin renal clearance in CF patients. This difference was due to enhanced glomerular filtration rate in those patients instead of increased tubular secretion. Ciprofloxacin had shown conflicting results. One IV dose study showed that the renal clearance was not difference between controls and CF patients (217) while another IV study showed a difference (232). Iothalamate was a marker of glomerular filtration and its clearance was not different between controls and CF patients (199).

2.3 Materials and Methods

2.3.1 Materials

The following materials were utilized: MDCK1, MDCK1-MDR1 (a gift from Dr. Ira Pastan of the National Institutes of Health), MDCK2, MDCK2-MDR1, MDCK2-MRP2, LLC-PK1, L-MRP1 and L-MDR1 cell lines (a gift from Prof. Dr. Piet Borst of the Dutch Cancer Institute), DME-H21 media, M-199 media, fetal bovine serum, phosphate buffered saline (PBS) Ca^{2+}, Mg^{2+}-free solution, Hank's BSS buffer, 0.25% trypsin (UCSF Cell Culture Facility, San Francisco, CA), colchicine, HEPES, trimethoprim, sulfamethoxazole, aztreonam, cefsulodin, dicloxacillin, vinblastine, cyclosporine, ketoconazole, para-amino hippurate, verapamil, tetra-ethyl ammonium, quinidine, sulfinpyrazone, indomethacin, probenecid, glycyl-sarcosine (Sigma, St.

Table 2.1 List of drugs chosen for transport studies and their renal clearance values in controls and cystic fibrosis patients

Drugs	Renal Clearance (ml/min/1.73m^2)		References
	Cystic Fibrosis	Controls	
Dicloxacillin[a,g]	282 ± 135	95 ± 28	195
Trimethoprim[a,b,h]	126 ± 30	82 ± 19	201
Sulfamethoxazole[b,h]	2.2 ± 1.7	3.1 ± 1.3	201
N4-acetyl-sulfamethoxazole	NA	NA	201
Cefsulodin[h]	140 ± 34	141 ± 36	196
Cefsulodin[c,h]	122 ± 19	92 ± 18	206
Cefsulodin[c,h]	118 ± 16	89 ± 5	206
Ciprofloxacin[d,h]	313 ± 121	309 ± 55	217
Ciprofloxacin[a,h]	464 ± 136	232 ± 92	232
Ciprofloxacin[g]	311 ± 143	253 ± 131	232
Ciprofloxacin[e,g]	282 ± 163	232 ± 12	225
Ciprofloxacin[f,g]	522 ± 176	396 ± 139	216
Iothalamate[h]	148 ± 29	143 ± 33	199

a = statistically significant difference from control, $P < 0.05$.
b = converted from L/h/kg.
c = increased CLr in CF is due to increased GFR.
d = converted from L/h.
e = units in ml/min
f = converted from ml/min
g = oral dose
h = IV dose
NA = not available

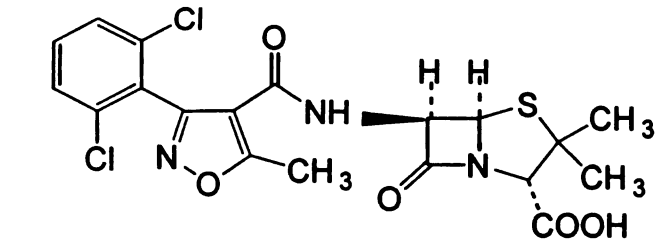

Dicloxacillin

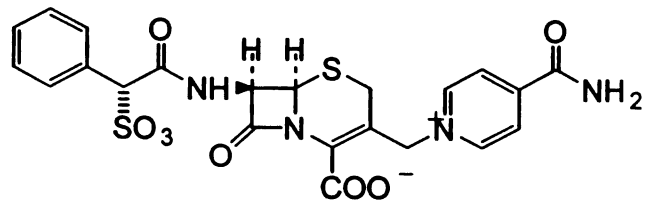

Cefsulodin

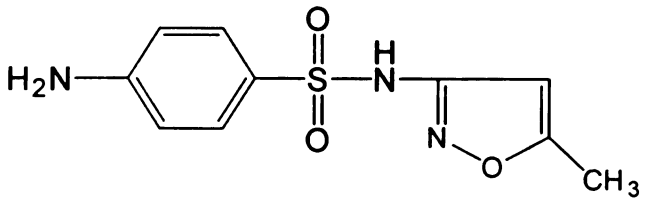

Sulfamethoxazole

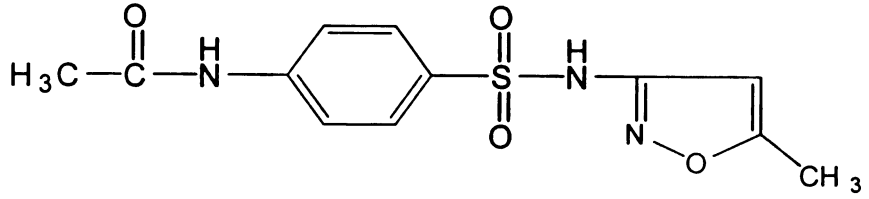

N4-acetylsulfamethoxazole

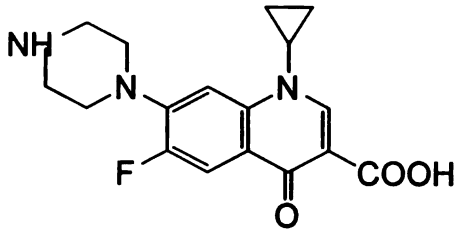

Ciprofloxacin

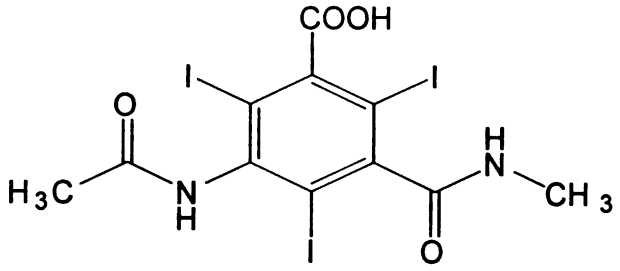

Iothalamic acid

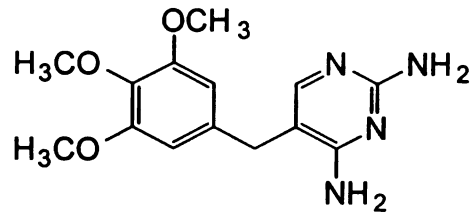

Trimethoprim

Figure 2.3 Structures of compounds chosen for transport studies

Louis, MO), N4-acetyl-sulfamethoxazole (Frinton Laboratories, Vineland, NJ), iothalamate (US Pharmacopeia, Rockville, MD), ciprofloxacin (a gift from Bayer, West Haven, CT), GG918 or GF120918 (a gift from Glaxo-Wellcome, Research Triangle Park, NC), Econo-Safe biodegradable counting cocktail (Research Product International Corp., Mount Prospect, IL), T75 culture flasks, PET cell culture inserts for six-well plate, 15 and 50 ml Falcon tubes (Becton Dickinson, Franklin Lakes, NJ), Falcon 2 ml aspirating pipets, 5, 10, 25 ml non-pyrogenic serological pipets, disposable cell scraper, hematocytometer, glass covers, disposable 16x125 mm borosilicate glass culture tubes (Fisher Scientific, Santa Clara, CA), Kimwipes EX-L (Kimberly-Clark, Roswell, GA), six-well plates (Corning, Corning, NY), inverted microscope TMS (Nikon Corp., Tokyo, Japan), CO_2 incubator (Revco Scientific, Asheville, NC), CO_2 (Praxair, Danbury, CT), Pipet-Aid (Drummond Scientific Company, Broomal, PA), Laboratory vacuum pump and compressor (KNF Neuberger Inc., Trenton, NJ), Baker SterilGARD Biological Safety Cabinet model SGII-400 (The Baker Company Inc., Sanford, ME), Millicell-ERS Transepithelial resistance measurement system (Millipore, Bedford, MA), Incubator Shaker II model 136400 (Boekel Scientific, Feasterville, PA), Mettler AE240 balance (Mettler-Toledo Inc., Columbus, OH), [^{14}C]-mannitol, [^{3}H]-digoxin (NEN, Boston, MA), [^{3}H]-vinblastine (Amersham, Piscataway, NJ), Laemmli sample buffer, dry milk, filter paper, nitrocellulose membrane, prestained SDS-PAGE broad range standard, 7.5% SDS-PAGE gel, 10X Tris/Glycine/SDS running bufer (Bio-Rad, Hercules, CA), ECL reagents, Hyperfilm (Amersham, Piscataway, NJ), bovine serum albumin (Gibco BRL Life Technologies, Grand Island, NY), RedTaq ReadyMix PCR Reaction Mix (Sigma, St. Louis, MO), X Systems centrifuge (Abbott Laboratories, Abbott Park, IL), human P-gp (S) and (AS) primers (Invitrogen Life Technologies, Carlsbad, CA), Pipetman (Rainin, Woburn, MA), Fisher Vortex Genie 2 (Fisher Scientific, Santa Clara, CA), ART RNase & DNase free tips (Molecular BioProduct, San Diego, CA), PCR Express (Thermo Hybaid, Ashford, Middlesex, United Kingdom), 0.2 ml PCR tubes (Ambion, Austin, TX) and Fisher Minifuge (Fisher Scientific, Santa Clara, CA).

2.3.2 Cell culture conditions

MDCK1, MDCK1-MDR1, MDCK2, MDCK2-MDR1, MDCK2-MRP2, LLC-PK1, L-MRP1 and L-MDR1 cells were seeded onto PET cell culture inserts of a 6-well plate system at a density of roughly

300,000 cells/insert. The growth media for MDCK1, MDCK1-MDR1, MDCK2 and MDCK2-MDR1 cells was Dulbecco's Modified Eagle's Medium (DMEM) supplemented with 10% fetal bovine serum (FBS) while LLC-PK1, L-MRP1 and L-MDR1 cells were grown in M-199 media supplemented with 10% FBS. For all cells that were transfected with the MDR1 gene, 80 ng/ml colchicine was added to the media to select for the transfectant cells. The cells were grown to confluency as a monolayer for 5-7 days at 37°C and 5% humidified CO_2-atmosphere. The media was changed every 2-3 days.

2.3.3 Characterization of cell lines

Cell integrity and monolayer confluency were tested by microscopy and transepithelial electrical resistance (TEER) measurements. On the day of the experiments, the culture media was removed and the cells were incubated for ~30 minutes in Hanks' buffer solution containing 22.5 mM Hepes. After equilibration, TEER values were measured using the Millicell-ERS Transepithelial resistance measurement system (Millipore, Bedford, MA). To compare P-gp, MRP1 and MRP2 expression in our cell lines, Western blot and RT-PCR were performed.

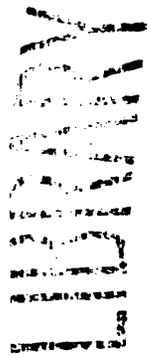

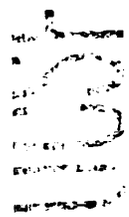

2.3.4 Western blot

Table 2.2 lists the recipes for preparing Western blot solutions. For Western blot, cells were grown in T75 flasks, rinsed with PBS Ca^{2+}, Mg^{2+}-free solution and scraped into 15 ml Falcon tubes. The tubes were centrifuged for 15 minutes at 1600 rpm (<6000 g) at 4°C. The supernatants were discarded and the pellets were washed again with PBS Ca^{2+}, Mg^{2+}-free solution and centrifuged again. The pellets were resuspended using lysis buffer pH 7.4 (10 mM KCl, 10 mM Tris-HCl, 1.5 mM $MgCl_2$). They were put on ice and sonicated for 20s (3x). The protein concentrations were determined by BioRad assay with bovine serum albumin as the standard. All samples were diluted to the same concentration and mixed with Laemmli sample buffer (1:3) and loaded onto 7.5% SDS-PAGE gels. The gels were run at 200 V for ~45 minutes. Before blotting the gels, they were incubated with blotting buffer for 15 minutes at 4°C. The gels were blotted to nitrocellulose membranes for 1 hour at 200 mA. Then the membranes were incubated for 2 hours at room temperature with 5% dry milk solution in

TBS. After that the membranes were washed with TTBS. Depending on the proteins of interest, the membranes were incubated overnight with either 50x diluted anti-MRP1 clone MRPr1 antibody (MC-201, Kamiya Biomedical, Seattle, WA), 500x diluted c219 (for detecting P-gp) antibody (Signet, Dedham, MA) or 50x diluted anti-MRP2 clone M2 III-6 (MC-206, Kamiya Biomedical, Seattle, WA). The next day, the membranes were washed several times with TTBS before incubating them for 1 hour at RT with their appropriate secondary antibody (3000x diluted goat anti-mouse (Gibco BRL Life Technologies, Grand Island, NY) for c219 and anti-MRP2 antibodies and goat anti-rat (Boehringer-Mangelheim, Indianapolis, IN) for anti-MRP1 antibody. The membranes were washed several times with TTBS and incubated with premix ECL reagent 1 & 2 for 1 min before developing the film.

Table 2.2 Recipes for Western blot solutions

Name of solution	Components	Amount	Final Concentration
Blotting buffer (store at 4°C)	Tris	3.03 g	25 mM
	Glycine	14.4 g	192 mM
	Methanol	200 ml	20% (v/v)
	DDI water	to make 1 L solution	
Running Buffer	10x Bio-Rad Tris/Glycine/SDS	100 ml	1X
	DDI water	to make 1 L solution	
Tris-buffered solution (TBS)	Tris	4.87 g	20 mM
	NaCl	58.44 g	0.5 M
	Concentrated HCl	to adjust pH to 7.4	to adjust pH to 7.4
	DDI water	to make 2 L solution	
Tween-TBS (TTBS)	Tween-20	0.5 ml	0.05% (v/v)
	TBS	to make 1 L solution	

2.3.5 RT-PCR

2.3.5.1 Primer design

To compare P-gp expression in our cell lines, we need to design primers for the human *MDR1* gene. Table 2.3 lists the exact sequences of the primers for the *MDR1* gene. This primer pair produces a 285 bp segment of the *MDR1* gene. For internal standard, we utilized the *18S*

Table 2.3 Primer sequences for *MDR1* gene

Primer Name	Sequences
Human P-gp primer (S)	5'-GCC TGG CAG CTG GAA GAC AAA TAC ACA AAA T-3'
Human P-gp primer (AS)	5'-AGA CAG CAG CTG ACA GTC CAA GAA CAG GAC T-3'

gene with the competimer technology from Ambion (Austin, TX). The expected product of the 18S gene is 489 bp.

2.3.5.2 One step semi-quantitative RT-PCR

The cells were rinsed in PBS Ca^{2+} Mg^{2+} free solution and RNA isolation was done according to the protocol outlined in TRIzol (Invitrogen Life Technologies, Carlsbad, CA). We performed the cDNA synthesis and PCR reaction in one step using the Qiagen OneStep RT-PCR Reaction Kit (Qiagen, Valencia, CA). The protocol is as outlined below:

1. RNA isolation and quantitation.
2. Preparation of RT-PCR reaction mix. Always prepare one extra reaction volume to account for pipetting loss. Table 2.4 lists the recipe for one reaction volume.

Table 2.4 RT-PCR reaction mix recipe for one reaction volume

Reagents	Volume (μl)	Final Concentration
Qiagen OneStep 5X buffer	10	1.25X
10 mM Qiagen OneStep dNTP Mix	2	0.4 mM
Qiagen OneStep Enzyme Mix	2	5% (v/v)
10 μM human P-gp primer (S)	3	0.75 μM
10 μM human P-gp primer (AS)	3	0.75 μM
Ambion 18S primer	0.5	1.25% (v/v)
Ambion 18S competimer	4.5	11.25% (v/v)
water	15	
total volume	40	

3. Aliquot 40 μl of solution from the master mix to a 0.2 ml PCR tube

4. Add 10 µl of 50 µg/ml RNA sample to each PCR tube

5. Vortex mix, briefly centrifuge and run the reactions in the PCR Express at:

50°C for 30 min

95°C for 15 min

94°C for 1 min ┐
59°C for 1 min ├ 26 cycles
72°C for 1 min ┘

72°C for 15 min

6. Run the RT-PCR products on 2% E-gel. Prerun the 2% E-gel at 66 V for 2 min with the comb on. After that, remove the comb, load 12 µl H_2O and 10 µl PCR product into each well, load 20 µl of 50 fold-diluted 50 bp DNA ladder into one well. Run the gel at 66 V for 30 min. The bands are visualized with the UV transilluminator and a picture is taken with a Polaroid camera.

2.3.6 Transport study protocol

The transport experiments were adapted with modifications from Zhang *et al.* (248). Most experiments were repeated at least twice and there were triplicates in each study. To determine if a drug is a substrate of P-gp, MRP1 or MRP2, bidirectional transport studies were performed in both the controls and P-gp, MRP1 or MRP2 overexpressing cell lines. The day before the transport studies, all cells were fed fresh media. On the day of the experiments, the cells were washed once and preincubated for ~30 minutes at 37°C in 5% CO_2 with Hank's Balanced Salt Solution containing 22.5 mM HEPES (HBSS-H). Drugs were dissolved in HBSS-H solution. To measure drug transport in the B→A direction, 2.5 ml of HBSS-H solution containing the drug was put into the basal (B) side and 1.5 ml of HBSS-H was put into the apical (A) side. At selected time points, 200 µl samples were taken from the A side and replaced with fresh HBSS-H. For measuring drug transport in the A→B direction, the drug solution was put into the A side and samples were taken from the B side. For inhibition studies, the inhibitor was put in both the A and B sides. During the studies, the cells were incubated in a shaking incubator at 37°C. To establish cell integrity, [^{14}C]-mannitol (a

paracellular marker) transport was measured for 1 hour at the end of the experiments. Transport of [^{3}H]-digoxin and [^{3}H]-vinblastine, known P-gp substrates, were also measured as positive controls.

We used the lowest concentration possible for the transport study and the drug concentrations were chosen in part based on what can be detected by HPLC for the A→B flux. The inhibitor concentrations were chosen based on concentrations used in published studies by other investigators.

2.3.7 Analytical methods

Samples were stored at -20°C until analysis by high performance liquid chromatography (HPLC) using methods adapted from Jehl *et al.* (274). Cefsulodin, dicloxacillin and trimethoprim were analyzed using an Ultrasphere ODS 150x2 mm (Phenomenex, Torrance, CA) column; sulfamethoxazole was analyzed with an Ultracarb ODS 150x4.6 mm (Phenomenex, Torrance, CA) column; ciprofloxacin, iothalamate and N4-acetyl-sulfamethoxazole were analyzed using a Zorbax SB-C18 250x4.6 mm (Phenomenex, Torrance, CA) column. The flow rate was 0.25 ml/min for cefsulodin, dicloxacillin and trimethoprim, 0.5 ml/min for sulfamethoxazole, 1 ml/min for ciprofloxacin, iothalamate and N4-acetyl-sulfamethoxazole. The organic mobile phase for cefsulodin, dicloxacillin, trimethoprim and sulfamethoxazole was acetonitrile (5 to 70% in 14.5 minutes for cefsulodin and dicloxacillin, 5 to 70% in 7 minutes for sulfamethoxazole and 20% isocratic for trimethoprim). The organic mobile phase for ciprofloxacin, iothalamate and N4-acetyl-sulfamethoxazole was methanol (50% isocratic). The aqueous mobile phases for cefsulodin, dicloxacillin, trimethoprim, sulfamethoxazole, ciprofloxacin and iothalamate (or N4-acetyl-sulfamethoxazole) were 5 mM tetrabutylammonium bromide (pH 3.7), 20 mM ammonium acetate (pH 5.8), 100 mM KH_2PO_4 (pH 2.7), 0.1% triethylamine (pH 5.9), 0.5% glacial acetic acid and 0.5% glacial acetic acid+0.25% triethylamine, respectively. Cefsulodin, dicloxacillin and trimethoprim were detected at 214 nm, iothalamate and N4-acetyl-sulfamethoxazole at 254 nm, sulfamethoxazole at 270 nm and ciprofloxacin at 280 nm.

2.3.8 Data analysis

The total amount of drugs transported into the other side was calculated according to the following formula:

$$\frac{\text{measured sample concentration X volume on sampling side}}{\text{cell growth area}}$$

In our studies the cell growth area was 4.2 cm^2. For transport in the B to A direction, the samples were taken from the A side which has a total volume of 1.5 ml. For transport in the A to B direction, the samples were taken from the B side which has a total volume of 2.5 ml.

In our studies, multiple samples were taken at different time points. To keep the volume of the sampling side constant, we replaced it with an equal volume of buffer solution. This will slightly decrease the actual concentration of measured sample concentration hence underestimating the total amount of drugs transported for the subsequent time points. Therefore, to account for the losses of amount transported due to sampling, we added the amount of drug lost in the previous sampling volumes to the above calculation to get an accurate total amount of drugs transported to the other side for subsequent time points.

Drug flux was calculated using the LINEST function from Microsoft Excel. The LINEST function calculated the slope of the line that best fits the amount of drugs transported *vs.* time plot. Flux values were calculated for each of the triplicates and were averaged to give us the average value of the flux and the standard deviation associated with it.

The apparent permeability value was calculated as follows:

$$P_{app} \pm SD\ (cm/s) = \frac{\text{average flux} \pm SD}{\text{dosing concentration}}$$

Statistical significance was tested by ANOVA using the Primer Express program created by Dr. Stanton Glantz (UCSF, San Francisco, CA).

2.4 Results of Transport Studies

2.4.1 Characterization of cell lines

Before conducting each transport study, cell integrity and monolayer confluency were confirmed by microscopy and transepithelial electrical resistance (TEER) measurements. Under the microscope, P-gp, MRP1 and MRP2 overexpressing cell lines (e.g., MDCK1-MDR1, MDCK2-MDR1, MDCK2-MRP2, L-MRP1, L-MDR1) appeared to have different morphologies compared to their respective control cell lines. MDCK1-MDR1 and L-MRP1 cells grew faster than their control cell lines, MDCK1 and LLC-PK1 cells, respectively. They also had higher TEER values. The average TEER values for MDCK1, MDCK1-MDR1, LLC-PK1 and L-MRP1 were 150, 1500, 165 and 240 Ω, respectively. However, TEER value measurement is not very accurate and precise. There were large variations associated with the values. Furthermore, for many cell lines such as MDCK1, MDCK2, MDCK2-MDR1, LLC-PK1 and L-MDR1, TEER values were very close to the values measured in the absence of any cells (~140 Ω). Therefore, to further monitor cell integrity and monolayer confluency, at the end of the experiments, we also measured [^{14}C]-mannitol (a paracellular marker) transport for 1 hour. As expected, we did not find any significant difference in the B to A and A to B transport of mannitol in our cell lines. Unlike TEER values, we also did not find large variations in the P_{app} of mannitol between controls and overexpressing cell lines. For example, there was about a 10-fold difference in TEER values between MDCK1 and MDCK1-MDR1 cells (~150 and 1500 Ω, respectively) but the P_{app} values for mannitol in those two cell lines were approximately the same (~5×10^{-7} cm/s). The mannitol P_{app} values in MDCK2, MDCK2-MRP2 and MDCK2-MDR1 cells are similar to MDCK1 and MDCK1-MDR1 cells. They are higher in LLC-PK1, L-MDR1 and L-MRP1 cells (~13×10^{-7}, 12×10^{-7} and 35×10^{-7} cm/s, respectively).

We also performed Western blot and RT-PCR studies to compare the expression of P-gp/*MDR1*, MRP1 and MRP2 among our cell lines. Figure 2.4 shows the result of an RT-PCR experiment to compare the expression of MDR1 mRNA among various cell lines. *18S* is the internal standard. As expected, expression of *MDR1* mRNA is much higher in P-gp overexpressing cell lines, MDCK1-MDR1 and MDCK2-MDR1 cells, compared to their control cell lines, MDCK1 and

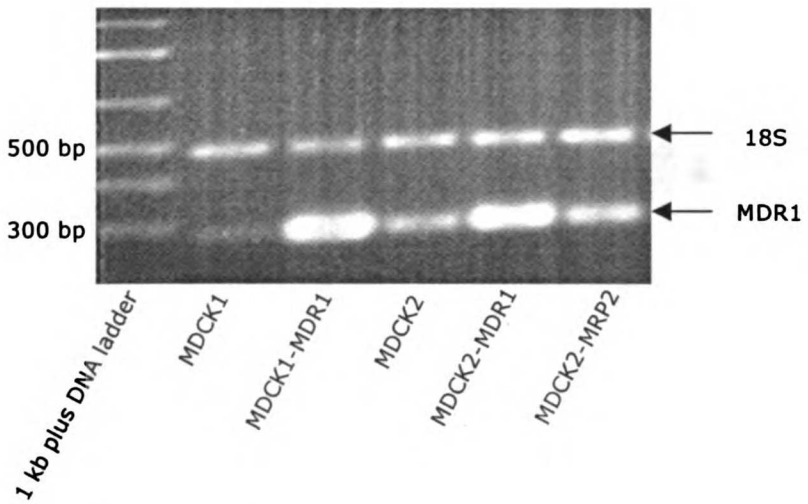

Figure 2.4 RT-PCR results of MDR1 mRNA comparison in several cell lines

MDCK2 cells, respectively. The results also show that the expression of *MDR1* mRNA is higher in MDCK2 cells compared to MDCK1 cells.

Figure 2.5 shows the Western blot results of P-gp expression comparison among various cell lines. The molecular weight of P-gp is around 170 kDa. Western blot results agree with the observations from RT-PCR studies (Figure 2.4). P-gp expression is higher in P-gp overexpressing cell lines, MDCK1-MDR1, MDCK2-MDR1 and L-MDR1 cells, compared to their control cell lines, MDCK1, MDCK2 and LLC-PK1 cells, respectively. The results also show that P-gp expression is higher in MDCK2 compared to MDCK1 or LLC-PK1 cells.

Figure 2.6 shows the Western blot results of MRP1 expression comparison among various cell lines. The molecular weight of MRP1 is around 190 kDa. As expected, MRP1 expression is much higher in the MRP1 overexpressing cell line, L-MRP1 cells, compared to its control cell line, LLC-PK1 cells, where MRP1 expression is not observed. The identity of the abundant lower band is not known but we think it could be the unglycosylated form of MRP1 protein. The results also show that MRP1 expression is similar in MDCK1, MDCK1-MDR1, MDCK2 and MDCK2-MDR1 cells.

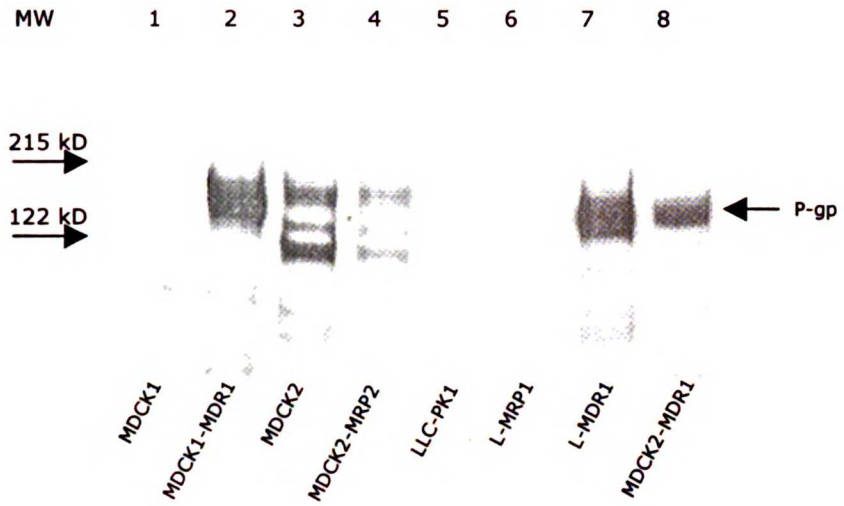

Figure 2.5 Western blot results of P-gp expression comparison among various cell lines

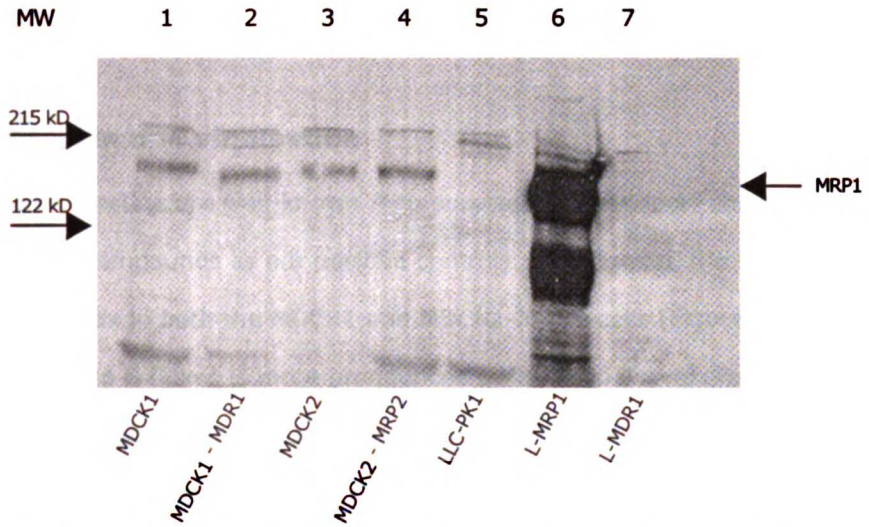

Figure 2.6 Western blot results of MRP1 expression comparison among various cell lines

Figure 2.7 shows the Western blot results of MPR2 expression comparison among various cell lines. The molecular weight of MRP2 is around 190 kDa. MRP2 expression is much higher in the MRP2 overexpressing cell line, MDCK2-MRP2 cells, compared to its control cell line, MDCK2 cells. It is interesting that no MRP2 expression is detected in a P-gp overexpressing cell line, MDCK1-MDR1 cells, which suggests that MRP2 expression is downregulated in that cell line, versus its control, MDCK1 cells. However, no downregulation of MRP2 expression is observed in another P-gp overexpressing cell line, the L-MDR1 cells.

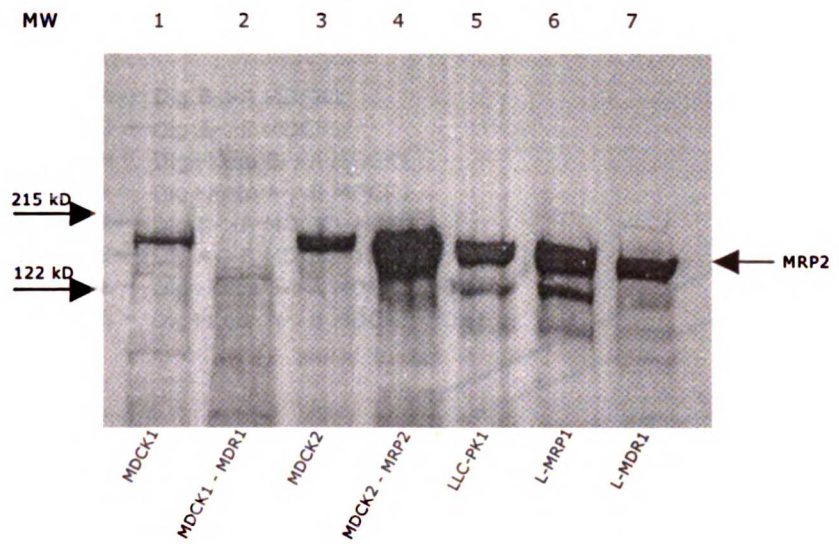

Figure 2.7 Western blot results of MRP2 expression comparison among various cell lines

2.4.2 Digoxin and vinblastine

Digoxin and vinblastine are well-known P-gp substrates. Transport studies were conducted using these two compounds as our positive controls. For digoxin, the B to A flux is higher than the A to B flux in both the MDCK1 and MDCK1-MDR1 cells (Figure 2.8). The difference in the B to A and A to B fluxes is more pronounced in the P-gp overexpressing cell line. The B to A/A to B ratio is about 7 in MDCK1 cells and about 35 in MDCK1-MDR1 cells (Table 2.5). In the presence of a P-gp inhibitor, ketoconazole, the digoxin B to A flux goes down and the A to B flux goes up in both the control and P-gp overexpressing cell lines (Figure 2.8). In the presence of ketoconazole, the B to A/A to B ratios of digoxin decrease to about 1 in both cell lines (Table 2.5). These are the classic patterns observed with a P-gp substrate. Therefore, digoxin is a substrate of P-gp, as reported previously in the literature (264, 275-279).

We also performed bidirectional transport studies of digoxin in LLC-PK1, L-MRP1 and L-MDR1 cells. The B to A flux is higher than the A to B flux in all three cell lines (Figure 2.9). However, there is not much difference in the B to A fluxes among those three cell lines (Table 2.6). There is also not much difference in the A to B fluxes between LLC-PK1 and L-MRP1 cells but the A to B transport is much lower in the L-MDR1 cells. The B to A/A to B ratio is about 3

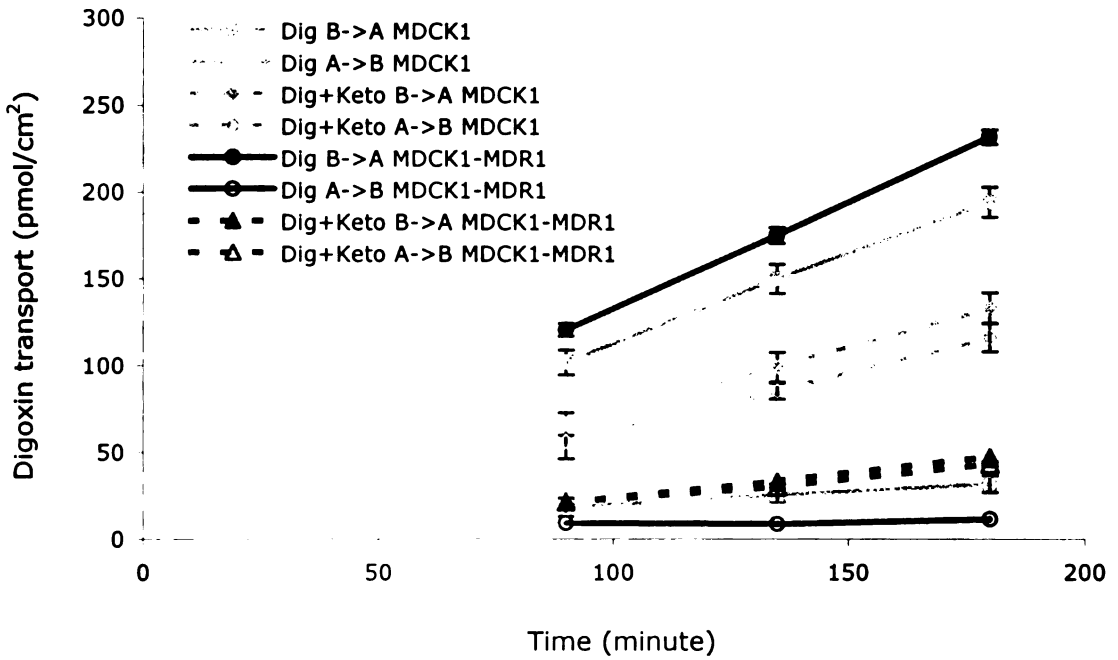

Figure 2.8 Bidirectional transport of 5 μM digoxin with and without 100 μM ketoconazole in MDCK1 (gray line) and MDCK1-MDR1 (black line) cells. ■,◆,●,▲= B→A and □,◇,○,△= A→B

Table 2.5 Bidirectional transport of 5 μM digoxin with and without 100 μM ketoconazole in MDCK1 and MDCK1-MDR1 cells.

Cell Line	Inhibitor	P_{app} x 10^{-7} (avg ± SD, n=3, cm/s)		B→A / A→B
		B→A	A→B	
MDCK1	-	35.6 (1.1)	5.0 (0.3)	7.2
	ketoconazole	26.4 (1.7)	23.7 (1.4)	1.1
MDCK1-MDR1	-	42.6 (0.6)	1.2 (0.5)	34.7
	ketoconazole	10.2 (0.5)	8.3 (0.7)	1.2

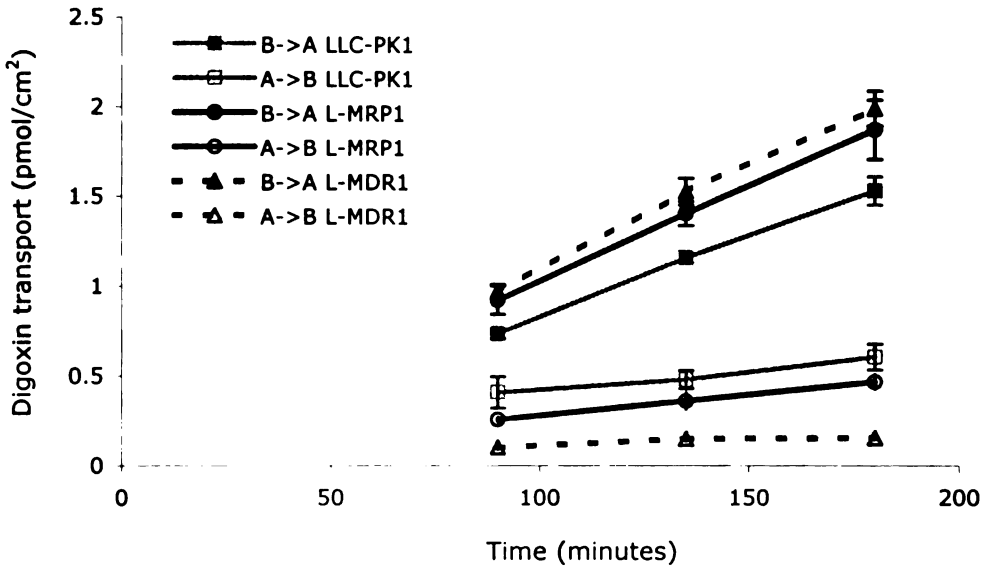

Figure 2.9 Bidirectional transport of 30 nM digoxin in LLC-PK1 (gray line), L-MRP1 (black line) and L-MDR1 (dashed line) cells. ■,●,▲= B→A and □,○,△= A→B

Table 2.6 Bidirectional transport of 30 nM digoxin in LLC-PK1, L-MRP1 and L-MDR1 cells

Cell Line	P_{app} x 10^{-7} (avg ± SD, n=3, cm/s)		B→A / A→B
	B→A	A→B	
LLC-PK1	49.2 (5.9)	15.1 (1.6)	3.2
L-MRP1	58.7 (5.4)	13.0 (1.8)	4.5
L-MDR1	62.9 (4.3)	2.9 (0.3)	22

in LLC-PK1, about 4 in L-MRP1 and about 22 in L-MDR1 cells (Table 2.6). The conclusion from these data is that digoxin is not a substrate of MRP1 but it is a substrate of P-gp. The bidirectional transport study result using LLC-PK1 and L-MDR1 cells agrees with that in MDCK1 and MDCK1-MDR1 cells.

As mentioned earlier, vinblastine is also a well-known P-gp substrate. For vinblastine, the B to A fluxes are larger than the A to B fluxes in LLC-PK1, L-MRP1 and L-MDR1 cells (Figure 2.10).

The B to A/A to B ratios are about 3-4 for all three cell lines (Table 2.7). Interestingly, there is no difference in the B to A and in the A to B fluxes among those three cell lines. These data could lead one to suggest that vinblastine is not a substrate of either MRP1 or P-gp. However, from literature data we know that vinblastine is a substrate of P-gp. Furthermore, preliminary transport studies performed in MDCK1 and MDCK1-MDR1 cells show differences between the B to A and the A to B fluxes in those two cell lines (data not shown).

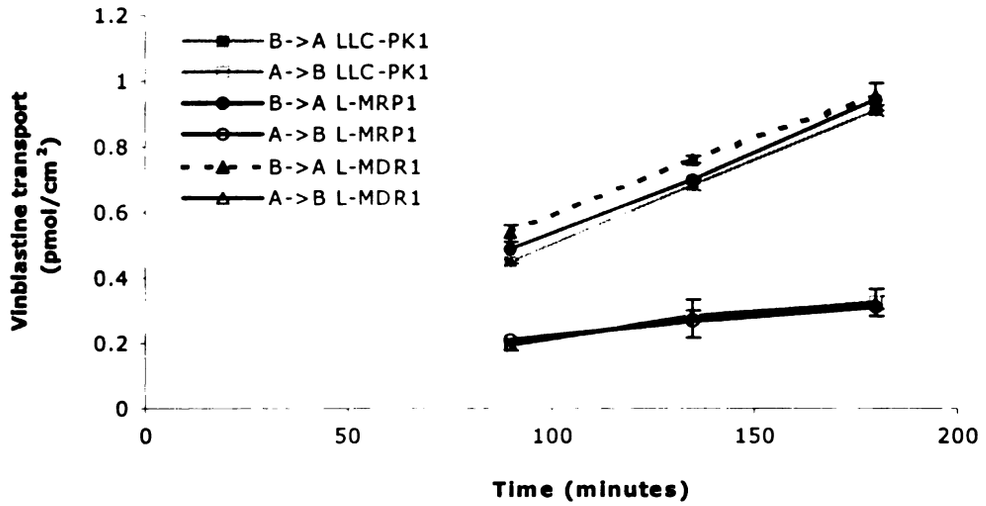

Figure 2.10 Bidirectional transport of 30 nM vinblastine in LLC-PK1 (gray line), L-MRP1 (black line) and L-MDR1 (dashed line) cells. ■,●,▲= B→A and □,○,△= A→B

Table 2.7 Bidirectional transport of 30 nM vinblastine in LLC-PK1, L-MRP1 and L-MDR1 cells

Cell Line	P_{app} x 10^{-7} (avg ± SD, n=3, cm/s)		B→A / A→B
	B→A	A→B	
LLC-PK1	28.3 (1.4)	7.7 (0.9)	3.7
L-MRP1	28.1 (1.1)	5.9 (0.3)	4.7
L-MDR1	25.6 (1.2)	8.0 (1.7)	3.2

Currently we do not know the cause of the discrepancies observed for vinblastine (but not digoxin) between MDCK1, MDCK1-MDR1 and LLC-PK1, L-MDR1 cells. Our Western blot results show that total P-gp expression is comparable between MDCK1-MDR1 and L-MDR1 cells (Figure 2.5). But it is possible that not all the P-gp observed in the Western blot is located on

the apical membrane or is functionally active. Another possibility could be that L-MDR1 cells express other transporters that are missing in MDCK1-MDR1 cells.

We concluded that LLC-PK1 and L-MDR1 cell lines might not be the right cell lines to use to determine if a drug is a substrate of P-gp. Therefore, to determine whether a drug is a substrate of P-gp or not, we chose to use the MDCK1 and MDCK1-MDR1 cell lines. However, we will also conduct transport studies using the other two P-gp overexpressing cell lines, L-MDR1 and MDCK2-MDR1 cells, to compare the results with MDCK1-MDR1 cells. To determine whether a drug is a substrate of MRP1 or MRP2, we will perform transport studies using LLC-PK1, L-MRP1 and MDCK2, MDCK2-MRP2 cell lines, respectively.

2.4.3 Dicloxacillin

Dicloxacillin has a higher renal clearance value in CF patients. We would like to determine if it is a substrate of P-gp, MRP1 or MRP2.

To determine if dicloxacillin is a substrate of P-gp, we compare the bidirectional transport study results in MDCK1 and MDCK1-MDR1 cells. The B to A fluxes are higher than the A to B fluxes in both the MDCK1 and MDCK1-MDR1 cells (Figure 2.11). The difference in the B to A and A to B fluxes is more pronounced in the P-gp overexpressing cell line. The B to A/A to B ratio is about 2 in MDCK1 cells and about 7 in MDCK1-MDR1 cells (Table 2.8). In this particular study, there is no difference in the A to B fluxes between MDCK1 and MDCK1-MDR1 cells. Normally for a P-gp substrate, the B to A flux is higher and the A to B flux is lower in MDCK1-MDR1 compared to MDCK1 cells. This is observed for other studies with lower concentrations of dicloxacillin (Table 2.9).

When the studies were performed at 4°C, where the active process was inhibited and the passive flow was reduced, the apparent permeabilities of dicloxacillin in MDCK1-MDR1 cells in both the B to A and A to B directions are decreased. In the study conducted in the absence of cells, fluxes are much greater (Table 2.8). In both cases, the B to A/A to B ratios are about 0.7. All these data indicate that dicloxacillin is a substrate of P-gp.

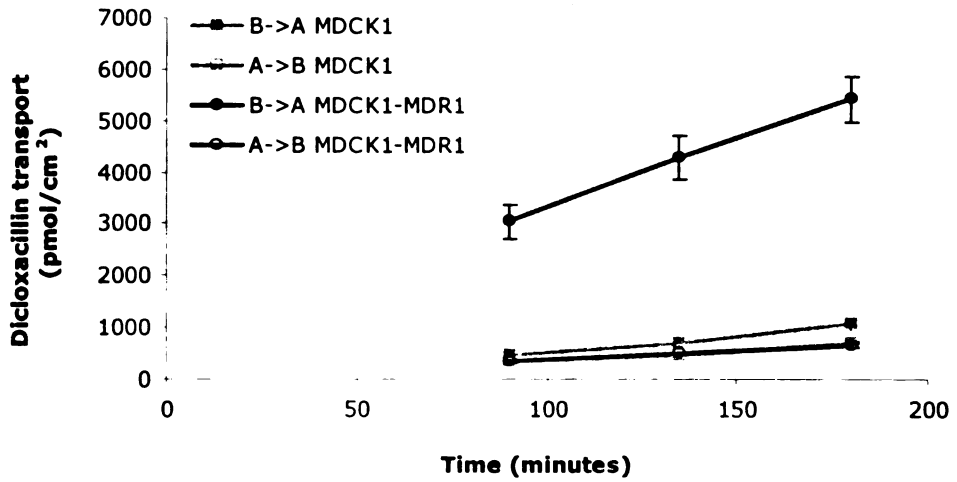

Figure 2.11 Bidirectional transport of 250 μM dicloxacillin in MDCK1 (gray line) and MDCK1-MDR1 (black line) cells. ■,●= B→A and □,○= A→B

Table 2.8 Bidirectional transport of 250 μM dicloxacillin in MDCK1 and MDCK1-MDR1 cells.

Cell Line	P_{app} x 10^{-7} (avg ± SD, n=3, cm/s)		B→A / A→B
	B→A	A→B	
MDCK1	4.5 (0.5)	2.5 (0.6)	1.8
MDCK1-MDR1	17.7 (1.1)	2.5 (0.2)	7.2
MDCK1-MDR1 4°c	0.5 (0.1)	0.7 (0.01)	0.7
No Cells	50.4 (3.9)	71.5 (8.1)	0.7

Table 2.9 Bidirectional transport of 25 and 100 μM dicloxacillin in MDCK1 and MDCK1-MDR1 cells.

Cell Line	Concentration (μM)	P_{app} x 10^{-7} (avg ± SD, n=3, cm/s)		B→A / A→B
		B→A	A→B	
MDCK1	25	2.8 (1.2)	3.1 (0.2)	0.9
	100	6.1 (0.9)	8.2 (0.8)	0.7
MDCK1-MDR1	25	29 (0.6)	1.4 (0.04)	20
	100	64 (4.7)	3.1 (0.3)	21

To confirm that dicloxacillin is a substrate of P-gp, we tested the effect of various inhibitors on dicloxacillin transport in MDCK1-MDR1 cells.

In the presence of P-gp inhibitors: cyclosporine, ketoconazole, GG918 and vinblastine, the B to A flux of dicloxacillin decreases (Figure 2.12) and no statistically significant change is observed for the A to B flux (Figure 2.13). PAH (para-amino hippurate), an inhibitor of organic anion transporters, has no statistically significant effects on dicloxacillin transport in MDCK1-MDR1 cells (Figure 2.12 and 2.13). P-gp inhibitors significantly decrease the B to A/A to B ratio while PAH has no effect (Figure 2.14). These data confirm that dicloxacillin is a substrate of P-gp.

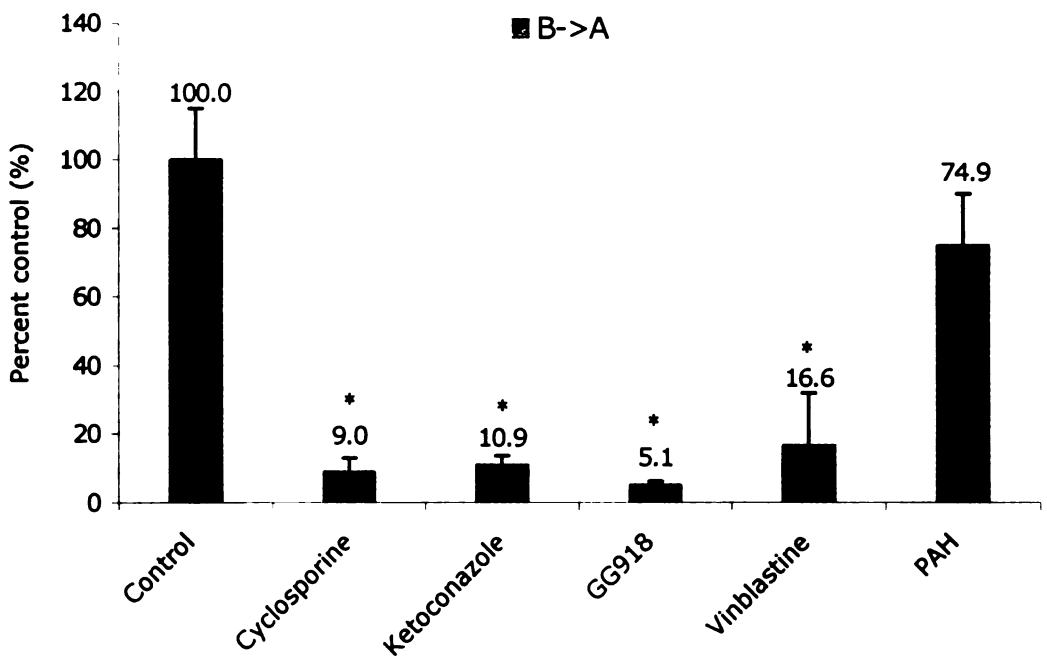

Figure 2.12 Effect of various inhibitors on 250 μM dicloxacillin (100 μM for cyclosporine and ketoconazole) B→A transport in MDCK1-MDR1 cells. The inhibitors are cyclosporine (20 μM), ketoconazole (100 μM), GG918 (2.5 μM), vinblastine (100 μM) and PAH (1000 μM). *P<0.01

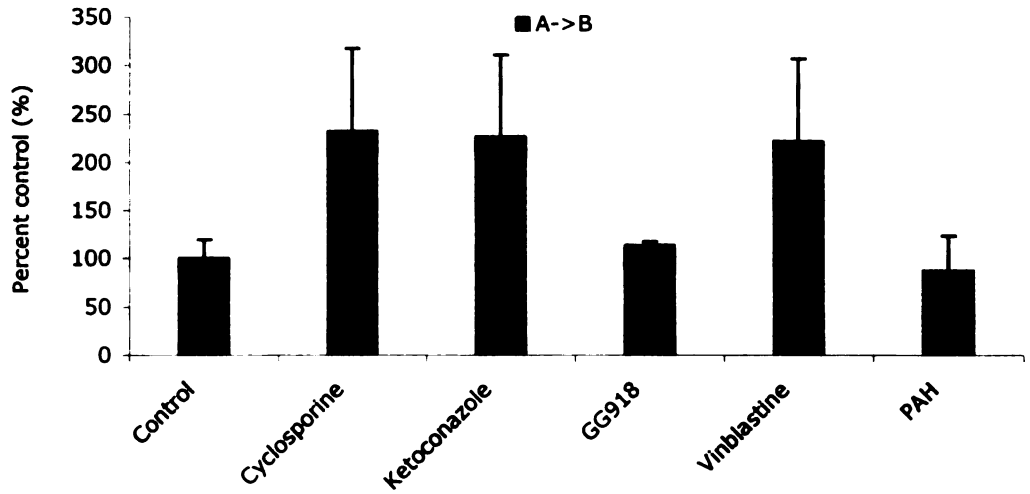

Figure 2.13 Effect of various inhibitors on 250 μM dicloxacillin (100 μM for cyclosporine and ketoconazole) A→B transport in MDCK1-MDR1 cells. The inhibitors are cyclosporine (20 μM), ketoconazole (100 μM), GG918 (2.5 μM), vinblastine (100 μM) and PAH (1000 μM). *P<0.01

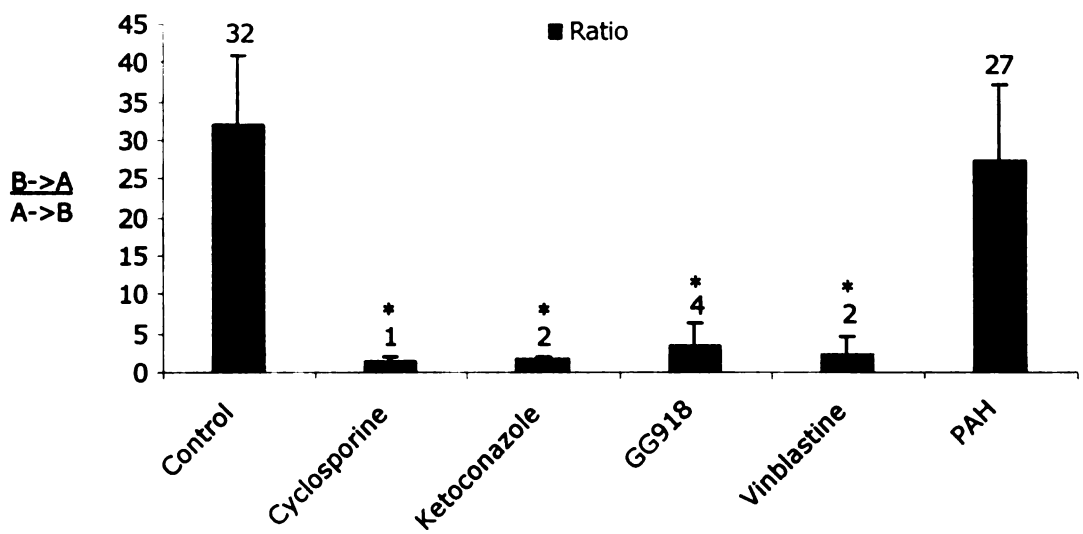

Figure 2.14 Effect of various inhibitors on 250 μM dicloxacillin (100 μM for cyclosporine and ketoconazole) B→A/A→B ratio in MDCK1-MDR1 cells. The inhibitors are cyclosporine (20 μM), ketoconazole (100 μM), GG918 (2.5 μM), vinblastine (100 μM) and PAH (1000 μM). *P<0.01

Next, we performed bidirectional transport studies for dicloxacillin in LLC-PK1, L-MDR1 and L-MRP1 cells. There is no significant difference observed in the bidirectional transport of dicloxacillin between LLC-PK1 and L-MDR1 cells (Figure 2.15). The B to A/A to B ratios are about 1 in both cell lines (Table 2.10). This data are similar to vinblastine, where transport studies in MDCK1 and MDCK1-MDR1 cells indicate that it is a substrate of P-gp while no difference is observed between LLC-PK1 and L-MDR1 cells. Comparison of dicloxacillin transport between LLC-PK1 and L-MRP1 cells shows that both the B to A and A to B fluxes are higher in L-MRP1 compared to LLC-PK1 cells but there is no difference observed between the B to A and A to B fluxes in both cell lines (Table 2.10). These data indicate that dicloxacillin is not a substrate of MRP1

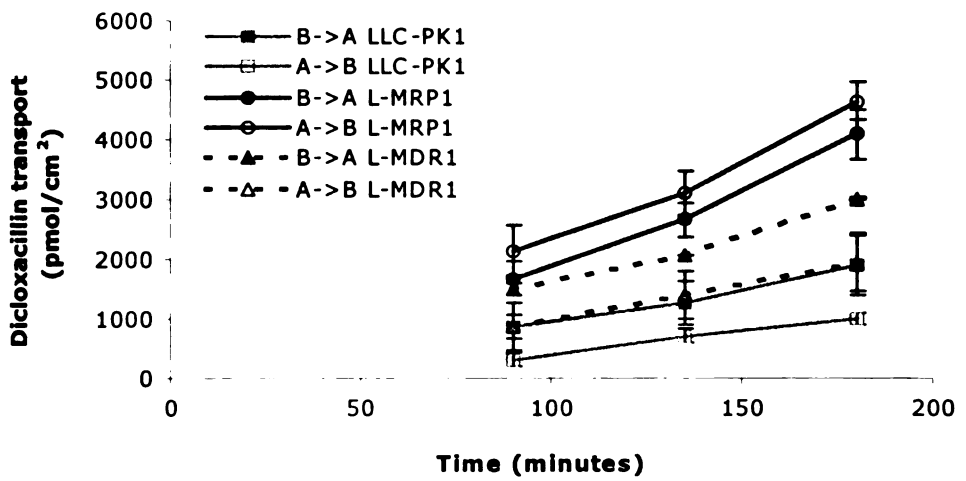

Figure 2.15 Bidirectional transport of 250 μM dicloxacillin in LLC-PK1 (gray line), L-MRP1 (black line) and L-MDR1 (dashed line) cells. ■,●,▲= B→A and □,○,△= A→B

Table 2.10 Bidirectional transport of 250 μM dicloxacillin in LLC-PK1, L-MRP1 and L-MDR1 cells.

Cell Line	P_{app} x 10^{-7} (avg ± SD, n=3, cm/s)		B→A / A→B
	B→A	A→B	
LLC-PK1	7.6 (2.6)	5.1 (0.2)	1.5
L-MRP1	17.9 (1.7)	18.6 (2.6)	1.0
L-MDR1	11.2 (0.8)	8.1 (2.3)	1.4

To determine if dicloxacillin is a substrate of MRP2, we conducted transport studies in MDCK2 and MDCK2-MRP2 cells. There is no difference in the dicloxacillin transport between these two cell lines (Figure 2.16). The B to A/A to B ratios are around 1 in both cell lines (Table 2.11). This indicates that dicloxacillin is not a substrate of MRP2. We also compared dicloxacillin transport between MDCK2 and MDCK2-MDR1 cells. The B to A and A to B fluxes are lower in MDCK2-MDR1 compared to MDCK2 cells. The B to A/A to B ratio is around 1 in the control cell line and 4 in the P-gp overexpressing cell line.

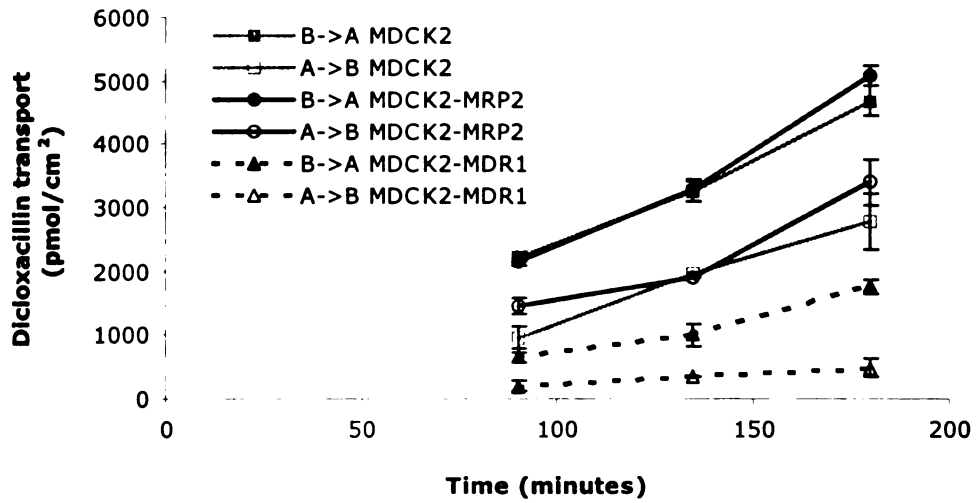

Figure 2.16 Bidirectional transport of 250 μM dicloxacillin in MDCK2 (gray line), MDCK2-MRP2 (black line) and MDCK2-MDR1 (dashed line) cells. ■,●,▲= B→A and □,○,Δ= A→B

Table 2.11 Bidirectional transport of 250 μM dicloxacillin in MDCK2, MDCK2-MRP2 and MDCK2-MDR1 cells.

Cell Line	P_{app} x 10^{-7} (avg ± SD, n=3, cm/s)		B→A / A→B
	B→A	A→B	
MDCK2	18.5 (1.5)	13.5 (1.7)	1.4
MDCK2-MRP2	21.9 (1.1)	14.4 (1.7)	1.5
MDCK2-MDR1	8.1 (0.8)	2.1 (0.5)	3.8

2.4.4 Trimethoprim

Trimethoprim also has a higher renal clearance value in CF patients. We would like to determine if it is a substrate of P-gp, MRP1 or MRP2. To determine if trimethoprim is a substrate of P-gp, we compare the bidirectional transport study results in MDCK1 and MDCK1-MDR1 cells. The B to A fluxes are higher than the A to B fluxes in both the MDCK1 and MDCK1-MDR1 cells (Figure 2.17). The difference in the B to A and A to B fluxes is more pronounced in the P-gp overexpressing cell line. The B to A/A to B ratio is about 2 in MDCK1 cells and about 55 in MDCK1-MDR1 cells (Table 2.12). When the study was performed at 4°C, the apparent permeabilities of trimethoprim in MDCK1-MDR1 cells in both the B to A and A to B directions are decreased, with a significantly larger decrease in the B to A direction. It is the opposite in the study conducted in the absence of cells (Table 2.12). At 4°C, the B to A/A to B ratio decreases to about 7 while in the absence of cells, it is about 0.6. All these data indicate that trimethoprim is a substrate of P-gp.

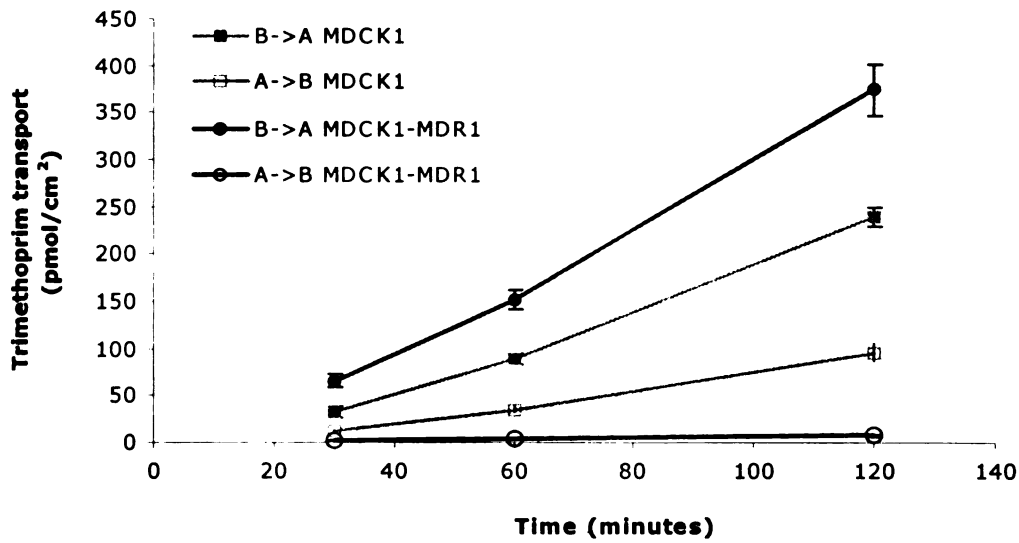

Figure 2.17 Bidirectional transport of 5 μM trimethoprim in MDCK1 (gray line) and MDCK1-MDR1 (black line) cells. ■,●= B→A and □,○= A→B

To confirm that trimethoprim is a substrate of P-gp, we tested the effect of various inhibitors on trimethoprim transport in MDCK1-MDR1 cells. In the presence of P-gp inhibitors, cyclosporine, ketoconazole, GG918, vinblastine and verapamil, the B to A flux of trimethoprim decreases (Figure 2.18) and the A to B flux increases (Figure 2.19). Sulfamethoxazole, the antibiotic that is dosed together with trimethoprim, TEA (tetra-ethyl ammonium), an inhibitor

Table 2.12 Bidirectional transport of trimethoprim in MDCK1 and MDCK1-MDR1 cells.

Cell Line	Concentration	P_{app} x 10^{-7} (avg ± SD, n=3, cm/s)		B→A / A→B
		B→A	A→B	
MDCK1	5 μM	77.8 (0.5)	31.9 (0.7)	2.4
MDCK1	25 μM	64.2 (3.7)	29.7 (2.5)	2.2
MDCK1	100 μM	78.3 (6.3)	78.5 (9.3)	1.0
MDCK1-MDR1	5 μM	77 (13.4)	2.2 (0.08)	34.6
MDCK1-MDR1	25 μM	104 (4.6)	1.3 (0.3)	79
MDCK1-MDR1	100 μM	128.7 (13.7)	2.6 (0.5)	50
MDCK1-MDR1	100 μM, 4°C	4.7 (2.4)	0.7 (0.5)	6.7
No cells	100 μM	143 (9)	255 (20)	0.6

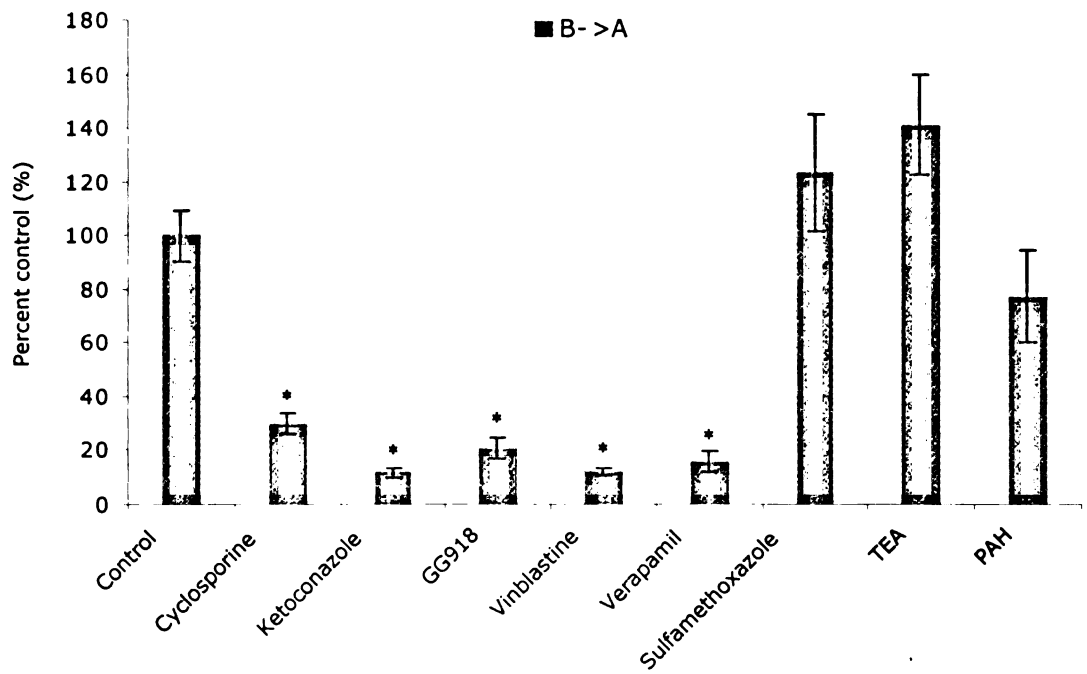

Figure 2.18 Effect of various inhibitors on 100 μM trimethoprim B→A transport in MDCK1-MDR1 cells. The inhibitors are cyclosporine (20 μM), ketoconazole (100 μM), GG918 (2.5 μM), vinblastine (100 μM), verapamil (50 μM), sulfamethoxazole (500 μM), TEA (500 μM) and PAH (500 μM). *P<0.01

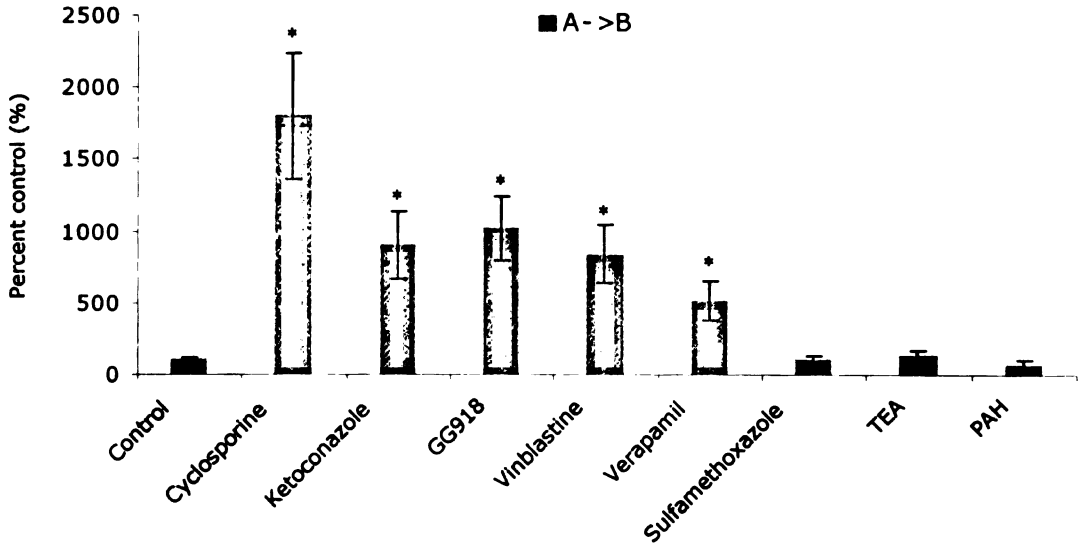

Figure 2.19 Effect of various inhibitors on 100 μM trimethoprim A→B transport in MDCK1-MDR1 cells. The inhibitors are cyclosporine (20 μM), ketoconazole (100 μM), GG918 (2.5 μM), vinblastine (100 μM), verapamil (50 μM), sulfamethoxazole (500 μM), TEA (500 μM) and PAH (500 μM). *P<0.01

of organic cation transporters and PAH, an inhibitor of organic anion transporters, have no effect on trimethoprim transport in MDCK1-MDR1 cells (Figures 2.18 and 2.19). P-gp inhibitors decrease the B to A/A to B ratio while non-P-gp inhibitors have no effect on the ratio (Figure 2.20). These data once again suggests that trimethoprim is a substrate of P-gp.

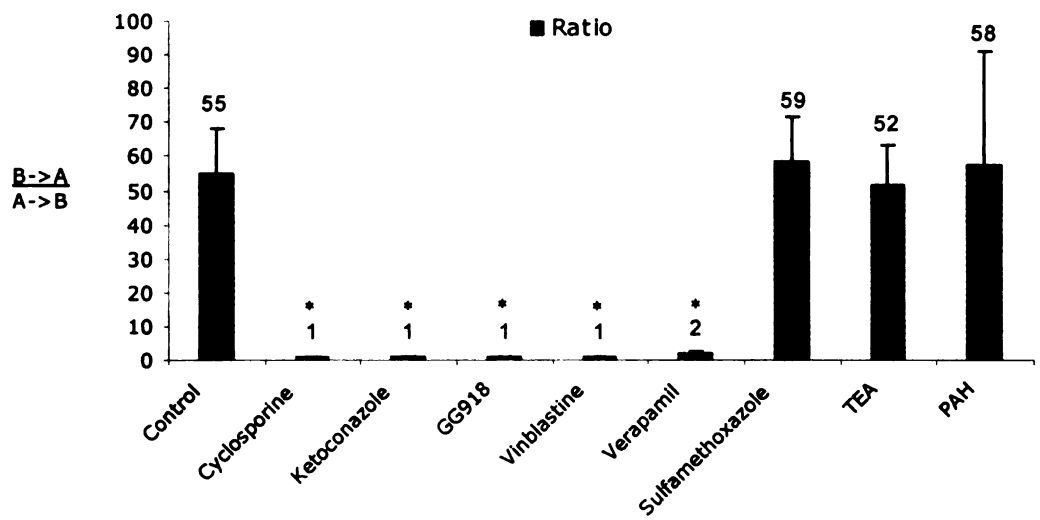

Figure 2.20 Effect of various inhibitors on 100 μM trimethoprim B→A/A→B ratio in MDCK1-MDR1 cells. The inhibitors are cyclosporine (20 μM), ketoconazole (100 μM), GG918 (2.5 μM), vinblastine (100 μM), verapamil (50 μM), sulfamethoxazole (500 μM), TEA (500 μM) and PAH (500 μM). *P<0.01

Next, we performed bidirectional transport studies for trimethoprim in MDCK2, MDCK2-MRP2 and MDCK2-MDR1 cells. There is no difference observed in the bidirectional transport of trimethoprim among those three cell lines (Figure 2.21). The B to A/A to B ratios are around 2-3 in all cell lines (Table 2.13). This indicates that trimethoprim is not a substrate of MRP2.

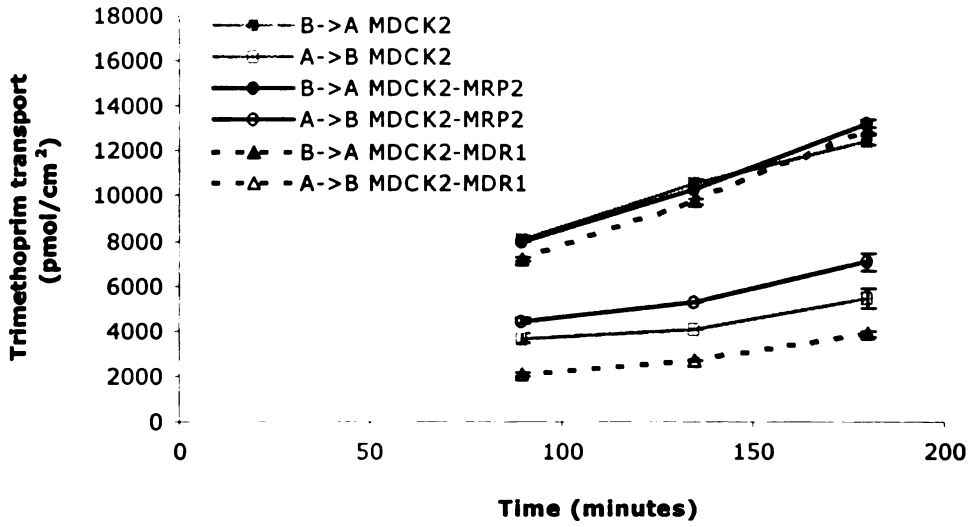

Figure 2.21 Bidirectional transport of 100 μM trimethoprim in MDCK2 (gray line), MDCK2-MRP2 (black line) and MDCK2-MDR1 (dashed line) cells. ■,●,□= B→A and □,○,Δ= A→B

Table 2.13 Bidirectional transport of 100 μM trimethoprim in MDCK2, MDCK2-MRP2 and MDCK2-MDR1 cells.

Cell Line	P_{app} x 10^{-7} (avg ± SD, n=3, cm/s)		B→A / A→B
	B→A	A→B	
MDCK2	81.7 (4.8)	33.7 (9.9)	2.4
MDCK2-MRP2	97.5 (7.3)	48.4 (6.8)	2
MDCK2-MDR1	106.4 (8.9)	33.5 (6.1)	3.2

It is interesting that there is no difference in trimethoprim transport between MDCK2 and MDCK2-MDR1 cells. Western blot and RT-PCR studies show higher amounts of P-gp in MDCK2-MDR1 compared to MDCK2 cells (Figures 2.4 and 2.5) and our bidirectional transport

and inhibition studies show that trimethoprim is a substrate of P-gp (Figures 2.17-2.20). This observation is similar to vinblastine and dicloxacillin, where transport studies in MDCK1 and MDCK1-MDR1 cells indicate that they are substrates of P-gp while no differences are observed between LLC-PK1 and L-MDR1 cells. Therefore, we concluded that MDCK2 and MDCK2-MDR1 cells, just like LLC-PK1 and L-MDR1 cell lines, might not be the right cell lines to use to determine if a drug is a substrate of P-gp.

To determine if trimethoprim is a substrate of MRP1, we conducted transport studies in LLC-PK1 and L-MRP1 cells. There is no difference in the bidirectional transport of trimethoprim between LLC-PK1 and L-MRP1 cells (Figure 2.22). The B to A/A to B ratios are about 1 in both cell lines (Table 2.14). This data indicate that trimethoprim is not a substrate of MRP1. We also compared trimethoprim transport between LLC-PK1 and L-MDR1 cells. There is a difference in trimethoprim transport between LLC-PK1 and L-MDR1 cells (Figure 2.23). The B to A flux is higher and the A to B flux is lower in L-MDR1 compared to LLC-PK1 cells. The B to A/A to B ratios in LLC-PK1 and L-MDR1 cells are about 1 and 5, respectively (Table 2.15). This data agrees with the results in MDCK1 and MDCK1-MDR1 cells and are similar to what we observed for digoxin.

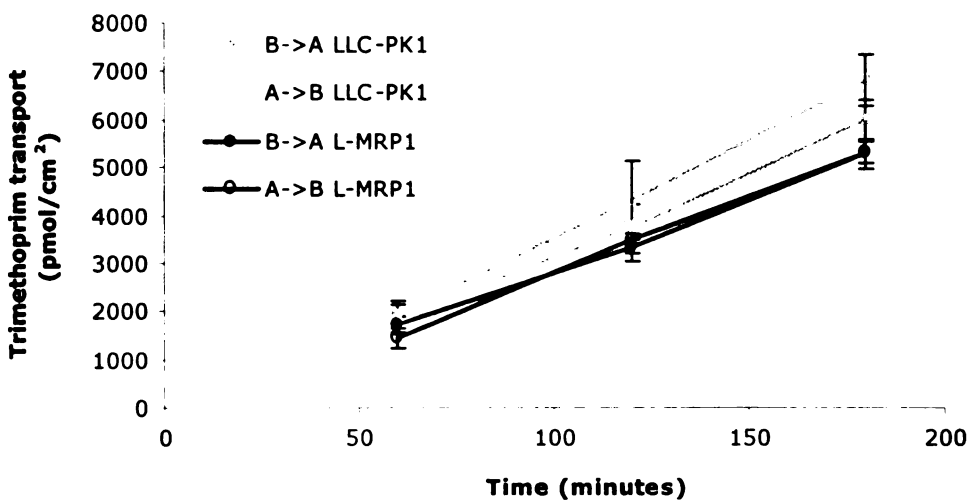

Figure 2.22 Bidirectional transport of 100 μM trimethoprim in LLC-PK1 (gray line) and L-MRP1 (black line) cells. ■,●= B→A and □,○= A→B

Table 2.14 Bidirectional transport of 100 μM trimethoprim in LLC-PK1 and L-MRP1 cells.

Cell Line	P_{app} x 10^{-7} (avg ± SD, n=3, cm/s)		B→A / A→B
	B→A	A→B	
LLC-PK1	57.3 (0.3)	67.6 (4.5)	0.8
L-MRP1	49.3 (2.3)	54.1 (0.5)	0.9

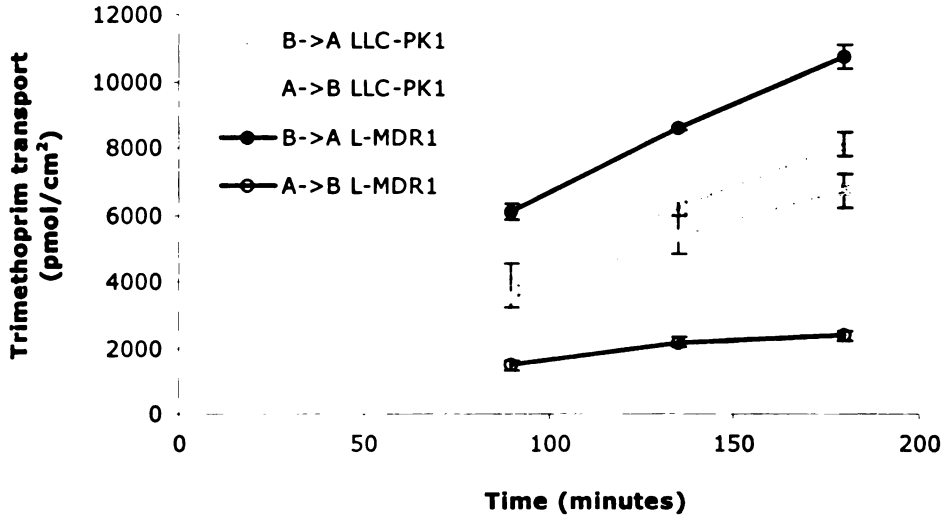

Figure 2.23 Bidirectional transport of 100 μM trimethoprim in LLC-PK1 (gray line) and L-MDR1 (black line) cells. ■,●= B→A and □,○= A→B

Table 2.15 Bidirectional transport of 100 μM trimethoprim in LLC-PK1 and L-MDR1 cells.

Cell Line	P_{app} x 10^{-7} (avg ± SD, n=3, cm/s)		B→A / A→B
	B→A	A→B	
LLC-PK1	58.7 (3.2)	74.6 (11.4)	0.8
L-MDR1	86.2 (10.9)	16.7 (0.3)	5.2

2.4.5 Sulfamethoxazole

Sulfamethoxazole does not show a higher renal clearance in CF patients. We would like to determine if it is a substrate of P-gp. To determine if sulfamethoxazole is a substrate of P-gp, we compare the bidirectional transport study results in MDCK1 and MDCK1-MDR1 cells. There

is no difference observed between the B to A and A to B fluxes for sulfamethoxazole in both the MDCK1 and MDCK1-MDR1 cells (Figure 2.24). The B to A/A to B ratios are about 1 in both cell lines (Table 2.16). This indicates that sulfamethoxazole is not a substrate of P-gp. We do observe that the B to A and A to B fluxes are slightly lower in MDCK1-MDR1 compared to MDCK1 cells. We proposed that this could be due to higher TEER values of MDCK1-MDR1 cells.

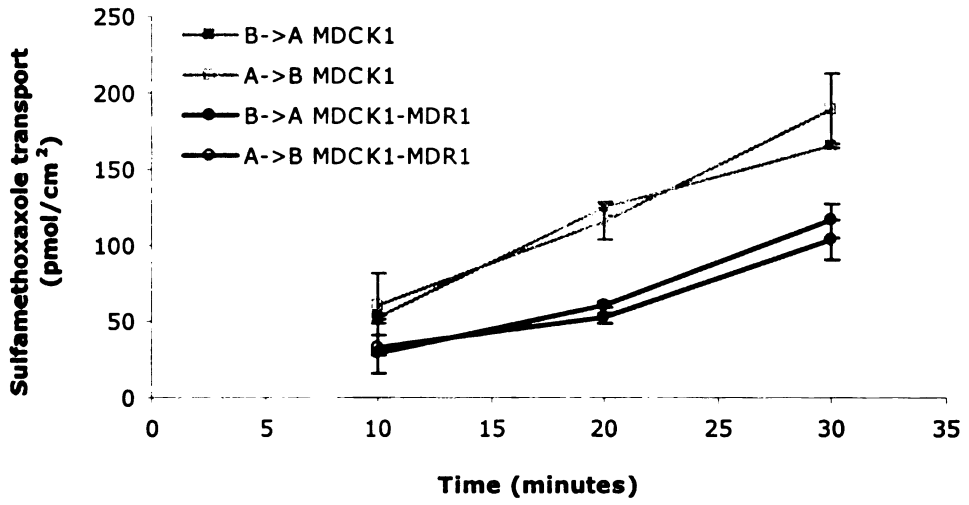

Figure 2.24 Bidirectional transport of 10 μM sulfamethoxazole in MDCK1 (gray line) and MDCK1-MDR1 (black line) cells. ■,● = B→A and □,○ = A→B

Table 2.16 Bidirectional transport of 10 μM sulfamethoxazole in MDCK1 and MDCK1-MDR1 cells.

Cell Line	P_{app} x 10^{-7} (avg ± SD, n=3, cm/s)		B→A / A→B
	B→A	A→B	
MDCK1	94 (10)	107 (24)	0.9
MDCK1-MDR1	73 (8)	60 (5)	1.2

2.4.6 N4-acetylsulfamethoxazole

N4-acetylsulfamethoxazole is a metabolite of sulfamethoxazole. Its formation clearance is increased in CF patients. We would like to determine if N4-acetylsulfamethoxazole is a substrate of P-gp. There is no difference between the B to A and A to B fluxes for N4-acetylsulfamethoxazole in the MDCK1 and MDCK1-MDR1 cells (Figure 2.25). The B to A/A to B ratios are about 1 in both cell lines (Table 2.17). This indicates that N4-acetylsulfamethoxazole is not a substrate of P-gp. Similar to sulfamethoxazole, we observe that the A to B flux is slightly lower in MDCK1-MDR1 compared to MDCK1 cells.

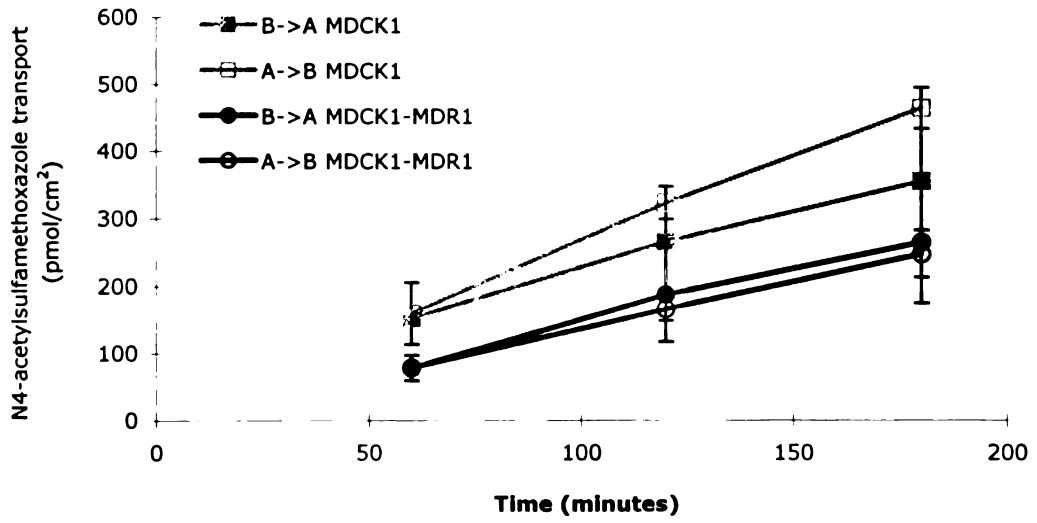

Figure 2.25 Bidirectional transport of 250 μM N4-acetylsulfamethoxazole in MDCK1 (gray line) and MDCK1-MDR1 (black line) cells. ■,●= B→A and □,○ = A→B

Table 2.17 Bidirectional transport of 250 μM N4-acetylsulfamethoxazole in MDCK1 and MDCK1-MDR1 cells.

Cell Line	P_{app} x 10^{-7} (avg ± SD, n=3, cm/s)		B→A / A→B
	B→A	A→B	
MDCK1	1.1 (0.3)	1.7 (0.4)	0.7
MDCK1-MDR1	1.0 (0.2)	0.9 (0.2)	1.1

2.4.7 Iothalamate

Iothalamate is a marker of glomerular filtration. It is neither secreted nor reabsorbed. The renal clearance of iothalamate is not different in CF patients, which indicates that GFR is not different in CF patients. We would like to determine if iothalamate is a substrate of P-gp. There is no difference between the B to A and A to B fluxes for iothalamate in the MDCK1 and MDCK1-MDR1 cells (Figure 2.26). The B to A/A to B ratios are about 1 in both cell lines (Table 2.18). This indicates that iothalamate is not a substrate of P-gp.

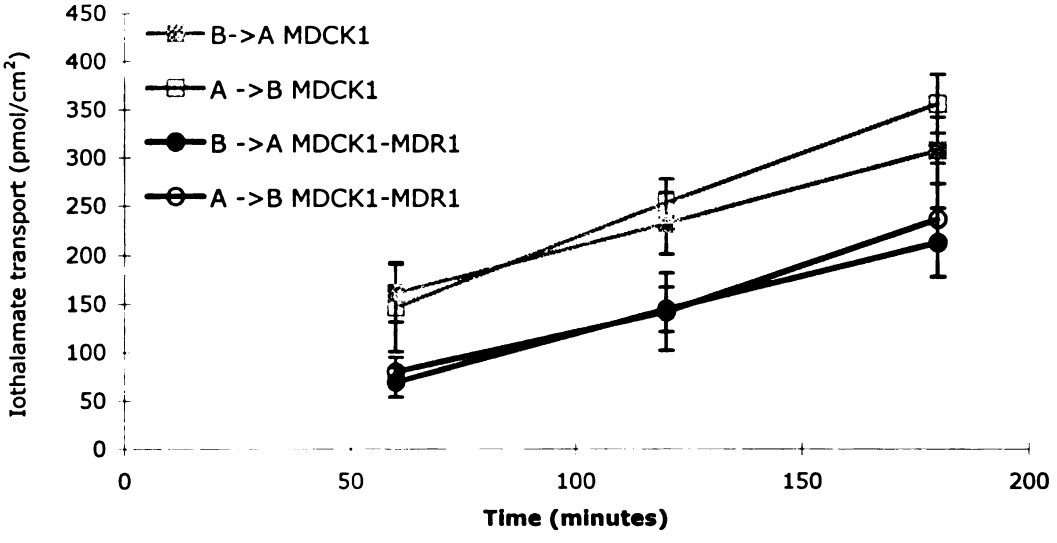

Figure 2.26 Bidirectional transport of 250 μM iothalamate in MDCK1 (gray line) and MDCK1-MDR1 (black line) cells. ■,●= B→A and □,○ = A→B

Table 2.18 Bidirectional transport of 250 μM iothalamate in MDCK1 and MDCK1-MDR1 cells.

Cell Line	P_{app} x 10^{-7} (avg ± SD, n=3, cm/s)		B→A / A→B
	B→A	A→B	
MDCK1	0.8 (0.1)	1.2 (0.1)	0.7
MDCK1-MDR1	0.8 (0.1)	0.9 (0.3)	0.9

2.4.8 Cefsulodin

Cefsulodin does not show enhanced active renal clearance in CF patients. We would like to determine if it is a P-gp substrate. There is no difference between the B to A and A to B fluxes for cefsulodin in the MDCK1 and MDCK1-MDR1 cells (Figure 2.27). The B to A/A to B ratios are about 1 in both cell lines (Table 2.19).

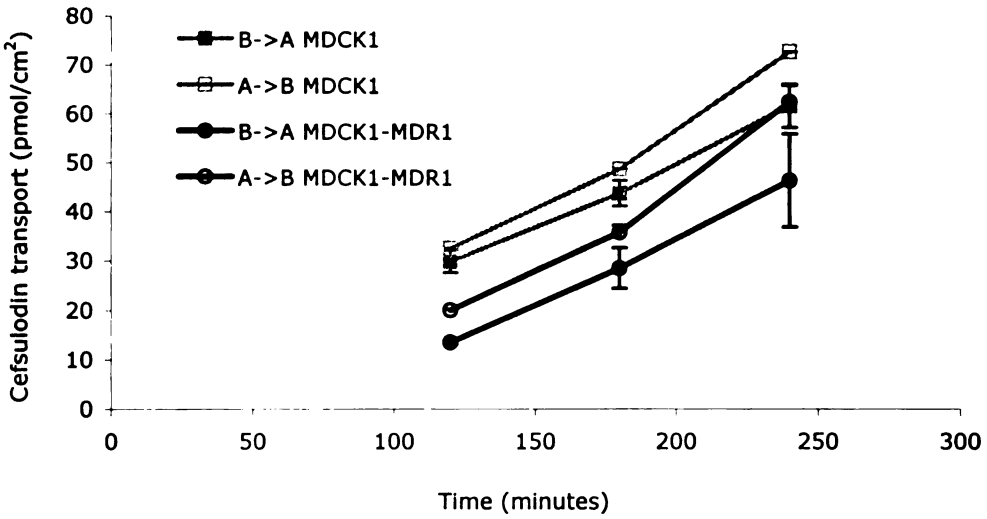

Figure 2.27 Bidirectional transport of 50 μM cefsulodin in MDCK1 (gray line) and MDCK1-MDR1 (black) cells. ■,●= B→A and □,○= A→B

Table 2.19 Bidirectional transport of 50 and 100 μM cefsulodin in MDCK1 and MDCK1-MDR1 cells.

Cell Line	Concentration	P_{app} x 10^{-6} (avg ± SD, n=3, cm/s)		B→A / A→B
		B→A	A→B	
MDCK1	50	8.8 (0.6)	11.2 (1.2)	0.8
	100	9.3 (1.4)	10.8 (0.4)	0.9
MDCK1-MDR1	50	10.1 (2.5)	11.8 (1.0)	0.8
	100	6.3 (1.4)	6.5 (1.1)	1.0

There is no significant difference observed in the bidirectional transport of cefsulodin between LLC-PK1 and L-MDR1 cells (Figure 2.28). The B to A/A to B ratios are about 1 in both cell

lines (Table 2.20). There is also no difference observed between the B to A and A to B fluxes in both LLC-PK1 and L-MRP1 cells. The B to A and A to B fluxes are higher in L-MRP1 compared to LLC-PK1 cells (Table 2.20), which might be attributed to leakier junctions in L-MRP1 cells, as shown by higher mannitol P_{app} value in those cells. All these data indicate that cefsulodin is not a substrate of MRP1

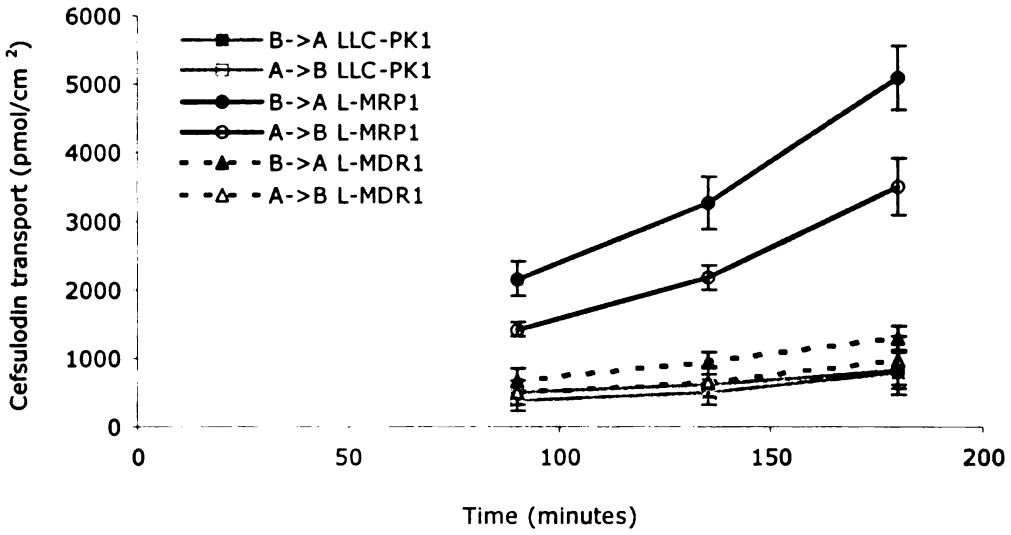

Figure 2.28 Bidirectional transport of 250 μM cefsulodin in LLC-PK1 (gray line), L-MRP1 (black line) and L-MDR1 (dashed line) cells. ■,●,▲= B→A and □,○,△= A→B

Table 2.20 Bidirectional transport of 250 μM cefsulodin in LLC-PK1, L-MRP1 and L-MDR1 cells.

Cell Line	P_{app} x 10^{-7} (avg ± SD, n=3, cm/s)		B→A / A→B
	B→A	A→B	
LLC-PK1	2.4 (0.6)	3 (0.4)	0.8
L-MRP1	21.8 (0.7)	15.3 (2.3)	1.4
L-MDR1	4.5 (0.7)	3.4 (1.2)	1.3

No difference is observed in the cefsulodin transport between MDCK2 and MDCK2-MRP2 cells (Figure 2.29). The B to A/A to B ratios are around 1 in both cell lines (Table 2.21). This indicates that cefsulodin is not a substrate of MRP2. Similar to dicloxacillin, the B to A and A

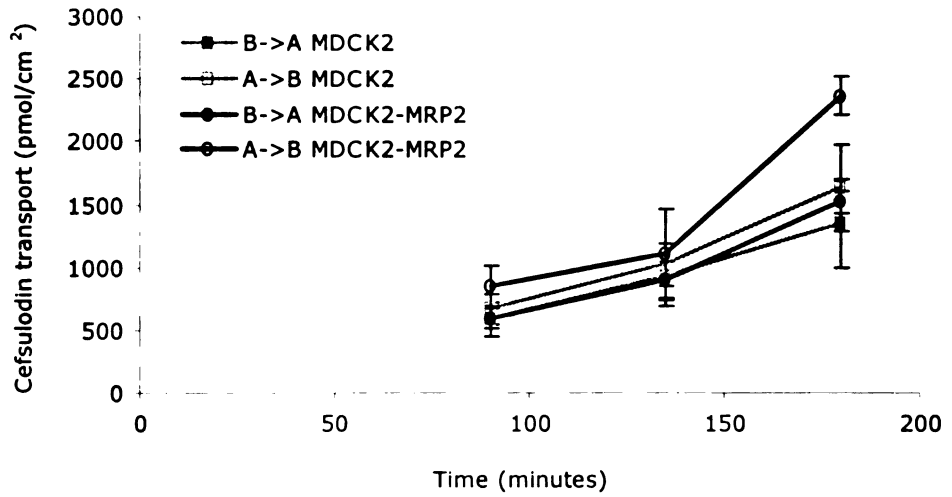

Figure 2.29 Bidirectional transport of 250 μM cefsulodin in MDCK2 (gray line) and MDCK2-MRP2 (black line) cells. ■,●= B→A and □,○= A→B

Table 2.21 Bidirectional transport of 250 μM cefsulodin in MDCK1 and MDCK1-MDR1 cells.

Cell Line	P_{app} x 10^{-7} (avg ± SD, n=3, cm/s)		B→A / A→B
	B→A	A→B	
MDCK2	5.7 (1.7)	7.2 (1.2)	0.8
MDCK2-MRP2	6.9 (0.2)	11.2 (1.1)	0.6
MDCK2-MDR1	1.1 (0.2)	1.4 (0.7)	0.8

to B fluxes are lower in MDCK2-MDR1 compared to MDCK2 cells. However, unlike dicloxacillin, there is no difference between the B to A and A to B flux for cefsulodin in MDCK2-MDR1 cells. The B to A/A to B ratio is around 1 for cefsulodin (Table 2.21) while it is around 4 for dicloxacillin (Table 2.11).

2.4.9 Ciprofloxacin

Ciprofloxacin shows conflicting renal clearance values in CF patients. We would like to determine if it is a substrate of P-gp, MRP1 or MRP2. For ciprofloxacin, the B to A flux is higher than the A to B flux in the MDCK1-MDR1 cells, with the B to A flux higher and A to B

flux lower compared to MDCK1 cells (Figure 2.30). The B to A/A to B ratio is about 15 in that cell line and it is abolished to about 1 at 4°C (Table 2.22). This indicates that ciprofloxacin is a substrate of P-gp. Interestingly, the B to A flux is lower than the A to B flux in MDCK1 cells. MDCK1 cells have an endogenous expression of P-gp, as shown by our RT-PCR studies (Figure 2.4). Normally for a P-gp substrate, e.g., digoxin, vinblastine, dicloxacillin and trimethoprim, the B to A flux is higher or equal to the A to B flux in MDCK1 cells. But it is the opposite for ciprofloxacin. The A to B flux is higher than the B to A flux, with the B to A/A to B ratio of about 0.4 in MDCK1 cells (Table 2.22). This suggests that ciprofloxacin, besides being a substrate of P-gp, is also a substrate of an absorptive transporter that pumps in the opposite direction of P-gp.

Currently we do not know whether it is an uptake transporter that is located on the apical membrane or an efflux transporter located on the basolateral membrane. We believe it is an energy dependent transporter because at 4°C, the difference between the A to B and B to A fluxes in MDCK1 cells is abolished, bringing the B to A/A to B ratio up from 0.4 to about 1 (Table 2.22).

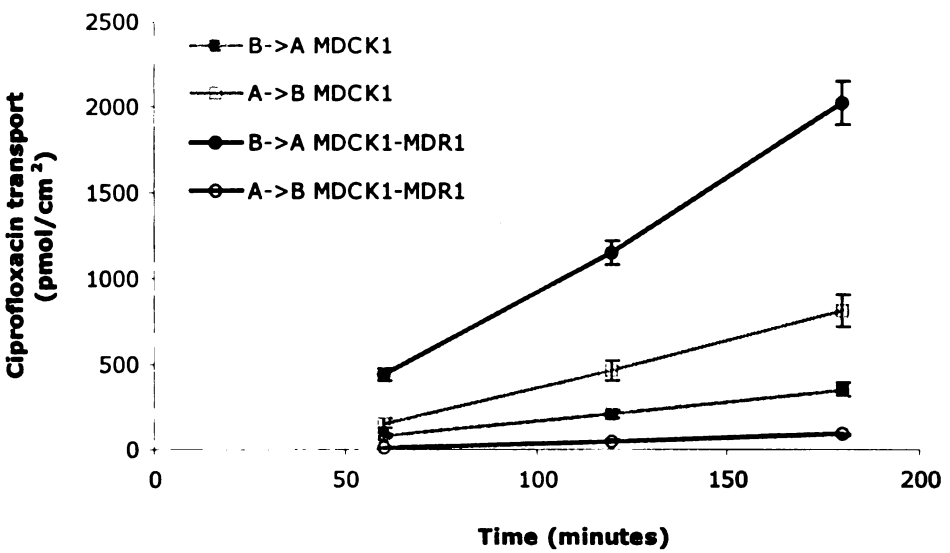

Figure 2.30 Bidirectional transport of 100 μM ciprofloxacin in MDCK1 (gray line) and MDCK1-MDR1 (black line) cells. ■,● = B→A and □,○ = A→B

Table 2.22 Bidirectional transport of 25 and 100 μM ciprofloxacin in MDCK1 and MDCK1-MDR1 cells.

Cell Line	Concentration	P_{app} x 10^{-7} (avg ± SD, n=3, cm/s)		B→A / A→B
		B→A	A→B	
MDCK1	25	4.5 (0.4)	10.6 (1.2)	0.4
MDCK1	100	3.8 (0.4)	9.2 (0.9)	0.4
MDCK1 4°C	25	2.1 (0.7)	1.7 (0.4)	1.2
MDCK1-MDR1	25	35.4 (1.0)	3.5 (0.4)	10
MDCK1-MDR1	100	21.9 (1.4)	1.0 (0.03)	22
MDCK1-MDR1 4°C	25	1.3 (0.4)	1.1 (0.2)	1.2
No cells	25	128.3 (2.8	153.7 (30.9)	0.8

To further test if ciprofloxacin is a P-gp substrate, we investigated the effect of various inhibitors on ciprofloxacin transport in MDCK1 and MDCK1-MDR1 cells. GG918, cyclosporine, ketoconazole, vinblastine, verapamil and quinidine are P-gp inhibitors. Dicloxacillin, trimethoprim and erythromycin are P-gp substrates. Glycosarcosine is an inhibitor of PEPT1, a pH-dependent uptake transporter. Probenecid and PAH are inhibitors of organic anion transporters. TEA is an inhibitor of organic cation transporters. Sulfinpyrazone and indomethacin are MRP1 and MRP2 inhibitors.

Figure 2.31 shows the effect of various inhibitors on ciprofloxacin B to A/A to B ratio in MDCK1 cells. In this study, in the absence of any inhibitors, the B to A/A to B ratio of ciprofloxacin is about 0.2. The ratio increases significantly to about 0.9, 1.2 and 2.5 with probenecid, sulfinpyrazone and indomethacin, respectively. P-gp inhibitors (GG918, cyclosporine, vinblastine, verapamil, quinidine) and a PEPT1 inhibitor (glycosarcosine) have no significant effects on ciprofloxacin transport in MDCK1 cells. The fact that glycosarcosine has no effect implies that ciprofloxacin is not a substrate of PEPT1. We have confirmed this further by running a pH gradient comparison study, where we do not see any difference (data not shown). It is interesting that in the presence of a MRP1 and MRP2 inhibitor, indomethacin, the B to A/A to B ratio flips from less than 1 to about 2.5. This suggests that indomethacin inhibits the activity of the unidentified absorptive transporter, and when this transporter is inhibited, P-gp effect can be observed. This data also implies that MRP1 could be that

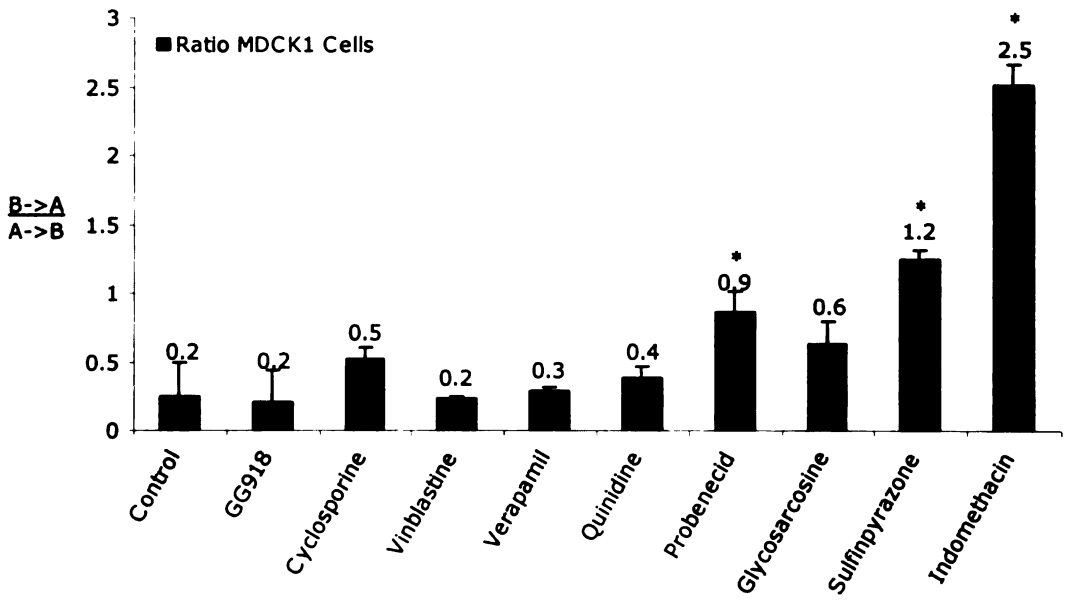

Figure 2.31 Effect of various inhibitors on 25 μM ciprofloxacin B→A/A→B ratio in MDCK1 cells. The inhibitors are GG918 (2.5 μM), cyclosporine (20 μM), vinblastine (100 μM), verapamil (50 μM), quinidine (100 μM), probenecid (100 μM), glycosarcosine (10 mM), sulfinpyrazone (1 mM) and indomethacin (100 μM). *P<0.01

absorptive transporter since indomethacin is an MRP1 inhibitor and MRP1 substrates show a higher A to B than B to A fluxes. The absorptive transporter could also be an organic anion transporter since probenecid also increases the B to A/A to B ratio of ciprofloxacin. Or it is possible that all these inhibitors are inhibiting the activity of a yet unknown transporter.

It is interesting that we do not observe any effects with P-gp inhibitors. We expect the B to A/A to B ratio to decrease with P-gp inhibitors. One explanation could be that the ratio is low and it is hard to reduce something that is already low. Another explanation could be that those inhibitors, besides inhibiting P-gp activity, could also inhibit the activity of the unidentified absorptive transporter. There is no such thing as a specific inhibitor of a transporter. Even GG918, which is thought to be a specific inhibitor of P-gp, is also known to inhibit BCRP, a breast cancer resistance protein (280). There is a third possibility of why we do not see the effects of P-gp inhibitors on ciprofloxacin transport in MDCK1 cells, which could conflict with what we observe with indomethacin. MDCK1 cells have endogenous expression of canine P-gp and it is possible that ciprofloxacin might not be a substrate of canine P-gp. Species-differences in substrate selectivity have been observed for P-gp substrates (281).

In MDCK1-MDR1 cells, the B to A flux significantly decreases in the presence of P-gp inhibitors (GG918, cyclosporine, ketoconazole, vinblastine, verapamil, trimethoprim, quinidine) while non-P-gp inhibitors (probenecid, PAH, glycosarcosine, sulfinpyrazone, TEA) have no effect (Figure 2.32). As expected with P-gp inhibitors, the A to B flux significantly increases with cyclosporine, ketoconazole and vinblastine (Figure 2.33). Trimethoprim, probenecid, indomethacin and TEA decrease the A to B flux. This could mean that they inhibit the activity of the unidentified absorptive transporter. Figure 2.34 shows the effect of various inhibitors on ciprofloxacin B to A/A to B ratios in MDCK1-MDR1 cells. As expected, P-gp inhibitors decrease the ratio while sulfinpyrazone and TEA increase the ratio, which is presumed to be due to inhibition of the function of the unidentified absorptive transporter.

All the data thus far suggest that ciprofloxacin is a substrate of P-gp. There is another interesting observation that further reinforces this conclusion. Ketoconazole is a classic P-gp inhibitor that is normally used in an inhibition study to confirm that a drug is a P-gp substrate. At the concentration of 100 μM, it is not toxic to the cells. However, we notice that when we utilize the same concentration of ketoconazole in the inhibition study of ciprofloxacin in MDCK1 cells, it disrupts the integrity of those cells, as shown by the increase of P_{app} of mannitol of approximately 6-fold in the presence of ketoconazole. As a result, the B to A and A to B fluxes of ciprofloxacin are much higher in the presence of ketoconazole compared to control (Figure 2.35). This phenomena is not observed in the inhibition study of digoxin with ketoconazole (Figure 2.8). We believe that it is the combination of ciprofloxacin and ketoconazole that is toxic to the cells and not the ketoconazole itself. This synergistic toxic effect is not observed in MDCK1-MDR1 cells. The P_{app} of mannitol does not change with ketoconazole in these cells. We believe that because MDCK1-MDR1 cells have significantly higher P-gp expression than MDCK1 cells, they are protected against the toxic effect of ciprofloxacin and ketoconazole. This is what happens in multidrug resistance cancer cells. They have higher expression of P-gp that pumps the chemotherapeutic drugs out from the cells.

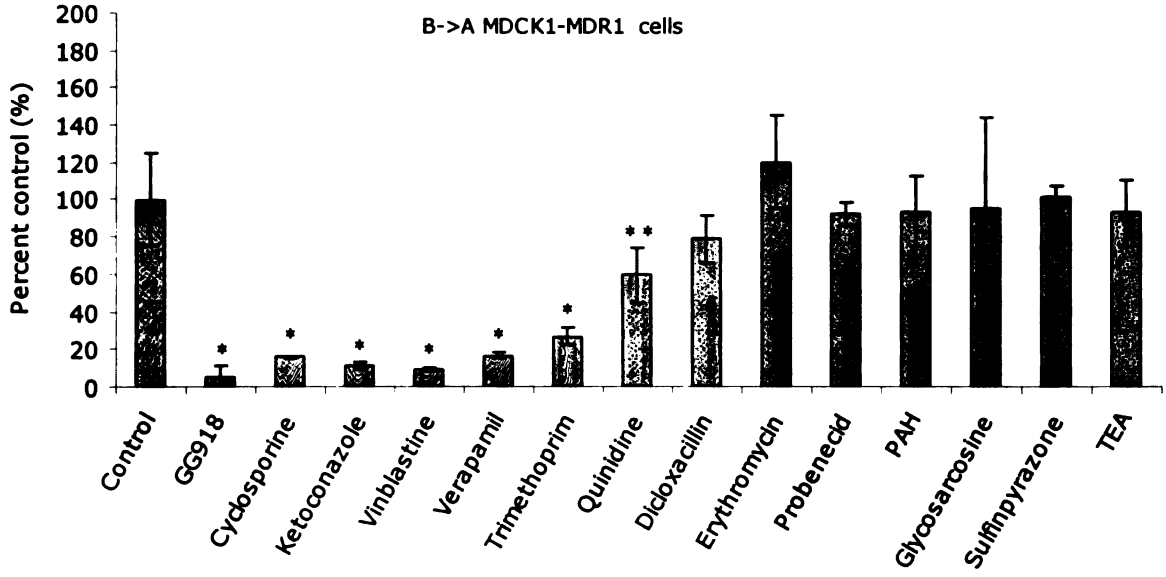

Figure 2.32 Effect of various inhibitors on 25 μM ciprofloxacin B→A transport in MDCK1-MDR1 cells. The inhibitors are GG918 (2.5 μM), cyclosporine (20 μM), ketoconazole (100 μM), vinblastine (100 μM), verapamil (50 μM), trimethoprim (100 μM), quinidine (100 μM), dicloxacillin (100 μM), erythromycin (100 μM), probenecid (100 μM), PAH (100 μM), glycosarcosine (10 mM), sulfinpyrazone (1 mM) and TEA (100 μM). *P<0.01 **P<0.05

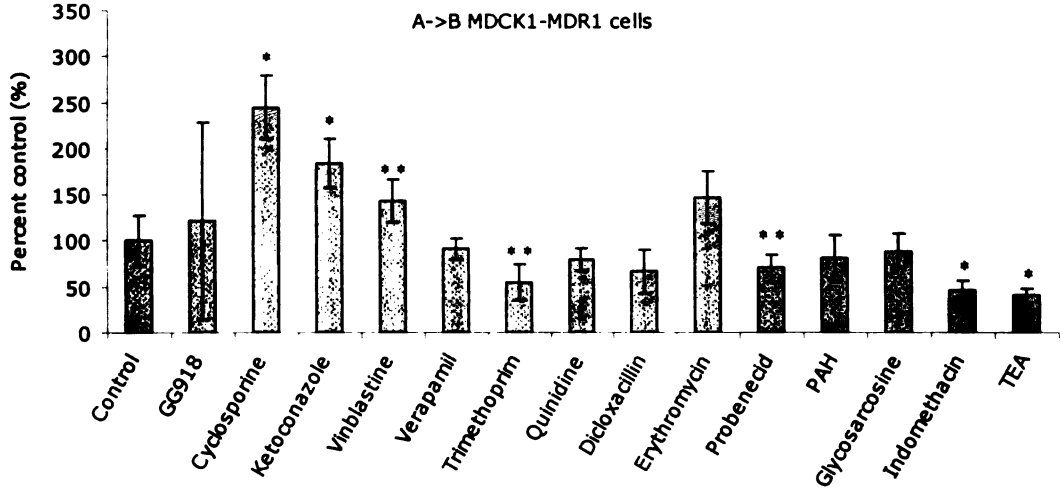

Figure 2.33 Effect of various inhibitors on 25 μM ciprofloxacin A→B transport in MDCK1-MDR1 cells. The inhibitors are GG918 (2.5 μM), cyclosporine (20 μM), ketoconazole (100 μM), vinblastine (100 μM), verapamil (50 μM), trimethoprim (100 μM), quinidine (100 μM), dicloxacillin (100 μM), erythromycin (100 μM), probenecid (100 μM), PAH (100 μM), glycosarcosine (10 mM), sulfinpyrazone (1 mM) and TEA (100 μM). *P<0.01 **P<0.05

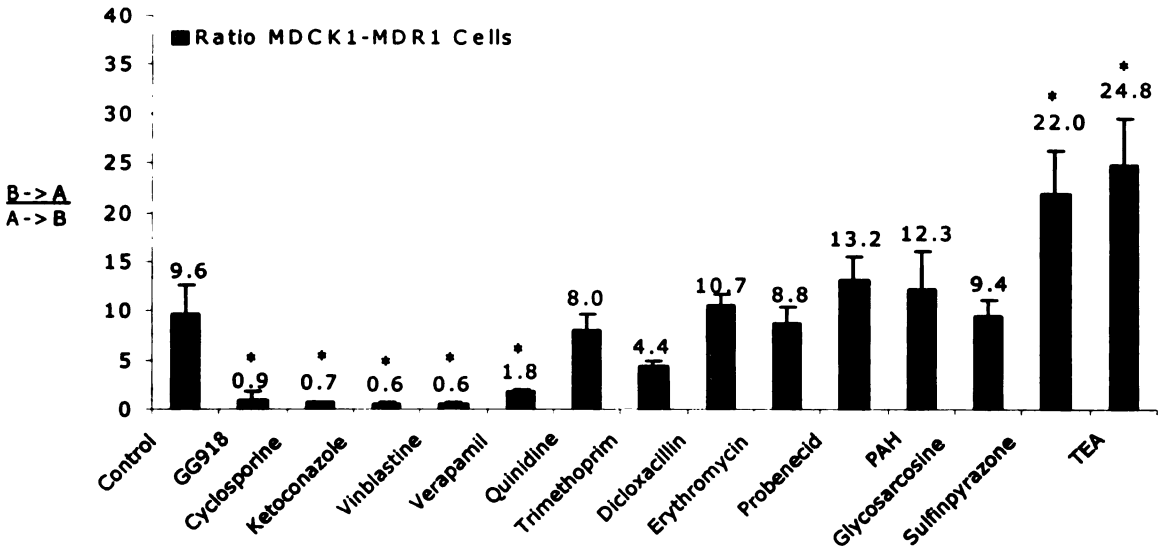

Figure 2.34 Effect of various inhibitors on 25 μM ciprofloxacin B→A/A→B ratio in MDCK1-MDR1 cells. The inhibitors are GG918 (2.5 μM), cyclosporine (20 μM), ketoconazole (100 μM), vinblastine (100 μM), verapamil (50 μM), trimethoprim (100 μM), quinidine (100 μM), dicloxacillin (100 μM), erythromycin (100 μM), probenecid (100 μM), PAH (100 μM), glycosarcosine (10 mM), sulfinpyrazone (1 mM) and TEA (100 μM). *P<0.01

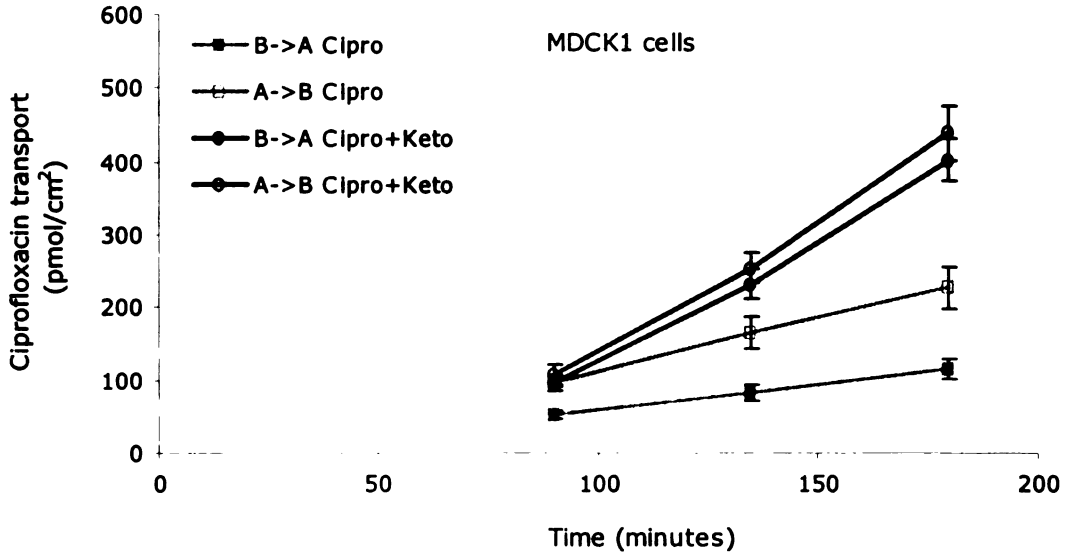

Figure 2.35 Bidirectional transport of 25 μM ciprofloxacin in MDCK1 cells without (gray line) and with 100 μM ketoconazole (black line) cells. ■,●= B→A and □,○ = A→B

In MDCK2 cells, the ciprofloxacin B to A flux is almost equal to the A to B flux (Figure 2.36). This is not what we observed in MDCK1 cells. Western blot and RT-PCR studies show that P-gp expression is higher in MDCK2 compared to MDCK1 cells (Figures 2.4 and 2.5). Therefore, we believe that in MDCK1 cells, which have lower expression of P-gp, the absorptive transporter plays a bigger role than P-gp, which then resulted in higher A to B than B to A fluxes for ciprofloxacin. In MDCK2 cells, where the P-gp expression is higher, the two transporters contribute to the same extent, with equal B to A and A to B fluxes, therefore we do not see the difference between the B to A and A to B fluxes in this cell line. This is only true if ciprofloxacin is a substrate of canine P-gp.

There is no difference in the ciprofloxacin transport between MDCK2 and MDCK2-MRP2 cells (Figure 2.36). The B to A/A to B ratios are around 1 in both cell lines (Table 2.23). This indicates that ciprofloxacin is not a substrate of MRP2. Similar to dicloxacillin and cefsulodin, the B to A and A to B fluxes are lower in MDCK2-MDR1 compared to MDCK2 cells (Figure 2.37). However, unlike dicloxacillin, there is no difference between the B to A and A to B flux for ciprofloxacin in MDCK2-MDR1 cells, with the B to A/A to B ratio of about 1 (Table 2.23). This is similar to what we observed for trimethoprim.

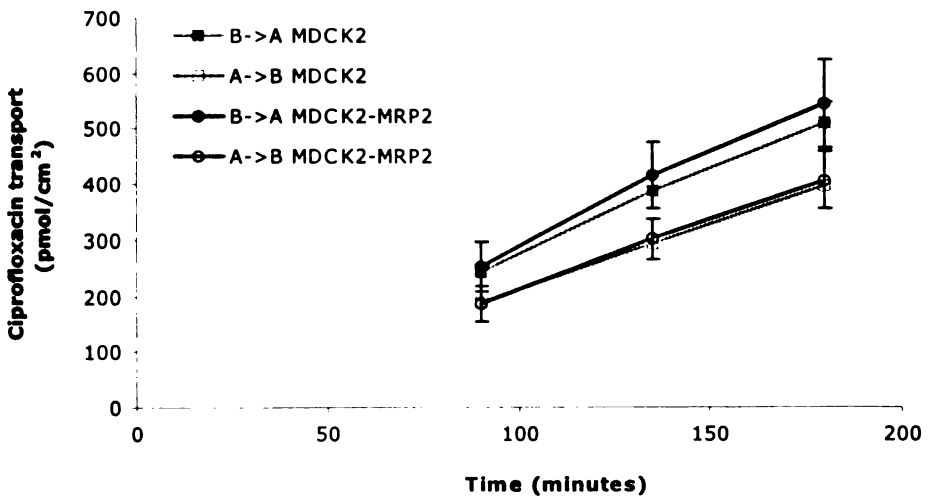

Figure 2.36 Bidirectional transport of 25 μM ciprofloxacin in MDCK2 (gray line) and MDCK2-MRP2 (black line) cells. ■,●= B→A and □,○ = A→B

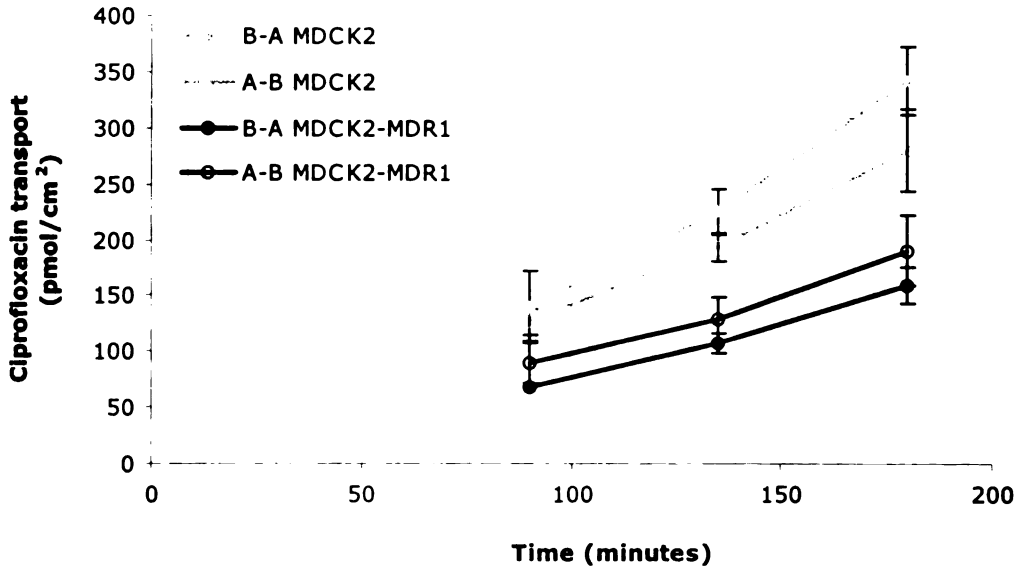

Figure 2.37 Bidirectional transport of 25 μM ciprofloxacin in MDCK2 (gray line) and MDCK2-MDR1 (black line) cells. ■,● = B→A and □,○ = A→B

Table 2.23 Bidirectional transport of 25 μM ciprofloxacin MDCK2, MDCK2-MRP2 and MDCK2-MDR1 cells.

Cell Line	P_{app} x 10^{-7} (avg ± SD, n=3, cm/s)		B→A / A→B
	B→A	A→B	
MDCK2	17.6 (3.6)	15.6 (2.5)	1.1
MDCK2-MRP2	15.0 (1.1)	11.3 (7.3)	1.3
MDCK2-MDR1	6.8 (1.2)	7.5 (1.2)	0.9

All the above data indicates that ciprofloxacin is a substrate of P-gp and an unidentified absorptive transporter. We tried to determine the identity of that unidentified transporter. As mentioned earlier, MRP1 is an efflux pump that is located on the basolateral membrane of epithelial cells and it pumps drugs out from the cells into the basolateral side. Therefore, an MRP1 substrate will exhibit a higher A to B than B to A flux, which is what we observed for ciprofloxacin in MDCK1 cells. Furthermore, MRP1 inhibitors appear to inhibit the transport of this unidentified transporter. Albeit low, MRP1 is expressed in MDCK1 cells (Figure 2.6). Therefore, ciprofloxacin could be a substrate of MRP1. We performed transport studies in LLC-

PK1 and L-MRP1 cells to determine if ciprofloxacin is indeed a substrate of MRP1. Figure 2.38 shows the result of the first transport study with ciprofloxacin in these cell lines. The B to A flux is lower and the A to B flux is higher in the MRP1 overexpressing cell line compared to LLC-PK1 cells. This is the expected pattern of an MRP1 substrate, with the exception that the A to B flux is not higher than the B to A flux in L-MRP1 cells (Table 2.24). However, we were not able to reproduce the result of our first transport study. Subsequent studies indicate that ciprofloxacin is not a substrate of MRP1. There is no ciprofloxacin transport difference observed between LLC-PK1 and L-MRP1 cells, nor is there any difference detected between the B to A and A to B fluxes in these two cell lines (Figure 2.39 and Table 2.25).

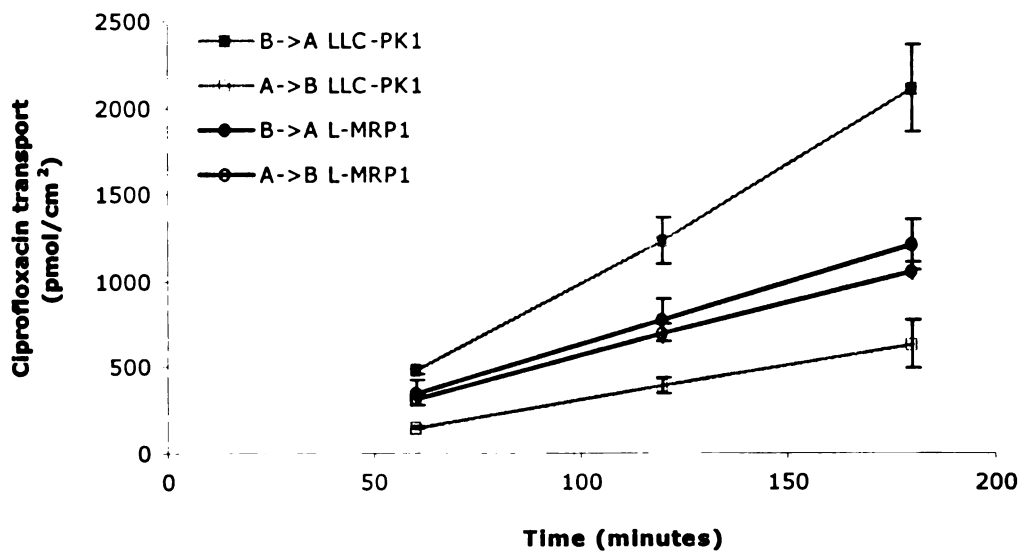

Figure 2.38 Bidirectional transport of 100 μM ciprofloxacin in LLC-PK1 (gray line) and L-MRP1 (black line) cells. ■,●= B→A and □,○ = A→B

Table 2.24 Bidirectional transport of 100 μM ciprofloxacin in LLC-PK1 and L-MRP1 cells.

Cell Line	P_{app} x 10^{-7} (avg ± SD, n=3, cm/s)		B→A / A→B
	B→A	A→B	
LLC-PK1	22.7 (3.3)	6.7 (1.9)	3.4
L-MRP1	12 (1.1)	10.4 (0.6)	1.2

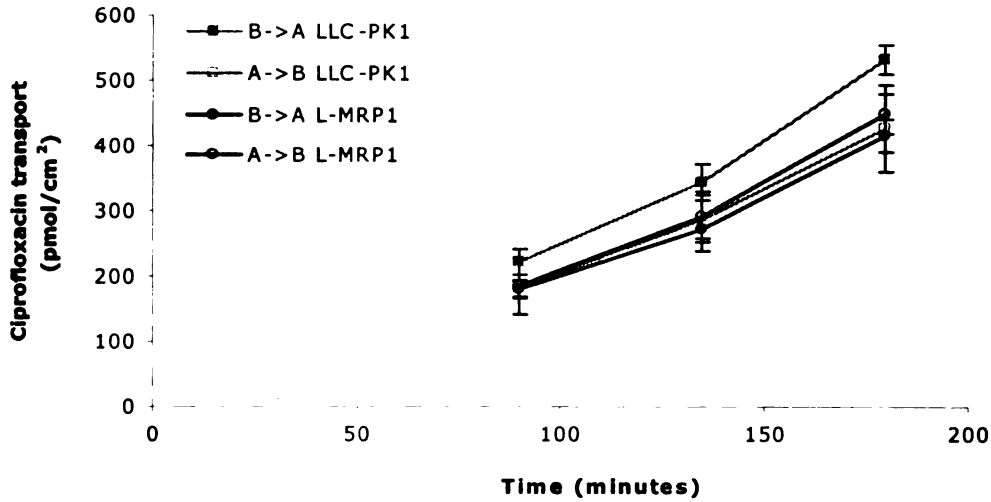

Figure 2.39 Bidirectional transport of 25 μM ciprofloxacin in LLC-PK1 (gray line) and L-MRP1 (black line) cells. ■,●= B→A and □,○ = A→B

Table 2.25 Bidirectional transport of 25 μM ciprofloxacin in LLC-PK1, L-MRP1 and L-MDR1 cells.

Cell Line	P_{app} x 10^{-7} (avg ± SD, n=3, cm/s)		B→A / A→B
	B→A	A→B	
LLC-PK1	23 (2.3)	18 (1.8)	1.3
L-MRP1	17.5 (0.9)	19.6 (1.0)	0.9
L-MDR1	22.6 (1.7)	12.8 (1.8)	1.8

There is no difference in the B to A fluxes of ciprofloxacin between LLC-PK1 and L-MDR1 cells but the A to B flux is slightly lower in L-MDR1 cells (Figure 2.40). The B to A/A to B ratio is about 1 in LLC-PK1 cells and 2 in L-MDR1 cells. The difference in ratios is not statistically significant (Table 2.25). These data are very similar to vinblastine and dicloxacillin, where transport studies in MDCK1 and MDCK1-MDR1 cells indicate that the drug is a substrate of P-gp while no difference is observed in LLC-PK1 and L-MDR1 cells.

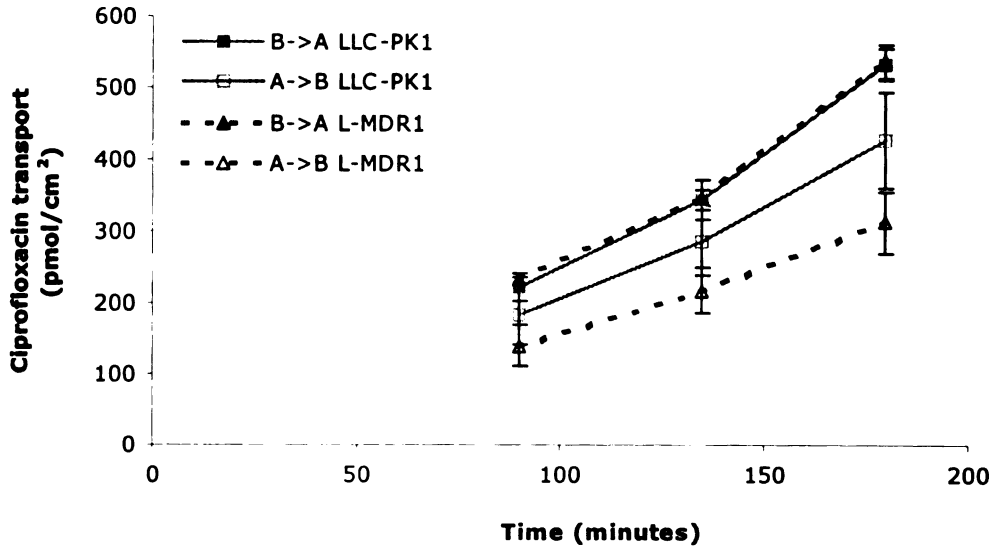

Figure 2.40 Bidirectional transport of 25 μM ciprofloxacin in LLC-PK1 (gray line) and L-MDR1 (dashed line) cells. ■,▲= B→A and □,Δ = A→B

2.4.10 Summary

We performed bidirectional transport studies of 7 compounds to determine if they are substrates of P-gp. Of the seven compounds, three are substrates of P-gp (dicloxacillin, trimethoprim, ciprofloxacin) and four are not substrates of P-gp (sulfamethoxazole, N4-acetylsulfamethoxazole, iothalamate, cefsulodin). Table 2.26 summarizes the results of our bidirectional transport studies

We also tested four compounds (dicloxacillin, trimethoprim, ciprofloxacin, cefsulodin) to find out if they are substrates of MRP1 and MRP2. None of the four compounds were found to be substrates of MRP1 and MRP2. This finding is not surprising because most MRP1 and MRP2 substrates are glucuronide conjugates of the parent drugs instead of the parent drugs themselves.

Table 2.26 Summary of bidirectional transport studies to deduce P-gp substrates

Drugs	CLr in CF patients	P-gp substrates?
Dicloxacillin	↑	YES
Trimethoprim	↑	YES
Sulfamethoxazole	↔	NO
N4-acetylsulfamethoxazole	NA	NO
Iothalamate	↔	NO
Cefsulodin	↔	NO
Ciprofloxacin	↔ ↑	YES

2.5 Discussion and Conclusions

It has been shown clinically that the renal clearance of many (but not all) drugs in CF patients is enhanced and to date, it is not known what causes the enhanced renal clearance. We hypothesize that the enhanced renal clearance is due to increased P-gp expression in CF patients resulting in increased tubular secretion of drugs that are substrates of P-gp. In this study we tested *in vitro* whether dicloxacillin, trimethoprim, sulfamethoxazole, N4-acetylsulfamethoxazole, iothalamate, cefsulodin and ciprofloxacin are substrates of P-gp. Dicloxacillin, trimethoprim and ciprofloxacin show enhanced active renal clearance while sulfamethoxazole, iothalamate and cefsulodin do not show enhanced active renal clearance in CF patients (Table 2.1).

Table 2.1 compares the renal clearance for several drugs between normal and CF patients and these are the drugs with which we chose to test our hypothesis. Ideally, we would like to have well-matched positive and negative controls. We want drugs that have similar fractions excreted into the urine, with high tubular secretion components and well-conducted

comparative studies in controls and CF patients. However, nothing is perfect in research and we did our best to choose representative compounds.

Dicloxacillin was the first drug shown to have enhanced renal clearance in CF patients, with a 3-fold increase in renal clearance compared to normals (195). Dicloxacillin was dosed orally but the bioavailability did not appear to be different since the fraction of dose excreted in the urine was similar between CF patients and controls. However, because a microbial assay was used to measure dicloxacillin concentrations and the drug is known to have an active metabolite, some of the reported increase might have been due to enhanced metabolic clearance.

For trimethoprim and sulfamethoxazole, HPLC assays were used to measure their concentrations but GFR was not studied in those patients thus we could not conclusively rule out the role of GFR on trimethoprim's enhanced renal clearance (201). No enhanced renal clearance was observed for sulfamethoxazole but the renal clearance value was much less than GFR. However, this does not rule out a significant contribution of tubular secretion for sulfamethoxazole. Even though sulfamethoxazole showed a net tubular reabsorption, it is possible that sulfamethoxazole is also secreted but the tubular reabsorption is larger and dominates the renal clearance. Sulfamethoxazole is mostly eliminated by metabolism and the metabolism to N4-acetylsulfamethoxazole accounts for approximately 44% of the dose. There was a 2.5-fold increase in the metabolic clearance of sulfamethoxazole to N4-acetylsulfamethoxazole in CF patients.

For cefsulodin, a study done in 1983 by the Karolinska group showed no increase in renal clearance of cefsulodin in CF patients (196). However, another study done by the same group in 1990 showed that the renal clearance was increased in CF patients but the increase was accounted for by an increase in GFR, therefore it was not due to an enhanced active secretion (206). The increased GFR is believed to be due to the patients' essential fatty acid status (205).

There were several studies done to compare the pharmacokinetic parameters of ciprofloxacin between controls and CF patients (216, 217, 225, 232). There were two studies with oral doses only (216, 225) and two studies with both oral and IV doses (217, 232). Oral dose studies showed no difference in the renal clearance of ciprofloxacin in CF patients. There is a conflicting result with IV dose studies. One study showed no difference (217) while another study showed a higher renal clearance of ciprofloxacin in CF patients (232). Because both oral and IV doses were given, the investigators were able to determine whether bioavailability changes in CF patients. Once again, one study showed no difference (217) while the other study showed a higher bioavailability of ciprofloxacin in CF patients (232). If bioavailability is really increased in CF patients, this may partly explain why no difference in the renal clearance was observed in the oral dose studies.

We believe that the observed enhanced renal clearance of drugs was not caused by changes in protein binding. Studies have shown that there is no difference in protein binding of trimethoprim, dicloxacillin, cefsulodin and sulfamethoxazole between control and CF patients, with fu values of 0.63, 0.05, 0.83 and 0.53, respectively, for the four drugs (195, 196, 201). Arvidsson *et al.* (196) and Hedman *et al.* (206) showed that the renal clearance of cefsulodin is very similar to inulin clearance, therefore cefsulodin does not show net tubular secretion or reabsorption. Dicloxacillin and ciprofloxacin, however, clearly showed net tubular secretion (CL_r >> fu x GFR) (195, 217-232). GFR was not measured by Hutabarat *et al.* (201) for their study with trimethoprim and sulfamethoxazole. By comparing fu x GFR (assuming GFR 100-120 ml/min) with the observed renal clearance values, trimethoprim showed a net tubular secretion while sulfamethoxazole showed a net tubular reabsorption.

To summarize, in CF patients, dicloxacillin, trimethoprim and ciprofloxacin show enhanced active renal clearance while sulfamethoxazole, iothalamate and cefsulodin do not show enhanced active renal clearance and we hypothesize that the increased renal clearance is due to increased tubular secretion caused by increased P-gp expression in CF patients. Therefore, according to our hypothesis, we would expect dicloxacillin, trimethoprim and ciprofloxacin to

be substrates of P-gp and sulfamethoxazole, iothalamate and cefsulodin not to be substrates of P-gp.

We were able to show with our bidirectional transport and inhibition study results in MDCK1 and MDCK1-MDR1 cells that dicloxacillin, trimethoprim and ciprofloxacin are substrates of P-gp while sulfamethoxazole, N4-acetylsulfamethoxazole, iothalamate and cefsulodin are not substrates of P-gp. Our bidirectional transport studies showed that the B→A/A→B ratios in MDCK1-MDR1 cells for dicloxacillin, trimethoprim and ciprofloxacin were significantly greater than 1, with average values of 20, 55 and 14, respectively, values that were very different from the ratios in MDCK cells (~1). Sulfamethoxazole, N4-acetylsulfamethoxazole, iothalamate and cefsulodin, on the other hand, showed no difference in B→A/A→B ratios (all ~1). This suggests that dicloxacillin, trimethoprim and ciprofloxacin are substrates of P-gp while sulfamethoxazole, N4-acetylsulfamethoxazole, iothalamate and cefsulodin are not. Inhibition studies with P-gp and non-P-gp inhibitors further reinforce this conclusion. P-gp inhibitors (e.g., cyclosporine, ketoconazole, vinblastine, GG918) decreased the B→A flux of dicloxacillin, trimethoprim and ciprofloxacin and increased the A→B flux of trimethoprim and ciprofloxacin in MDCK1-MDR1 cells, bringing the B→A/A→B ratios to about 1.

Bidirectional transport studies in MDCK2 and MDCK2-MDR1 cells indicate that dicloxacillin, trimethoprim and ciprofloxacin might not be substrates of P-gp and bidirectional transport studies in LLC-PK1 and L-MDR1 cells indicate that dicloxacillin and ciprofloxacin might not be substrates of P-gp. Currently we do not know the cause of the discrepancy between these P-gp overexpressing cell lines. Vinblastine, a well-known P-gp substrate, also did not show a difference between LLC-PK1 and L-MDR1 cells. It is possible that besides P-gp, the expression of another transporter is upregulated in MDCK1-MDR1 cells and this transporter is responsible for the observed B to A/A to B difference between MDCK1 and MDCK1-MDR1 cells for dicloxacillin, trimethoprim, ciprofloxacin and vinblastine and the activity of this transporter is inhibited by the P-gp inhibitors used in our studies. Another explanation could be that MDCK2-MDR1 and L-MDR1 may not be the right cell lines to use to determine whether a drug is a substrate of P-gp. Western blot studies have shown that P-gp expression is elevated in

MDCK2-MDR1 and L-MDR1 cells compared to MDCK2 and LLC-PK1 cells, respectively, but we do not know whether the P-gp expression is located on the membrane. Further studies need to be performed to characterize these P-gp overexpressing cell lines.

In addition to determining if our drugs are substrates of P-gp, we also ran bidirectional transport studies in MRP1 (L-MRP1) and MRP2 (MDCK2-MRP2) overexpressing cell lines to see if these drugs are also substrates of MRP1 and/or MRP2. Our results showed that dicloxacillin, trimethoprim, ciprofloxacin and cefsulodin are not substrates of either MRP1 or MRP2. However, we discovered that ciprofloxacin, besides being a substrate of P-gp, is also a substrate of an unidentified absorptive transporter. This could partly explain the conflicting renal clearance values observed in CF patients. The renal clearance of ciprofloxacin may depend on the relative expression of P-gp and this transporter that works in the opposite direction of P-gp.

To conclude, thus far, our in vitro studies appear to support the hypothesis that P-gp may be responsible for the enhanced renal clearance in CF patients.

Chapter 3

Mice Breeding and Genotyping

3.1 Overview

We hypothesize that enhanced renal clearance of antibiotics in cystic fibrosis patients is due to elevated P-gp expression in the kidney of those patients. Thus far, our *in vitro* studies appear to support the hypothesis. It seemed logical to next perform *in vivo* pharmacokinetic studies to test if P-gp expression level affects the renal clearance values of antibiotics that are substrates of P-gp, like the ones that show enhanced renal clearance in cystic fibrosis patients. To do this we require *in vivo* models that exhibit different expression levels of P-gp.

P-gp knockout mice have been constructed by Schinkel and coworkers (282-286). Cystic fibrosis mouse models have also been constructed by several investigators (56, 287-295). If our hypothesis is correct and if cystic fibrosis mice mimic cystic fibrosis patients, we would expect the CF mice to have a higher P-gp expression compared to wild type mice, yielding mice with different P-gp expression levels. The level of P-gp expression in those mice would be as follows: CF mice > wild type mice > P-gp knockout mice. P-gp knockout and CF mice are bred in different strains of mice hence we have two strains of wild type mice. Therefore, for the *in vivo* pharmacokinetic experiments, we have four groups of mice: P-gp wild type (FVB), P-gp knockout (*mdr1ab (-/-)*), CF wild type (C57Bl/6J) and CF (ΔF508) mice.

P-gp wild type and P-gp knockout mice can be purchased from Taconic (Germantown, New York). On the other hand, we needed to breed our own CF mice due to the difficulty in obtaining CF mice commercially. Table 3.1 lists the published mouse information such as breeding age, breeding life, litter size, etc.

Table 3.1 Mouse information. Adapted from The UCSF Animal Care and Use Training Manual (296)

Item	Normal Value	Reference
Breeding age, female	28-49 days	297
Breeding age, male	28-49 days	297
Estrous cycle	4-5 days, postpartum	298
gestation	19-21 days	297
Birth weight	1-1.5 g	297
Weaning age	21 days	297
Begin dry food	10 days	298
Litter size	4-12	297
Time to remate	Postpartum	298
Breeding life, female	6-10 litters	298
Breeding life, male	18 months	298
Mating ratio	Pairs, 1 male - 3 females	298
Life span	1.5 yr avg, 3 yr max	297
Weight, adult male	20-40 g	297
Weight, adult female	25-40 g	297
Blood volume	5.85 ml/100g	297
Daily food consumption	5g/8 weeks of age	297
Daily water consumption	6.7 ml/8 weeks of age	297
Daily urinary output	0.5-1ml	297
Maximum safe bleed	7.7 ml/kg	formulary
Respiration rate	163 breaths/min	297
Heart rate	310-840 beats/min	297
Chromosome number	40	298
Rectal temperature	37.5°C	297

3.2 Cystic Fibrosis Mouse Models

3.2.1 Introduction

At the present time, ten models of cystic fibrosis mice have been constructed. Grubb and Boucher (299) have written a very comprehensive review of all types of CF mice available to date. In essence, there are two types of CF mice, a complete *cftr* gene knockout or a specific point mutation in the *cftr* gene. Table 3.2 lists all the CF mouse models constructed to date.

Table 3.2 Mouse models of cystic fibrosis. Adapted from Grubb and Boucher (299)

Type	CF Mouse	Molecular Technique	Reference	Year
Cftr	*cftr*^{tm1Unc}	inframe stop (exon 10)	287	1992
knockouts	*cftr*^{tm1Hgu}	insertion (exon 10)	288	1992
	cftr^{tm1Cam}	insertion (exon 10)	289	1993
	cftr^{tm1Bay}	duplication (exon 3)	290	1993
	cftr^{tm3Bay}	inframe stop (exon 2)	291	1995
	cftr^{tm1Hsc}	insertion (exon 1)	56	1996
ΔF508	*cftr*^{tm1Kth}	homologous recombination	292	1995
	cftr^{tm1Eur}	homologous recombination	293	1995
	cftr^{tm2Cam}	homologous recombination	294	1996
G551D	*cftr*^{TgHm1G551D}	homologous recombination	295	1996

The first CF mouse model constructed was the *cftr*^{tm1Unc}, completed in 1992, three years after the *CFTR* gene was cloned. Around the same time, *cftr*^{tm1Hgu} was created. Thus far, six *cftr* knockouts have been constructed. Gene targeting strategies used to create the knockout models lead to absence of *cftr* production, which is expected to mimic cystic fibrosis disease. However, the majority of the CF patients (>70%) have ΔF508 mutation, which is a loss of three nucleotides (CTT) that lead to a deletion of phenyalanine at position 508. Therefore the ΔF508 mouse models were created three to four years later. As in human, ΔF508 mutation in mice causes an abnormal processing of *cftr* and most proteins do not reach the plasma membrane. The *cftr*^{TgHm1G551D} model was created to study the effect of G551D mutation, which

is also a relatively common mutation in CF patients. Patients with this mutation show a genotype/phenotype correlation in that the incidence of meconium ileus is reduced threefold compared to patients with ΔF508 mutation. G551D mutation produces *CFTR* protein that is processed normally but has a reduced cAMP-regulated Cl^- activity (299).

All of the CF mouse models were generated using the same general technique. First, the *cftr* gene is mutated, then cloned into a targeting vector and inserted into murine embryonic stem cells. In a small number of stem cells, homologous recombination occurs that integrate the mutated *cftr* gene into the *cftr* locus of the stem cells. The next step is to screen the stem cells that have the mutated gene. Once the stem cells are isolated, they are expanded and injected into blastocytes and transplanted into a pseudo-pregnant mother. Mice that contain the *cftr* mutated gene can be identified by coat color since they are chimera of normal and mutant cells, which have different coat color. The chimera are bred together and of the chimera that have the mutated gene in their germ cells, a quarter of their pups will be homozygous mutant (299).

The hallmark of the CF mouse model is the intestinal pathology, with accumulation of mucus in the crypts of Lieberkuhn, goblet cell hypertrophy, hyperplasia and eosinophilic concentration in the crypts. A majority of CF mouse pups (50-95%) die because of the intestinal complications. There are two distinct time periods of death, the first is within 5 days of birth and the second is shortly after weaning. The death rate in the second period can be reduced by placing the CF mice on a liquid diet or a less expensive alternative, substituting the drinking water with Colyte (an electrolyte solution containing 6% polyethylene glycol). Most CF mice exhibit the same symptoms with the exception of $cftr^{tm1Hgu}$, $cftr^{tm1Eur}$ and $cftr^{TgHm1G551D}$ mice (299).

$Cftr^{tm1Hgu}$ is one of the six *cftr* knockout mouse models. Because $cftr^{tm1Hgu}$ mice are created by insertion rather than the replacement gene method, exon skipping and aberrant splicing produce some normal *cftr* mRNA, which explains why $cftr^{tm1Hgu}$ mice have a milder

gastrointestinal phenotype compared to the other *cftr* knockout mice. As much as 20% of wild type mRNA is detectable in their intestines (up to 10% in their airway epithelia) (299).

Cftr^{tm1Eur} (ΔF508) mice do not express any wild type mRNA. However, they express normal levels of ΔF508 mRNA, which may allow more of the mutant protein to be correctly processed and more protein to reach the plasma membrane. Once it reaches the membrane, ΔF508 *cftr* protein can function as a Cl^- channel, albeit with a decrease in open channel probability. Therefore, *cftr*^{tm1Eur} mice also do not exhibit very severe intestinal complications. The other two ΔF508 models, *cftr*^{tm1Kth} and *cftr*^{tm2Cam} mice, express much lower levels of ΔF508 mRNA and they exhibit a more severe intestinal pathology than *cftr*^{tm1Eur} mice (299).

Cftr^{TgHm1G551D} mice have milder intestinal symptoms because G551D mutation produces *cftr* protein that is processed normally but has reduced cAMP-regulated Cl^- activity. Therefore this mouse model mimics the patients with G551D mutation (299).

Cftr^{tm1Hsc} exhibit the same symptoms as other CF mice, with severe intestinal pathology, no functioning *cftr* and early death. However, there is a subset of *cftr*^{tm1Hsc} mice designated class III mice that have normal survival rates and normal body mass. The intestinal tract of these mice show an alternative Ca^{2+}-activated Cl^- channel (Cl_A), that may compensate for the loss of *cftr*. It is thought that there might be modifier gene(s) in chromosome 7 that modulate the severity of disease in these class of mice (299).

Pulmonary pathology is the major cause of death in CF patients. However, unlike human, all the CF mouse models (knockouts, ΔF508 and G551D) do not show any pathology in the lower airways and only a minor pathology in the upper airways. There are two hypotheses as to why CF mice do not exhibit marked pathology in the lung. First, murine airway (but not intestinal) epithelia cells have intracellular Ca^{2+}-activated Cl^- channel (Cl_A) which seems to play a small role in normal mice but is quite active in CF mice. It is thought that this Cl_A might replace the function of defective *cftr*, therefore protecting the lungs. Second,

hyperpolarization of Na^+ is thought to cause lung pathology in CF patients and this hyperpolarization is absent in the lower airways of CF mice (299).

There are two phenotypic markers of CF mice. They are relatively smaller compared to normal mice and they have very white incisor teeth. The white teeth are present in all CF mice regardless of their intestinal disease severity, even in CF mice that are corrected by the insertion of human *CFTR* gene (299, 300). The enamel of the incisor teeth in normal mice are hard and yellow-brown as they mature while it is soft and chalky white in CF mice (299). This is due to abnormal enamel development. Several studies have compared the mineral contents between normal and CF mouse enamels (301-303). All reports agree that the CF mouse enamel has a decreased calcium content. However, there are discrepancies in the analysis of mineral content between normal and CF mice. Arquitt *et al.* (301) reported that the calcium-phosphorus ratio is decreased in CF mouse enamel, while Wright *et al.* (302) reported no difference. Gawenis *et al.* (303) noted no difference in potassium levels and a reduced iron content in CF while Arquitt *et al.* (301) showed an increase in both potassium and iron levels in CF teeth. Arquitt *et al.* (301) suggested that these discrepancies could be partially explained by measurement techniques and the areas of tissue sampled. However, it is interesting that Arquitt *et al.* (301) report a higher iron content in CF mouse enamel since it is thought that the iron is responsible for the yellow-brown pigmentation of mouse incisors (304). Since CF mice have chalky white incisors, we would expect the iron content to be lower in CF enamel as shown by Gawenis *et al.* (303). Arquitt *et al.* (301) argued that since the iron levels found in CF teeth are consistent with previous reports (305, 306), other factors beside iron deficiency are responsible for the white opaque coloration in CF mouse enamel. It is also interesting that, unlike the incisors, there is no difference in the mineral content of the slow-growing brachydont molar teeth even though both incisors and molar teeth buds express *cftr* mRNA (303, 301). Arquitt *et al.* (301) hypothesized that the discrepancy could be due to developmental differences between molars and incisors or the way the *cftr* channel is utilized during incisor amelogenesis versus molar amelogenesis. From these studies, it is clear that the exact mechanism responsible for the abnormal enamel development in CF mice remains to be elucidated.

In humans, most males are infertile and females have reduced fertility. In CF mice it is reversed. Male CF mice are fertile and generate normal size litters. Even though the female CF mice do not show pathology in the reproductive tract, they show a marked reduced fertility. However, it has been reported that female *cftr*^{tm1Kth} mice exhibit normal fertility (299). From our personal experience with *cftr*^{tm1Kth} and *cftr*^{tm1Eur} mice, it appears that the fertility in CF female mice is indeed reduced.

3.2.2 Breeding of CF mice

Due to the reduced fertility of CF female mice and the high mortality rate associated with intestinal pathology, it is very challenging to obtain viable CF homozygous mice. *Cftr*^{tm1Kth} and *cftr*^{tm1Unc} mice may be purchased from the Jackson Laboratory (Bar Harbor, Maine). However, they are not readily available. It takes at least six months from the day of order to obtain a limited number of mice and they are very expensive (~$300/mouse). Therefore, we decided to breed CF mice in our animal care facility.

We chose to breed the ΔF508 CF model since ~70% of CF patients have this mutation. To initiate the breeding project, we were able to obtain several heterozygote male and female *cftr*^{tm1Kth} (The Jackson Laboratory, Bar Harbor, Maine) and *cftr*^{tm1Eur} mice (Mathias Lab, UCSF, San Francisco). As shown in Table 3.2, both *cftr*^{tm1Kth} and *cftr*^{tm1Eur} are ΔF508 mice model. Since *cftr* is a recessive gene, according to Mendelian rule, from mating a heterozygote female with the heterozygote male mouse, a quarter of the pups will be homozygous CF mice, a quarter will be homozygous wild type and the remaining half will be heterozygotes (Figure 3.1). However, because of the high mortality associated with CF mice, in reality we expect a much lower yield of CF mice. To decrease the mortality associated with intestinal pathology, drinking water was substituted with Colyte solution (GoLytely, PEG 3350, Braintree, Braintree, Massachusetts).

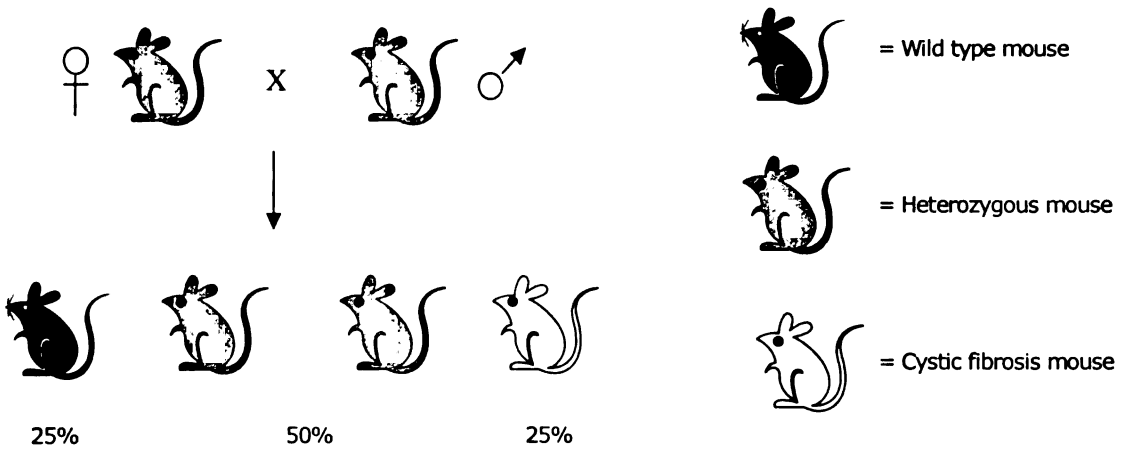

Figure 3.1 A cartoon representation of the expected offsprings from mating two heterozygous mice

To obtain a higher percentage of homozygous CF mice, after we obtained the homozygous male CF mice, we mated the homozygous male with the heterozygous female (the homozygous female mice have reduced fertility). Figure 3.2 depicts the theoretical expectation, but as stated above, the actual percentage of homozygous CF mice will be lower than 50%.

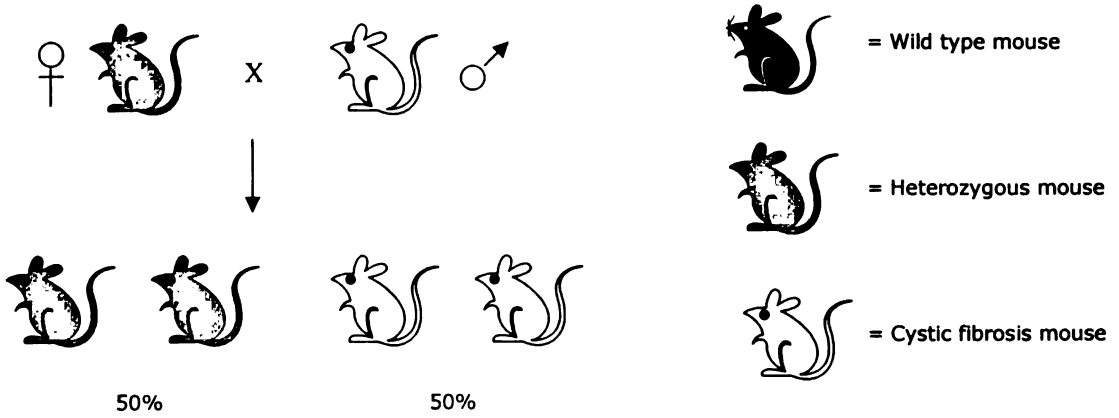

Figure 3.2 A cartoon representation of the expected offsprings from mating a heterozygous female with the homozygous CF mouse

3.2.3 Genotyping

To determine the genotype of each mouse, DNA is isolated from a small segment of mouse tail and a segment of the DNA is amplified by polymerase chain reaction (PCR) with the appropriate primers. Depending on whether the DNA is from a wild type, knockout or heterozygous mouse, the PCR results will be different for each type of mouse.

3.2.3.1 How to genotype *cftr*^{tm1Eur} mice

Cftr^{tm1Eur} mice were genotyped according to the protocol provided by Dr. Xiaohui Fang (Mathias Lab, UCSF, San Francisco). To genotype *cftr*^{tm1Eur} mice, a PCR product is generated using MCF1 (sense) and MCF3 (antisense) primers (Table 3.3) that produce a 450 bp band that is then subjected to *Ssp*I enzyme. The PCR product from the *cftr*^{tm1Eur} mice contains an *Ssp*I restriction site (AATATT), which is digested to two bands (150 and 300 bp). This restriction site is absent from the wild type mice. In creating the ΔF508 construct (deletion of CTT that leads to deletion of phenylalanine at position 508 in exon 10), the creator also changes the C base (3 bp before the deletion of CTT) with a T base. The single point mutation does not change the amino acid that it codes (both TCA and TTA code for isoleucine) but it creates a recognition site for *Ssp*I enzyme (see Figure 3.3). *Ssp*I is an enzyme that is isolated from *Sphaerotilus species* and it digests in the middle of AATATT sequences.

*Ssp*I recognition sequence:

5′-AAT↓ATT-3′
3′-TTA↑TAA-5′

Table 3.3 Primer sequences for genotyping *cftr*^{tm1Eur} mice

Primer Name	Sequences
MCF1 (sense)	5'-CCC TTT TCA AGG TGA GTA GTC AAG-3'
MCF3 (antisense)	5'-GCC TAG AAA AGT CCC TGT ATC ATG-3'

Wild type mice

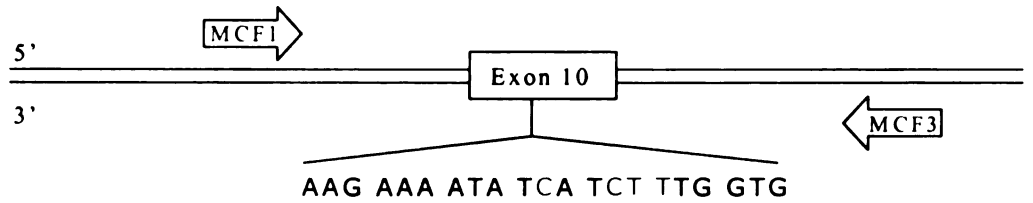

Cftr^{tm1Eur} mice

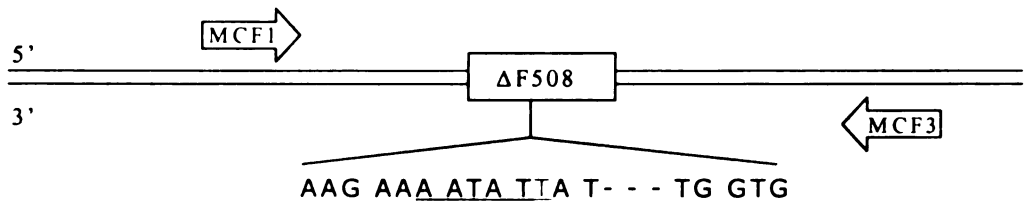

Figure 3.3 A cartoon representation of the difference in DNA sequences between wild type and *cftr*^{tm1Eur} mice. The underlined sequence is the *SspI* recognition site.

A heterozygous *cftr*^{tm1Eur} mouse will have two different alleles of *cftr*, one wild type and one mutant *cftr*. The wild type *cftr* allele will yield a PCR product that does not contain an S*sp*I recognition site while the mutant allele will yield a PCR product that contains an S*sp*I recognition site. Therefore, after S*sp*I digestion, from a heterozygous mouse we expect to see three bands: 150, 300 (product of S*sp*I) and 450 (uncut PCR product) bp. Table 3.4 lists the expected results after digesting with S*spI* enzyme for the three different mouse types .

Table 3.4 Expected PCR result after digesting with S*sp*I enzyme for *cftr*^{tm1Eur} mice

Homozygous Wild Type	**Heterozygote**	**Homozygous *cftr*^{tm1Eur} Mice**
	150 bp	150 bp
	300 bp	300 bp
450 bp	450 bp	

3.2.3.2 How to genotype *cftr*^{tm1Kth} mice

Cftr^{tm1Kth} mice were genotyped according to the protocol provided by Jackson Lab (Bar Harbor, Maine). To genotype *cftr*^{tm1Kth} mice, a PCR product is generated using IMR 269 (sense), IMR 270 (antisense) and IMR 271 (sense) primer pairs (Table 3.5). IMR 269 recognizes neo^r sequences that are not present in the DNA of wild type mice. Therefore DNA from wild type mice will only have one ~430 bp band that is the PCR product of IMR 270 and IMR 271 primer pairs. On the other hand, DNA from *cftr*^{tm1Kth} mice do have neo^r sequences, therefore IMR 269 and IMR 270 produce a 300 bp band. Because of the insertion of neo^r gene, IMR 270 and IMR 271 produce a band that is larger than 3 kb that may not show in the gel because the PCR condition is not optimized to amplify a large size PCR product (Figure 3.4).

Table 3.5 Primer sequences for genotyping *cftr*^{tm1Kth} mice

Primer Name	Sequences
IMR 269 (sense, neo^r)	5'-TTC AAG CCC AAG CTT TCG CGA G-3'
IMR 270 (antisense, common)	5'-CTC CCT TCT TCT AGT CAC AAC CG-3'
IMR 271 (sense, wt)	5'-CAT CTT GAT AGA GCC ACG GTG C-3'

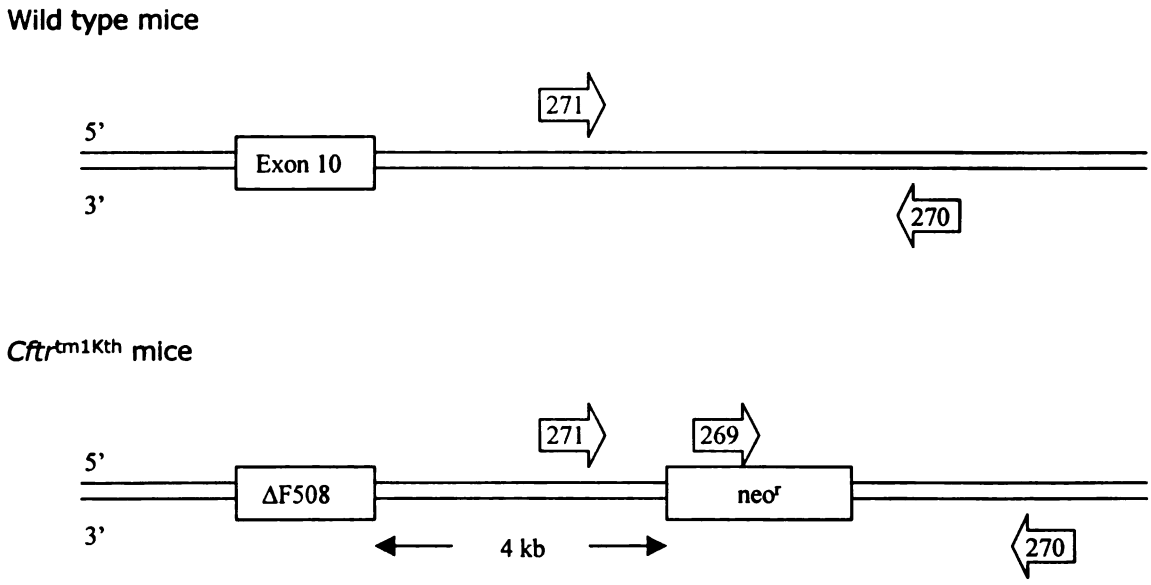

Figure 3.4 A cartoon representation of the difference in DNA sequences between wild type and *cftr*^{tm1Kth} mice

DNA from heterozygous mice will contain one allele without the neo^r and one allele with the neo^r sequences. Hence, we expect two different size bands, 300 bp (*cftr* mutant allele) and 430 bp (wild type *cftr* allele) (Table 3.6)

Table 3.6 Expected PCR result with IMR 269, 270 and 271 primers

Homozygous Wild Type	**Heterozygote**	**Homozygous *cftr*^{tm1Kth} Mice**
	300 bp	300 bp
430 bp	430 bp	

3.2.3.3 How to detect ΔF508 allele

Sections 3.2.3.1 and 3.2.3.2 describe how to genotype *cftr*^{tm1Eur} and *cftr*^{tm1Kth} mice. Those genotyping methods are based on how the knockout mice are constructed. There is another way to genotype the mice based on whether or not the mice have the ΔF508 allele in their *cftr* gene. This method was provided by Jackson Lab (Bar Harbor, Maine). Since ΔF508 allele resulted from the CTT deletion, we can design different primers for wild type and ΔF508 alleles of the *cftr* gene. The two primers will only differ in the last three nucleotides of their forward primer: primer for wild type gene ending with CTT while the primer for ΔF508 allele will skip the CTT and takes on the next three nucleotides from the *cftr* gene, TGG (Table 3.7).

Table 3.7 Primer sequences for genotyping the presence of ΔF508 gene

Primer Name	**Sequences**
IMR 272 (sense, wt)	5'-GGT ACT ATC AAA GAA AAT ATC ATC TT-3'
IMR 273 (sense, ΔF508)	5'-GGT ACT ATC AAA GAA AAT ATC ATT GG-3'
IMR 274 (antisense, common)	5'-TTA TCA CAA CAC TGA CAC AAG TAG C-3'

Both primer pairs will generate a 160 bp product. To genotype for the presence or absence of ΔF508 allele, run one PCR reaction with wild type primer pair and run another reaction with ΔF508 allele primer pair. Homozygous wild type mice will show bands only from the reactions

with the wild type primers, homozygous knockout will have bands from the ΔF508 allele primer pair while the heterozygous mice will have bands from both reactions. This method has the advantage over the other two methods in that it directly shows whether or not the mice have the intended ΔF508 allele. However, for every mouse you need to run two reactions instead of one to determine its genotype. Therefore, we did not employ this method to genotype the mice but it is presented here for reference purposes.

3.3 P-glycoprotein Mouse Models

3.3.1 Introduction

In humans there is only one gene (*MDR1*) that codes for P-gp but in mouse, there are two genes. They are called *mdr1a* (also called *mdr3* or *abcb1a*) and *mdr1b* (also called m*dr1* or *abcb1b*). *Mdr2* (also called *abcb4*) is a gene that encodes a protein that is closely related to P-gp (307). Figure 3.5 shows a schematic representation of these three genes in the mouse chromosome.

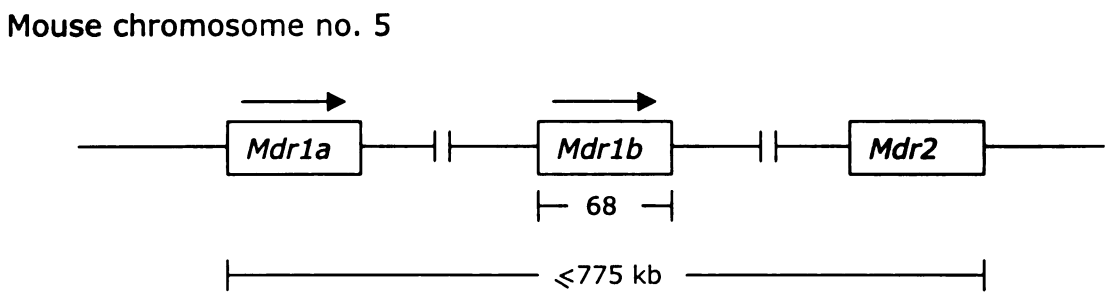

Figure 3.5 Schematic representation of the mouse P-glycoprotein gene locus. The arrows represent the direction of transcription. Adapted from Borst and Schinkel (307)

Mdr1a and *mdr1b* are the homologues of the human *MDR1* gene. They encode functional P-gp that can transport drugs. *Mdr1a* is expressed in the intestine, blood brain barrier and blood testis barrier, while *mdr1b* is highly expressed in the adrenal glands, pregnant uterus and ovaries. Both genes are also expressed in liver, kidney, heart, lung and spleen (284). *Mdr2* is the homologue of the human *MDR3* (also known as *MDR2*) gene. This gene does not encode a protein that can transport drugs. *Mdr2* is only expressed in a few tissues, with the highest

concentration in the liver, on the canalicular membrane of the hepatocyte. It is known to transport phosphatidylcholine, one of the major constituents of bile (307).

Mdr1a (-/-), *mdr1b* (-/-), *mdr2* (-/-) and the double knockout, *mdr1ab* (-/-) mice have been constructed in the laboratories of Dr. Alfred Schinkel (282-285, 308, 309). All four types of *mdr* knockout mice are viable and fertile with no visible phenotypic differences. The complete loss of the *mdr1a* gene does not appear to have a lethal effect on mice. Besides the *mdr1a* (-/-) mice created by Dr. Schinkel, there is a naturally occurring *mdr1a* (-/-) mice in CF-1 (Carworth Farm) strain mice (310, 311), which is available from Charles River Laboratories (Wilmington, Massachusetts). Even though mice deficient in the *mdr1a* gene have no visible phenotypic differences, these mice are hypersensitive to drugs that are transported by P-gp. The loss of *mdr1a* could be fatal to the mice if they are exposed to certain drugs, such as ivermectin, which is a substrate of P-gp (282, 308, 312-314). The *mdr1a* (-/-) mice have completely lost all detectable P-gp in gut epithelia and brain capillaries and the absence of the *mdr1a* gene does not lead to an activation of the *mdr1b* gene in these tissues, as well as in brain, heart, lung, muscles, spleen, thymus, testis, ovary and uterus. However, in liver and kidney there was a more than two-fold increase in *mdr1b* expression (307). Thus it appears that the pharmacological role of the *mdr1a* gene is to protect the brain against entry of a range of xenobiotics and drugs and in limiting the entry of these drugs from the intestinal lumen (284).

As with *mdr1a* (-/-) mice, *mdr1b* (-/-) mice display normal viability and fertility. P-gp expression is not detectable in adrenal gland membrane immunoblots. However, unlike *mdr1a* (-/-) mice, there is no compensation for the loss of *mdr1b* gene in *mdr1b* (-/-) mice. Utilizing the RNAse protection assay, *mdr1a* expression is not significantly altered in the adrenal gland, uterus, liver, kidney, heart, lung, skeletal muscle, stomach, jejunum, colon, cecum, spleen, thymus, testis, ovary, uterus and brain of *mdr1b* (-/-) mice. Pregnancy and litter size are also normal in *mdr1b* (-/-) mice. The lack of effects of *mdr1b* gene loss could be explained by the fact that the more abundant *mdr1a* gene could be taking over its function (284).

Mdr2 (-/-) mice show liver defects. The bile of the homozygous knockout mice have no detectable level of phosphatidylcholine (PC) while the heterozygous mice show half the normal level of PC. When the lack of *mdr2* gene is compensated by the *MDR3* gene (human homolog of the *mdr2*), driven by the albumin promoter, the PC levels in the bile were normal and the liver pathology was not observed (307).

The *mdr1ab* (-/-) mice do not have the protective function of P-gp since both the genes that code for P-gp are knocked out. The *mdr1ab* (-/-) mice are viable and fertile and they do not show any abnormalities. Just like *mdr1a* (-/-) mice, they lack the protective function of the blood brain barrier, and an increase in digoxin accumulation was exhibited in the brain, adrenal glands, testis (male) and ovaries (female) (284). Since this model lacks both *mdr1a* and *mdr1b* genes, we chose to use this mice model in our pharmacokinetic studies.

Because the *mdr1ab* (-/-) mice are fertile, obtaining the knockout mice is not a problem. You simply mate the homozygous female with the homozygous male knockout mice. The P-gp knockout mice are available for purchase from Taconic (Germantown, New York). The corresponding wild type mice (FVB) are also available from Taconic. Since there is no phenotypic difference between the wild type and knockout mice, we need to run a PCR reaction to confirm the genotype of the mice. Since it is a P-gp double knockout, we need to test for both the *mdr1a* and *mdr1b* gene.

3.3.2 Genotyping

Mdr1ab (-/-) mice were genotyped according to the protocol provided by Taconic (Germantown, New York). To genotype *mdr1ab* (-/-) mice, perform both the genotyping protocols for *mdr1a* (-/-) and *mdr1b* (-/-) mice.

3.3.2.1 How to genotype *mdr1a* (-/-) mice

For *mdr1a*, the HSAS1 and HSAS2 primer pair (Table 3.8) will recognize the DNA sequence from the wild type mice to produce a PCR fragment of 411 bp while the HSAS7 and HSAS8

primer pair (Table 3.8) will only recognize the DNA sequence from the knockout mice to generate a PCR band of 481 bp. The heterozygous mice will have both bands but since we only buy homozygous wild type or knockout mice, we will not expect to see a double band in our PCR result (Table 3.9).

Table 3.8 Primer sequences for genotyping *mdr1a* gene

Primer Name	**Sequences**
HSAS1 (sense, wild type)	5'-CAG CTC CAT CCA ACA ACT TC-3'
HSAS2 (antisense, wild type)	5'-GAC ACA GGT ACT GTC CAC AG-3'
HSAS7 (sense, knockout)	5'-ATG TCC TGC GGG TAA ATA GC-3'
HSAS8 (antisense, knockout)	5'-CGT CAG GAC ATT GTT GGA GC-3'

Table 3.9 Expected PCR results for *mdr1a* gene

Homozygous Wild Type	**Heterozygote**	**Homozygous Knockout**
411 bp	411 bp	
	481 bp	481 bp

3.3.2.2 How to genotype *mdr1b* (-/-) mice

For *mdr1b*, the HSAS3 and HSAS6 primer pair (Table 3.10) will recognize the DNA sequence from the wild type mice to produce a PCR fragment of 540 bp while the HS5NEO and HS3NEO2 primer pair (Table 3.10) will only recognize the DNA sequence from the knockout mice to generate a PCR band of 453 bp. The heterozygote mice will have both bands but since we only have homozygous wild type or knockout mice, we will not expect to see a double band in our PCR result (Table 3.11).

Table 3.10 Primer sequences for genotyping *mdr1b* gene

Primer Name	Sequences
HSAS3 (sense, wt)	5'-GAG AAA CCA TGT CCT TCC AG-3'
HSAS6 (antisense, wt)	5'-AAG CTG TGC ATG ATT CTG GG-3'
HS5NEO (sense, KO)	5'-TGT CAA GAC CGA CCT GTC CG-3'
HS3NEO2 (antisense, KO)	5'-TAT TCG GCA AGC AGG CAT CG-3'

Table 3.11 Expected PCR results for *mdr1b* gene

Homozygous Wild Type	Heterozygote	Homozygous Knockout
	453 bp	453 bp
540 bp	540 bp	

3.4 Materials and Methods

3.4.1 Materials

3.4.1.1 DNA isolation

Mice tail fragments, DNeasy Tissue Kit (Qiagen, Valencia, CA), Type 16500 Dri-bath (Barnstead Thermolyne (Dubuque, IA), RNase free tube (Ambion, Austin, TX), X Systems centrifuge (Abbott Laboratories, Abbott Park, IL) were utilized for DNA isolation.

3.4.1.2 PCR

RedTaq ReadyMix PCR Reaction Mix (Sigma, St. Louis, MO), *Ssp*I enzyme (Gibco BRL Life Technologies, Grand Island, NY), X Systems centrifuge (Abbott Laboratories, Abbott Park, IL), MCF1, MCF3, IMR 269, 270 and 271, HSAS 1, 2, 3, 6, 7 and 8, HS5NEO and HS3NEO2 primers (Invitrogen Life Technologies, Carlsbad, CA), Pipetman (Rainin, Woburn, MA), Fisher Vortex Genie 2 (Fisher Scientific, Santa Clara, CA), ART RNase & DNase free tip (Molecular BioProduct, San Diego, CA), PCR Express (Thermo Hybaid, Ashford, Middlesex, United

Kingdom), 0.2 ml PCR tubes (Ambion, Austin, TX), Fisher Minifuge (Fisher Scientific, Santa Clara, CA) were utilized for the PCR reaction.

3.4.1.3 Electrophoresis

2% E-gel, E-gel power base and 50 bp DNA ladder (Invitrogen Life Technologies, Carlsbad, CA), UV transilluminator and photo-documentation system (Fisher Biotech, Pittsburgh, PA), Black and White film (Polaroid, Cambridge, MA) and BioRad Power Pac 300 (BioRad, Hercules, CA) were utilized for electrophoresis.

3.4.2 Polymerase Chain Reaction (PCR)

PCR is a technique that can exponentially amplify a segment of DNA of interest. It was invented by Dr. Kary Mullis who won the 1993 Nobel Prize in chemistry for his work. DNA containing the gene of interest is amplified by heat-stable DNA polymerase. The DNA synthesis is primed with the help of primers, specific oligonucleotide sequences that are complementary to the 5' and 3' end of the gene segment. Each round of PCR in the exponential phase doubles the amount of template DNA therefore it can greatly increase the original amount of DNA (315).

3.4.2.1 DNA isolation

DNA isolation from mice tails was done according to the protocol provided in the DNeasy Tissue Kit by Qiagen (Valencia, CA). Briefly the protocol is as follows:
Cut ~1 cm tails from mice, put into a 1.5 ml Eppendorf tubes. Add 180 µl buffer ATL (tissue lysis buffer). Add 20 µl Proteinase K, mix by vortexing and incubate at 55° C in a dry bath overnight. The next day, vortex mix samples for 15 seconds, add 400 µl buffer AL-ethanol mixture and vortex mix again. Pipet the mixture into a DNeasy mini column. Centrifuge the column for 1 min at 13,000 rpm (or >6000 g). Place the column into a new collection tube and add 500 µl buffer AW1, centrifuge for 1 min at 13,000 rpm (or >6000 g). Put the column into a new collection tube and add 500 µl buffer AW2 and centrifuge for 3 min at 13,000 rpm (or >6000 g). Move the column to a new collection tube and add 100 µl buffer AE. Incubate

at room temperature for 1 min then centrifuge for 1 min at 13,000 rpm (or >6000 g) to elute DNA. Use the eluted DNA for the PCR reaction and store the remaining DNA at -20°C.

3.4.2.2 Reaction mix for genotyping CF mice

Tables 3.12 and 3.13 list the PCR solution recipe for genotyping CF mice.

Table 3.12 PCR reaction mix recipe to genotype *cftr*^{tm1Eur} mice

Reagents	Volume (µl)	Final Concentration
RedTaq ReadyMix PCR Mix (2X)	12.5	1X
40 µM MCF1 primer (S)	0.25	0.4 µM
40 µM MCF3 primer (AS)	0.25	0.4 µM
Tail DNA	2	8% (v/v)
H2O	10	
Total volume	25	

Table 3.13 PCR reaction mix recipe to genotype *cftr*^{tm1Kth} mice

Reagents	Volume (µl)	Final Concentration
RedTaq ReadyMix PCR Mix (2X)	12.5	1X
40 µM IMR 269 primer (S)	0.25	0.4 µM
40 µM IMR 270 primer (S)	0.25	0.4 µM
40 µM IMR 271 primer (AS)	0.25	0.4 µM
Tail DNA	2	8% (v/v)
H2O	9.75	
Total volume	25	

Table 3.14 *Ssp*I enzyme recipe for digesting PCR product

Reagents	Volume (µl)
*Ssp*I enzyme	0.5
10 x buffer solution	0.5
PCR product	10
water	4.0
Total volume	15

3.4.2.3 Reaction mix for genotyping P-gp mice

HSAS1 and HSAS2 primers amplify a segment of the *mdr1a* gene from the wild type P-gp mice while HSAS7 and HSAS8 amplify a segment of the *mdr1a* gene from the P-gp knockout mice. The PCR product from the wild type gene is 411 bp while the knockout mice produces a 484 bp band. Because the E-gel condition cannot resolve these two bands clearly, instead of mixing these two primer pairs together, we run the two primer pairs separately for each sample. HSAS1 and 2 primer pair produce a 411 bp band from the wild type tail DNA while no bands are produced from the HSAS7 and 8 primer pair. The reverse is true for the P-gp mice, a 481 bp band comes from HSAS7 and 8 while no bands appear from HSAS1 and 2. Tables 3.15, 3.16 and 3.17 list the recipe for making the PCR reaction mixture solution for genotyping P-gp mice.

Table 3.15 PCR reaction mixture recipe to genotype *mdr1a* wild type gene

Reagents	**Volume (μl)**	**Final Concentration**
RedTaq ReadyMix PCR Mix (2X)	12.5	1X
10 μM HSAS1 primer (S)	1.25	0.5 μM
10 μM HSAS2 primer (AS)	1.25	0.5 μM
Tail DNA	3	12% (v/v)
H2O	7.0	
Total volume	25	

Table 3.16 PCR reaction mixture recipe to genotype *mdr1a* (-/-) gene

Reagents	**Volume (μl)**	**Final Concentration**
RedTaq ReadyMix PCR Mix (2X)	12.5	1X
10 μM HSAS7 primer (S)	1.25	0.5 μM
10 μM HSAS8 primer (AS)	1.25	0.5 μM
Tail DNA	3	12% (v/v)
H2O	7.0	
Total volume	25	

Table 3.17 PCR reaction mixture recipe to genotype *mdr1b* gene

Reagents	**Volume (μl)**	**Final Concentration**
RedTaq ReadyMix PCR Mix (2X)	12.5	1X
10 μM HSAS3 primer (S)	1.25	0.5 μM
10 μM HSAS6 primer (AS)	1.25	0.5 μM
10 μM HS5NEO primer (S)	1.25	0.5 μM
10 μM HS3NEO primer (AS)	1.25	0.5 μM
DNA	3	12% (v/v)
H2O	4.5	
Total volume	25	

3.4.2.4 PCR thermal cycling conditions for *cftr* gene

PCR thermal cycling conditions for *cftr*^{tm1Eur} and *cftr*^{tm1Kth} mice are as follows:

stage 1: 95°C for 3 min

stage 2: 95°C for 30 s
59°C for 30 s
72°C for 1 min
} 35 cycles

stage 3: 72°C for 15 min

3.4.2.5 PCR thermal cycling conditions for *mdr1a* & *b* gene

PCR thermal cycling conditions for mdr1ab KO mice are:

stage 1: 95°C for 3 min

stage 2: 94°C for 45 s
55°C for 1 min
72°C for 1 min
} 35 cycles

stage 3: 72°C for 15 min

3.4.2.6 Electrophoresis conditions

To visualize the PCR products, we need to run them on a gel. It is done as follows: Prerun the 2% E-gel at 66 V for 2 min with the comb on. After that, remove the comb, load 12 μl H_2O and 10 μl PCR product into each well, load 20 μl of 50 fold-diluted 50 bp DNA ladder into one well, run at 66 V for 30 min. The bands are visualized with the UV transilluminator and a picture is taken with a Polaroid camera. For the PCR products from genotyping *cftr*^{tm1Eur} mice, we digest the PCR products first with S*sp*I enzyme for 2 hours at 37°C before loading the digested product on the gel.

3.5 Results

Figure 3.6 shows a representative sample of the genotyping results for *cftr*^{tm1Eur} mice. The bands shown are the PCR products digested with S*sp*I enzyme for 2 hours at 37°C. Lanes 6 and 11 show only one intact band at 450 bp; therefore the DNAs amplified by the PCR come from homozygous wild type mice. Lanes 7, 8 and 10 have three bands (150, 300 and 450 bp); therefore those are from heterozygous mice. Lane 9 has two digested bands (150 and 300 bp); therefore it is from a homozygous *cftr*^{tm1Eur} mice.

Figure 3.7 shows a representative sample of the genotyping results for *cftr*^{tm1Kth} mice. The bands shown are the products of PCR amplification of a segment of the *cftr* gene. Lanes 7, 8 and 10 show only one intact band at 430 bp; therefore the DNAs amplified by the PCR come from homozygous wild type mice. Lanes 2, 6, 9 and 11 have three bands (300, 430 and 800 bp); therefore those are from heterozygous mice. Theoretically there should only be two bands (300 and 430 bp) amplified from the DNA of heterozygous mice. The extra band at ~800 bp is probably the result of a non-specific interaction. Lanes 1, 3, 4 and 5 have only one band at 300 bp; therefore they are from homozygous *cftr*^{tm1Eur} mice.

Figure 3.8 shows a representative sample of the genotyping results for P-gp mice. Lanes 1 to 6 show the PCR product from FVB wild type mice while lanes 7 to 11 show the PCR product from FVB knockout mice. Lanes 1, 2, 4, 5, 7, 8 and 10 show the PCR amplification products of

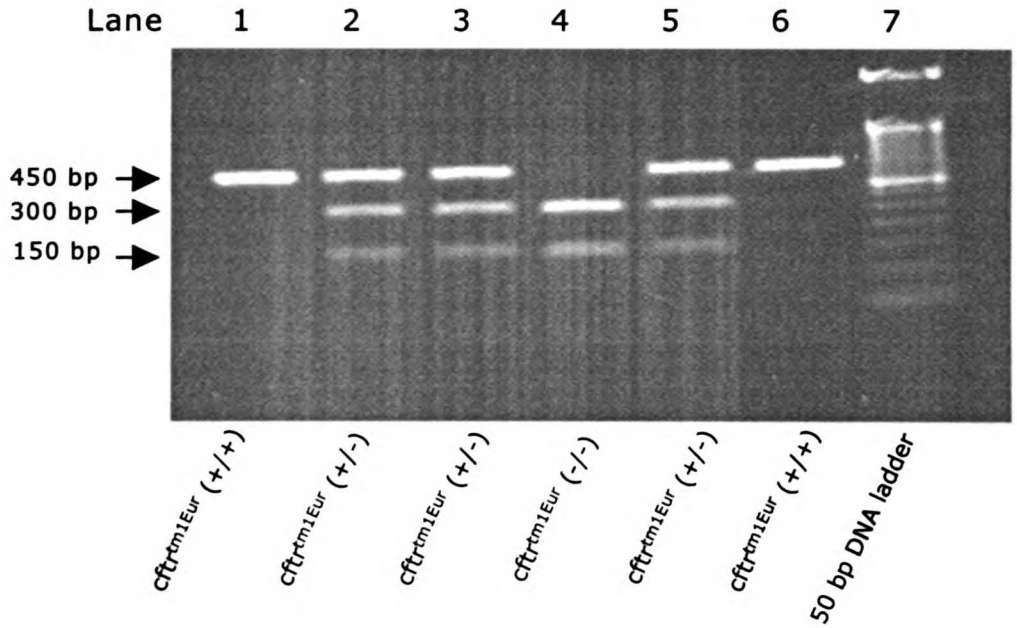

Figure 3.6 A representative sample of genotyping results of *cftr*^{tm1Eur} mice.

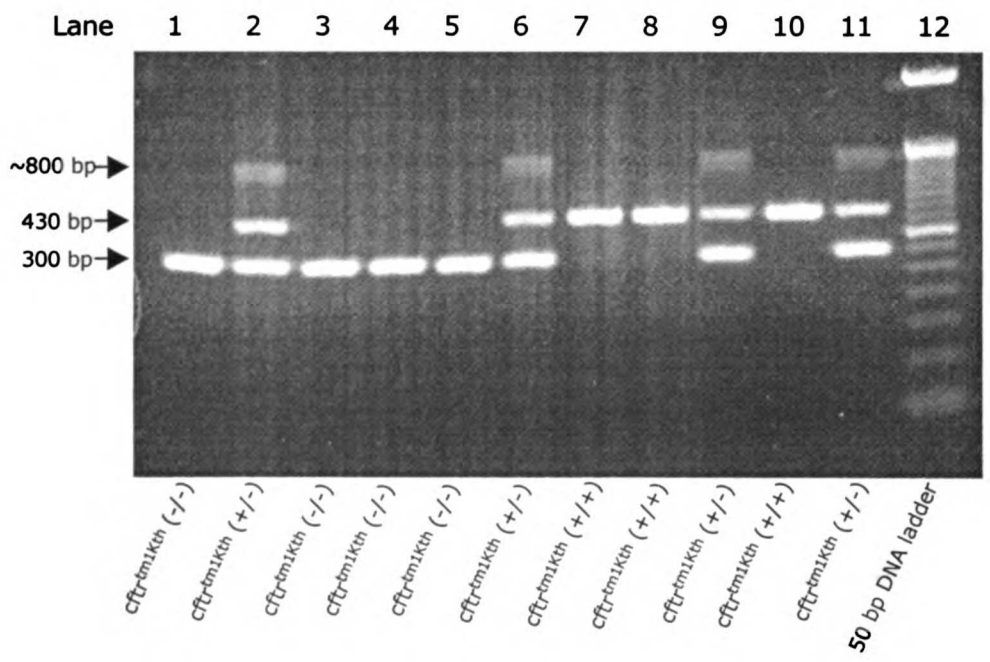

Figure 3.7 A representative sample of genotyping results of *cftr*^{tm1Kth} mice.

a segment of the *md1a* gene while lanes 3, 6, 9 and 11 are amplification products of a segment of the *md1b* gene. Lanes 1, 4 and 7 are the products amplified using the wild-type *mdr1a* gene primers; therefore we observed bands at 411 bp from DNAs of FVB wild-type mice no.1 and no. 2 while it was absent from lane 7 where the DNA come from a FVB knockout mouse no. 1. Due to lack of gel lanes we did not run the PCR product amplified with the wild type primer for FVB knockout mouse no. 2 but we did run it in another gel and there were no bands observed (data not shown), as expected. Lanes 2, 5, 8 and 10 are PCR products amplified with knockout *mdr1a* gene primers; therefore lanes 2 and 5 do not show any bands since the DNAs are from FVB wild type mice while lanes 8 and 10 show a band at 481 bp, as expected since the DNAs come from FVB knockout mice. Lanes 3, 6, 9 and 11 are PCR products amplified with both wild type and knockout *mdr1b* gene primers; therefore we should see bands in all lanes but with different sizes. Lanes 3 and 6 show a band at 540 bp, which is expected from DNAs of FVB wild type mice, while lanes 9 and 11 show a band at 453 bp, which is expected from DNAs of FVB knockout mice. Therefore the genotype of the mice are confirmed. FVB wild type mice have wild type copy of the *mdr1a* and *mdr1b* genes while FVB P-gp double knockout mice do not have functional *mdr1a* and *mdr1b* genes. Because the knockout mice are double knockout, for practical purposes we do not have to genotype for both *mdr1a* and *mdr1b* genes. If the mouse has been genotyped to contain a wild type *mdr1a* gene, it should have a wild type *mdr1b* gene and vice versa, as shown in our genotyping results here. Since the *mdr1b* gene is easier to genotype than the *mdr1a* gene (wild type and knockout *mdr1b* gene products can be separated in 2% E-gel), *mdr1b* was selected as the gene of choice to be tested.

3.6 Discussion

P-gp knockout mice are readily available for purchase from Taconic (Germantown, NY). There is no observable phenotypic differences between wild type and P-gp knockout mice. Therefore to confirm their genotype we did PCR analysis of their *mdr1a* and *mdr1b* genes. While P-gp knockout mice are easily acquired, CF mice are hard to obtain commercially. Therefore we bred the CF mice in our animal care facility. We were able to obtain two strains of CF heterozygous mice to begin the project. *Cftr*^{tm1Eur} heterozygous mice were generously

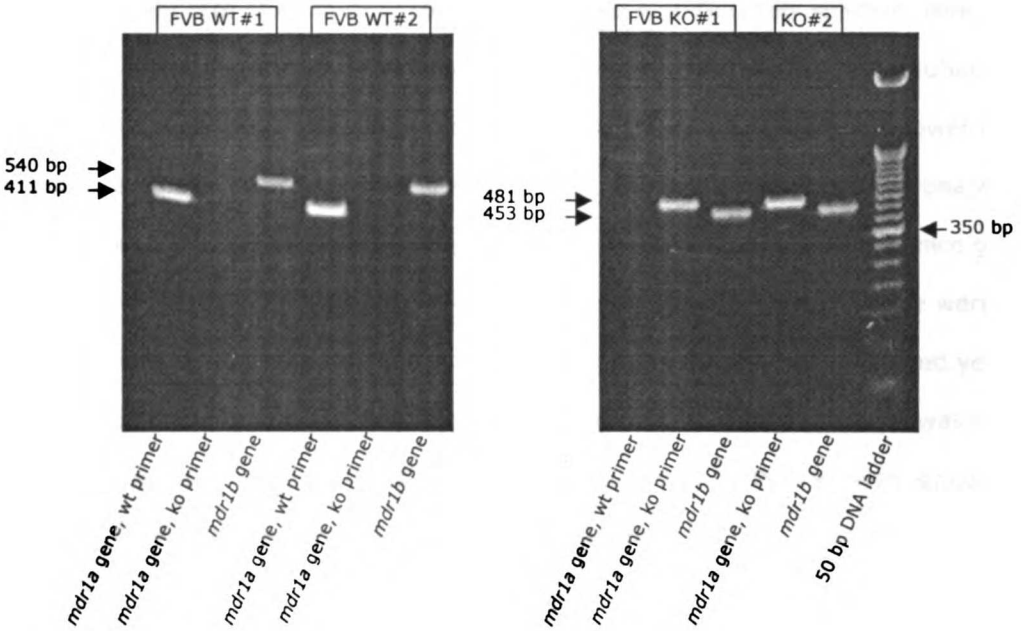

Figure 3.8 A representative sample of genotyping results of P-gp double knockout mice. **WT = wild type, ko = knockout.**

provided by the Mathias lab (UCSF, San Francisco, CA) while *cftr*^{tm1Kth} heterozygous mice were commercially obtained from Jackson Laboratories (Bar Harbor, ME). Both strains of mice contain the ΔF508 mutation that is present in about ~70% of the human CF population.

We began the breeding project with more *cftr*^{tm1Eur} heterozygous female mice and at an earlier time compared to *cftr*^{tm1Kth} heterozygous mice, therefore the majority of our CF offsprings are of *cftr*^{tm1Eur} strain. We did not observe any phenotypic differences in the two strains, though we did not investigate this thoroughly or in a systematic way. Both strains of CF mice exhibit a high mortality rate, white incisor teeth and lower body weight. These phenomena only appeared in homozygous CF mice and were not observable in heterozygous CF mice. The heterozygous mice are indistinguishable from the wild type mice.

To lower the high mortality rate of CF mice associated with intestinal problems, we substituted the drinking water with GoLytely solution (Braintree, Braintree, MA), which has been shown to

lower the mortality rate of CF mice (316). The mice fed with GoLytely solution have soft, wet stools instead of dry, hard ones. To eliminate the possible effect of GoLytely solution, we also fed it to the wild type mice. Even with the GoLytely solution, the CF mice had lower body weights compared to wild type or heterozygous mice. The body weight phenomena was most noticeable when the mice were very young and it appeared to decrease as the mice got older. The white incisor teeth in CF mice, however, were less noticeable when the mice were young and became more pronounced as the mice got older. This was due to pronounced yellowing of the teeth of adult wild type mice compared to the young ones. This phenotype was useful as a rough genotype of CF mice that was confirmed subsequently by PCR analysis since the white teeth phenotype was not accurate, especially in the young mice.

Theoretically the expected yield of CF mice offspring from mating two heterozygous mice is 25%. However, from our experience, the actual yield is much lower than that. In reality it is about 5-10%. This lower yield is not due to reduced pup size (they are normal compared to wild type) but rather to high mortality rates in the first few days of life. Once the CF mice passed the first few days, they were more likely to survive but occasionally, some do die shortly after 1 month. If they pass this stage, they almost always survive past 6 months.

Once we obtained homozygous CF mice, we tried to mate the homozygous males with the homozygous female CF mice. Even though we were able to get offsprings (all CF mice) from one homozygous female CF mice, the mother died not long after giving birth and we put the pups with another mouse that just gave birth. Despite this effort, the pups died shortly thereafter. It was apparent that the fertility was reduced in female CF mice but not in male CF mice, as reported. Therefore, to increase the yield of CF mice, we mated a homozygous male CF mouse to four heterozygous female CF mice. The CF mice yield was increased by this method but it was also lower than the expected 50% theoretical value.

In summary, we bought our P-gp double knockout mice from Taconic and we bred our own CF mice. We were able to breed two strains of homozygous CF mice. Because of the lower yield of CF mice due to a high mortality rate, it took us about 1 year to establish a breeding colony

that would produce enough homozygous CF mice to carry out our pharmacokinetic experiments.

Chapter 4

In Vivo Pharmacokinetic Studies in Mice

4.1 Overview

The overall goal of this project is to determine the cause of enhanced renal clearance of drugs in CF patients. We hypothesize that enhanced renal clearance of antibiotics in CF patients is due to elevated P-gp expression in their kidneys. Thus far, the results from our first specific aim, the *in vitro* bidirectional transport studies, appear to support the hypothesis. Therefore, we proceeded with our second specific aim, where we performed *in vivo* pharmacokinetic studies to determine if the amount of P-gp expression affects the renal clearance values of antibiotics that are substrates of P-gp.

4.2 Study Design

We conducted pharmacokinetic studies with P-gp and non-P-gp substrates in four groups of mice that have different expression levels of P-gp: P-gp wild type (FVB), P-gp knockout (FVB-MDR1AB-MM), CF wild type (C57Bl/6J) and CF mice (ΔF508). Renal clearance values of P-gp and non-P-gp substrates were compared in these four mice groups to determine if there is a correlation between amounts of P-gp expression and renal clearance values. The results of *in vitro* studies showed that trimethoprim and ciprofloxacin are substrates of P-gp while sulfamethoxazole and iothalamate are not substrates of P-gp (Chapter 2). Therefore, we predicted that the renal clearances (CLr) of trimethoprim and ciprofloxacin would be lower in P-gp knockout mice, where the P-gp expression is absent (Table 4.1). We expected the renal clearances of trimethoprim and ciprofloxacin to be higher in CF mice, where according to our hypothesis, P-gp expression is elevated. We expected to see no difference in renal clearance values of sulfamethoxazole and iothalamate among those four groups of mice because sulfamethoxazole and iothalamate are not P-gp substrates. Iothalamate is a marker of glomerular filtration rate. It is assumed that the compound is not secreted, reabsorbed or

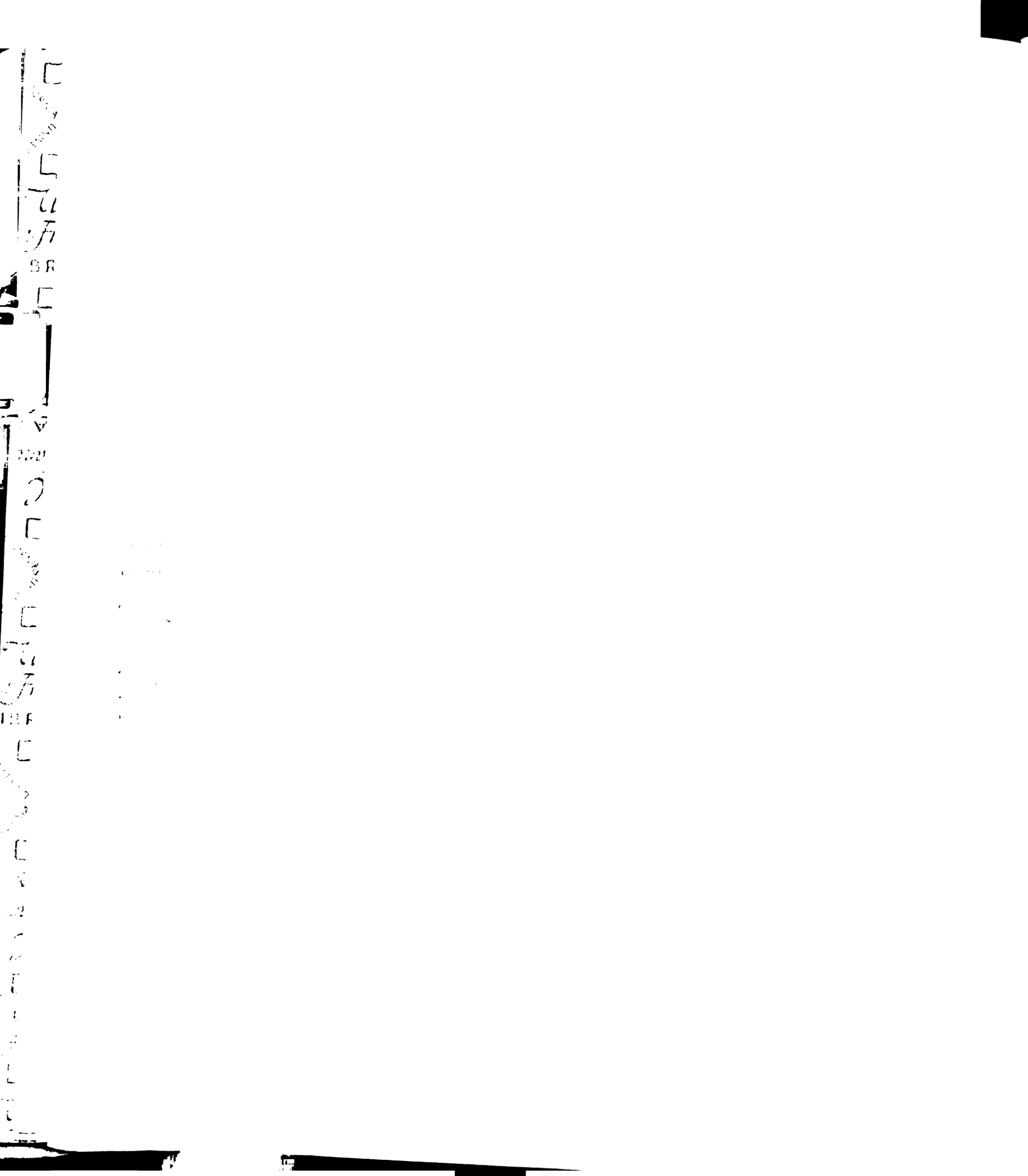

Table 4.1 Expected renal clearance (CLr) results from pharmacokinetic studies in four groups of mice

Group	Mice Strain	Description	Expected CLr			
			TMP	SMZ	IoA	CIP
1	FVB	control mice	1	1	1	1
2	FVB-MDR1AB-MM	Mdr1a and Mdr1b KO mice	< 1	1	1	< 1
3	C57Bl/6J	control mice	1	1	1	1
4	C57Bl/6J-cftr$^{tm1.Kth}$ C57Bl/6J-cftr$^{tm1.Eur}$	ΔF508 CF mice	> 1	1	1	> 1

TMP = trimethoprim
SMZ = sulfamethoxazole
IoA = iothalamate
CIP = ciprofloxacin

metabolized. Due to a limited number of CF mice, instead of measuring P-gp expression in the kidneys of these mice before the *in vivo* pharmacokinetic experiments, we will measure it after the *in vivo* experiments.

Renal clearance is calculated using this equation:

$$CLr = \frac{Ae_{inf}}{AUC_{0\text{-}inf}}$$

where Ae_{inf} is the total amount of drug eliminated into the urine and it is measured using mice metabolic cages (Figure 4.1). $AUC_{0\text{-}inf}$ is the total area under the curve of the plasma concentration-time plot.

Table 4.2 shows a comparison of several physiological parameters between human and mouse.

4.3 Drug Characteristics

Sulfamethoxazole is a synthetic sulfanilamide anti-infective. It acts on the folic acid pathway. Sulfamethoxazole is a structural analog that mimics para-aminobenzoic acid (PABA), an essential natural metabolite of bacteria. PABA is a precursor for the synthesis of

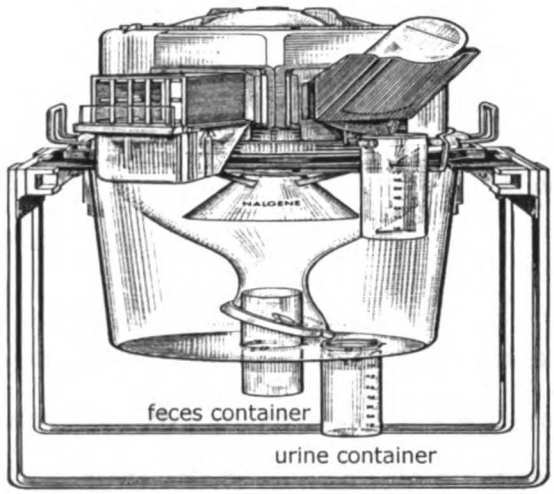

Figure 4.1 A drawing of a mice metabolic cage. Adapted from the information sheet of Nalgene Metabolic Cage for Mice System (Rochester, NY)

Table 4.2 Various physiological parameters in mouse and human. Adapted from Davies and Morris (317).

Physiological Parameters	**Mouse (0.02 kg)**	**Human (70 kg)**
Kidney weight (g)	0.32	310
Surface area (m^2)	0.008	1.85
Total plasma protein (100 ml)	6.2	7.4
Plasma albumin (g/100 ml)	3.27	4.18
Plasma α-1-AGP (g/100 ml)	1.25	0.18
Hematocrit (%)	45	44
Total ventilation (L/min)	0.025	7.98
Respiratory rate (min^{-1})	163	12
Heart rate (beats/min)	624	65
Oxygen consumption (ml/hr/g body wt)	1.59	0.2
Total body water (ml)	14.5	42000
Intracellular fluid (ml)	-	23800
Extracellular fluid (ml)	-	18200
Plasma volume (ml)	1	3000
Kidney blood flow (ml/min)	1.3	1240
Liver blood flow (ml/min)	1.8	1450
Urine flow (ml/day)	1	1400
Bile flow (ml/day)	2	350
GFR (ml/min)	0.28	125
Cardiac output (ml/min)	8	5600

tetrahydrofolate, the metabolically active form of folic acid. Sulfamethoxazole competes with PABA for the synthesis of dihydropteroic acid which leads to depletion of the folate pool. Sulfamethoxazole is also incorporated into folate analogs that then inhibit the folate-utilizing enzymes. Because the mode of action of sulfamethoxazole is at the level of DNA synthesis, it is only bacteriostatic in a poor growth media and bacteriocidal in rich growth medium lacking thymine, such as blood and urine (318).

Table 4.3 lists various properties of sulfamethoxazole and Figure 4.2 shows its metabolites. In humans, sulfamethoxazole is mostly metabolized, with N4-acetylsulfamethoxazole accounting for about 44% of the sulfamethoxazole dose. Thirty percent of measured drug and metabolites is accounted for by N4-acetylsulfamethoxazole in the blood and 60% in the urine. Other metabolites are found at minute concentrations. N4-hydroxysulfamethoxazole is thought to contribute to sulfamethoxazole toxicity with long term use (319).

Table 4.3 Properties of trimethoprim (TMP), sulfamethoxazole (SMZ), ciprofloxacin (CIP) and iothalamate (IoA) in humans

	TMP	SMZ	CIP	IoA	References
Molecular Formula	$C_{14}H_{18}N_4O_3$	$C_{10}H_{11}N_3O_3S$	$C_{17}H_{18}FN_3O_3$	$C_{11}H_9I_3N_2O_4$	320
Molecular Weight (kDa)	290.3	253.28	331.35	613.92	320
pKa	6.6	5.7	6, 8.8	-	320
Bioavailability	~100	~100	60 ± 12	-	236
Urinary excretion (%)	63 ± 10	14 ± 2	65 ± 12	-	236
protein binding (%)	37 ± 5	62 ± 5	40	-	236
Clearance (ml/min/kg)	1.9 ± 0.3	0.32 ± 0.04	6.0 ± 1.2	-	236
Volume of distribution (L/kg)	1.6 ± 0.2	0.21 ± 0.02	1.8 ± 0.4	-	236
Half life (hours)	10 ± 2	10.1 ± 4.6	4.1 ± 0.9	-	236

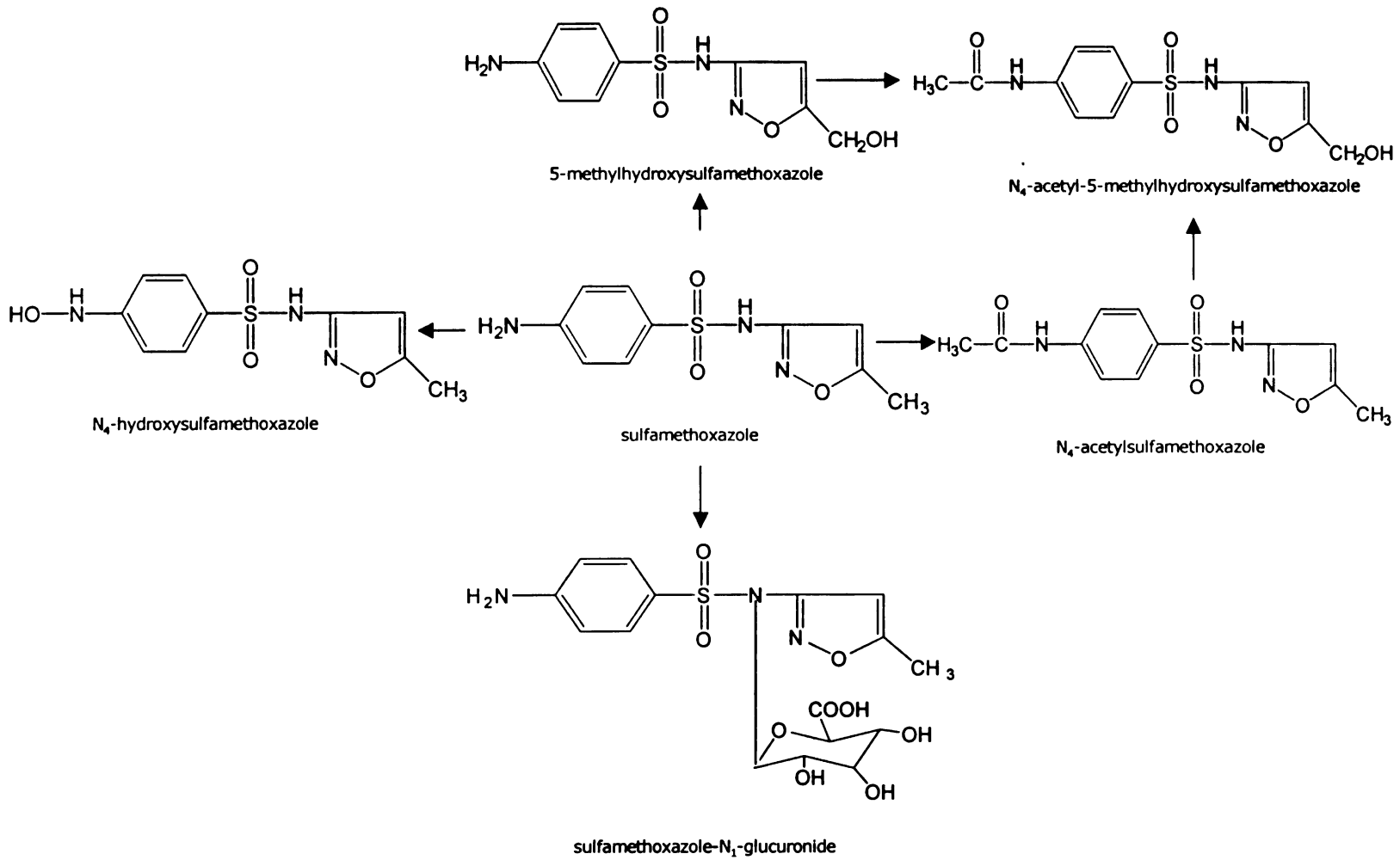

Figure 4.2 Structures of sulfamethoxazole and its metabolites

Trimethoprim is a synthetic folate-antagonist anti-infective. It also acts on the folic acid pathway. It inhibits the reduction of dihydrofolic acid to tetrahydrofolic acid by dihydrofolate reductase. It is a potent, reversible inhibitor of dihydrofolate reductase. Inhibition of the synthesis of tetrahydrofolic acid, inhibits bacterial thymidine synthesis. It does not affect human dihydrofolate reductase because trimethoprim has a hundred thousand-fold higher affinity to the bacterial form of the enzyme (318). Table 4.3 lists various properties of trimethoprim and Figure 4.3 shows its metabolites. In humans, trimethoprim is mostly eliminated unchanged into the urine. Ten percent of a radiolabeled trimethoprim dose is accounted for by trimethoprim metabolites in the blood and about 20-40% in the urine. Trimethoprim 3-oxide represents about 2.1% of trimethoprim dose in the urine while 1-hydroxytrimethoprim is minute. 3- and 4-Demethyltrimethoprim are further glucuronidated (321).

Trimethoprim is often dosed together with sulfamethoxazole in a 1:5 ratio. This represents the double blockage of the folate synthesis. Sulfamethoxazole blocks folate synthesis, therefore reducing the amount of folate that competes with trimethoprim for binding with dihydrofolate reductase.

Ciprofloxacin is a synthetic fluoroquinolone anti-infective. Fluoroquinolones have an expanded spectrum of activity and potency compared with nonfluorinated quinolones. Currently quinolones are the second most widely used class of antibiotics. However, their frequency of use is still far behind the beta-lactams. The mechanism(s) of action of ciprofloxacin has not been fully elucidated. It is thought to inhibit the activity of DNA topoisomerase, a type II DNA topoisomerase commonly known as DNA-gyrase. This enzyme is required for bacterial DNA replication and also contributes to mRNA synthesis and repair and DNA recombination and transposition. The target of ciprofloxacin appears to be the A, and maybe also the B subunit of the enzyme. At low concentrations, just above its minimum inhibitory concentration, the drug is bacteriocidal, while at high concentrations, it is bacteriostatic (318). Table 4.3 lists various properties of ciprofloxacin and Figure 4.4 shows its metabolites. In humans, ciprofloxacin is mostly eliminated unchanged into the urine. Nineteen percent of a

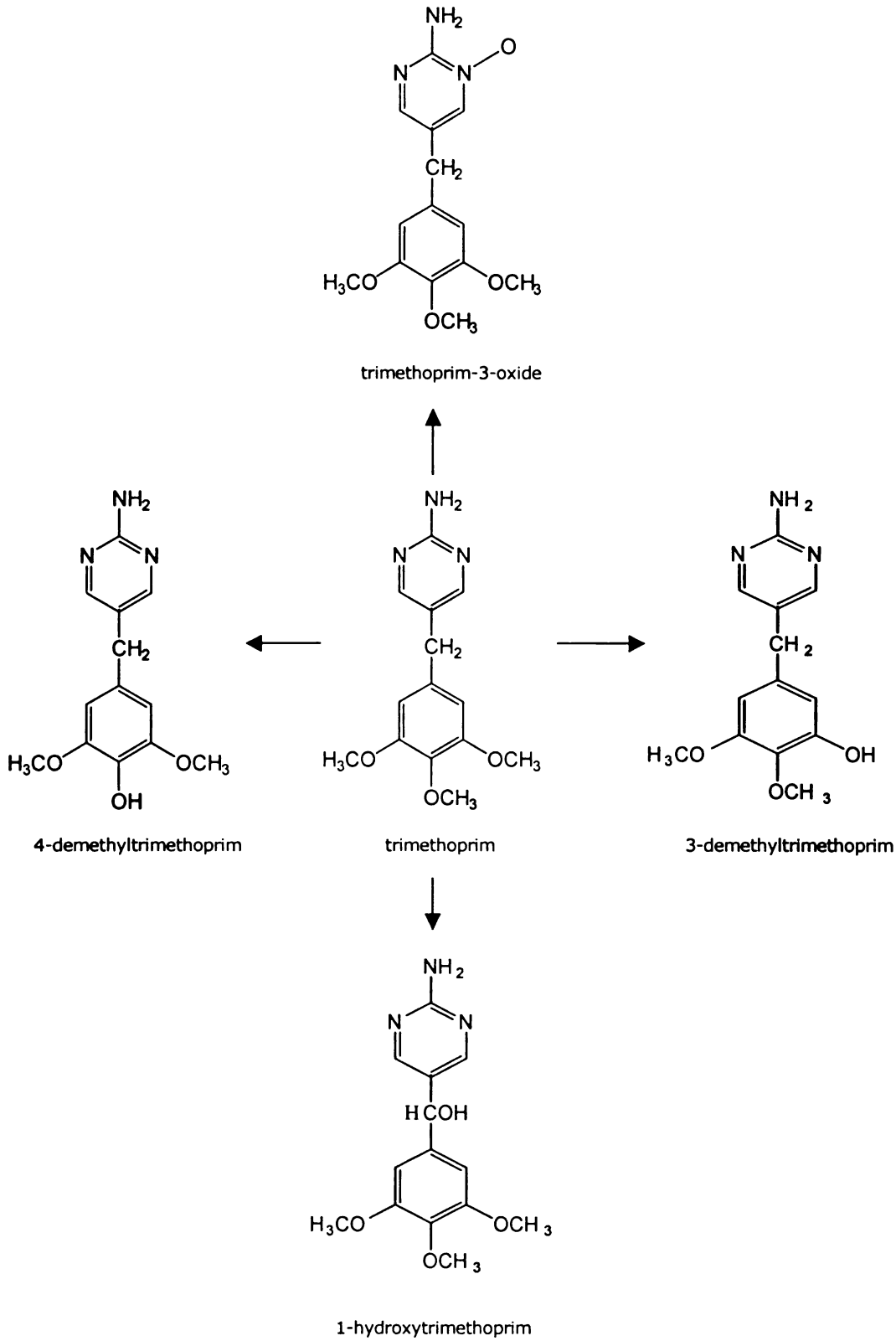

Figure 4.3 Structures of trimethoprim and its metabolites

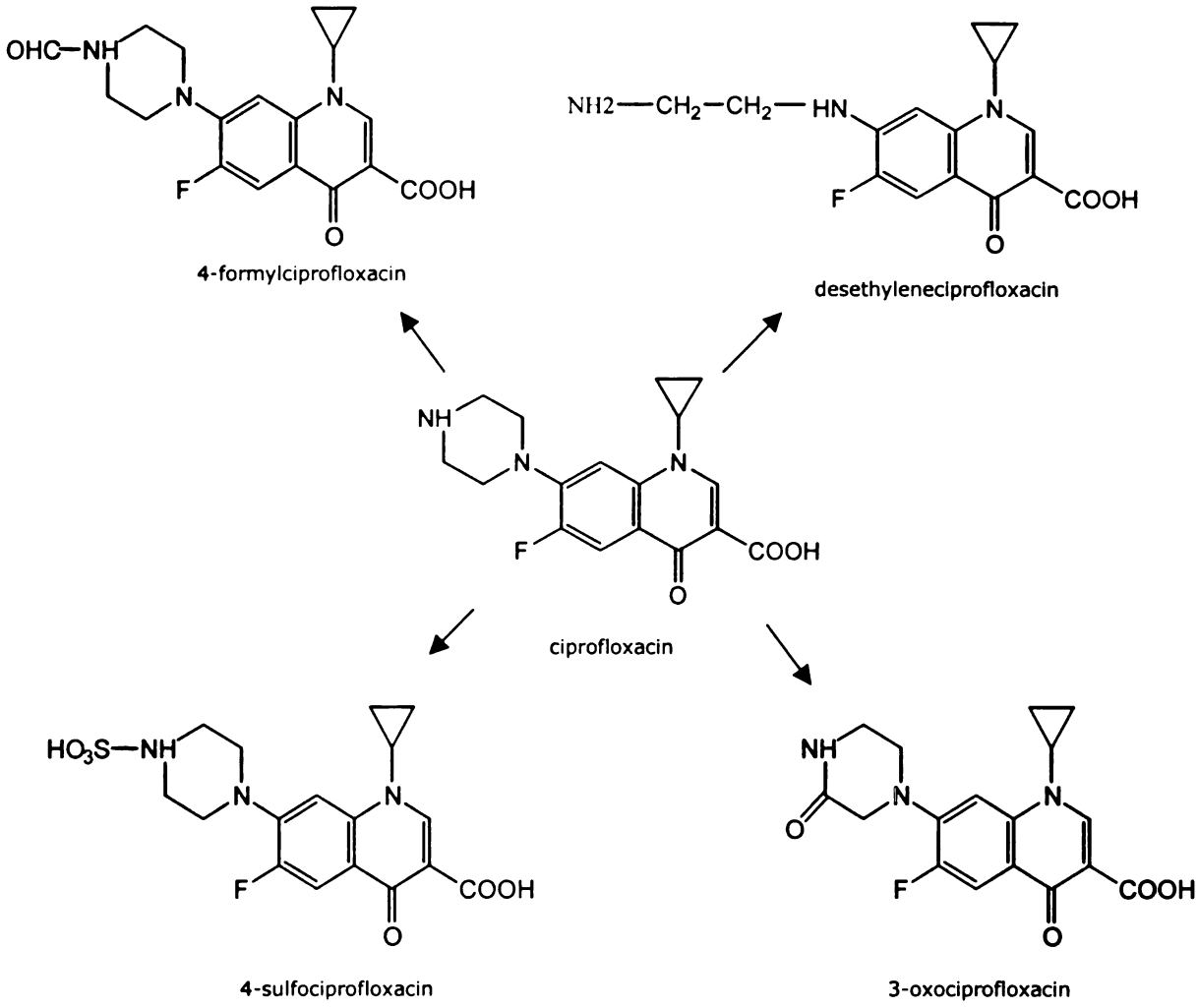

Figure 4.4 Structures of ciprofloxacin and its metabolites

ciprofloxacin dose is excreted as metabolites in both urine and feces. Sulfociprofloxacin and oxociprofloxacin represent 10% and 7%, respectively, of the dose metabolized. Desethyleneciprofloxacin only accounts for 1.8% of a ciprofloxacin dose while formylciprofloxacin accounts for less than 0.1% percent of a ciprofloxacin dose (322).

4.4 Materials and Methods

4.4.1 Materials

The following materials were utilized: FVB wild type and FVB MDR1AB-MM (P-gp double knockout) mice (Taconic, Germantown, NY), CF wild type and CF knockout mice (bred at UCSF Animal Facility, San Francisco, CA), trimethoprim (16 mg/ml) and sulfamethoxazole (80 mg/ml) IV solution (Elkins-Sinn, Cherry Hill, NJ), ciprofloxacin IV solution (Bayer, West Haven, CT), iothalamate meglumine (60%) IV solution (Mallinckrodt, St. Louis, MO), 5% dextrose injectable (Baxter, Deerfield, IL), iothalamate USP standard, carbidopa USP standard (U.S. Pharmacopeia, Rockville, MD), ofloxacin (Allergan Investigation Laboratories, Irvine, CA), N4-acetylsulfamethoxazole (Frinton Laboratories, Vineland, NJ), 30G1/2 needles, 1 ml syringes, scalpel surgical no. 11 (Becton Dickinson, Franklin Lakes, NJ), mouse decapicone disposable mouse restrainers (Braintree Scientific, Braintree, MA), mouse hot box (Aladdin Enterprises, San Francisco, CA), mouse metabolic cages (Nalgene, Rochester, NY), Pipetman (Rainin, Woburn, MA), timer (Phenomenex, Torrance, CA), balance (Sartorius, Edgewood, NY), heparinized capillary tubes for micro-hematocrit (VWR, West Chester, PA), CRITOSEAL (Oxford, St. Louis, MO), carbide point scriber (Cole Hardware, San Francisco, CA), micro hematocrit centrifuge (IEC, Needham Heights, MA), X Systems centrifuge (Abbott Laboratories, Abbott Park, IL), liquid nitrogen (UCSF Storeroom, San Francisco, CA), 5 L liquid nitrogen dewar (SPI Supplies, West Chester, PA), 2 ml cryogenic vial (Corning, Corning, NY), 400 µl microcentrifuge tubes for insertion in Waters 96 autosampler (E & K Scientific Products, Campbell, CA), Micromass Quattro LC, Quattro Ultima (Micromass, Manchester, United Kingdom), 4.6 x 150mm Hypersil BDS-C_{18} 5µ column (Keystone Scientific Inc., Bellefonte, PA), sulfadimethoxine, methanol, formic acid, acetonitrile (Sigma, St. Louis, MO), Waters 96 autosampler (Waters, Milford, MA) and LC-10 AD pump (Shimadzu, Kyoto, Japan).

4.4.2 Study protocol

There were two different sets of experiments. In one set, trimethoprim, sulfamethoxazole and iothalamate were dosed together. In another set, ciprofloxacin and iothalamate were dosed together. Trimethoprim and sulfamethoxazole were dosed together because clinically they are

dosed together in a 1:5 ratio. Iothalamate was used to monitor glomerular filtration rate in each study.

4.4.2.1 Drug dosing

The drugs were administered intravenously via the mouse tail vein. The dosing regimens for both sets of experiments are listed in Tables 4.4 and 4.5. It was not possible to collect both urine and plasma samples at the same time. Therefore, the drugs were dosed twice, about one week apart, to collect urine samples in one experiment and plasma samples in the second experiment.

Table 4.4 Dosing regimen for trimethoprim, sulfamethoxazole and iothalamate

Drugs	Dose (mg/kg)	Concentration (mg/ml)	Injection Volume (ml/kg)
Trimethoprim	20	2	10
Sulfamethoxazole	100	10	10
Iothalamate	50	5	10

Table 4.5 Dosing regimen for ciprofloxacin and iothalamate

Drugs	Dose (mg/kg)	Concentration (mg/ml)	Injection Volume (ml/kg)
Ciprofloxacin	25	2.5	10
Iothalamate	44	4.4	10

4.4.2.2 Urine collection

Urine samples were collected using mice metabolic cages, designed to separate feces into one container and urine into another container (see Figure 4.1). Before the experiments, the mice were put in the mice metabolic cage to let them get accustomed to it. During the actual urine collection experiments, the mice were dosed with drugs and placed in the metabolic cages along with water and food overnight. The mice were removed the next day and the urine

containers were removed. The cages were washed to collect residual urine that was on the cage. All the urine solutions were centrifuged to remove solid contaminants and the total volumes were measured. Urine samples were saved at -80°C until the concentration of drugs in the urine was determined by LC/MS/MS.

4.4.2.3 Plasma collection

The plasma collection was performed several days apart from the urine collection. Plasma samples were collected by nicking the mouse tail artery with a surgical scalpel no. 11 at selected time points. The sampling points for trimethoprim and sulfamethoxazole were at 2, 15, 30, 60, 90, 120, 150 and 180 minutes. The sampling points for ciprofloxacin were at 2, 30, 60, 90 and 120 minutes. Due to the limited amount of blood in mice, a very small volume (~20 μl) of blood was collected at early time points, where the concentrations were high, and a larger volume (~40 μl) was collected for later time points, where the concentrations were low. The blood was collected into heparinized capillaries and the capillaries were centrifuged immediately to collect the plasma. Plasma samples were saved at -80°C until analysis by LC/MS/MS. At the end of the experiment, the mice were euthanized and the organs were collected in liquid N_2 and saved at -80°C for later use in P-gp expression studies.

4.4.3 Sample preparation

4.4.3.1 Plasma sample preparation

Due to the high sensitivity of LC/MS/MS, we diluted the earlier time point samples several fold with blank mouse plasma before processing them. The following is the protocol for plasma sample preparation: 10 μl of plasma sample was mixed with 140 μl of 70% acetonitrile containing internal standard solution (50 ng/ml dideoxy inosine, ofloxacin and sulfadimethoxine). The sample was vortex mixed and centrifuged for 15 minutes. The supernatant was aliquoted: 110 μl to one tube and set aside for trimethoprim, sulfamethoxazole or ciprofloxacin measurement. To another tube, 90 μl of water was added to the aliquoted 30 μl supernatant and this was set aside for iothalamate analysis.

4.4.3.2 Urine sample preparation

To prepare urine samples for analysis, 20 µl of urine sample was mixed with 20 µl internal standard solution (50 ng/ml dideoxy inosine, ofloxacin and sulfadimethoxine) and 160 µl of water. The solution was centrifuged and the supernatant was set aside for analysis.

4.4.4 Sample analysis

Concentrations of ciprofloxacin, iothalamate, sulfamethoxazole, N4-acetylsulfamethoxazole and trimethoprim in plasma and urine were quantified using an LC/MS/MS (liquid chromatography/mass spectrophotometry/mass spectrophotometry) system. This was done in collaboration with Dr. Emil Lin from the Drug Studies Unit (South San Francisco, CA). The actual sample measurements were performed by Dr. Yong Huang.

Samples were injected at a flow rate of 0.8 ml/min onto a 5 µm BDS-C_{18} (4.6 X 150 mm) analytical column. The mobile phase for ciprofloxacin, sulfamethoxazole, N4-acetylsulfamethoxazole and trimethoprim consisted of a mixture of methanol, acetonitrile, 0.1% formic acid with 5 mM formate ammonium in the ratio of 3:1:6 (v/v). The mobile phase for iothalamate consisted of methanol and 0.1% formic acid in the ratio of 14: 86 (v/v).

Postcolumn, twenty five percent of the original flow was diverted into the electrospray MS/MS. The mass spectrophotometer was operated in the positive mode. Ultra-high purity nitrogen was used as the drying and electrospray ionization gas. Argon was used as the collision gas. The cone voltage was set at 26, 30, 30, 30 and 40 V for trimethoprim, ciprofloxacin, sulfamethoxazole, N4-acetylsulfamethoxazole and iothalamate, respectively. The collision energy was set at 16, 20, 23, 23 and 24 eV for ciprofloxacin, iothalamate, sulfamethoxazole, N4-acetylsulfamethoxazole and trimethoprim, respectively. Multiple reaction monitoring was applied for recording of analytes. The m/z values of parent and daughter ions are as followed: 254>156 (sulfamethoxazole), 291>230 (trimethoprim), 332>314 (ciprofloxacin), 615>361 (iothalamate) and 296>134 (N4-acetylsulfamethoxazole).

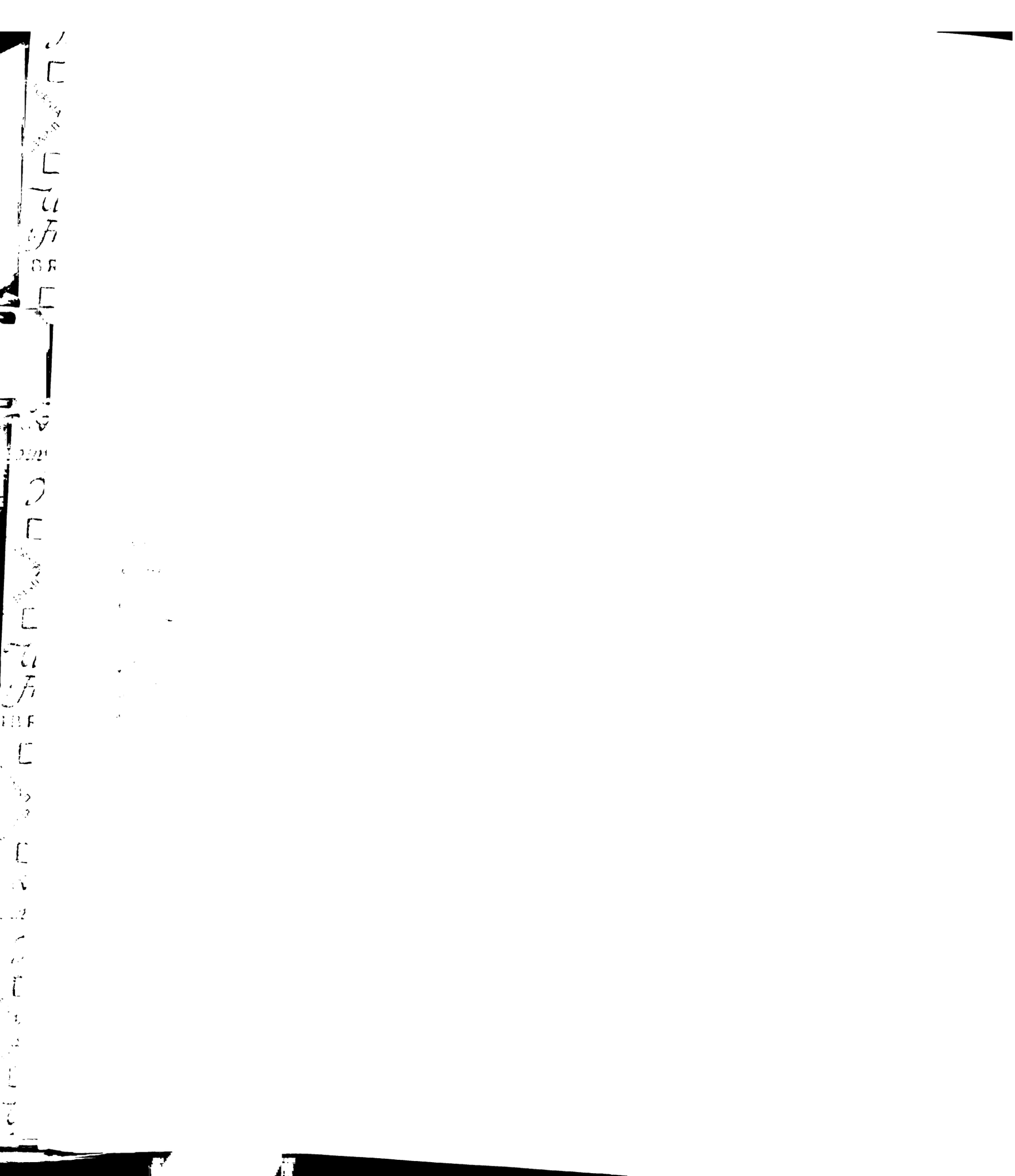

4.4.5 Pharmacokinetic data analysis

Pharmacokinetic (PK) parameters were calculated using WinNonlin Professional software, version 2.1 (Pharsight, Mountain View, CA). Noncompartmental analysis for IV bolus input (Model 201) was employed to estimate the PK parameters of trimethoprim, ciprofloxacin, sulfamethoxazole and iothalamate.

Clearance (CL) is the volume of plasma that is completely cleared of drug per unit time. It is calculated using this equation:

$$CL = \frac{Dose}{AUC_{0\text{-}inf}}$$

AUC (area under the curve) is the total area under the plasma concentration-time (C *vs.* t) curve. To calculate AUC, the total area is divided into segments. The area of each segment is calculated using the linear trapezoid method and the total AUC is calculated by adding these segments together. Therefore, the total AUC can be calculated as :

$$AUC^{0-\infty} = AUC^{0-t(last)} + AUC^{t(last)-\infty}$$

$$= \sum \left\{ \frac{Cp^0 + Cp^1}{2} \cdot t^1 \right\} + \left\{ \frac{Cp^1 + Cp^2}{2} \cdot (t^2 - t^1) \right\} + \quad \ldots + \frac{Cp^{last}}{kel}$$

where k_{el} is the elimination rate constant calculated from the terminal slope of a semilog plot of a plasma concentration-time curve.

The elimination half-life ($t_{1/2}$) is the amount of time for the plasma concentration to fall to half its original value. The elimination half-life ($t_{1/2}$) is calculated using this equation:

$$t_{1/2} = \frac{0.693}{k_{el}}$$

The renal clearance (CLr) is defined as the ratio of the rate of urinary excretion to plasma concentration. It is the volume of plasma cleared of drug per unit time by the kidneys. It is calculated as follows:

$$CLr = \frac{Ae_{inf}}{AUC_{0\text{-}inf}} = fe \times CL$$

where fe is the fraction of dose excreted into the urine, calculated from the total amount of drug eliminated into the urine divided by the dose.

Mean residence time (MRT) is the average amount of time a molecule remains in a system. MRT for a bolus intravenous dose is calculated from this equation:

$$MRT = \frac{AUMC}{AUC}$$

where AUMC is the area under the moment curve. It is similar to AUC, with the exception that it is the total area under the plasma concentration X time *vs.* time (C•t *vs.* t) curve.

Vss is the steady state volume of distribution. It is calculated by this equation:

$$Vss = CL \times MRT$$

Fraction of dose metabolized (fm) is estimated from the fraction of metabolite excreted into the urine. The inherent assumption is that the metabolite is not further metabolized.

CLf is the formation clearance. It is calculated by multiplying the fraction of dose metabolized by the total clearance.

$$CLf = fm \times CL$$

4.4.6 Statistical analysis

ANOVA (analysis of variance) was performed on all the data sets. Data were analyzed using the Primer Express software created by Dr. Stanton Glantz (UCSF, San Francisco, CA). The acceptable level of significance was $P < 0.05$

4.5 Results

4.5.1 Trimethoprim

Figure 4.5 shows the plot of plasma concentration *vs.* time for trimethoprim in P-gp wild type and P-gp knockout mice. We observe no significant difference in the concentration-time profiles of trimethoprim between P-gp wild type and knockout mice. Figure 4.6 shows the plot of plasma concentration *vs.* time for trimethoprim in CF wild type and CF mice (referred to in the figure as CF KO). The concentration-time profiles in CF wild type mice appear to be different from CF mice. Figure 4.7 shows the plot of average plasma concentration *vs.* time in these four groups of mice and the average pharmacokinetic parameters for each group are listed in Table 4.6.

There is no statistically significant difference in the total clearance of trimethoprim between P-gp wild type and knockout mice. The total clearance appears different between CF wild type and CF mice but the difference is not statistically significant. The total clearance of trimethoprim in mice (~4.5 ml/min) is larger than the published mouse liver blood flow but not greater than cardiac output (1.8 and 8.0 ml/min, respectively, see Table 4.2). This suggests that in mice, trimethoprim is a high extraction ratio drug while it is a low extraction ratio drug in human, and that metabolism may be significantly extrahepatic. The total clearance of trimethoprim in humans (133 ml/min/70 kg, see Table 4.3) is much lower than the liver blood flow (1450 ml/min/70 kg, see Table 4.2).

The renal clearance is significantly higher in CF mice compared to CF wild type mice resulting in a higher fraction of trimethoprim excreted into the urine in CF mice. This agrees with our hypothesis that P-gp expression is higher in CF mice kidneys and higher P-gp expression leads to larger renal clearance of drugs that are substrates of P-gp. However, no difference in renal clearance is observed between P-gp wild type and knockout mice. This suggests that higher renal clearance in CF mice cannot be attributed to P-gp.

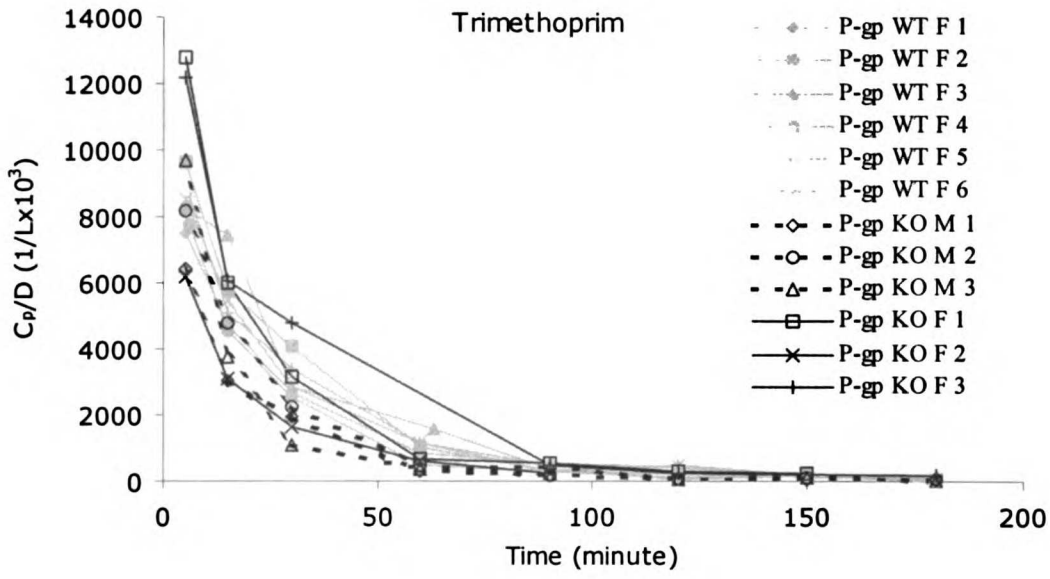

Figure 4.5 Comparison of plasma concentration-time profiles of trimethoprim between P-gp wild type (P-gp WT) and P-gp knockout mice (P-gp KO). Grey lines = P-gp WT, black lines = P-gp KO. Solide lines = female mice, dashed lines = male mice. F = female, M = male. The units for the y-axis are plasma concentration normalized with dose and multiplied by 1000.

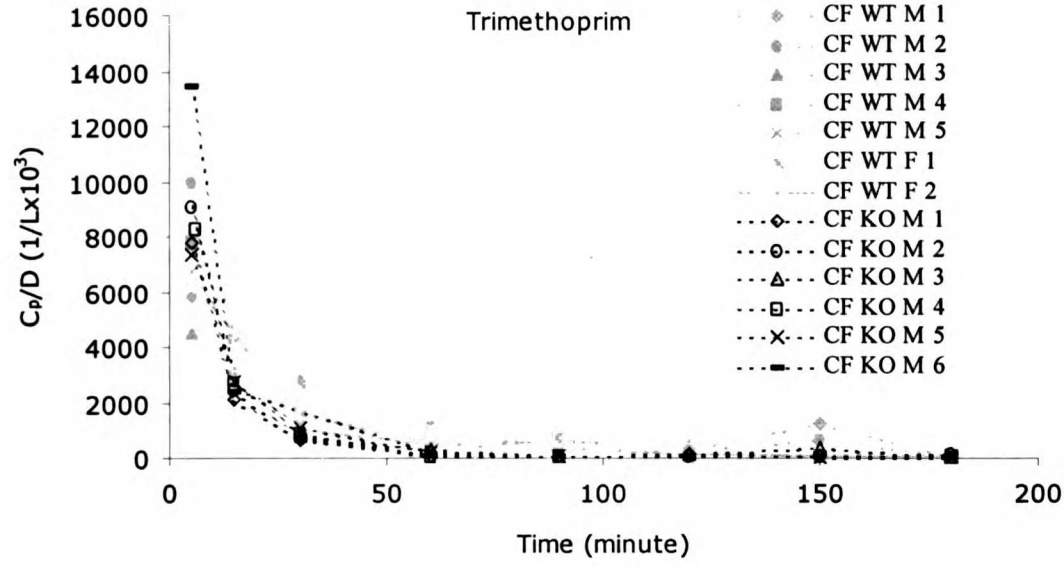

Figure 4.6 Comparison of plasma concentration-time profiles of trimethoprim between CF wild type (CF WT) and CF mice (CF KO). Grey lines = CF WT, black lines = CF KO. Solid lines = female mice, dashed lines = male mice. F = female, M = male. The units for the y-axis are plasma concentration normalized with dose and multiplied by 1000.

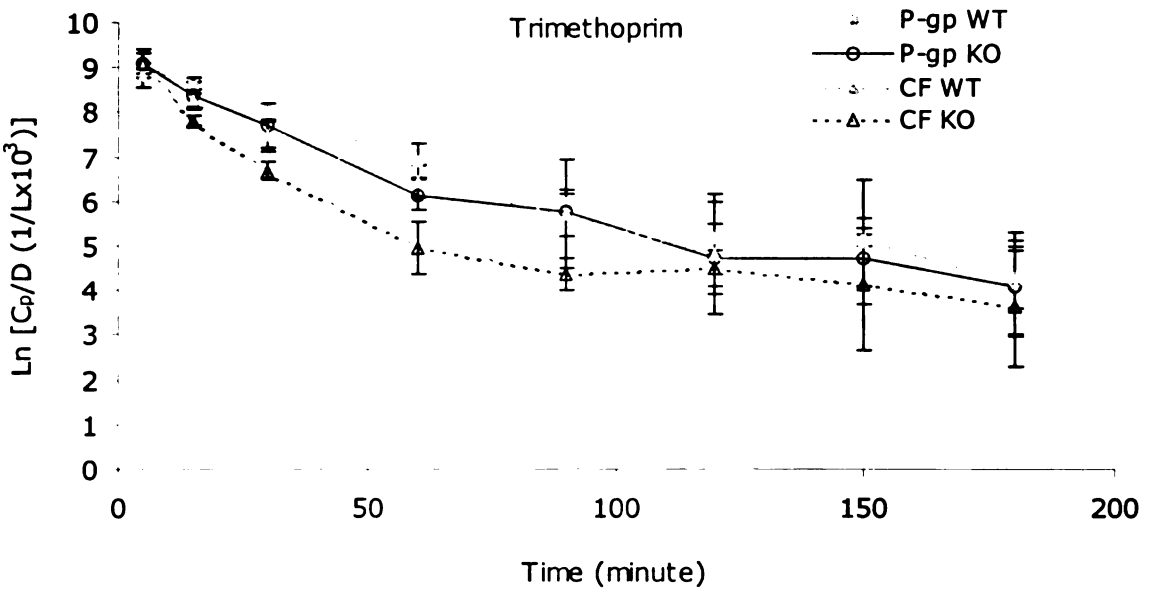

Figure 4.7 Comparison of average plasma concentration-time profiles of trimethoprim between P-gp wild type (P-gp WT), P-gp knockout (P-gp KO), CF wild type (CF WT) and CF mice (CF KO). Solid grey line = P-gp WT, solid black line = P-gp KO, dashed grey line = CF WT, dashed black line = CF KO. The units for the y-axis are the natural logarithm of plasma concentration normalized with dose and multiplied by 1000.

Table 4.6 Average pharmacokinetic parameters of trimethoprim in mice (avg ± SD, N= 5-7)

Parameters	**P-gp WT**	**P-gp KO**	**CF WT**	**CF KO**
CL (ml/min) [d]	3.5 (0.4)	4.3 (1.5)	4.7 (1.1)	5.6 (1.1)
CLr (ml/min) [b,d,f]	0.42 (0.05)	0.42 (0.14)	0.47 (0.11)	0.72 (0.14)
fe_{urine} (%) [a,b,c,d,f]	11.8 (0.1)	9.6 (0.1)	10.1 (0.9)	12.7 (0.2)
Vss (ml) [b,c,e]	107 (18)	103 (30)	162 (64)	86 (18)
$t_{1/2,z}$ (min) [b,d,f]	20.1 (3.4)	16.8 (2.6)	19.3 (5.9)	10.7 (2.3)
$MRT_{0-\infty}$ (min) [b,d,e,f]	30.3 (3.5)	24.4 (2.4)	34.8 (11.3)	15.3 (2.0)

a P<0.05 for P-gp WT and KO
b P<0.05 for CF WT and KO
c P<0.05 for P-gp WT and CF WT
d P<0.05 for P-gp WT and CF KO
e P<0.05 for P-gp KO and CF WT
f P<0.05 for P-gp KO and CF KO

In humans, about 63% of trimethoprim is excreted unchanged into urine. However, in mice as well as in other species, fraction of dose excreted into the urine is much lower (10%, 22%, 15%, 3% and 2% in mice, dogs, pigs, cows and goats, respectively (323-328). Because renal elimination only contributes about ten percent of total clearance of trimethoprim in mice, a 50% increase in the renal clearance of trimethoprim in CF mice does not translate into a pronounced higher total clearance. Renal clearance of trimethoprim (~0.50 ml/min) in mice is larger than the published mouse GFR (~0.28 ml/min, see Table 4.2), and it is also larger than the renal clearance of iothalamate, our GFR marker (~0.20 ml/min, see Table 4.12). This indicates that there is a net renal tubular secretion for trimethoprim. We did not measure the extent of protein binding in mice but in humans it is about 37%. Using this value for our calculation, the net tubular secretion is about 0.32 ml/min (CLr - fu x GFR = 0.5 - 0.63 X 0.28).

There is a statistically significant difference in volume of distribution at steady state, half-life and mean residence time of trimethoprim between CF wild type and CF mice (Table 4.6). Trimethoprim is highly distributed into tissues, as shown by the large Vss values (~115 ml). This value is much greater than the published mice plasma volume and total body water (1 and 14.5 ml, respectively). Half-life and mean residence time are shorter in CF mice due to an apparently higher total clearance and lower Vss compared to CF wild type mice.

To determine sex effects on trimethoprim drug disposition, the data were separated between male and females. There are six female P-gp wild type, two female CF wild type, five male CF wild type, six male CF mice and three male and three female P-gp knockout mice. Not much variation is observed between female P-gp wild type and CF wild type mice; therefore, the data from those two groups were combined. Figure 4.8 shows the plot of average plasma concentration *vs.* time and Table 4.7 lists the average pharmacokinetic parameters for each group. There is no comparison of renal clearance and fraction of drug excreted into the urine based on sex because we mixed male and female mice in urine collection experiments. This is a flaw in our experimental design because we did not control for the sex effects.

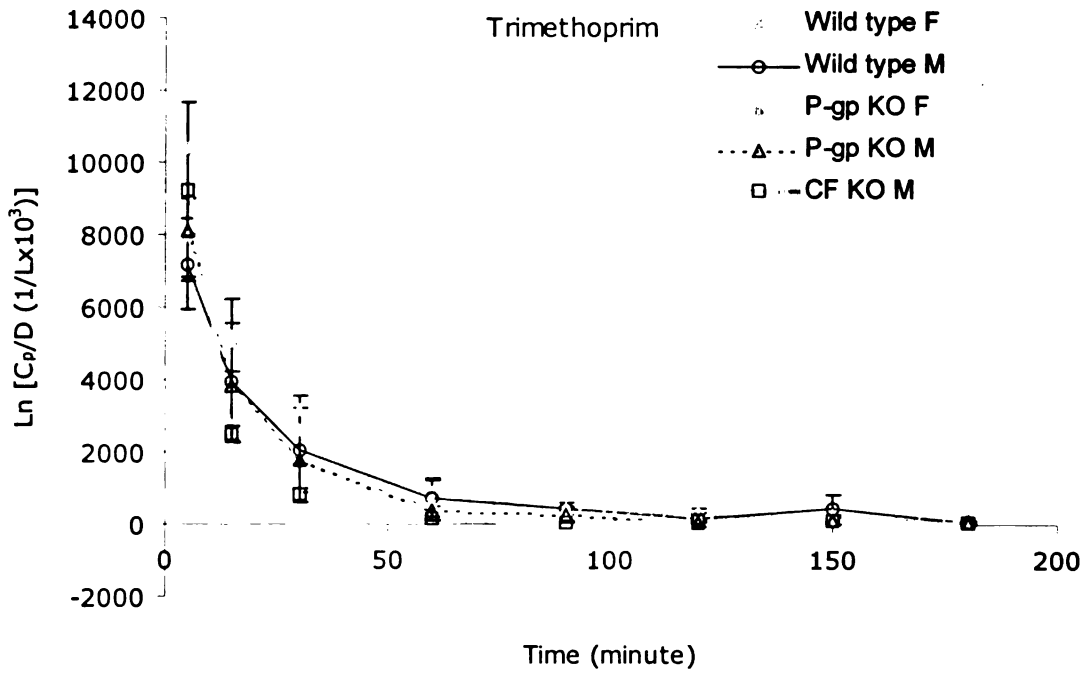

Figure 4.8 Comparison of average plasma concentration-time profiles of trimethoprim among wild type female, wild type male, P-gp knockout female and male and CF knockout male. Thin grey line = wild type female, solid black line =wild type male, dashed grey line = P-gp knockout female, dashed black line = P-gp knockout male, thick grey line = CF knockout male. The units for the y-axis are the natural logarithm of plasma concentration normalized with dose and multiplied by 1000. F = female, M = male. KO = knockout

Table 4.7 Average pharmacokinetic parameters of trimethoprim in mice based on sex (avg ± SD)

Parameters	WT Female N = 8	WT Male N = 5	P-gp KO Female N = 3	P-gp KO Male N = 3	ΔF508 CF Male N = 6
CL (ml/min)	3.9 (0.8)	4.6 (1.2)	3.7 (1.9)	5.0 (0.7)	5.6 (1.1)
Vss (ml)	120 (30)	158 (71)	93 (39)	114 (21)	86 (18)
$t_{1/2,z}$ (min)[e,f]	20 (4)	20 (6)	17 (4)	17 (2)	11 (2.3)
$MRT_{0-\infty}$ (min) [e,f]	31 (4)	35 (13)	26 (2)	23 (1)	15 (2)

a P<0.05 for WT female and male
b P<0.05 for P-gp KO female and male
c P<0.05 for WT female and P-gp KO female
d P<0.05 for WT male and P-gp KO male
e P<0.05 for WT male and ΔF508 male
f P<0.05 for WT female and ΔF508 male

We observe no significant difference in either the concentration-time profiles or in the calculated pharmacokinetic parameters of trimethoprim between males and females in wild type and P-gp knockout mice. This indicates lack of a sex effect on trimethoprim disposition. Comparison of wild type (males and females) and male CF mice reveals a statistically significant difference in the half-life and mean residence time of trimethoprim.

As mentioned earlier, the clearance of trimethoprim is larger than the liver blood flow. Trimethoprim is equally distributed between plasma and red blood cells with a 1:1 ratio; therefore, the plasma clearance is equal to the blood clearance. In fact, the measured clearance of trimethoprim exceeds the sum of liver and renal blood flows. The clearance of a drug should not be larger than the blood flow that delivers it to the elimination organs. Since this suggests extrahepatic and extrarenal metabolism, we decided to determine whether trimethoprim is stable in mouse blood and whether this could explain the high clearance.

To determine the stability of trimethoprim in blood, we added 100 μl of 50 mg/ml trimethoprim to 0.5 ml mouse blood in an Eppendorf tube. For water samples, we used 0.5 ml water instead of blood. Some samples were incubated at 37°C, some at room temperature and some were centrifuged to separate the plasma. At selected time points, 50 μl samples were removed. To process the samples for analysis, 100 μl water was added to the sample. The mixture was vortex mixed and 200 μl ZnSO4/MeOH solution (3:7) containing 150 μg/ml β-OH theophylline was added as internal standard. The mixture was vortex mixed and centrifuged for 10 minutes at >6,000 g at 4°C. The supernatants were saved at 4°C until analysis. Table 4.8 shows the result of trimethoprim stability study. The result indicates that trimethoprim is stable in mouse blood. There is not much difference in the concentration of trimethoprim between samples incubated at room temperature or at 37°C, nor is there much difference between samples collected at 10 *vs.* 240 minutes.

Table 4.8 Results of trimethoprim stability study in mouse blood

Incubation Time (minute)	Water (HPLC area, avg ± SD, n=2, μg/ml)		Blood (HPLC area, avg ± SD, n=2, μg/ml)		Plasma (HPLC area, avg ± SD, n=2, μg/ml)
	Room Temperature	37°C	Room Temperature	37°C	Room Temperature
10	-	-	3103 (373)	3271 (101)	3804 (113)
30	-	-	2929 (309)	3182 (25)	-
90	-	-	3176 (49)	2979 (284)	-
240	3321 (125)	3321 (125)	3000 (47)	2912 (155)	-

4.5.2 Ciprofloxacin

Figure 4.9 shows the plot of plasma concentration *vs.* time for ciprofloxacin in P-gp wild type and P-gp knockout mice. We observe no significant difference in the concentration-time profiles of ciprofloxacin between P-gp wild type and knockout mice. Figure 4.10 shows the plot of plasma concentration *vs.* time for ciprofloxacin in CF wild type and CF mice. We also observe no significant difference in the concentration-time profiles of ciprofloxacin between CF wild type and CF mice. Figure 4.11 shows the plot of average plasma concentration *vs.* time in these four groups of mice and the average pharmacokinetic parameters for each group are listed in Table 4.9.

There is no statistically significant difference in any of the pharmacokinetic parameters calculated for ciprofloxacin among P-gp wild type, P-gp knockout, CF wild type and CF mice. The total clearance of ciprofloxacin in mice is about 1 ml/min. This is lower than the published mouse liver blood flow (1.8 ml/min). The extraction ratio of ciprofloxacin in mice is almost doubled compared to humans (~0.6 and 0.3, respectively).

Renal elimination contributes about thirty 36% of total ciprofloxacin elimination in mice. This is lower than the fraction excreted in urine in humans (about 65%, see Table 4.3). The renal clearance of ciprofloxacin in mice is about 0.37 ml/min. This is slightly larger than the published GFR in mice (0.28 ml/min) and larger than the renal clearance of iothalamate

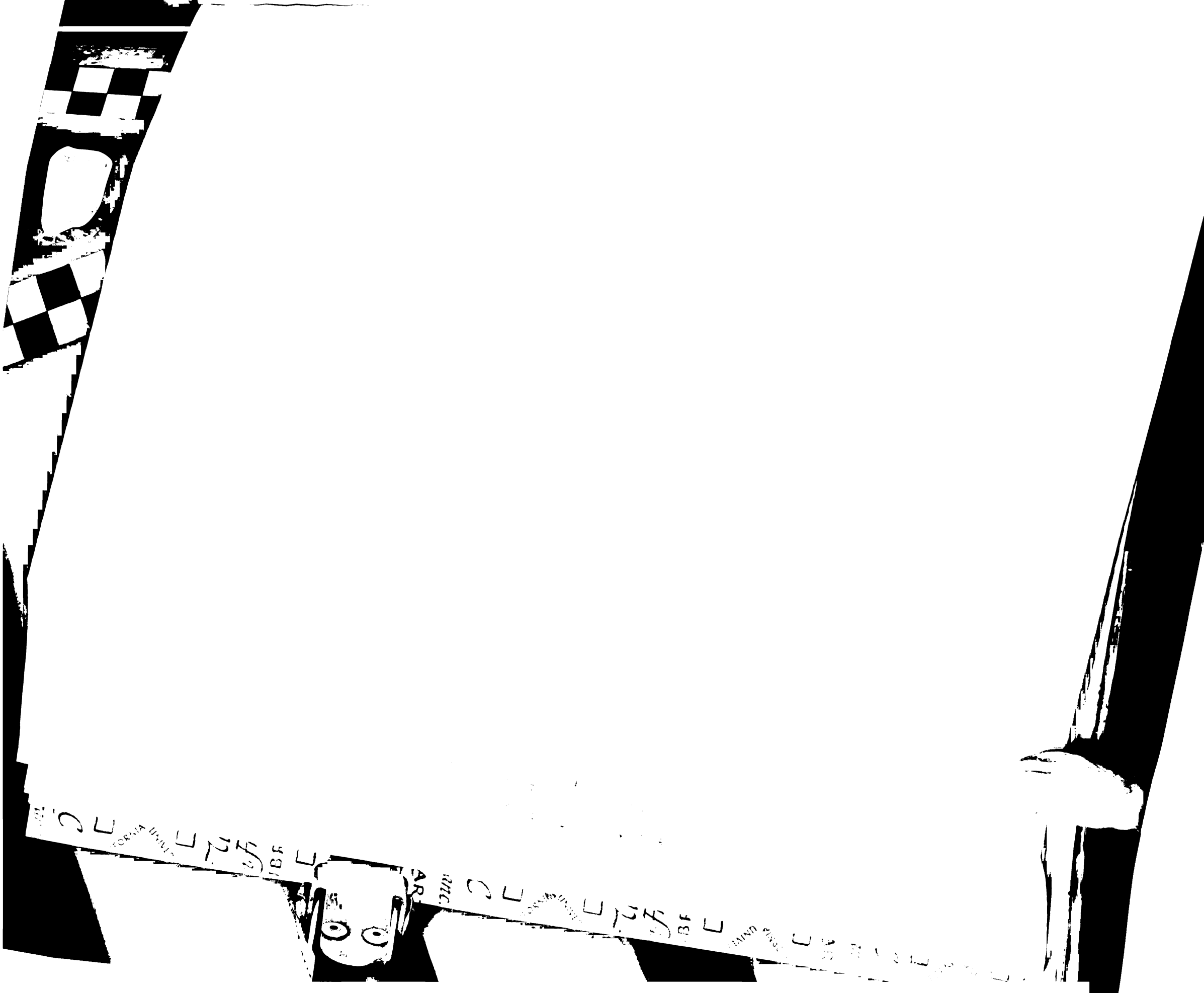

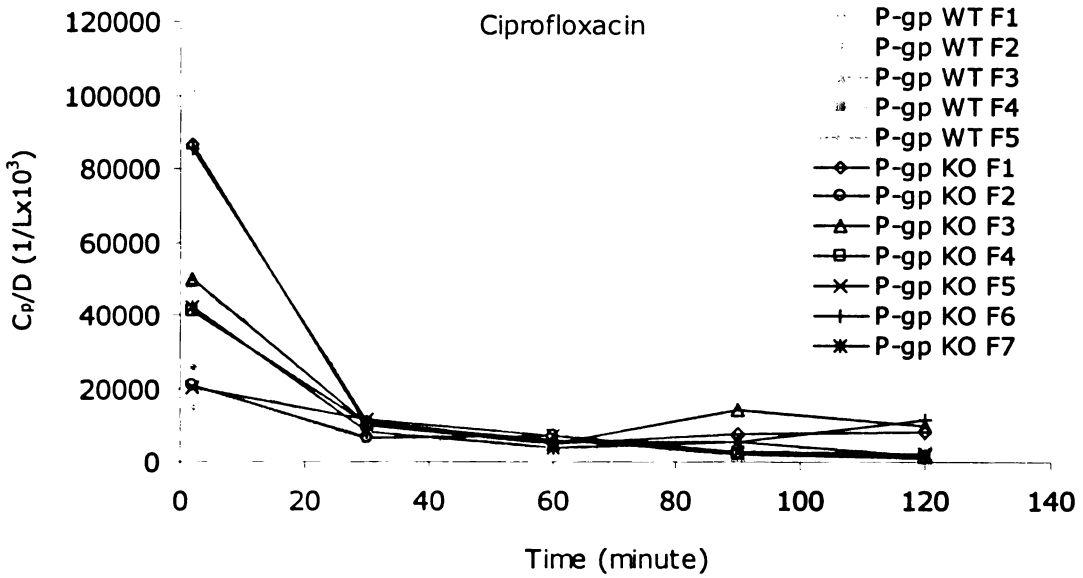

Figure 4.9 Comparison of plasma concentration-time profiles of ciprofloxacin between P-gp wild type (P-gp WT) and P-gp knockout mice (P-gp KO). Grey lines = P-gp WT, black lines = P-gp KO. F = female. The units for the y-axis are plasma concentration normalized with dose and multiplied by 1000.

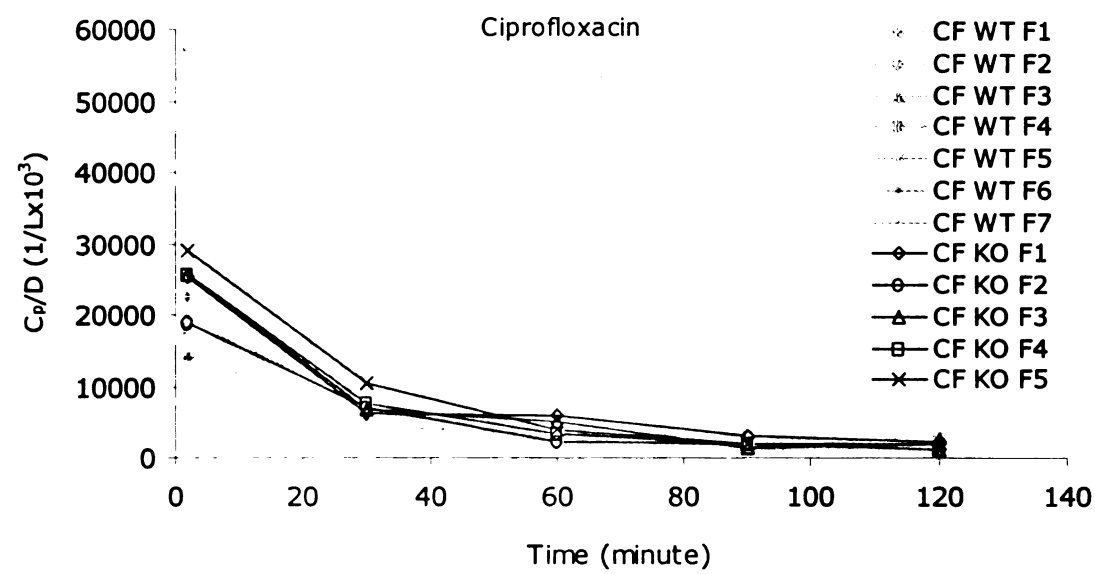

Figure 4.10 Comparison of plasma concentration-time profiles of ciprofloxacin between CF wild type (CF WT) and CF mice (CF KO). Grey lines = CF WT, black lines = CF KO. F = female. The units for the y-axis are plasma concentration normalized with dose and multiplied by 1000.

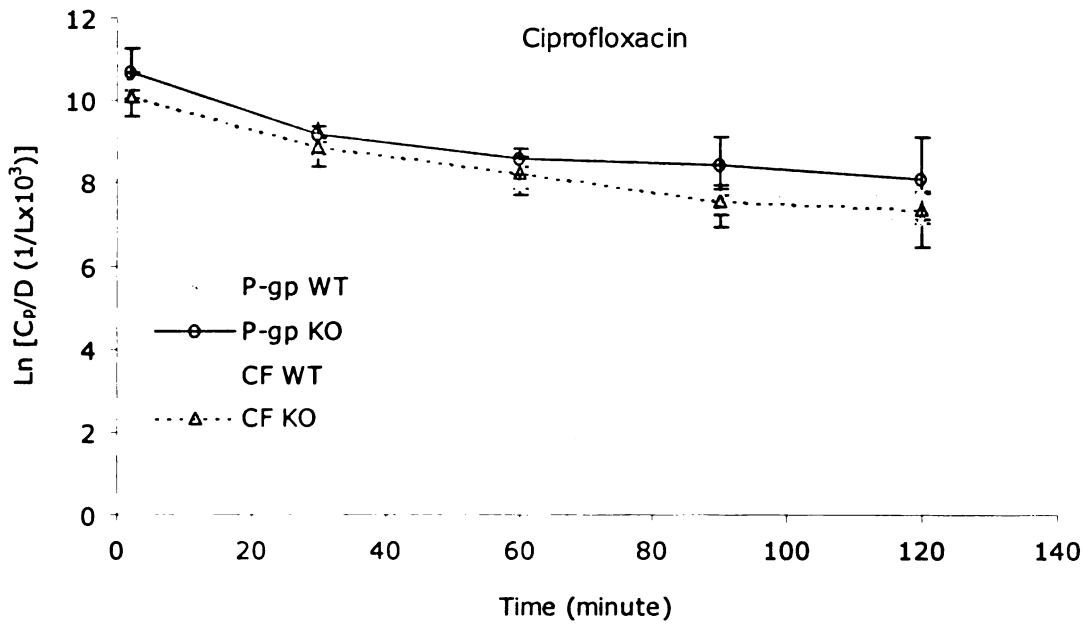

Figure 4.11 Comparison of average plasma concentration-time profiles of ciprofloxacin between P-gp wild type (P-gp WT), P-gp knockout (P-gp KO), CF wild type (CF WT) and CF mice (CF KO). Solid grey line = P-gp WT, solid black line = P-gp KO, dashed grey line = CF WT, dashed black line = CF KO. The units for the y-axis are the natural logarithm of plasma concentration normalized with dose and multiplied by 1000.

Table 4.9 Average pharmacokinetic parameters of ciprofloxacin in mice (avg ± SD, n=5-7)

Parameters	**P-gp WT**	**P-gp KO**	**CF WT**	**CF KO**
CL (ml/min)	0.92 (0.49)	0.81 (0.26)	1.17 (0.34)	1.16 (0.16)
CLr (ml/min)	0.28 (0.17)	0.29 (0.17)	0.50 (0.28)	0.39 (0.11)
fe_{urine} (%)	30.8 (7.4)	35.5 (8.8)	42.3 (9.9)	33.7 (8.5)
Vss (ml)	32.3 (23.0)	30.9 (14.8)	35.8 (13.8)	42.7 (11.0)
$t_{1/2,z}$ (min)	24.9 (2.5)	32.0 (4.9)	31.0 (16.9)	27.9 (3.5)
$MRT_{0-\infty}$ (min)	32.5 (7.0)	37.3 (9.2)	30.5 (10.2)	36.3 (4.7)

(~0.20 ml/min, see Table 4.12). This indicates that there is a net renal tubular secretion for ciprofloxacin in mice. We did not measure the extent of protein binding in mice but in humans it is about 40%. Using this value for our calculation, the net tubular secretion is about 0.20

ml/min (CLr - fu x GFR = 0.37 - 0.60 X 0.28). The lack of a difference in renal clearance observed between P-gp wild type and knockout mice suggests that tubular secretion of ciprofloxacin in mice cannot be attributed to P-gp. This result is similar to the observed no change in the renal clearance in mdr1a (-/-) mice for grepafloxacin, a member of the fluoroquinolone family and a P-gp substrate (329).

Ciprofloxacin is highly distributed into tissues, as shown by the large Vss values (~36 ml). This value is much greater than the published mice plasma volume and total body water (1 and 14.5 ml, respectively).

All ciprofloxacin experiments were performed on female mice; therefore, no comparison of sex effects can be made for ciprofloxacin.

4.5.3 Sulfamethoxazole

Figure 4.12 shows the plot of plasma concentration *vs.* time for sulfamethoxazole in P-gp wild type and P-gp knockout mice. We observe no significant difference in the concentration-time profiles of sulfamethoxazole between P-gp wild type and knockout mice. Figure 4.13 shows the plot of plasma concentration *vs.* time for sulfamethoxazole in CF wild type and CF mice. We also observe no significant difference in the concentration-time profiles of sulfamethoxazole between CF wild type and CF mice. Figure 4.14 shows the plot of average plasma concentration *vs.* time in these four groups of mice and the average pharmacokinetic parameters for each group are listed in Table 4.10.

Unlike humans, the half-life of sulfamethoxazole in mice (~125 minutes) is different from the half-life of trimethoprim (~17 minutes) in mice. Therefore, the 180 minute plasma collection period is only slightly over one half-life for sulfamethoxazole. A significant portion of area under the curve and area under the moment curve is based on extrapolated values, which is presented in Table 4.11. Therefore, a reliable estimate of pharmacokinetic parameters for sulfamethoxazole cannot be obtained. The only parameter where we have confidence is the

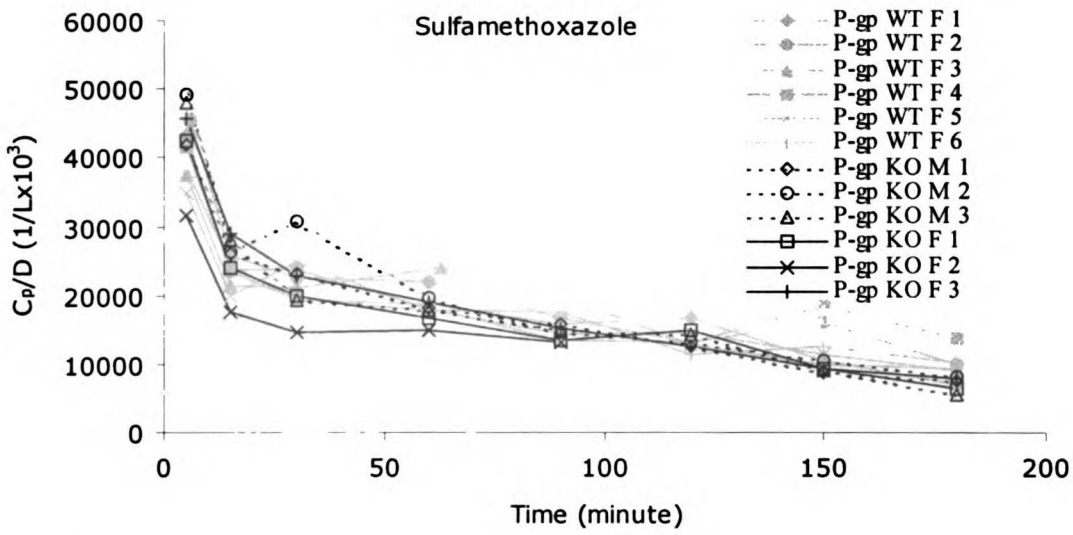

Figure 4.12 Comparison of plasma concentration-time profiles of sulfamethoxazole between P-gp wild type (P-gp WT) and P-gp knockout mice (P-gp KO). Grey lines = P-gp WT, black lines = P-gp KO. Solid lines = female mice, dashed lines = male mice. F = female, M = male. The units for the y-axis are plasma concentration normalized with dose and multiplied by 1000.

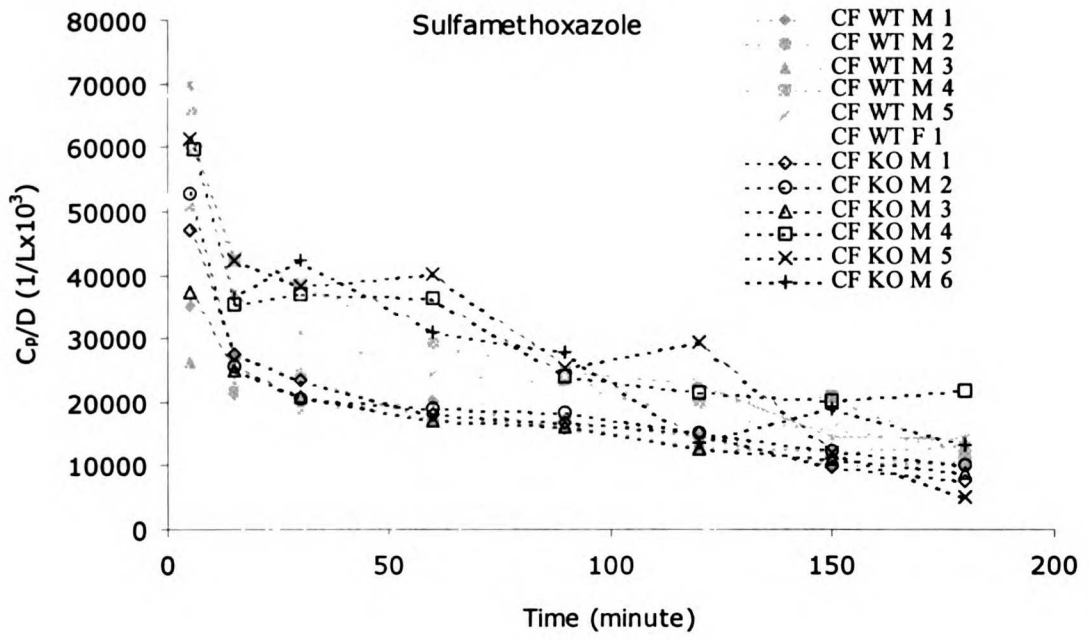

Figure 4.13 Comparison of plasma concentration-time profiles of sulfamethoxazole between CF wild type (CF WT) and CF mice (CF KO). Grey lines = CF WT, black lines = CF KO. Solid lines = female mice, dashed lines = male mice. F = female, M = male. The units for the y-axis are plasma concentration normalized with dose and multiplied by 1000.

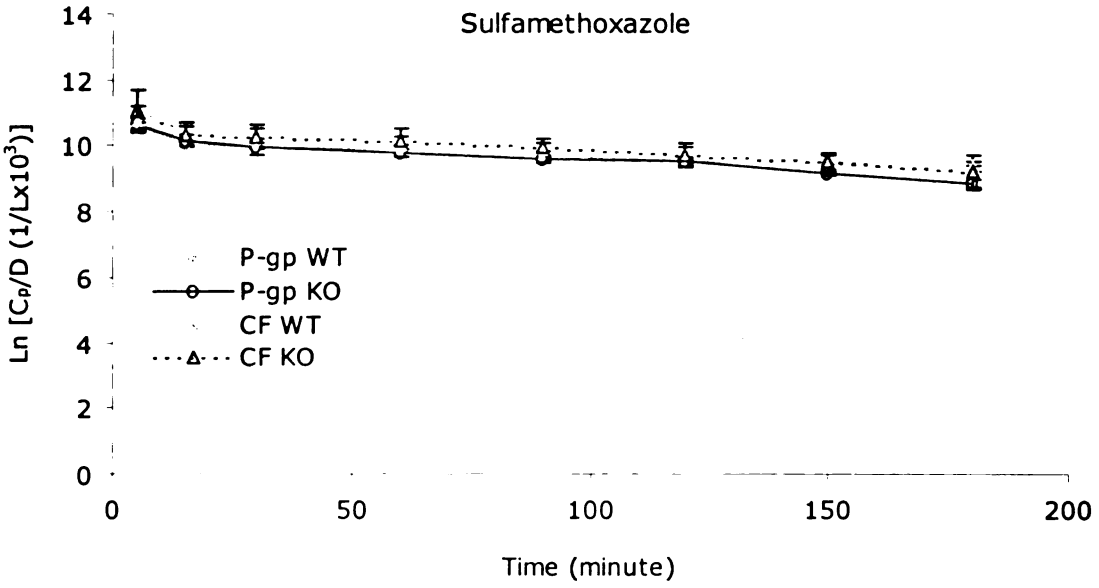

Figure 4.14 Comparison of average plasma concentration-time profiles of sulfamethoxazole between P-gp wild type (P-gp WT), P-gp knockout (P-gp KO), CF wild type (CF WT) and CF mice (CF KO). Solid grey line = P-gp WT, solid black line = P-gp KO, dashed grey line = CF WT, dashed black line = CF KO. The units for the y-axis are the natural logarithm of plasma concentration normalized with dose and multiplied by 1000.

Table 4.11 Average pharmacokinetic parameters of sulfamethoxazole in mice (avg ± SD, n=5-7)

Parameters	**P-gp WT**	**P-gp KO**	**CF WT**	**CF KO**
CL (ml/min) [a,e,f]	0.19 (0.04)	0.24 (0.03)	0.17 (0.02)	0.18 (0.05)
CLr (ml/min) [b]	0.029 (0.013)	0.031 (0.014)	0.030 (0.003)	0.040 (0.012)
fe_{urine} (%) [b,d,f]	15.0 (6.1)	13.2 (5.7)	17.7 (0.03)	22.8 (2.0)
Vss (ml)	36 (3)	34 (10)	31 (10)	26 (8)
$t_{1/2,z}$ (min)	145 (42)	111 (50)	128 (34)	114 (38)
$MRT_{0-\infty}$ (min)	198 (65)	151 (72)	181 (55)	159 (57)
CLf (ml/min)	0.010 (0.002)	0.013 (0.005)	0.011 (0.002)	0.012 (0.004)
AUC extrapolated (%)	38 (10)	31 (20)	36 (10)	30 (14)
AUMC extrapolated (%)	75 (9)	65 (16)	73 (9)	64 (21)

a P<0.05 for P-gp WT and KO
b P<0.05 for CF WT and KO
c P<0.05 for P-gp WT and CF WT
d P<0.05 for P-gp WT and CF KO
e P<0.05 for P-gp KO and CF WT
f P<0.05 for P-gp KO and CF KO

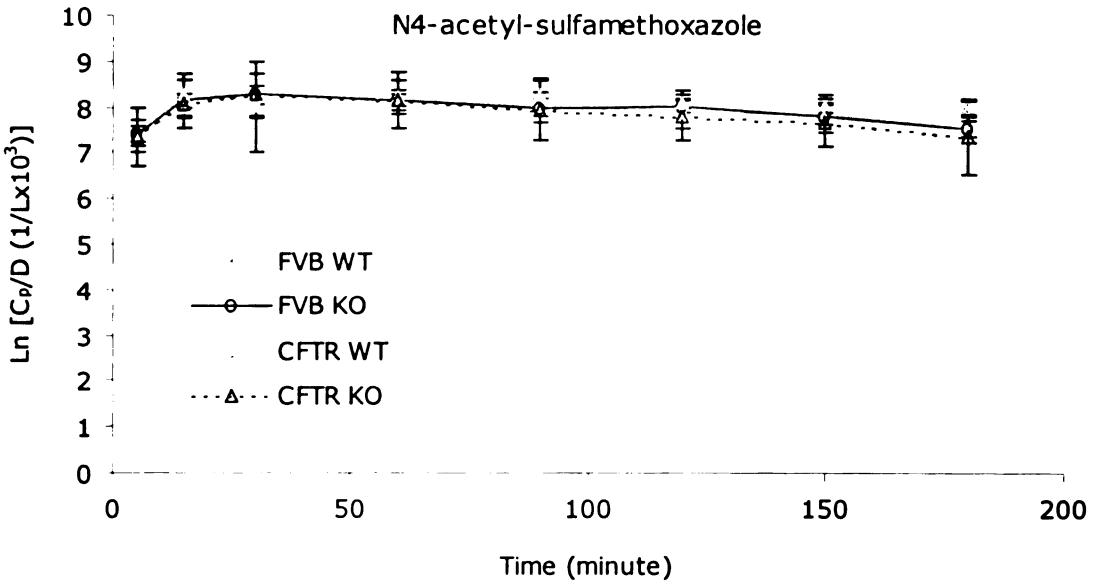

Figure 4.15 Comparison of average plasma concentration-time profiles of N4-acetylsulfamethoxazole between P-gp wild type (P-gp WT), P-gp knockout (P-gp KO), CF wild type (CF WT) and CF mice (CF KO). Solid grey line = P-gp WT, solid black line = P-gp KO, dashed grey line = CF WT, dashed black line = CF KO. The units for the y-axis are the natural logarithm of plasma concentration normalized with dose and multiplied by 1000.

fraction of sulfamethoxazole excreted into the urine because urine was collected for over 12 hours. In interpreting the results, we have to keep this in mind.

Similar to trimethoprim, the renal clearance of sulfamethoxazole is significantly higher in CF mice compared to CF wild type mice resulting in a higher fraction of sulfamethoxazole excreted into the urine in CF mice. No difference is observed between P-gp wild type and knockout mice. This suggests that higher renal clearance in CF mice is not caused by P-gp. The renal clearance in mice (~0.03 ml/min) is much lower than the published GFR in mice (0.28 ml/min) and also lower than the renal clearance of iothalamate (~0.20 ml/min, see Table 4.12). This suggests that there is a net renal tubular reabsorption for sulfamethoxazole in mice, as in humans. We did not measure the extent of protein binding in mice but in humans it is about 62%. Using this value for our calculation, the net tubular reabsorption is about 0.07 ml/min (fu x GFR - CLr = 0.38 X 0.28 - 0.03). Higher renal clearance in CF mice could be due to a decrease in tubular reabsorption of sulfamethoxazole. Because renal elimination only contributes about 17% of total clearance of sulfamethoxazole in mice, a 30%

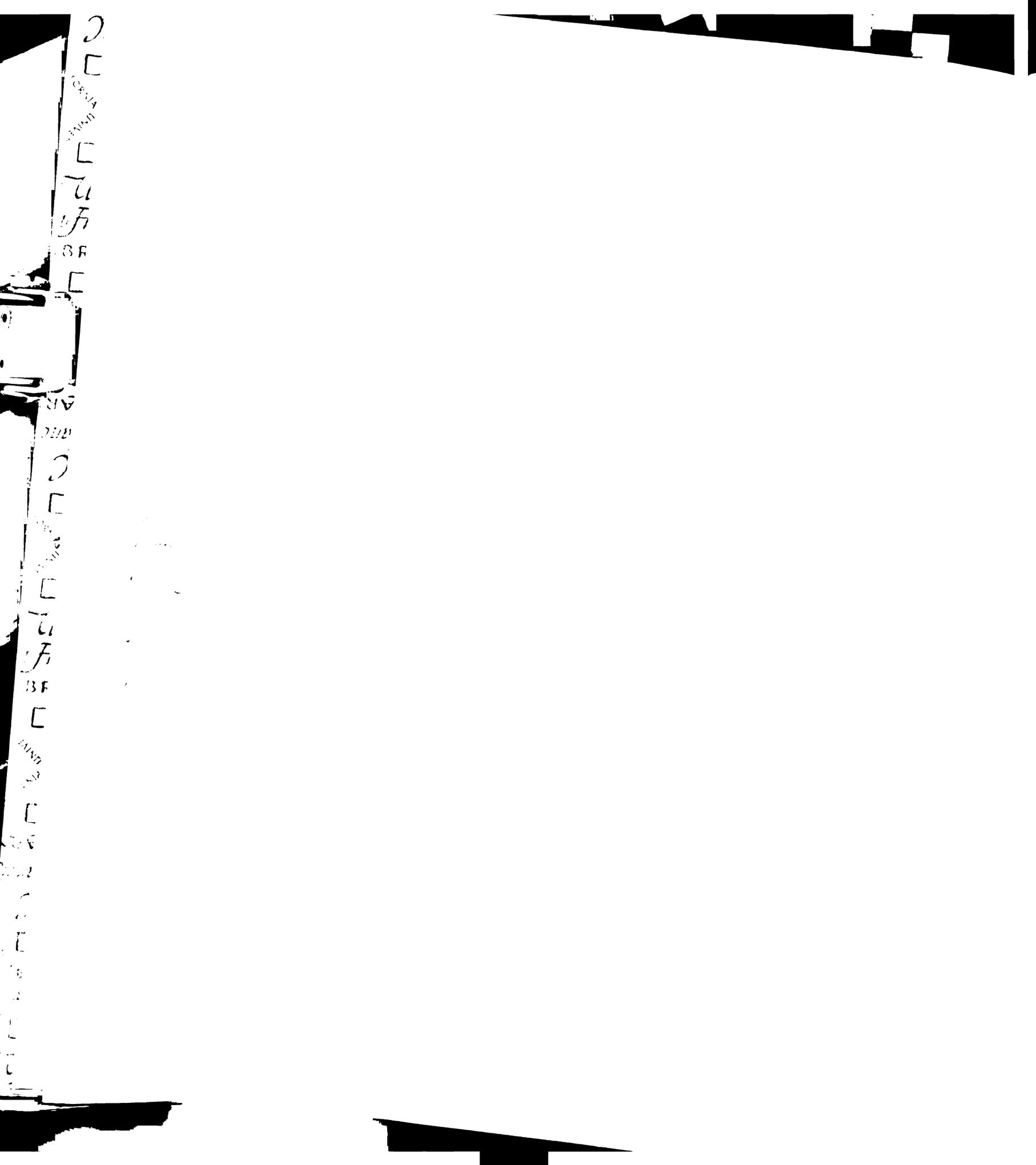

increase in renal clearance does not translate into a higher total clearance. The extent of renal elimination is similar between mice and humans (~17 and 14%, respectively).

The total clearance of sulfamethoxazole is higher in P-gp knockout mice compared to P-gp wild type mice. Because there is no difference in the renal clearance, the observed higher total clearance is due to an increase in nonrenal elimination pathways. We observe no significant difference in the formation clearance of N4-acetylsulfamethoxazole, the major metabolite of sulfamethoxazole between P-gp wild type and knockout mice (Figure 4.15). Therefore, the increase in total clearance is due to enhanced elimination by other pathways in P-gp knockout mice. In CF patients, there is a reported 2.5-fold increase in the formation clearance of N4-acetylsulfamethoxazole (201). However, we observe no difference in the formation clearance of N4-acetylsulfamethoxazole between CF wild type and CF mice (Figure 4.15).

To determine the sex effects on sulfamethoxazole drug disposition, the data were analyzed as described earlier for trimethoprim. Figure 4.16 shows the plot of average plasma concentration *vs.* time curves and Table 4.11 lists the average pharmacokinetic parameters for each group. We observe no significant difference in either the concentration-time profiles or in the calculated pharmacokinetic parameters of sulfamethoxazole between males and females in wild type and P-gp knockout mice. This indicates lack of sex effect on sulfamethoxazole disposition. The total clearance is significantly higher in male and female P-gp knockout compared to male and female wild type mice and male CF mice.

4.5.4 Iothalamate

Figures 4.17-4.19 show the iothalamate plots from the experiments where iothalamate was dosed together with trimethoprim and sulfamethoxazole. Figure 4.17 shows the plot of plasma concentration *vs.* time for iothalamate in P-gp wild type and P-gp knockout mice. We observe no significant difference in the concentration-time profiles of iothalamate between P-gp wild type and knockout mice. Figure 4.18 shows the plot of plasma concentration *vs.* time for iothalamate in CF wild type and CF mice. The concentration -time profiles in CF wild type mice appear to be different from CF mice. Figure 4.19 shows the plot

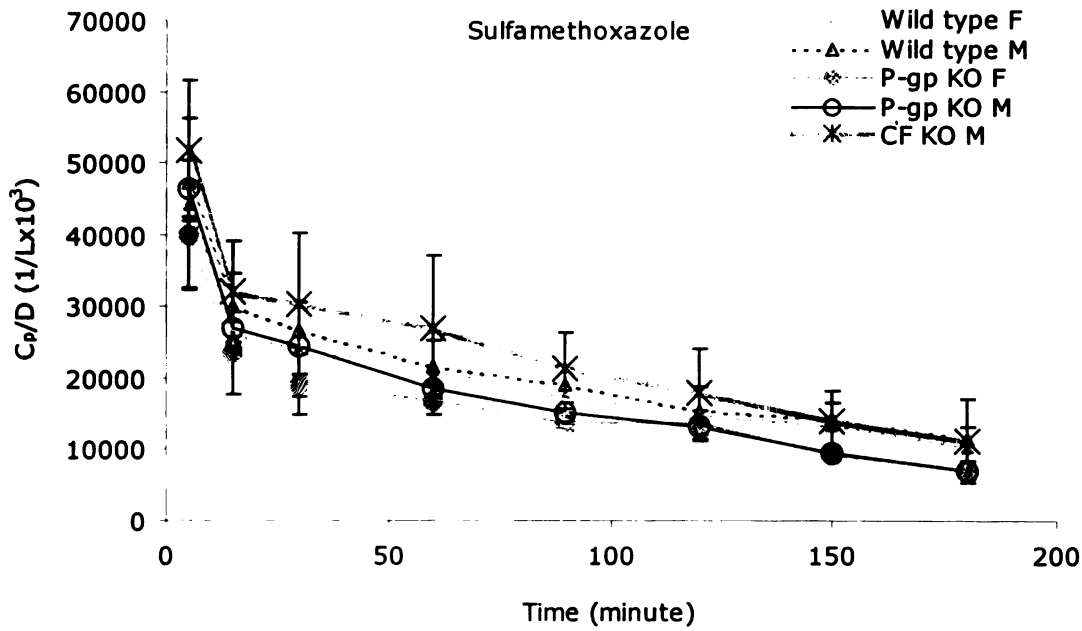

Figure 4.16 Comparison of average plasma concentration-time profiles of sulfamethoxazole among wild type female, wild type male, P-gp knockout female and male and CF knockout male. Thin grey line = wild type female, solid black line =wild type male, dashed grey line = P-gp knockout female, dashed black line = P-gp knockout male, thick grey line = CF knockout male. The units for the y-axis are the natural logarithm of plasma concentration normalized with dose and multiplied by 1000. F = female, M = male. KO = knockout

Table 4.11 Average pharmacokinetic parameters of sulfamethoxazole based on sex in mice (avg ± SD, n=5-7)

Parameters	WT Female N = 8	WT Male N = 5	P-gp KO Female N = 3	P-gp KO Male N = 3	ΔF508 CF Male N = 6
CL (ml/min)	0.18 (0.03)	0.17 (0.02)	0.22 (0.04)	0.24 (0.02)	0.18 (0.05)
Vss (ml)	35 (6)	30 (8)	38 (13)	30 (4)	26 (8)
$t_{1/2,z}$ (min)	144 (38)	130 (33)	132 (70)	95 (14)	114 (38)
$MRT_{0-\infty}$ (min)	199 (55)	184 (55)	184 (99)	127 (22)	159 (57)

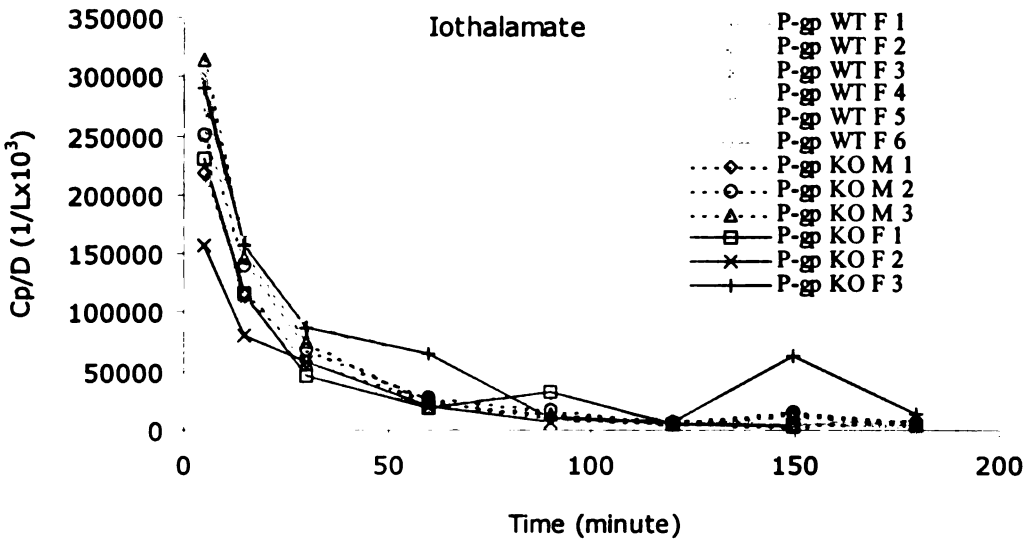

Figure 4.17 Comparison of plasma concentration-time profiles of iothalamate between P-gp wild type (P-gp WT) and P-gp knockout mice (P-gp KO). Grey lines = P-gp WT, black lines = P-gp KO. Solid lines = female mice, dashed lines = male mice. F = female, M = male. The units for the y-axis are plasma concentration normalized with dose and multiplied by 1000.

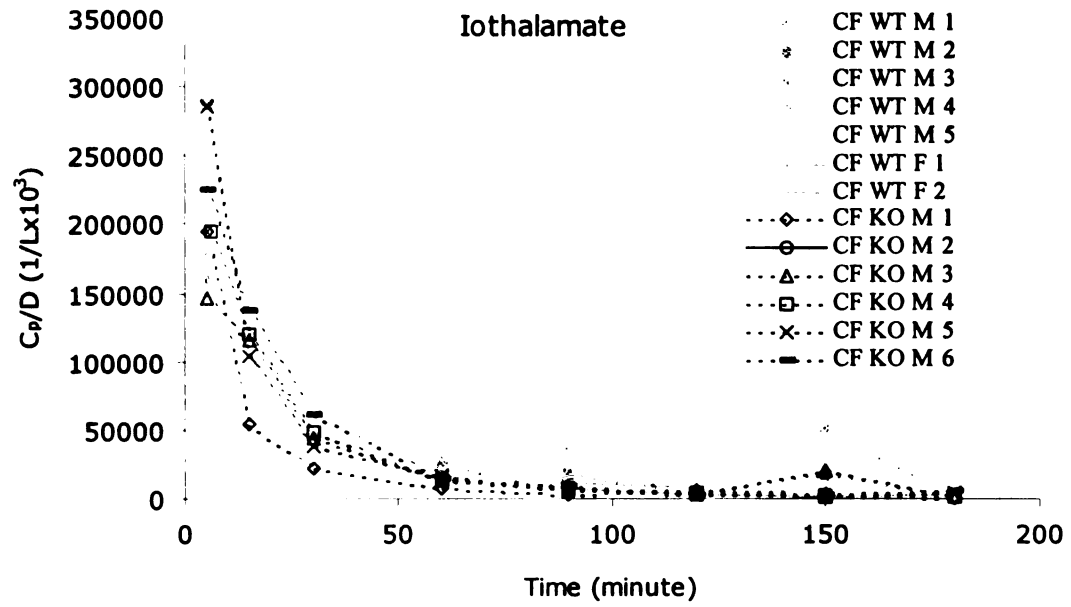

Figure 4.18 Comparison of plasma concentration-time profiles of iothalamate between CF wild type (CF WT) and CF mice (CF KO). Grey lines = CF WT, black lines = CF KO. Solid lines = female mice, dashed lines = male mice. F = female, M = male. The units for the y-axis are plasma concentration normalized with dose and multiplied by 1000.

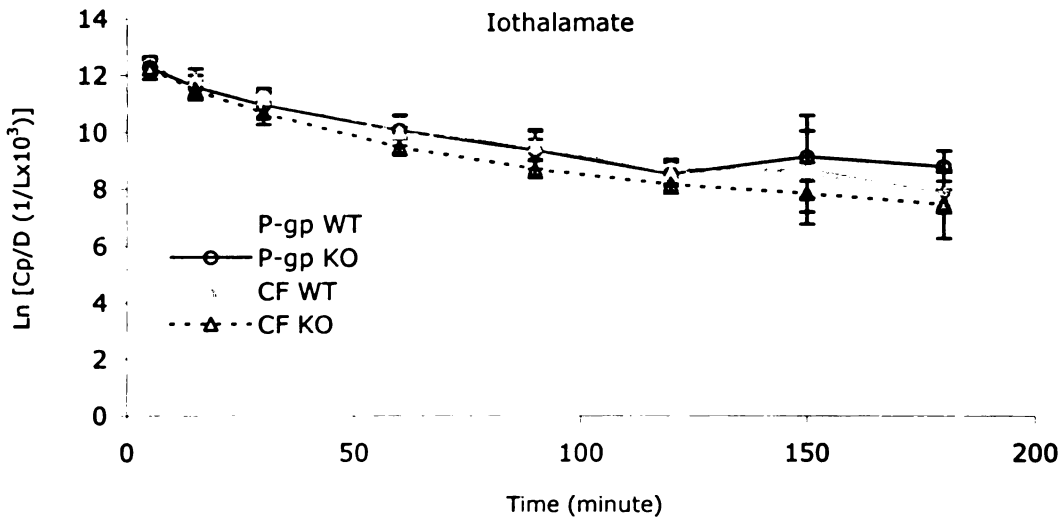

Figure 4.19 Comparison of average plasma concentration-time profiles of iothalamate between P-gp wild type (P-gp WT), P-gp knockout (P-gp KO), CF wild type (CF WT) and CF mice (CF KO). Solid grey line = P-gp WT, solid black line = P-gp KO, dashed grey line = CF WT, dashed black line = CF KO. The units for the y-axis are the natural logarithm of plasma concentration normalized with dose and multiplied by 1000.

of average plasma concentration *vs.* time in these four groups of mice and the average pharmacokinetic parameters for each group are listed in Table 4.12.

Table 4.12 Average pharmacokinetic parameters of iothalamate in mice (avg ± SD, n=5-7)

Parameters	**P-gp WT**	**P-gp KO**	**CF WT**	**CF KO**
CL (ml/min) [b,d,f]	0.28 (0.05)	0.31 (0.09)	0.29 (0.02)	0.41 (0.08)
CLr (ml/min) [b,d,f]	0.16 (0.04)	0.13 (0.04)	0.19 (0.01)	0.33 (0.06)
fe_{urine} (%) [a,b,d,e,f]	58.1 (12.6)	43.4 (3.3)	64.7 (0.5)	81.2 (2.4)
Vss (ml)	9.0 (1.7)	10.8 (1.6)	10.4 (4.6)	11.2 (2.9)
$t_{1/2,z}$ (min)	23.4 (4.6)	24.2 (3.3)	24.0 (7.4)	20.7 (1.6)
$MRT_{0-\infty}$ (min)	32.1 (3.0)	36.0 (6.3)	35.3 (14.3)	27.7 (6.1)

a P<0.05 for P-gp WT and KO
b P<0.05 for CF WT and KO
c P<0.05 for P-gp WT and CF WT
d P<0.05 for P-gp WT and CF KO
e P<0.05 for P-gp KO and CF WT
f P<0.05 for P-gp KO and CF KO

The total and renal clearances of iothalamate are similar between P-gp wild type and knockout mice and they are higher in CF mice compared to CF wild type mice. Higher total clearance in CF mice is completely accounted for by the increase in the renal clearance. This suggests that glomerular filtration rate is higher in CF mice. The fraction of iothalamate excreted in the urine is lower than 1 in all four groups of mice and we observe a statistically significant difference in fe_{urine} values between P-gp wild type and knockout mice and between CF wild type and CF mice. We expected a higher fraction excreted in the urine for iothalamate because it is a marker of GFR and it is assumed that it is not secreted, reabsorbed or metabolized and has minimal protein binding in humans. However, renal elimination only contributes about 62% of total clearance of iothalamate in our experiments. This leads to lower renal clearance of iothalamate (~0.20 ml/min) compared to the published GFR in mice (~0.28 ml/min, Table 4.2), but the total clearance of iothalamate (~0.29 ml/min) is comparable to the published GFR value in mice.

To our knowledge, GFR in mice is estimated based on the total clearance instead of direct renal clearance measurements (330-332). Most iothalamate experiments are not mass-balanced. The disappearance of iothalamate from plasma is not mass-balanced by its appearance in the urine. Even though iothalamate is completely removed by the kidneys in humans, the elimination pathways might be different in other species. Griep *et al.* (333) reported that 0-22% of iothalamate is excreted into the bile in aglomerular fish but bile excretion is not observed in humans. Blaufox *et al.* (334) reported a clearance of 0.07 ml/min/100 g in an anephric rat, suggesting extrarenal elimination of iothalamate. Pihl *et al.* (335) reported that the total clearance of iothalamate in dogs is 10-13% higher than the renal clearance. Gagnon *et al.* (336) reported an iothalamate to inulin clearance ratio of 0.9 in dogs and 1 in humans. Nielsen *et al.* (337) reported that the renal clearance of iothalamate is slightly lower than the total clearance in pigs (65 and 73 ml/min, respectively). All these examples show that iothalamate is not completely removed by the kidneys in fish, rats, dogs and pigs. It is not known whether extrarenal elimination of iothalamate also occurs in mice. After an extensive search of the literature, we did not find any report with regard to mass balance experiments or comparison of total and renal clearance values of iothalamate in mice.

Currently we do not know the cause of the low fraction of iothalamate excreted in the urine in mice. Iothalamate is a very stable compound and when we spiked iothalamate to mice metabolic cages and let stand overnight we were able to get close to 100% recovery. A pilot study showed that iothalamate was not excreted in the feces in mice. Further studies need to be performed to determine if iothalamate is metabolized in mice and whether this is responsible for differences in fe_{urine} values observed between P-gp wild type and knockout mice and CF wild type and CF mice.

To determine the sex effects on iothalamate drug disposition, the data were analyzed as described earlier for trimethoprim. Figure 4.20 shows the plot of average plasma concentration *vs.* time curves and Table 4.13 lists the average pharmacokinetic parameters for each group. We observe no significant difference in either the concentration profiles or in the calculated pharmacokinetic parameters of iothalamate between male and female in wild type and P-gp knockout mice. This indicates lack of sex effect on iothalamate disposition.

Figure 4.21 shows the plot of average plasma concentration *vs.* time for iothalamate from experiments where it was dosed together with ciprofloxacin. The plot is very similar to the plot of iothalamate dosed together with trimethoprim and sulfamethoxazole (Figure 4.19), with the exception that there is no significant difference observed in the concentration-time profiles of iothalamate between CF wild type and CF mice. The fractions of iothalamate eliminated into the urine also show no difference among P-gp wild type, P-gp knockout, CF wild type and CF mice (72.9 ± 0.9, 68.7 ± 10.9, 75.7 ± 11.1, 80 ± 13.3 percent, respectively). Therefore, there is no difference in the renal clearance of iothalamate between P-gp wild type and P-gp knockout mice and between CF wild type and CF knockout mice. Previous experiments with iothalamate showed a higher renal clearance of iothalamate in CF mice compared to CF wild type mice. This difference could be due to the sex effect (male CF mice in trimethoprim-sulfamethoxazole-iothalamate *vs.* female CF mice in ciprofloxacin-iothalamate experiments) or it could be attributed to chance.

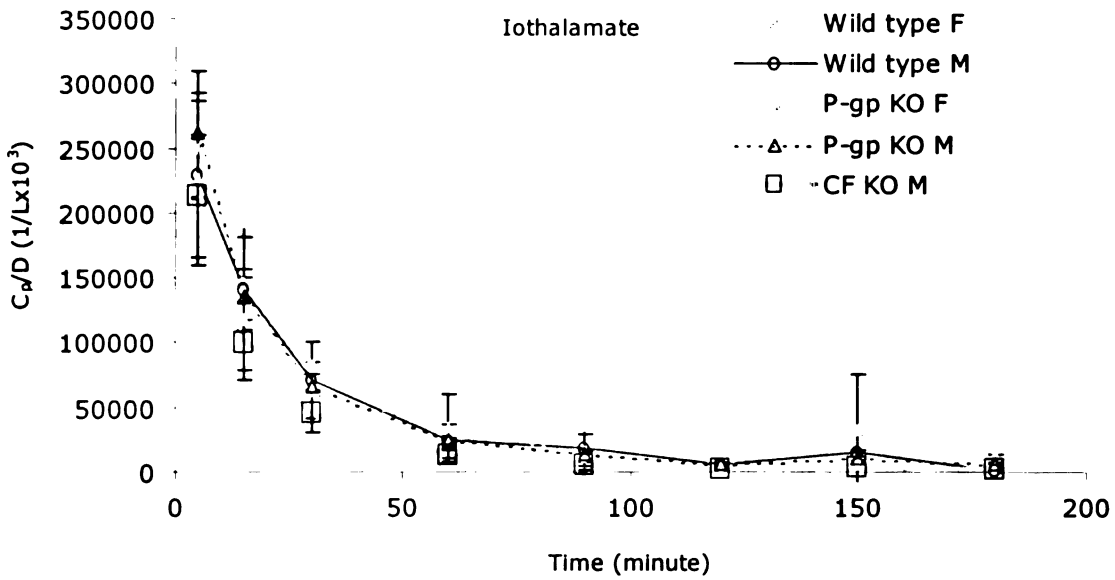

Figure 4.20 Comparison of average plasma concentration-time profiles of iothalamate among wild type female, wild type male, P-gp knockout female and male and CF knockout male. Thin grey line = wild type female, solid black line =wild type male, dashed grey line = P-gp knockout female, dashed black line = P-gp knockout male, thick grey line = CF knockout male. The units for the y-axis are the natural logarithm of plasma concentration normalized with dose and multiplied by 1000. F = female, M = male. KO = knockout

Table 4.13 Average pharmacokinetic parameters of iothalamate based on sex in mice (avg ± SD)

Parameters	**WT Female N = 8**	**WT Male N = 5**	**P-gp KO Female N = 3**	**P-gp KO Male N = 3**	**ΔF508 CF Male N = 6**
CL (ml/min)[f]	0.28 (0.04)	0.29 (0.02)	0.34 (0.12)	0.29 (0.04)	0.41 (0.08)
Vss (ml)	9 (2)	11 (5)	11 (1)	11 (2)	11 (3)
$t_{1/2,z}$ (min)	22 (6)	26 (5)	24 (5)	24 (2)	21 (2)
$MRT_{0-\infty}$ (min)	31 (4)	37 (15)	35 (9)	37 (4)	28 (6)

a P<0.05 for WT female and male
b P<0.05 for P-gp KO female and male
c P<0.05 for WT female and P-gp KO female
d P<0.05 for WT male and P-gp KO male
e P<0.05 for WT male and ΔF508 male
f P<0.05 for WT female and ΔF508 male

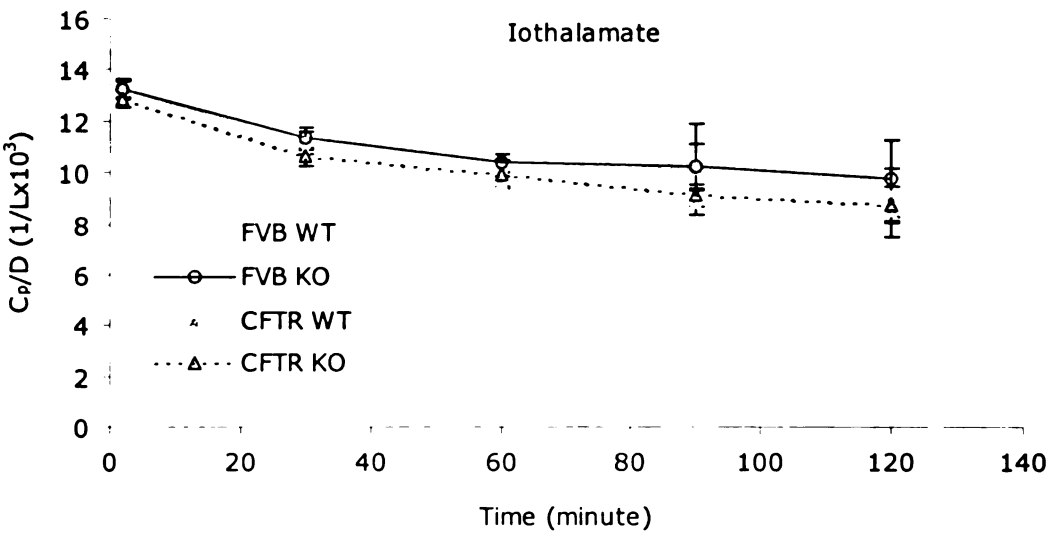

Figure 4.21 Comparison of average plasma concentration-time profiles of iothalamate between P-gp wild type (P-gp WT), P-gp knockout (P-gp KO), CF wild type (CF WT) and CF mice (CF KO). Solid grey line = P-gp WT, solid black line = P-gp KO, dashed grey line = CF WT, dashed black line = CF KO. The units for the y-axis are the natural logarithm of plasma concentration normalized with dose and multiplied by 1000.

4.5 Discussion and Conclusions

We observe that the renal clearance of trimethoprim and sulfamethoxazole are higher in CF mice compared to CF wild type mice. However, the renal clearance of iothalamate that was dosed together with trimethoprim and sulfamethoxazole is also higher in CF mice compared to CF wild type mice. This, together with the observation of no difference in the renal clearance of trimethoprim and sulfamethoxazole between P-gp wild type and knockout mice, suggests that the observed higher renal clearance is due to higher GFR instead of higher tubular secretion caused by increased P-gp expression. However, no difference in the renal clearance of iothalamate, dosed together with ciprofloxacin, was observed between CF wild type and CF mice. This suggests that GFR is not higher in CF mice, an opposite result to that described above for the trimethoprim and sulfamethoxazole study. This discrepancy could potentially be explained by a sex effect. Due to a limited number of CF mice, trimethoprim and sulfamethoxazole experiments were performed in male CF mice while ciprofloxacin experiments were performed in female CF mice. Therefore, GFR could be increased in male

but not female CF mice. However, we cannot conclusively rule out the possibility that the differences we observed are due to chance since the differences we observe for the renal clearance of trimethoprim, sulfamethoxazole and iothalamate between CF wild type and CF mice are not that large. This could be due to lack of power in the experiments due to the small sample size.

It is interesting that we do not see any difference in the concentration-time profiles of P-gp substrates (trimethoprim and ciprofloxacin) between P-gp wild type and knockout mice. One explanation could be that trimethoprim and ciprofloxacin are substrates of human but not mice P-gp. Another explanation could be that they are not very good substrates of P-gp, consistent with conflicting results in several P-gp overexpressing cell lines (Chapter 2). A third explanation could be that the effect of P-gp on plasma concentration cannot be observed from dosing the drugs intravenously. Indinavir, saquinavir and nelfinavir are substrates of P-gp. Intravenous administration of these drugs to P-gp knockout mice (*mdr1a* (-/-)) show no difference in their plasma concentration profiles compared to wild type mice but the brain concentrations of saquinavir, indinavir and nelfinavir in *mdr1a* (-/-) mice were elevated 7, 10 and 36-fold, respectively (338). Following oral administration, unlike intravenous administration, the plasma concentrations of indinavir, saquinavir and nelfinavir in P-gp knockout mice were increased 2, 4 and 5-fold, respectively (338). *In vitro* studies have shown that saquinavir and ritonavir are substrates of both human and mouse P-gp (339-341). This suggests that mechanisms other than P-gp are important for the elimination of these drugs and P-gp in the intestine is important for the oral bioavailability of drugs that are substrates of P-gp.

There are other examples of the effect of P-gp on limiting drug accumulation in the brain but no effect was observed on plasma concentration or total clearance. Savolainen *et al.* (342) reported no change in nelfinavir total clearance with GG918, a P-gp inhibitor, but the brain to plasma ratio increased 100-fold. van Asperen *et al.* (343) reported no change in vinblastine steady state plasma concentration between wild type and *mdr1a* (-/-) mice but the brain concentration in *mdr1a* (-/-) mice was increased by 10-fold. Leusch *et al.* (344) reported a

10-fold increase in apafant brain to plasma ratio in *mdr1a* (-/-) mice but no change was observed in total clearance. This lack of difference in total clearance in *mdr1a* (-/-) mice was due to enhanced biliary and renal elimination that compensated for the decrease in the intestinal elimination of apafant. Desrayaud *et al.* (345) reported 10-fold higher PSC833 (a P-gp inhibitor) in the brain of *mdr1a* (-/-) mice but no change was observed in the plasma concentration or metabolism and elimination of PSC833. These examples show that the contribution of P-gp to drug accumulation in the brain is undisputed but the effect of P-gp on systemic clearance, especially renal clearance, is less clear cut.

There are conflicting reports in the literature with regard to the importance of P-gp in the renal clearance of P-gp substrates. The following are examples that P-gp does not play a major role in the renal elimination of P-gp substrates. Schwarz *et al.* (346) reported that erythromycin, a P-gp substrate, increased the Cmax and $AUC_{0\text{-}24h}$ of talinolol in humans but no change in the renal clearance was observed. R-verapamil, a P-gp inhibitor, also had no effect on the renal clearance of talinolol in humans (347). Boyd *et al.* (348) reported that atorvastatin, a P-gp substrate, increased the steady state Cmax and $AUC_{0\text{-}24h}$ of digoxin in humans by 20% and 15%, respectively, but the renal clearance of digoxin was unaffected. Schinkel *et al.* (285) reported that plasma and brain concentrations of digoxin in *mdr1ab* (-/-) mice were increased by 3 and 27-fold, respectively, but no change in urinary excretion rate was observed. Song *et al.* (349) reported that PSC833 reduced the biliary but not the renal clearance of digoxin in rats. Mayer *et al.* (350) reported that PSC833 increased the urinary excretion of digoxin in wild type mice, bringing it to the same level observed in *mdr1ab* (-/-) mice and that PSC833 further enhanced the urinary excretion of digoxin in *mdr1ab* (-/-) mice. Yamaguchi *et al.* (329) reported no change in the renal clearance of grepafloxacin and levofloxacin with cyclosporine, a P-gp substrate, in rats and no change in the renal clearance of grepafloxacin was observed between wild type and *mdr1ab* (-/-) mice while the brain concentration was 2.7-fold higher in the knockout animals.

The following examples are reports in the literature that indicate the significance of P-gp in the renal clearance of P-gp substrates. Kurata *et al.* (351) reported that the renal clearance of

digoxin was 32% lower in human subjects with 2627TT/3435TT compared to 2627GG/3435CC *MDR1* genotypes and renal clearance was intermediate in subjects with 2627GT/343CT genotype. Kovarik *et al.* (352) reported that PSC833 reduced the renal clearance of digoxin in humans by 62%. Jalava *et al.* (353) reported that itraconazole, a P-gp inhibitor, decreased the renal clearance of digoxin by 20% in humans. Kawahara *et al.* (354) reported that the renal clearance of digoxin was decreased in *mdr1a* (-/-) mice. However, Mayer *et al.* (355) reported that urinary excretion of digoxin was doubled in *mdr1a* (-/-) mice, presumably due to increased *mdr1b* expression in the kidneys of *mdr1a* (-/-) mice. Hori *et al.* (278) reported that in the presence of quinidine or verapamil in the perfusate, urinary excretion of digoxin was decreased by 50% in the isolated perfused rat kidney. *In vivo* experiments in the canine kidney using the single-pass multiple indicator dilution method showed that cyclosporine, a P-gp inhibitor, reduced the urinary excretion of digoxin (275), vinblastine and vincristine (356). Song *et al.* (349) reported that PSC833 reduced the biliary and renal clearances of vincristine in rats. Tsuruoka *et al.* (357) reported that the decay half-life of intracellular fluorescence of rhodamine 123, a P-gp substrate, in isolated perfused mouse proximal tubule was significantly increased with verapamil to the same extent as the half-life observed in *mdr1ab* (-/-) mice and no effect of verapamil was observed in *mdr1ab* (-/-) mice. Leusch *et al.* (344) reported that the renal clearance of apafant was doubled in *mdr1a* (-/-) mice.

All the examples above show that the role of P-glycoprotein on renal clearance is not completely understood. There are many other transporters in the kidneys, in addition to P-gp, that may play an important role in renal drug elimination. More research is needed to determine the contribution of P-gp in drug elimination by the kidneys.

As mentioned earlier, many reports in the literature have shown a significant increase in brain concentrations for P-gp substrates with no change in plasma concentration *vs.* time profiles in P-gp knockout mice. We did not measure the brain concentrations of trimethoprim and ciprofloxacin in our studies. It may be worthwhile to reexamine the concentrations of these two drugs in the brains of wild type and P-gp knockout mice.

In conclusion, we do not observe a correlation between P-gp expression and the renal clearance values of P-gp substrates, trimethoprim and ciprofloxacin, in mice. This indicates that P-gp is not the predominant mechanism for the urinary excretion of trimethoprim and ciprofloxacin in mice. This lack of a P-gp effect in mice could potentially explain the discrepancy between observed higher renal clearance of trimethoprim and ciprofloxacin in CF patients versus similar renal clearance values of trimethoprim and ciprofloxacin between CF wild type and CF mice.

Currently it is not known whether P-gp plays a role in the renal elimination of trimethoprim and ciprofloxacin in humans. The renal clearance of ciprofloxacin in humans was shown to be reduced by probenecid (358). The renal clearance of trimethoprim was not affected by ganciclovir but the renal clearances of ganciclovir and didanosine were decreased by trimethoprim (359, 360). It is possible that the urinary excretions of trimethoprim and ciprofloxacin are not governed by P-gp but rather by another yet unknown transporter and the expression of this transporter could be upregulated in CF patients. Further studies need to be performed to determine the significance of P-gp in the renal elimination of trimethoprim and ciprofloxacin in humans.

Chapter 5

In Vivo Pharmacokinetic Studies in Rats

5.1 Overview

In vivo pharmacokinetic studies reveal no difference in the pharmacokinetic parameters of two P-gp substrates, trimethoprim and ciprofloxacin, between P-gp wild type and P-gp double knockout mice (Chapter 4). Therefore, we decided to perform *in vivo* inhibition studies to determine the effect of a P-gp inhibitor, GF120918 (GG918), on the pharmacokinetic parameters of P-gp and non-Pgp substrates. We utilized rats instead of mice because of the ease of performing pharmacokinetic studies in rats. Rats have more blood than mice; therefore we can perform many more sampling points in rats to get an accurate drug pharmacokinetic profile.

5.2 Study Design

To conduct inhibition studies in rats, P-gp (trimethoprim, ciprofloxacin) and non-P-gp substrates (sulfamethoxazole, iothalamate) were dosed together with and without GG918. Iothalamate is our marker of glomerular filtration rate. The pharmacokinetic parameters of P-gp and non-P-gp substrates are compared in the presence and absence of GG918 to determine if GG918 has any effect on the disposition of P-gp and non-P-gp substrates. Our *in vitro* studies have shown that GG918 does inhibit the activity of P-gp in MDCK1-MDR1 cells (Chapter 2). Therefore, we predict that GG918 will have effects on the pharmacokinetic parameters of trimethoprim and ciprofloxacin in rats and no effect is expected with sulfamethoxazole.

5.3 Materials and Methods

5.3.1 Materials

The following materials were utilized: Sprague-Dawley rats (Hilltop Lab Animals, Scottsdale,

PA), Animal Tissue Cleanser Concentrate (AIMS, Budd Lake, NJ), saline (Abbott, Chicago, IL), PE 10 intramedic polyethylene tubing (Becton Dickinson, Rutherford, NJ), ketamine HCl/xylazine (Sigma, St. Louis, MO), GG918 (a gift from Glaxo Wellcome), trimethoprim (16 mg/ml) and sulfamethoxazole (80 mg/ml) IV solution (Elkins-Sinn, Cherry Hill, NJ), 10 mg/ml ciprofloxacin IV solution (Bayer, West Haven, CT), 5% dextrose injectable (Baxter, Deerfield, IL), ofloxacin (Allergan Investigation Laboratories, Irvine, CA), N4-acetylsulfamethoxazole (Frinton Laboratories, Vineland, NJ), sulfadimethoxine, DMSO, Tween-20 (Sigma, St. Louis, MO), 1000 U/ml heparin solution (Elkins-Sinn, Cherry Hill, NJ), 23G1 needles, 1 ml syringes (Becton Dickinson, Franklin Lakes, NJ), rat scale (Taconic, Germantown, NY), timer (Phenomenex, Torrance, CA), Pipetman (Rainin, Woburn, MA), X Systems centrifuge (Abbott Laboratories, Abbott Park, IL), 400 µl microcentrifuge tubes for insert in Waters 96 autosampler (E & K Scientific Products, Campbell, CA), Micromass Quattro LC, Quattro Ultima (Micromass, Manchester, United Kingdom), 4.6 x 150mm Hypersil BDS-C_{18} 5u column (Keystone Scientific Inc., Bellefonte, PA), methanol, formic acid, acetonitrile (Sigma, St. Louis, MO), Waters 96 autosampler (Waters, Milford, MA), LC-10 AD pump (Shimadzu, Kyoto, Japan) and rat metabolic cages (Kroetz lab, San Francisco, CA).

5.3.2 Drug dosing

Each of the drugs, ciprofloxacin, trimethoprim, sulfamethoxazole and iothalamate, were dosed with and without GG918. The drugs were administered intravenously via the rat tail vein. The dosing characteristics are listed in Table 5.1. Due to a solubility problem with GG918, 1 mg/ml is the highest concentration of GG918 that we could prepare. We believe that dosing GG918 at 2 mg/kg will be sufficient because *in vitro* studies show that GG918 is a very effective P-gp inhibitor. A concentration of 2.5 µM GG918 inhibited the activity of P-gp in the bidirectional transport of 250 µM dicloxacillin (Chapter 2).

5.3.3 Urine and feces collection

Urine and feces samples were collected using rat metabolic cages. Rat metabolic cages were designed to separate feces into one container and urine into another container. They are very

Table 5.1 Dosing characteristics for inhibition studies in rats

Drugs	Dose (mg/kg)	Concentration (mg/ml)	Injection Volume (ml/kg)
Ciprofloxacin	5	2.5	2
Trimethoprim	5	2.5	2
Sulfamethoxazole	5	2.5	2
Iothalamate	10	5	2
GG918	2	1	2

similar to mice metabolic cages, with the exception that they are bigger. Before the experiments, the rats were put in the metabolic cages to let them get accustomed to it. During the actual urine collection experiments, the rats were dosed with drugs and placed in the metabolic cages along with water and food overnight. The rats were removed the next day and the urine and the feces containers were removed. The cages were washed to collect residual urine that was on the cage. All the urine solutions were centrifuged to remove solid contaminants and the total volumes measured. Urine samples were stored at -80°C until the concentrations of drugs in the urine were determined by LC/MS/MS. Urine samples were also collected during plasma collection periods from the cannulated bladder. Drugs in feces were extracted by homogenizing the feces samples with 50 ml of acetonitrile:0.1% formic acid solution in a 1:1 ratio. Homogenates were centrifuged to collect supernatants. Supernatants were stored at -80°C until the concentrations of drugs in the supernatants were determined by LC/MS/MS.

5.3.4 Plasma collection

The plasma collection was performed several days apart from the urine collection. Plasma samples were collected at selected time points from a cannulated jugular vein using a 23G1 needle attached to a 1 ml syringe. The sampling time points were at 0, 1, 2.5, 5, 10, 15, 30, 45, 60, 75, 90, 120, 150, 180, 210, 240 and 300 minutes. Blood was collected into a heparinized syringe and centrifuged immediately to obtain plasma. Plasma samples were stored at -80°C until analysis by LC/MS/MS. During the plasma collection experiments, urine

samples were also collected by attaching a PE10 tubing to the cannulated bladder. Urine samples were collected into Eppendorf tubes.

5.3.5 Sample preparation

5.3.5.1 Plasma sample preparation

Due to the high sensitivity of LC/MS/MS, we diluted the earlier time point samples several fold with control rat plasma before processing them, as follows: 10 μl of plasma sample was mixed with 140 μl of 70% acetonitrile containing internal standard solution (50 ng/ml dideoxy inosine, ofloxacin and sulfadimethoxine). The sample was vortex mixed and centrifuged for 15 minutes. The supernatant was saved for LC/MS/MS analysis.

5.3.5.2 Urine and feces sample preparation

To prepare urine and feces samples for analysis, 20 μl of urine or feces sample was mixed with 20 μl internal standard solution (50 ng/ml dideoxy inosine, ofloxacin and sulfadimethoxine) and 160 μl of water. The solution was centrifuged and the supernatant was set aside for analysis.

5.3.6 Sample analysis

Concentrations of ciprofloxacin, iothalamate, sulfamethoxazole, N4-acetylsulfamethoxazole and trimethoprim in plasma and urine were quantified using an LC/MS/MS (liquid chromatography/mass spectrophotometry/mass spectrophotometry) system. This was done in collaboration with Dr. Emil Lin from the Drug Studies Unit (South San Francisco, CA). The actual sample measurements were performed by Dr. Yong Huang.

Samples were injected at a flow rate of 0.8 ml/min onto a 5 μm BDS-C_{18} (4.6 X 150 mm) analytical column. The mobile phase for ciprofloxacin, sulfamethoxazole, N4-acetylsulfamethoxazole and trimethoprim consisted of a mixture of methanol, acetonitrile, 0.1% formic acid with 5 mM formate ammonium in the ratio of 3:1:6 (v/v). The mobile phase for iothalamate consisted of methanol and 0.1% formic acid in the ratio of 14: 86 (v/v).

Postcolumn, 25% of the original flow was diverted into the electrospray MS/MS. The mass spectrophotometer was operated in the positive mode. Ultra-high purity nitrogen was used as the drying and electrospray ionization gas. Argon was used as the collision gas. The cone voltage was set at 26, 30, 30, 30 and 40 V for trimethoprim, ciprofloxacin, sulfamethoxazole, N4-acetylsulfamethoxazole and iothalamate, respectively. The collision energy was set at 16, 20, 23, 23 and 24 eV for ciprofloxacin, iothalamate, sulfamethoxazole, N4-acetylsulfamethoxazole and trimethoprim, respectively. Multiple reaction monitoring was applied for recording of analytes. The m/z values of parent and daughter ions are as followed: 254>156 (sulfamethoxazole), 291>230 (trimethoprim), 332>314 (ciprofloxacin), 615>361 (iothalamate) and 296>134 (N4-acetylsulfamethoxazole).

5.3.7 Pharmacokinetic data analysis

Pharmacokinetic (PK) parameters were calculated using WinNonlin Professional software, version 2.1 (Pharsight, Mountain View, CA). Noncompartmental analysis for IV bolus input (Model 201) was employed to estimate the PK parameters of trimethoprim, ciprofloxacin, sulfamethoxazole and iothalamate.

Clearance (CL) is the volume of plasma that is completely cleared of drug per unit time. It is calculated using this equation:

$$CL = \frac{Dose}{AUC_{0\text{-}inf}}$$

AUC (area under the curve) is the total area under the plasma concentration-time (C *vs.* t) curve. To calculate AUC, the total area is divided into segments. The area of each segment is calculated using the linear trapezoid method and the total AUC is calculated by adding these segments together. Therefore, the total AUC can be calculated as :

$$AUC^{0-\infty} = AUC^{0-t(last)} + AUC^{t(last)-\infty}$$

$$= \sum \left\{ \frac{Cp^0 + Cp^1}{2} \cdot t^1 \right\} + \left\{ \frac{Cp^1 + Cp^2}{2} \cdot (t^2 - t^1) \right\} + \quad \ldots + \frac{Cp^{last}}{kel}$$

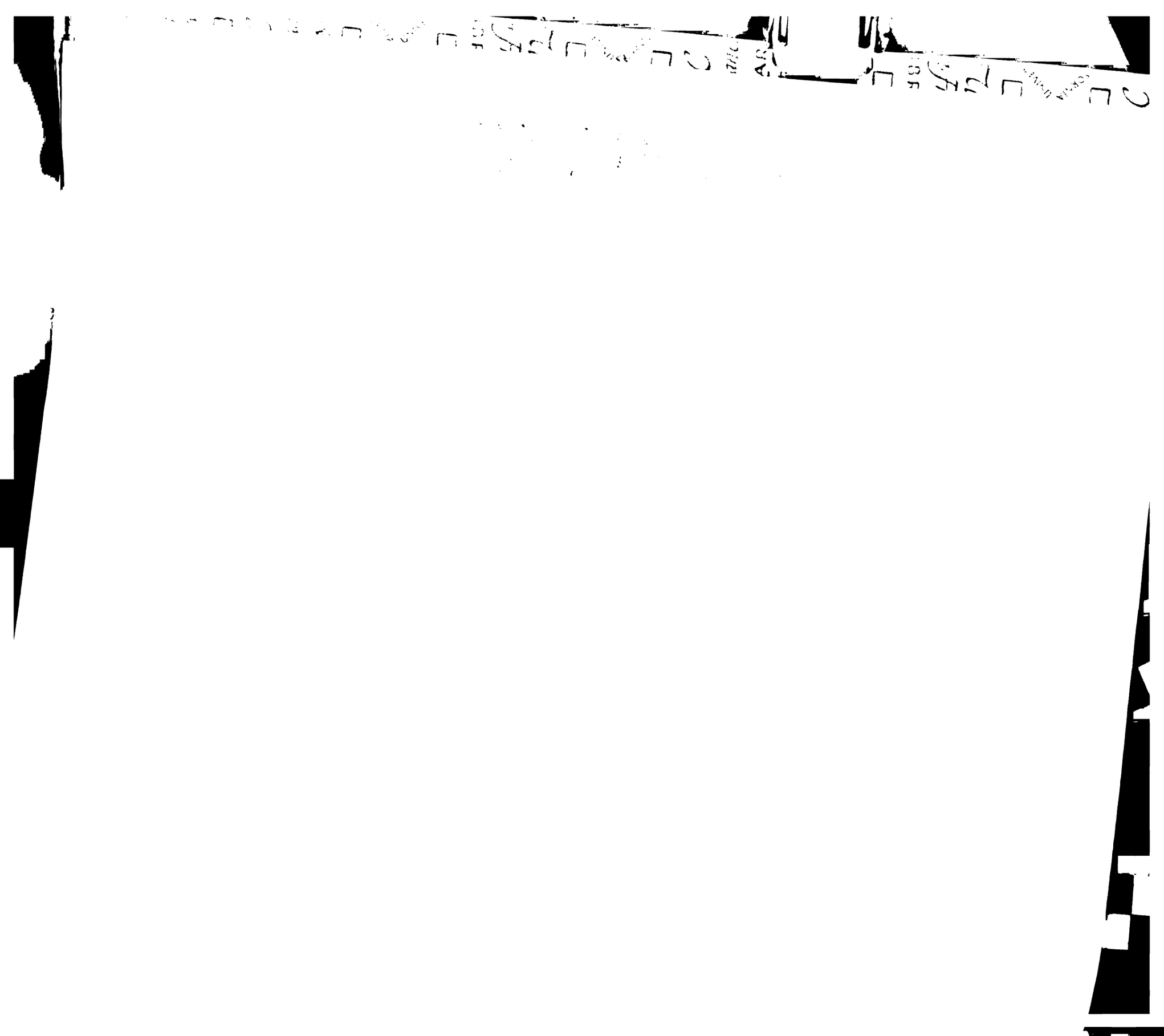

where k_{el} is the elimination rate constant calculated from the terminal slope of a semilog plot of a plasma concentration-time curve.

The elimination half-life ($t_{1/2}$) is the amount of time for the plasma concentration to fall to half its original value. The elimination half-life ($t_{1/2}$) is calculated using this equation:

$$t_{1/2} = \frac{0.693}{k_{el}}$$

The renal clearance (CLr) is defined as the ratio of the rate of urinary excretion to plasma concentration. It is the volume of plasma cleared of drug per unit time by the kidneys. It is calculated as follows:

$$CLr = \frac{Ae_{inf}}{AUC_{0\text{-}inf}} = fe \times CL$$

where fe is the fraction of dose excreted into the urine, calculated from the total amount of drug eliminated into the urine divided by the dose.

Mean residence time (MRT) is the average amount of time a molecule remains in a system. MRT for a bolus intravenous dose is calculated from this equation:

$$MRT = \frac{AUMC}{AUC}$$

where AUMC is the area under the moment curve. It is similar to AUC, with the exception that it is the total area under the plasma concentration X time *vs.* time (C•t *vs.* t) curve.

Vss is the steady state volume of distribution. It is calculated by this equation:

$$Vss = CL \times MRT$$

Fraction of dose metabolized (fm) is estimated from the fraction of metabolite excreted into the urine. The inherent assumption is that the metabolite is not further metabolized.

CLf is the formation clearance. It is calculated by multiplying the fraction of dose metabolized by the total clearance.

$$CLf = fm \times CL$$

5.3.8 Statistical analysis

ANOVA (analysis of variance) was performed on all the data sets. Data were analyzed using Primer Express software created by Dr. Stanton Glantz (UCSF, San Francisco, CA). The acceptable level of significance was $P < 0.05$.

5.4 Results

5.4.1 Trimethoprim

Figure 5.1 shows the plot of plasma concentrations *vs.* time for trimethoprim in the presence and absence of GG918. The plot of average plasma concentration *vs.* time is shown in Figure 5.2. We observe no significant difference in the concentration-time profiles of trimethoprim in the presence of GG918. However, the concentration-time profiles of trimethoprim are significantly different between male and female rats. Male rats have significantly lower area under the curve and higher clearance than female rats. The average pharmacokinetic parameters are listed in Table 5.2.

None of the calculated pharmacokinetic parameters show any statistically significant difference in female rats in the presence of GG918 versus "No Inhibitor". For male rats, even though we cannot determine the statistical significance in the presence of GG918 because there is only have one male rat per treatment group, the pharmacokinetic parameters do not appear to be different with GG918. Because no effect of GG918 is observed on the pharmacokinetic parameters of trimethoprim, we pooled the data from experiments in the absence of GG918 with the data from experiments with GG918 in female and male rats. Statistical tests between male and female rats were then performed on the combined parameters. The results show a statistically significant difference between male and female rats in the total clearance (CL), fraction of drug excreted into the urine (fe_{urine}) and volume of distribution at steady state (Vss).

Table 5.3 shows a comparison of several physiological parameters between rats and humans. The total clearance of trimethoprim in female rats (~9 ml/min) is lower than the published rat

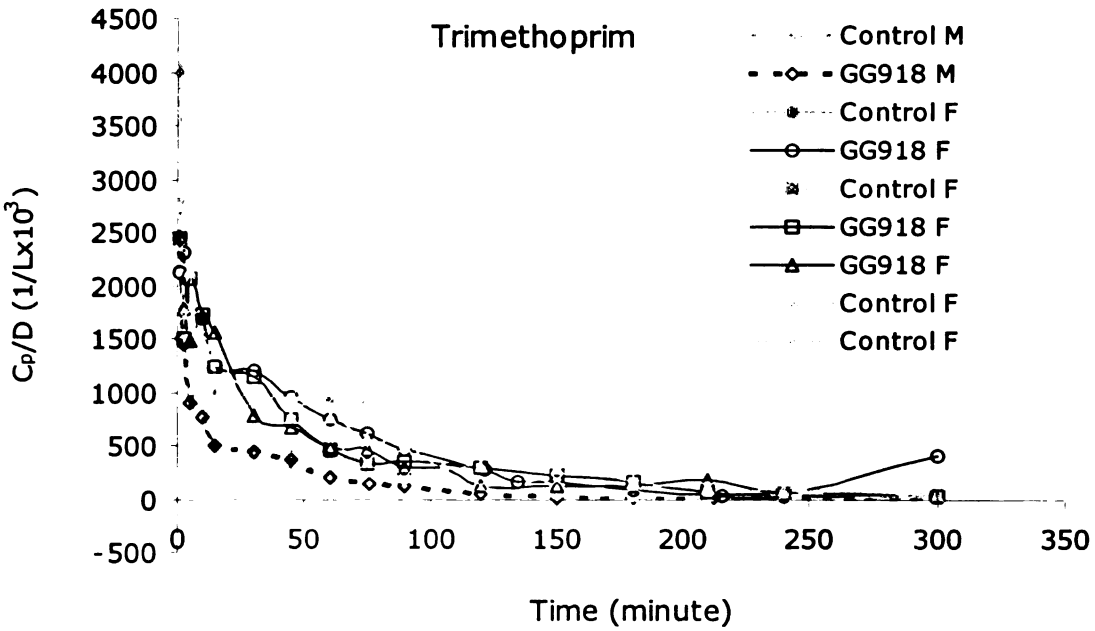

Figure 5.1 Comparison of plasma concentration-time profiles of trimethoprim (TMP) in the presence and absence of GG918. Grey lines = TMP control, black lines = TMP with GG918. Solid lines = female rats. Dashed lines = male rats. F = female, M = male. The units for the y-axis are plasma concentration normalized with dose and multiplied by 1000.

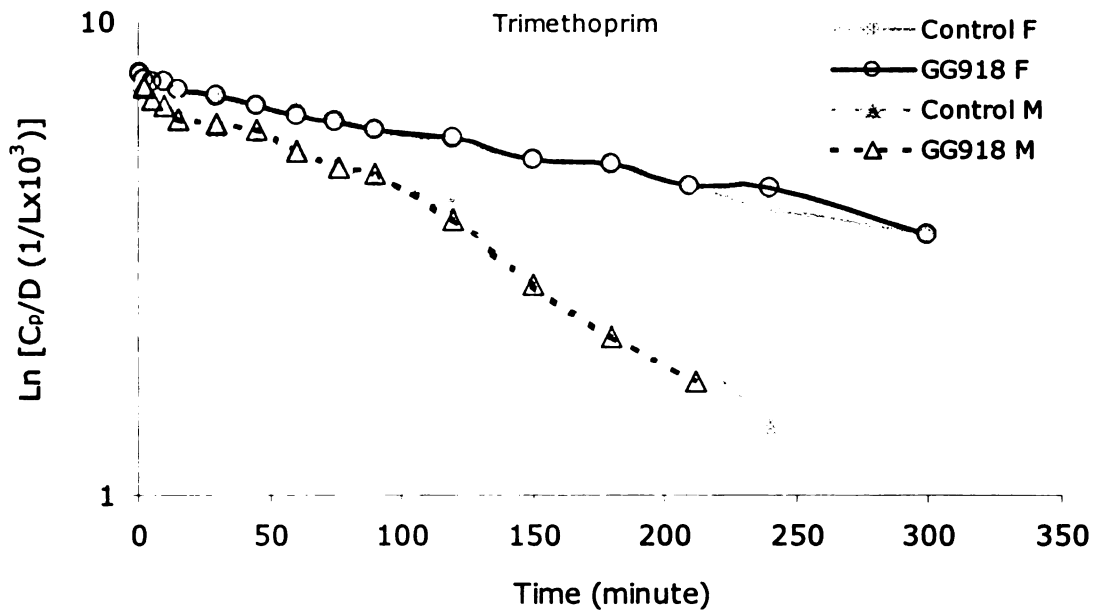

Figure 5.2 Comparison of average plasma concentration-time profiles of trimethoprim in the presence and absence of GG918. Grey lines = control, black lines = with GG918. Solid lines = female rats, dashed lines = male rats. F = female, M = male. The units for the y-axis are the natural logarithm of plasma concentration normalized with dose and multiplied by 1000.

Table 5.2 Average pharmacokinetic parameters of trimethoprim in female and male rats in the presence and absence of GG918 (avg ± SD)

Parameters	Female Rats No Inhibitor N = 4	Female Rats With GG918 N= 3	Male Rat No Inhibitor N = 1	Male Rat With GG918 N= 1
CL (ml/min)[a]	9.9 (1.3)	8.5 (1.6)	23.3	24.7
CLr (ml/min)	2.0 (0.4)	1.6 (0.4)	1.6	1.8
fe_{urine} (%)[a]	19.9 (3.1)	18.4 (2.6)	6.9	7.2
fe_{feces} (%)	0.4 (0.4)	0.3 (0.1)	0.02	0.08
Vss (ml)[a]	626 (66)	697 (95)	881	933
$t_{1/2,z}$ (min)	50 (7)	49 (12)	32	29
$MRT_{0-\infty}$ (min)	67 (8)	86 (29)	38	38

a = Comparison of combined female *vs.* male (no inhibitor+GG918) PK parameters. $P < 0.05$

Table 5.3 Various physiological parameters in rats and humans. Adapted from Davies and Morris (317).

Physiological Parameters	Rat (0.25 kg)	Human (70 kg)
Kidney weight (g)	2.0	310
Surface area (m^2)	0.023	1.85
Total plasma protein (100 ml)	6.7	7.4
Plasma albumin (g/100 ml)	3.16	4.18
Plasma α-1-AGP (g/100 ml)	1.81	0.18
Hematocrit (%)	46	44
Total ventilation (L/min)	0.12	7.98
Respiratory rate (min^{-1})	85	12
Heart rate (beats/min)	362	65
Oxygen consumption (ml/hr/g body wt)	0.84	0.2
Total body water (ml)	167	42000
Intracellular fluid (ml)	92.8	23800
Extracellular fluid (ml)	74.2	18200
Plasma volume (ml)	7.8	3000
Kidney blood flow (ml/min)	9.2	1240
Liver blood flow (ml/min)	13.8	1450
Urine flow (ml/day)	50	1400
Bile flow (ml/day)	22.5	350
GFR (ml/min)	1.31	125
Cardiac output (ml/min)	74	5600

liver blood flow (13.8 ml/min). The total clearance of trimethoprim in male rats (~24 ml/min) is slightly higher than the combined published rat liver and kidney blood flows (~23 ml/min) but not greater than cardiac output (74 ml/min).

No difference in the renal clearance (~1.8 ml/min) of trimethoprim was observed between male and female rats. This lack of difference in the renal clearance indicates that the observed higher total clearance in male rats is probably due to enhanced metabolism in those rats. Our group has reported previously that the expression of cytochrome P4503A2 (the rat isoform of human 3A4) enzyme is different between male and female rats, with no detectable expression in female rats (361). This could explain the observed significantly higher nonrenal elimination in male rats. To test this hypothesis, we could perform inhibition studies to determine the effect of 3A2 inhibitors on nonrenal clearance of trimethoprim in male and female rats. If the hypothesis is correct, we expect to see a decrease in the clearance in male but not female rats. Another potential experiment could be to perform an induction study to increase the expression of 3A2 enzyme in female rats and determine whether there is a correlation between 3A2 enzyme expression level and clearance value.

The renal clearance of trimethoprim (~1.8 ml/min) is higher than the published rat glomerular filtration rate (1.31 ml/min). This indicates a net renal tubular secretion for trimethoprim in rats. We did not measure the extent of protein binding in rats but in humans it is about 37%. Using this value for our calculation, the net tubular secretion is about 0.97 ml/min (CLr - fu x GFR = 1.8 - 0.63 X 1.31). However, we observe no effect of GG918 on the renal clearance of trimethoprim which suggests that tubular secretion is not mediated by P-gp but rather by other transporter(s). Trimethoprim is not excreted into feces as shown by the low value of fraction of trimethoprim excreted into the feces (<1%).

Trimethoprim is highly distributed into tissues, as shown by the large volume of distributions. There is a statistically significant difference in the volume of distribution at steady state (Vss) for trimethoprim between female and male rats (~657 and 907 ml, respectively). This indicates a sex effect on trimethoprim distribution in rats.

5.4.2 Ciprofloxacin

Figure 5.3 shows the plot of plasma concentrations *vs.* time for ciprofloxacin in the presence and absence of GG918. The plot of average plasma concentration *vs.* time is shown in Figure 5.4. We observe no significant difference in the concentration-time profiles of ciprofloxacin in the presence of GG918. Unlike what is observed for trimethoprim, there is no large difference in the concentration-time profiles of ciprofloxacin between male and female rats. The average pharmacokinetic parameters are listed in Table 5.4. There is one outlier in the female rat without GG918 treatment group. The result of an outlier test (q test) shows that we can reject the data with greater than 95% confidence. The average pharmacokinetic parameters in the absence of this outlier data are listed in Table 5.5.

Tables 5.4 and 5.5 show that none of the calculated pharmacokinetic parameters show any statistically significant difference in female rats with GG918 versus without. For male rats, there appears to be potential differences with and without GG918 for fraction of dose excreted into the urine (fe_{urine}), renal clearance (CLr) and fraction of the dose excreted into the feces (fe_{feces}). Because we only have one rat per group, we cannot determine whether the difference is statistically significant. However, since we do not observe the effect of GG918 on fe_{urine}, CLr and fe_{feces} the variability of these two parameters is relatively large in female rats, we believe that the difference values we observed could be due to chance or inherent variability between those two rats.

Because no effect of GG918 is observed on the pharmacokinetic parameters of ciprofloxacin, we pooled the data from experiments in the absence of GG918 with the data from experiments with GG918 in female and male rats. Statistical tests between male and female rats were then performed on the combined parameters. The data in Table 5.5 show statistically significant differences between male and female rats in the total and renal clearance, fraction of drug excreted into the urine (fe_{urine}) and feces (fe_{feces}) and in the volume of distribution at steady state (Vss).

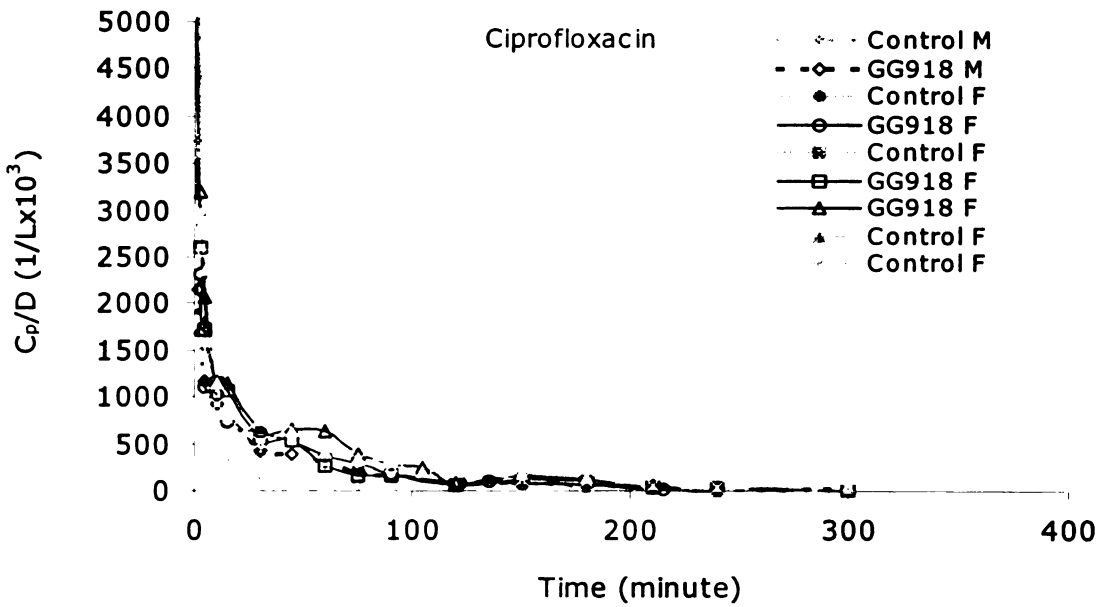

Figure 5.3 Comparison of plasma concentration-time profiles of ciprofloxacin (CIP) in the presence and absence of GG918. Grey lines = CIP control, black lines = CIP with GG918. Solid lines = female rats. Dashed lines = male rats. F = female, M = male. The units for the y-axis are plasma concentration normalized with dose and multiplied by 1000.

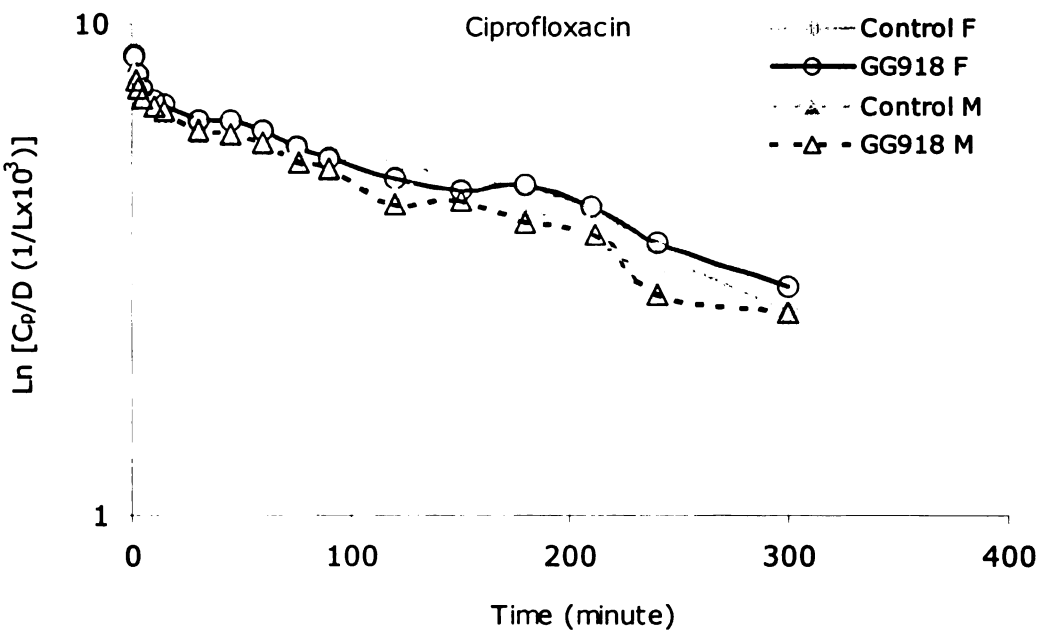

Figure 5.4 Comparison of average plasma concentration-time profiles of ciprofloxacin in the presence and absence of GG918. Grey lines = control, black lines = with GG918. Solid lines = female rats, dashed lines = male rats. F = female, M = male. The units for the y-axis are the natural logarithm of plasma concentration normalized with dose and multiplied by 1000.

Table 5.4 Average pharmacokinetic parameters of ciprofloxacin in female and male rats in the presence and absence of GG918 (avg ± SD)

Parameters	Female Rats No Inhibitor N = 4	Female Rats With GG918 N= 3	Male Rat No Inhibitor N = 1	Male Rat With GG918 N= 1
CL (ml/min)	14.0 (7.8)	12.2 (2.1)	15.8	16.5
CLr (ml/min)	4.8 (2.9)	3.7 (0.8)	7.8	10.7
fe_{urine} (%)[a]	34.6 (7.4)	30.1 (4.0)	49.2	64.9
fe_{feces} (%)[a]	9.2 (1.5)	8.0 (3.2)	0.8	3.7
Vss (ml)	761 (286)	595 (43)	961	900
$t_{1/2,z}$ (min)	55 (14)	44 (10)	44	52
$MRT_{0-\infty}$ (min)	59 (15)	49 (6)	61	54

a = Comparison of combined female *vs.* male (no inhibitor+GG918) PK parameters. $P < 0.05$

Table 5.5 Average pharmacokinetic parameters of ciprofloxacin without the outlier in female and male rats in the presence and absence of GG918 (avg ± SD)

Parameters	Female Rats No Inhibitor N = 3	Female Rats With GG918 N= 3	Male Rat No Inhibitor N = 1	Male Rat With GG918 N= 1
CL (ml/min)[a]	10.1 (1.4)	12.2 (2.1)	15.8	16.5
CLr (ml/min)[a]	3.5 (0.9)	3.7 (0.8)	7.8	10.7
fe_{urine} (%)[a]	31.6 (7.6)	30.1 (4.0)	49.2	64.9
fe_{feces} (%)[a]	9.7 (1.4)	8.0 (3.2)	0.8	3.7
Vss (ml)[a]	624 (107)	595 (43)	961	900
$t_{1/2,z}$ (min)	57 (16)	44 (10)	44	52
$MRT_{0-\infty}$ (min)	63 (15)	49 (6)	61	54

a = Comparison of combined female *vs.* male (no inhibitor+GG918) PK parameters. $P < 0.05$

The total clearance of ciprofloxacin in female rats (~11 ml/min) is lower while in male rats (~16 ml/min) it is higher than the published rat liver blood flow (13.8 ml/min, Table 5.3). Subtracting the renal clearance from the total clearance values show that the clearance by nonrenal routes (e.g., metabolism, biliary, intestinal) are about the same in male and female rats (~6.9 and 7.6 ml/min, respectively). This suggests that the observed higher total

clearance in male rats are mostly due to higher renal clearance. The lack of difference in nonrenal clearance between male and female rats suggests that ciprofloxacin is not metabolized by the 3A2 enzyme in rats. However, McLellan *et al.* (362) reported that ciprofloxacin decreased the N-demethylation of erythromycin by 3A4 in humans and 3A2 in rats by a competitive mechanism. Ciprofloxacin was also reported to inhibit the activity of 1A1 enzyme and had no effect on the activity of 2E1 and 4A1 enzymes (362). It is known, however, that inhibitors of metabolism by a specific enzyme may not be substrates for that enzyme, even when the inhibition is thought to be competitive.

The renal clearance in both female and male rats (~3.6 and 9.3 ml/min, respectively) is much higher than the published rat glomerular filtration rate (1.31 ml/min, Table 5.3). This indicates a significant net renal tubular secretion for ciprofloxacin in rats. We did not measure the extent of protein binding in rats but in humans it is about 40%. Using this value for our calculation, the net tubular secretion is about 2.8 ml/min (CLr - fu x GFR = 3.6 - 0.60 X 1.31) in female and 8.5 ml/min (CLr - fu x GFR = 9.3 - 0.60 X 1.31) in male rats. Because we observe no effect of GG918 on the renal clearance of ciprofloxacin, the results suggest that tubular secretion is not mediated by P-gp but by other transporter(s) and the expression of this transporter is higher in male than female rats. A potential candidate can be found by examining ciprofloxacin drug-drug interactions. Naora *et al.* (363) and Al-Khamis *et al.* (364) reported that fenbufen and famotidine, respectively, decreased the total clearance of ciprofloxacin in rats, presumably due to inhibition of ciprofloxacin tubular secretion. Probenecid was reported to reduce the renal clearance of ciprofloxacin in humans (358). These data suggest that the activity of this unknown transporter is affected by famotidine, probenecid and fenbupen.

There is a significant difference in fraction of dose excreted into feces between male and female rats (~2 and 9%, respectively). The fraction of dose excreted into the feces is lower in male compared to female rats which is the opposite that observed for fraction of dose excreted into the urine. This suggests that intestinal and renal excretion of ciprofloxacin may be mediated by two different mechanisms.

In humans and rats, the appearance of ciprofloxacin in feces is mostly due to transintestinal secretion rather than biliary excretion (322, 365-374). Because we observe no effect of GG918 on the fe_{feces} values, the results suggest that intestinal secretion of ciprofloxacin is not attributed to P-gp. Dautrey *et al.* (369) reported that inhibition studies in rats with quinidine, verapamil, cyclosporine, cephalexin and azlocillin increased the AUC, decreased the biliary, intestinal and total clearance of ciprofloxacin while pefloxacin reduced the intestinal elimination of ciprofloxacin, but sparfloxacin had no effect. Intestinal secretion of grepafloxacin in rats was decreased by 50% with cyclosporine (329). Intestinal secretion of grepafloxacin was decreased by 38% in *mdr1ab* (-/-) mice and cyclosporine inhibited the intestinal secretion of grepafloxacin to the similar level observed in *mdr1ab* (-/-) mice (329).

Ciprofloxacin is highly distributed into tissues, as shown by the large volume of distributions. There is a statistically significant difference in the volume of distribution at steady state (Vss) for ciprofloxacin between male and female rats (~931 and 610 ml, respectively). This indicates a sex effect on ciprofloxacin distribution in rats.

5.4.3 Sulfamethoxazole

Figure 5.5 shows the plot of plasma concentrations *vs.* time for sulfamethoxazole in the presence and absence of GG918. The plot of average plasma concentration *vs.* time is shown in Figure 5.6. We observe no significant difference in the concentration-time profiles of sulfamethoxazole with GG918. There is also no significant difference in the concentration-time profiles of a major sulfamethoxazole metabolite, N4-acetylsulfamethoxazole (Figures 5.7-5.8). There is no significant difference in the concentration-time profiles of sulfamethoxazole between male and female rats. This lack of difference conclusion must be tempered by the time length of plasma collection. Unlike mice, the half-life of sulfamethoxazole in rats is very long (~350 minutes) and the 300 minute collection period does not even yield samples for one half-life. Therefore, a reliable estimate of pharmacokinetic parameters for sulfamethoxazole cannot be obtained. Based on the observed early concentration *vs.* time profiles, GG918 has no effect on sulfamethoxazole disposition, as expected since it is not a substrate of P-gp. The

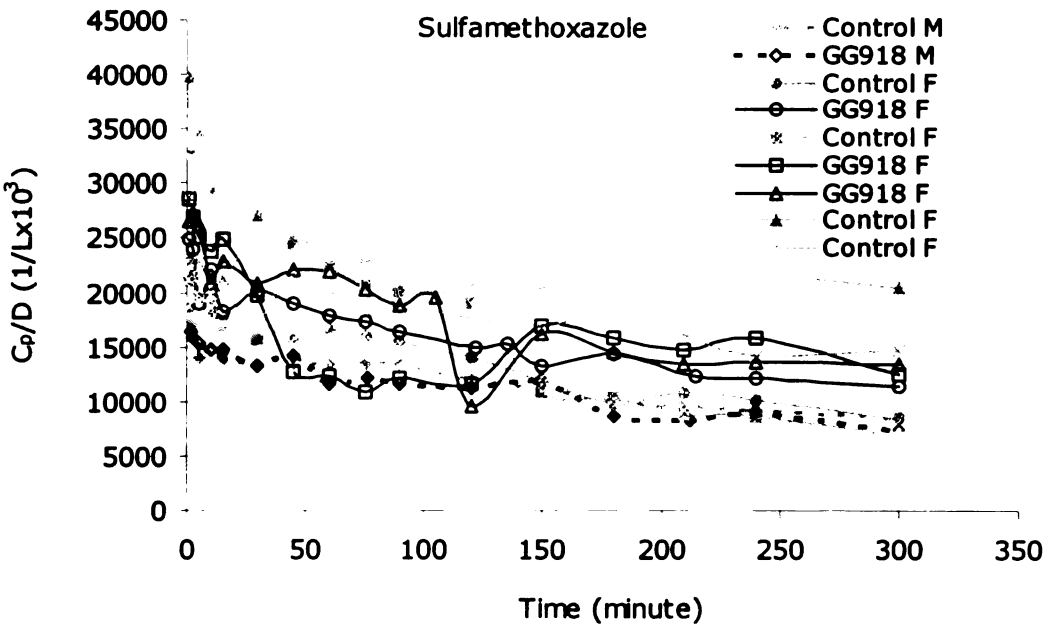

Figure 5.5 Comparison of plasma concentration-time profiles of sulfamethoxazole (SMZ) in the presence and absence of GG918. Grey lines = SMZ control, black lines = SMZ with GG918. Solid lines = female rats. Dashed lines = male rats. F = female, M = male. The units for the y-axis are plasma concentration normalized with dose and multiplied by 1000.

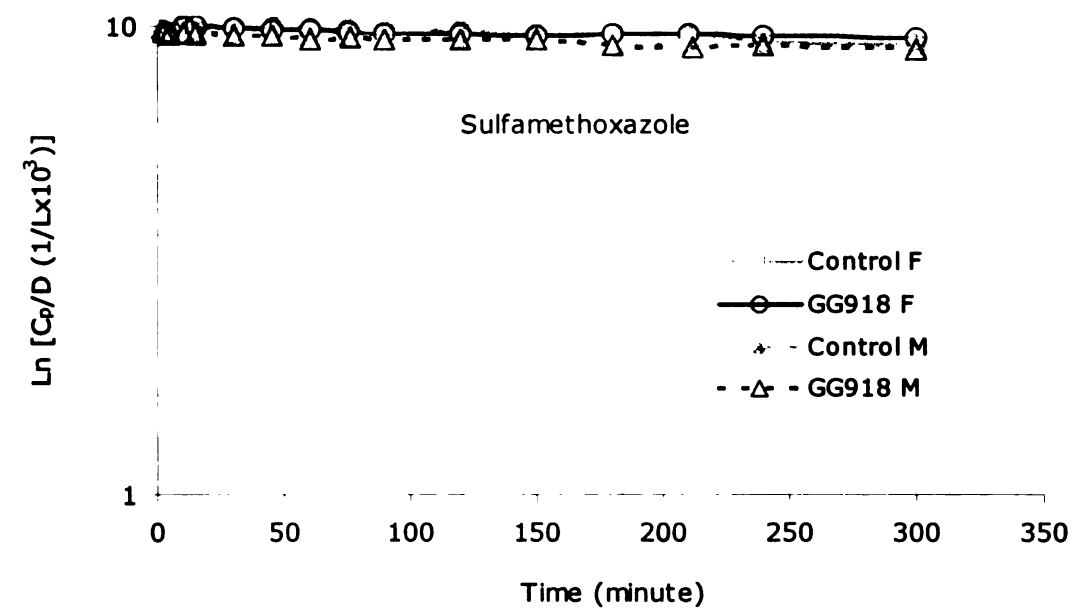

Figure 5.6 Comparison of average plasma concentration-time profiles of sulfamethoxazole in the presence and absence of GG918. Grey lines = control, black lines = with GG918. Solid lines = female rats, dashed lines = male rats. F = female, M = male. The units for the y-axis are the natural logarithm of plasma concentration normalized with dose and multiplied by 1000.

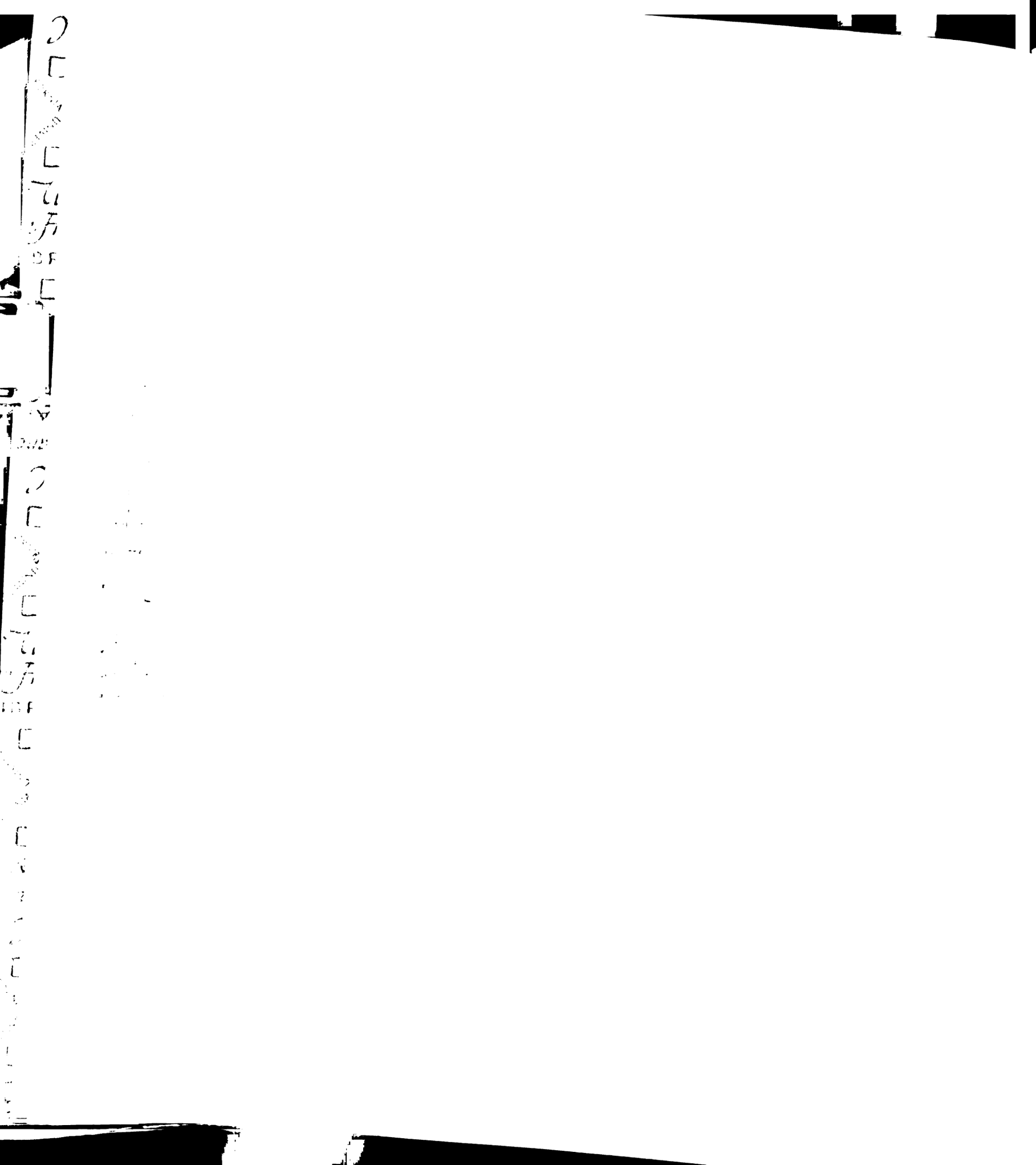

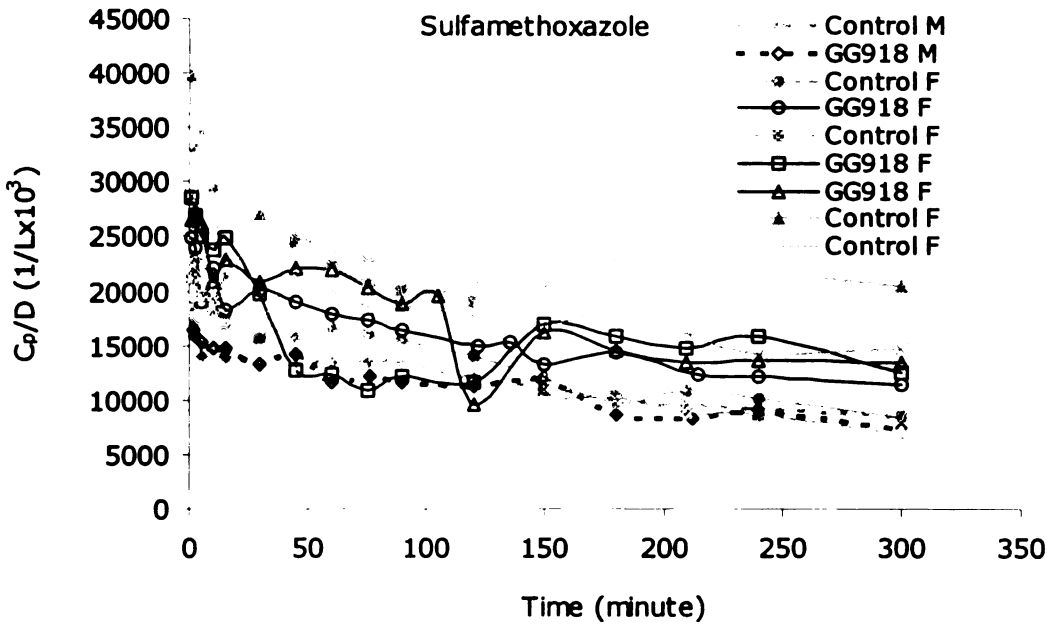

Figure 5.5 Comparison of plasma concentration-time profiles of sulfamethoxazole (SMZ) in the presence and absence of GG918. Grey lines = SMZ control, black lines = SMZ with GG918. Solid lines = female rats. Dashed lines = male rats. F = female, M = male. The units for the y-axis are plasma concentration normalized with dose and multiplied by 1000.

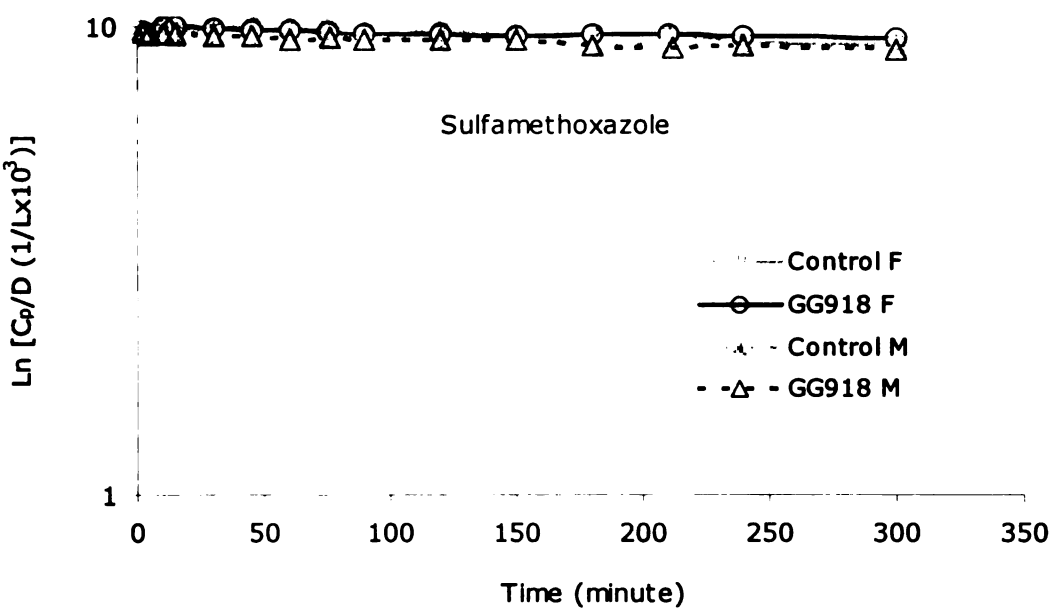

Figure 5.6 Comparison of average plasma concentration-time profiles of sulfamethoxazole in the presence and absence of GG918. Grey lines = control, black lines = with GG918. Solid lines = female rats, dashed lines = male rats. F = female, M = male. The units for the y-axis are the natural logarithm of plasma concentration normalized with dose and multiplied by 1000.

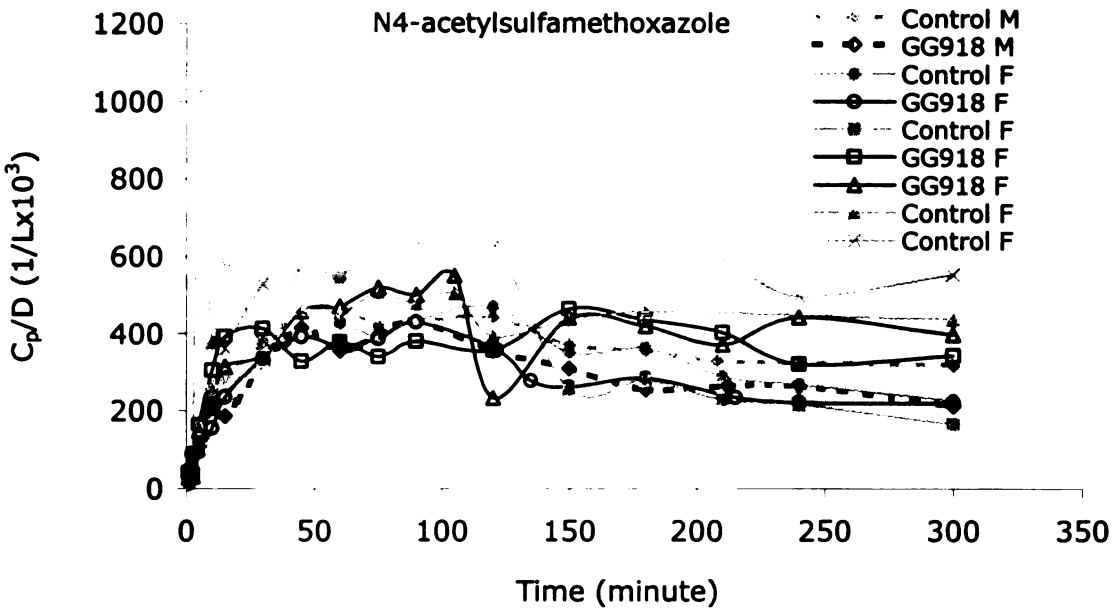

Figure 5.7 Comparison of plasma concentration-time profiles of N4-acetylsulfamethoxazole (N4-SMZ) in the presence and absence of GG918. Grey lines = N4-SMZ control, black lines = N4-SMZ with GG918. Solid lines = female rats. Dashed lines = male rats. F = female, M = male. The units for the y-axis are plasma concentration normalized with dose and multiplied by 1000.

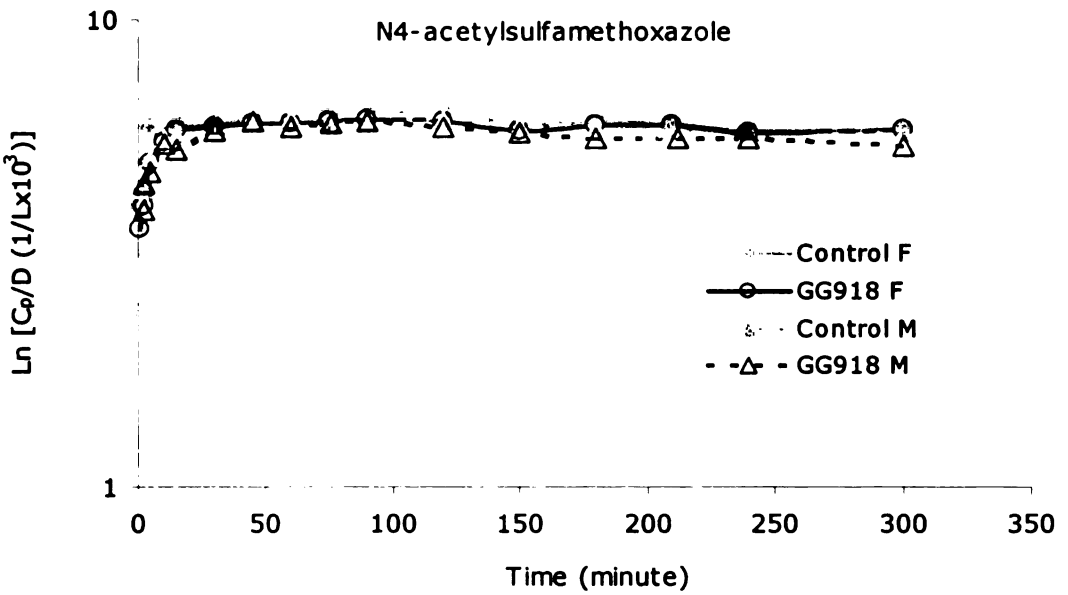

Figure 5.8 Comparison of average plasma concentration-time profiles of N4-acetylsulfamethoxazole in the presence and absence of GG918. Grey lines = control, black lines = with GG918. Solid lines = female rats, dashed lines = male rats. F = female, M = male. The units for the y-axis are the natural logarithm of plasma concentration normalized with dose and multiplied by 1000.

metabolism of sulfamethoxazole to N4-acetylsulfamethoxazole by N-acetyltransferase is not affected by GG918 over the 5 hour time course evaluated.

5.4.4 Iothalamate

We were not able to obtain reliable plasma concentration *vs.* time data for iothalamate in rats due to problems in LC/MS/MS analysis. We did not repeat the analysis because iothalamate is not the focus of our studies. We did, however, obtain a reliable measure of the fraction of iothalamate excreted into urine. Table 5.6 lists the fraction of trimethoprim, ciprofloxacin, sulfamethoxazole, N4-acetylsulfamethoxazole and iothalamate excreted into the urine in four female rats. The fe values were calculated from the concentration of drugs in the urine collected from the cannulated bladder during plasma collection experiments. We were only able to collect urine from four out of seven female rats due to imperfection in urinary bladder cannulation.

Table 5.7 lists the fraction of trimethoprim, ciprofloxacin, sulfamethoxazole, N4-acetylsulfamethoxazole and iothalamate excreted into the urine in seven female and two male rats. The fe values were calculated from the concentration of drugs in the urine collected using the rat metabolic cages. With the exception of fe values for sulfamethoxazole, the fe values measured by these two methods are comparable. The fe values for sulfamethoxazole are lower in urinary bladder cannulation method because urine was only collected for about five hours, the length of our plasma collection experiments while it was collected for about twenty two hours in rat metabolic cages, and the half-life of sulfamethoxazole in rats is greater than 5 hours.

We prefer rat metabolic cages over urinary bladder cannulated method to estimate renal clearance in rats due to several reasons. Even though urinary bladder cannulation method allows simultaneous urine and plasma collections in the experiments, the success is highly dependent upon perfect cannulation. We were only able to get good urine collection in four out of seven rats due to imperfect bladder cannulation in three rats. Furthermore, urinary bladder cannulated rats are still able to excrete urine via the normal route therefore care must

Table 5.6 Fraction of drugs excreted into the urine estimated using urinary bladder cannulation method.

Rat No.	Inhibitor	fe TMP (%)	fe CIP (%)	fe SMZ (%)	fe N4-SMZ (%)	fe IoA (%)
Female no. 1	-	22.5	29.1	20.9	3.6	72.9
Female no. 2	GG918	15.6	17.1	6.4	1.3	32.9
Female no. 4	GG918	17.1	30.5	11.9	3.4	64.2
Female no. 7	-	16.4	22.4	NA	2.4	68.3

Table 5.7 Fraction of drugs excreted into the urine estimated using rat metabolic cages method.

Rat No.	Inhibitor	fe TMP (%)	fe CIP (%)	fe SMZ (%)	fe N4-SMZ (%)	fe IoA (%)
Male no. 1	-	6.9	49.2	10.1	3.9	68.4
Male no. 2	GG918	7.2	64.9	14.4	6.0	63.9
Female no. 1	-	17.4	40.7	36.0	5.5	70.0
Female no. 2	GG918	21.4	28.9	36.4	2.7	50.7
Female no. 3	-	22.6	34.3	29.3	7.0	85.0
Female no. 4	GG918	16.8	34.6	31.7	2.9	76.0
Female no. 5	GG918	17.0	26.9	27.8	2.6	72.9
Female no. 6	-	22.5	39.1	43.7	2.6	96
Female no. 7	-	16.9	24.2	25.4	4.0	59

be taken to ensure complete collection into the cannulae. Lastly, bladder cannulation is a fairly invasive procedure.

5.5 Discussion and Conclusions

We observe no change in the pharmacokinetic parameters of trimethoprim, ciprofloxacin and sulfamethoxazole in the presence of GG918. This indicates that P-gp has no effect on the disposition of trimethoprim, ciprofloxacin and sulfamethoxazole in rats. This data agree with the results of pharmacokinetic studies performed in P-gp wild type and knockout mice where no significant difference is observed in the concentration-time profiles of trimethoprim, ciprofloxacin and sulfamethoxazole between those two groups of mice.

There are several possibilities for the lack of GG918 effect on the disposition of trimethoprim and ciprofloxacin. One explanation could be that trimethoprim and ciprofloxacin are not substrates of rat P-gp. Another possibility could be that the effect of P-gp cannot be observed easily from dosing the drugs intravenously. Paclitaxel (Taxol) is a substrate of P-gp. *In vivo* studies in humans and mice have shown that GG918 increased the oral bioavailability of paclitaxel (375, 376). In wild type mice, GG918 increased the plasma AUC of oral paclitaxel by 6.6-fold (376). When paclitaxel was given intravenously, the AUC also showed a statistically significant increase with GG918 but it was only a 1.4-fold change. No effect of GG918 was observed on the plasma AUC of paclitaxel in P-gp knockout mice (*mdr1ab* (-/-)). This suggests that the effect observed for paclitaxel with GG918 in wild type mice was due to inhibition of P-gp activity. A third possibility could be that the concentration of GG918 in rats was not high enough to inhibit the P-gp activity. GG918 is a poorly water soluble compound. The highest possible dose of GG918 that we could administer was 2 mg/kg. We believed that GG918 is effective at this dose because *in vitro* studies indicate that GG918 is a very effective inhibitor of P-gp. However, we did not measure the concentration of GG918 in the rat plasma and subsequent experiments by a colleague in our lab (Chi-Yuan Wu) showed that GG918 was eliminated quite rapidly in the isolated perfused rat liver. It remains to be seen whether rapid elimination of GG918 also occurs *in vivo* in rats. Hyafil *et al.* (377) reported a half-life of 2.7 hours for GG918 in mice. If a similar half-life is observed in rats, this means that GG918 concentrations fall to 25% of the initial concentration (2 half-lives) during our 5-hour study. Whether the concentration of GG918 is sufficient to inhibit the activity of P-gp also depends on the volume of distribution. Large volume of distribution means smaller concentration in the plasma. A fourth possibility could be that P-gp is not important in the disposition of trimethoprim and ciprofloxacin in rats.

In conclusion, we do not observe any effects of GG918 on the pharmacokinetic parameters of trimethoprim, ciprofloxacin and sulfamethoxazole, indicating lack of P-gp contribution to the disposition of these drugs in rats.

Chapter 6

P-glycoprotein and CFTR Expression in Various Mouse Models

6.1 Introduction

Our hypothesis stated that enhanced renal clearance of several drugs observed in CF patients is due to elevated P-gp expression in the kidneys of those patients. Our *in vitro* study results appear to support the hypothesis; drugs that show enhanced renal clearance (i.e. trimethoprim, dicloxacillin, ciprofloxacin) are substrates of P-gp while those that do not (i.e. sulfamethoxazole, cefsulodin) are not substrates of P-gp. The results of our *in vivo* pharmacokinetic studies in mice are inconclusive. There is no difference in the renal clearance for ciprofloxacin and sulfamethoxazole among P-gp wild type, P-gp knockout, CF wild type and ΔF508 CF mice. The renal clearance of trimethoprim is higher in ΔF508 CF mice compared to CF wild type mice. However, no difference in the renal clearance of trimethoprim is observed between P-gp wild type and knockout mice. To determine whether the increased renal clearance of trimethoprim observed in ΔF508 CF mice is due to increased P-gp expression, we investigate here if there is a difference in the P-gp expression level in the kidneys of CF wild type and ΔF508 CF mice. In addition, we will also determine if the *CFTR* expression varies in the kidneys of P-gp wild type and knockout mice.

Ideally, we would also like to examine if the P-gp expression level is indeed elevated in the kidneys of CF patients. However, kidney biopsy is a very invasive procedure and we have no access to kidneys from CF cadavers. As an alternative, we will utilize cultured cell lines from CF patients. Kidney cell lines from CF patients are not available but there is a cell line called CFPAC-1, which originated from the pancreas of a CF patient with the ΔF508 mutation in his *CFTR* gene. Dr. Mitchell Drumm (378) has stably transfected the CFPAC-1 cell line with a vector containing wild type *CFTR* gene. The resulting cell line is called CFPAC-1 pLJ CFTR. Here, we will compare the expression level of *MDR1* between CFPAC-1 and CFPAC-1 pLJ CFTR

cells. According to the hypothesis, the P-gp expression should be higher in CFPAC-1 cells compared to CFPAC-1 pLJ CFTR cells. P-gp expression should be decreased in CFPAC-1 pLJ CFTR cells due to the presence of the wild type *CFTR* gene.

MDR1 and *CFTR* expression comparison in mice kidneys will be performed with real-time relative quantitative RT-PCR while the *MDR1* expression comparison between CFPAC-1 and CFPAC-1 pLJ CFTR cells will be performed with traditional semi-quantitative RT-PCR because of the small sample numbers.

6.2 Real-Time Quantitative PCR

Dr. David Ginzinger has written a comprehensive review on gene quantification using real-time PCR (379). Real-time quantitative PCR is a method that reliably detects and measures products generated during each cycle of PCR that are directly proportional to the actual amount of starting template prior to the start of the PCR. Real-time PCR differs from traditional PCR in that we can monitor the PCR products as they are accumulating instead of just looking at the end product of the PCR process, which is what is measured in traditional PCR. PCR is comprised of two phases: the exponential phase and the plateau phase. The plateau phase occurs when the PCR process is no longer generating template at an exponential rate due to reagent limitation or byproduct accumulation. Therefore, to accurately determine the actual amount of starting template, we can only extrapolate back from the exponential phase and not from the plateau phase. From real-time PCR, a plot of fluorescence signal (a measure of PCR product) *vs.* PCR cycle number (Figure 6.1) is generated. This plot will enable us to visualize the location of the exponential and the plateau phases. The program associated with the PCR machine will calculate a fluorescence signal threshold value for the exponential phase of the reaction. This threshold value is calculated as ten times the standard deviation of the average signal of the baseline fluorescent signal. This threshold value defines the cycle threshold or C_T, which is the number of PCR cycles required to generate enough fluorescence to reach this value. The C_T values are directly proportional to the amount of starting template and are used to calculate mRNA expression levels. The black and the gray lines in Figure 6.1 represent two different hypothetical samples. The black line

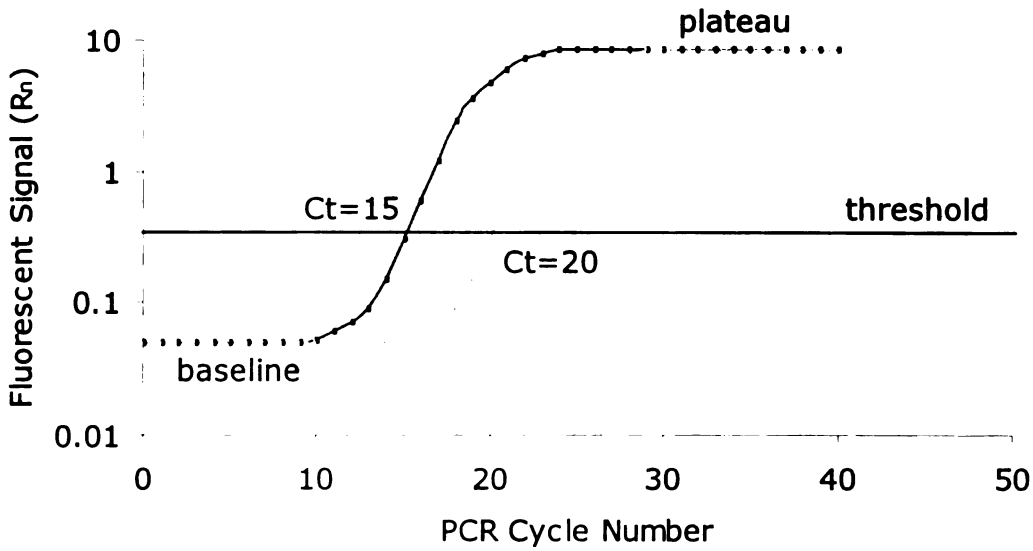

Figure 6.1 A hypothetical amplification plot from a run of real-time PCR (Adapted from Ginzinger (379)).

crosses the threshold value at C_T = 15 while the gray line crosses at C_T = 20. Therefore there is a difference of 5 cycles between the two samples and since the PCR is exponential in nature, the actual difference in the starting amount of the two samples are $2^{-(\Delta Ct)}$ or 32 fold difference (379).

Several compounds are available to generate fluorescent signal as an indicator of PCR products being formed in the real-time PCR. SYBR Green I intercalating dyes, Taqman probe and molecular beacon are the most common compounds used. SYBR Green I is a dye that when excited by light generates a fluorescent signal when it intercalates to double strand DNA. Taqman probe is a short sequence of DNA designed to hybridize to the gene of interest between the forward and reverse primers. Unlike primers, the 5' of the probe contains a fluorescent molecule while the 3' end contains a quenching molecule. The most common dye for the 5' end is FAM (6-carboxyfluorescein) while TAMRA (6-carboxy tetramethyl rhodamine) is the most common for the 3' end. When the probe hybridizes to the template DNA during DNA synthesis, the 5' nuclease activity of the DNA polymerase will cleave the dye on the 5'

end, releasing it from the quenching effect of the 3' end molecule. Therefore, as PCR progresses, more fluorescent molecules are being released, yielding a higher fluorescent signal. This method has an advantage over SYBR Green I because it is specific, however, it is more costly because you have to design a probe for each gene of interest. Molecular beacon is similar to Taqman probe but there is no 5' end cleavage involved. The 5' and 3' end dyes are in proximity with each other due to a hairpin loop design. When the probe hybridizes to the template, the 5' end is sufficiently far from the 3' end molecule (usually DABCYL) that quenching does not occur (379).

Quantitation of gene expression with real-time PCR can be done in two ways: standard curve quantitation and relative (comparative) quantitation. Standard curve quantitation uses a known concentration of samples to generate a standard curve and the unknown sample concentrations are determined based on this standard curve. Relative or comparative quantitation uses arithmetic formulas to compare the concentrations among samples. The concentration of the gene of interest is normalized to a reference sample and the quantitation is done relative to a control gene (with the assumption that the control gene expression is constant among samples). The formula for the relative quantitation is:

$$2^{-\Delta\Delta C_T}$$

$\Delta C_T = C_{T,X} - C_{T,R}$, the difference in threshold cycle of target and control gene

$\Delta\Delta C_T = \Delta C_{T,S} - \Delta C_{T,RS}$, the difference in ΔC_T of sample and reference sample

An inherent assumption in that formula is that the efficiency of the PCR process for both the target and control gene are the same or similar and preferably over 90%. PCR efficiency is determined from a plot of C_T as a function of log(10) cDNA concentration. The slope of the line is used to calculate efficiency. PCR efficiency = $[10^{(1/-S)}] - 1$. For a detailed derivation of these formulas, see Applied Biosystems' User Bulletin #2 (379, 380).

6.3 Materials and Methods

6.3.1 RNA Isolation

6.3.1.1 Materials

Kidneys of P-gp wild type and P-gp double knockout (FVB MDR1AB-MM) mice (Taconic, Germantown, NY), CF wild type and CF mice (bred at UCSF Animal Facility, San Francisco, CA), TRIzol (Invitrogen Life Technologies, Carlsbad, CA), pellet pestle disposable with tubes (Kontes Glass Company, Vineland, NJ), RNase free tubes (Ambion, Austin, TX), X Systems centrifuge (Abbott Laboratories, Abbott Park, IL), diethyl pyrocarbonate (Sigma, St. Louis, MO) and UV Spectrophotometer (Fisher Biotech, Pittsburgh, PA) were utilized for RNA isolation.

6.3.1.2 RNA Isolation

The kidneys were from the P-gp wild type, P-gp knockout, CF wild type and ΔF508 CF mice used for the pharmacokinetic studies. After collection, the kidneys were frozen immediately in liquid nitrogen and stored at -80°C. RNA was isolated according to the protocol provided with the TRIzol reagent. A small piece of kidney was homogenized with 1 ml of TRIzol reagent in an Eppendorf tube with pellet pestle. The homogenate was centrifuged at 13,000 rpm (12,000 g), 4°C for 10 minutes to remove insoluble materials. The supernatant was transferred to a new RNase DNase free tube and incubated at room temperature for 5 minutes to permit complete dissociation of nucleoprotein complexes. Then 0.2 ml chloroform was added to the tube. The tube was capped and shaken vigorously by hand for 15 seconds and incubated for 2-3 minutes at room temperature, then centrifuged at 13,000 rpm, 4°C for 15 minutes. The aqueous phase was transferred to a new tube and the RNA was precipitated by adding 0.5 ml isopropyl alcohol and mixing well. The sample was incubated for 10 minutes at room temperature and then centrifuged at 13,000 rpm, 4°C for 10 minutes. The RNA precipitate appeared as a white pellet on the wall of the tube. The supernatant was removed and the RNA pellet was washed with 1 ml of 75% ethanol. The sample was mixed by vortexing and centrifuged at 13,000 rpm, 4°C for 3 minutes. The ethanol was removed and the pellet was air dried at room temperature. We were careful not to let the RNA pellet dry

completely, which makes it difficult to resuspend the RNA. The RNA pellet was dissolved with 200 µl DEPC-treated water (0.1% of diethyl pyrocarbonate water, autoclaved, to inactivate RNase). The RNA concentration was determined by measuring its absorbance at 260 nm (A_{260} of 1 equals 40 µg/ml). All RNA samples were diluted to 50 µg/ml, aliquoted and stored at -80°C.

6.3.2 cDNA synthesis

6.3.2.1 Materials

10X PCR buffer, 25 mM $MgCl_2$ (Applied Biosystems, Foster City, CA), 40 U/µl RNaseOUT Recombinant Ribonuclease Inhibitor (Gibco BRL Life Technologies, Grand Island, NY), 3 µg/µl Random Primers, 25 mM dNTP, 200 U/µl M-MLV Reverse Transcriptase (Invitrogen Life Technologies, Carlsbad, CA), PCR Express (Thermo Hybaid, Ashford, Middlesex, United Kingdom), 0.2 ml PCR tubes (Ambion, Austin, TX), Fisher Minifuge (Fisher Scientific, Santa Clara, CA), Pipetman (Rainin, Woburn, MA) and ART RNase & DNase free tips (Molecular BioProduct, San Diego, CA) were utilized for cDNA synthesis.

6.3.2.2 cDNA synthesis

The cDNA synthesis was performed according to the protocol suggested by the UCSF Genome Analysis Core Facility. The protocol is as outlined below:

1. Preparation of master mix. Always prepare one extra reaction volume to account for pipetting loss. Table 6.1 lists the recipe for one reaction volume.

Table 6.1 Formula for the preparation of master mix for cDNA synthesis

Reagents	Volume (µl)	Final Concentration
10X PCR Buffer	15	1X
40 U/µl RNaseOut Inhibitor	1.5	0.4 U/µl
25 mM dNTPs	6	1 mM
200 U/µl M-MLV Reverse Transcriptase	1.375	2.5 U/µl
3 mg/ml Random Primers	7.5	0.15 mg/ml
25 mM $MgCl_2$	45	7.5 mM
RNAse-treated H_20	58.125	
Total volume for one reaction volume	135	

2. Aliquot 135 µl of solution from the master mix to a 0.2 ml PCR tube
3. Add 15 µl of 50 µg/ml RNA sample to each PCR tube
4. Vortex mix, briefly centrifuge and incubate the reactions sequentially in the PCR 5. Express at:
    - 25°C for 10 min
    - 48°C for 40 min
    - 95°C for 5 min
5. Store the synthesized cDNA samples at -20°C.

6.3.3 Real-time PCR

6.3.3.1 Materials

2X Taqman Universal PCR Master Mix, Optical Adhesive Cover starter kit, MicroAmp Optical 96-well reaction plates (Applied Biosystems, Foster City, CA), *cftr, mdr1a, mdr1b* and *gapdh* primers, *cftr, mdr1a, mdr1b* and *gapdh* probes (Integrated DNA Tech, Coralville, IO), Eppendorf RepeaterPlus, 0.1 and 0.2 ml CombitipPlus tips (Eppendorf, Hamburg, Germany) and ABI Prism 7700 Sequence Detection System (Applied Biosystems, Foster City, CA) were utilized for real-time PCR.

6.3.3.2 Primer and probe design

Cftr, mdr1a and *mdr1b* are mouse genes of interest while mouse *gapdh* serves as the control gene. The primers and Taqman probes were designed with the help of Dr. David Ginzinger from the UCSF Cancer Center using the Primer Express program (Applied Biosystems, Foster City, CA). Table 6.2 lists the sequences for each primer and probe used in the study while Table 6.3 lists the complete sequences of the amplicons for each gene amplified in the PCR reactions. The probes were designed to span the exon/intron boundary to prevent erroneous results from contaminating genomic DNA (if present). The amplicons are less than 150 bp to ensure a good PCR efficiency.

Table 6.2 Primer and probe sequences for Taqman real-time PCR assay

Primer Name	**Sequences**
Mouse *cftr* primer (S)	5'-ACG CCC CTA TGT CGA CCA-3'
Mouse *cftr* primer (AS)	5'-GCT CCA ATC ACA ATG AAC ACC A-3'
Mouse *cftr* probe	FAM-CAG CAA GCT GAA AGC AGG TGG GAT TCT-TAMRA
Mouse *mdr1a* primer (S)	5'-ACC CCC GAG ATT GAC AGC TAC-3'
Mouse *mdr1a* primer (AS)	5'-GAC TCC ACT AAA TTG CAC ATT TCC T-3'
Mouse *mdr1a* probe	FAM-CGC AAG GCC TAA AGC CGA ATA TGT TGG-TAMRA
Mouse *mdr1b* primer (S)	5'-TCA TTG TAT TGG GCG GAA TTA TT-3'
Mouse *mdr1b* primer (AS)	5'-GTG CGG AAG TTT TCA ATT GCT-3'
Mouse *mdr1b* probe	FAM-TTG TCT GGC CAA GCC TTG AAG GAC AA-TAMRA
Mouse *gapdh* primer (S)	5'-TGC ACC ACC AAC TGC TTA G-3'
Mouse *gapdh* primer (AS)	5'-GGA TGC AGG GAT GAT GTT C-3'
Mouse *gapdh* probe	FAM-CAG AAG ACT GTG GAT GGC CCC TC-TAMRA

Table 6.3 Complete amplicon sequences for Taqman real-time PCR

Amplicon Name	**Sequences**
Mouse *cftr* (139 bp)	5'-ACGCCCCTATGTCGACCATCAGCAAGCTGAAAGCAGGTGGGATTCTT AACAGATTCTCCAAAGATATAGCAATTTTGGATGACTTTCTGCCTCTTAC CATTTTTGACTTCATTCAGTTGGTGTTCATTGTGATTGGAGC-3'
Mouse *mdr1a* (78 bp)	5'-ACCCCCGAGATTGACAGCTACAGCACGCAAGGCCTAAAGCCGAATA TGTTGGAAGGAAATGTGCAATTTAGTGGAGTC-3'
Mouse *mdr1b* (118 bp)	5'-TCATTGTATTGGGCGGAATTATTGAAATGAAGCTGTTGTCTGGCCAA GCCTTGAAGGACAAGAAACAGCTTGAGATCTCTGGGAAGATTGCTACA GAAGCAATTGAAAACTTCCGCAC-3'
Mouse *gapdh* (177 bp)	5'-TGCACCACCAACTGCTTAGCCCCCCTGGCCAAGGTCATCCATGACAA CTTTGGCATTGTGGAAGGGCTCATGACCACAGTCCATGCCATCACTGCC ACCCAGAAGACTGTGGATGGCCCCTCTGGAAAGCTGTGGCGTGATGGC CGTGGGGCTGCCCAGAACATCATCCCTGCATCC-3'

6.3.3.3 PCR efficiency test

PCR efficiency is determined according to the protocol outlined below:

1. A 10-fold serial dilution of cDNA (1000 ng RNA/100 µl reverse transcriptase reaction) is performed (1, 1:10, 1:100, 1:1000).

2. A master mix solution is prepared for each cDNA concentration. Always prepare one extra reaction volume to account for pipetting loss. Also take into account that each sample is run in triplicate. The recipe for one reaction volume is:

   Taqman Universal Master Mix 2X = 12.5 µl

   H_2O = 2.5 µl

   cDNA = 5.0 µl

3. Prepare probe and primer mix solution for each gene of interest. Always prepare one extra reaction volume to account for pipetting loss. Also take into account that each sample is run in triplicate. The recipe for one reaction volume is:

   50 µM (S) and (AS) primer = 0.25 µl

   20 µM probe = 0.25 µl

   H_2O = 4.5 µl

4. With repeater pipetter, aliquot 20 µl of master mix and 5 µl of probe and primer mix solution into a well of a MicroAmp Optical 96-well reaction plate. Each sample is run in triplicate. Repeat this for all cDNA concentrations and genes of interests.

5. Run the PCR in the ABI 7700 System with the following thermal cycler condition:

   stage 1 : 95°C for 12 min

   stage 2 : 95°C for 15 s
   60°C for 1 min] 45 cycles

6. Plot the C_T *vs.* log(10) of cDNA concentration and determine the slope of the line to calculate the PCR efficiency. A slope of 3.3 is 100% efficiency.

6.3.3.4 Reverse transcription linearity test

This is very similar to the PCR efficiency test with the exception that the different cDNA concentrations used in the PCR reaction are not from a serial dilution but rather from the cDNA made with a different starting amount of RNA. The cDNAs are synthesized according to the protocol outlined in section 6.3.3 with different concentrations of RNA (for example: 12.5, 25, 50 and 100 μg/ml). The linearity is determined in the same way as the efficiency test. A slope of 3.3 means that the reverse transcription reaction is linear.

6.3.3.5 Relative quantitation of unknown samples

Unknown sample quantitation is determined according to the protocol outlined below:

1. A master mix solution is prepared. Always prepare one extra reaction volume to account for pipetting loss. Also take into account that each sample is run in triplicate. The recipe for one reaction volume is:

   Taqman Universal Master Mix 2X = 12.5 μl

   50 μM (S) and (AS) primer = 0.25 μl

   probe = 0.25 μl

   H_2O =7.0 μl

2. With repeater pipetter, aliquot 20 μl of master mix and 5 μl of unknown cDNA solution into a well of a MicroAmp Optical 96-well reaction plate. Each sample is run in triplicate. Repeat this for all unknown samples and genes of interests.
3. Run the PCR in the ABI 7700 System with the same thermal cycler condition as the PCR efficiency test.
4. Determine the relative amounts/concentrations of unknown samples using the formula outlined in section 6.2.

6.3.4 Semi-quantitative RT-PCR

6.3.4.1 Materials

CFPAC-1 cells (ATCC, Manassas, VA), CFPAC-1 pLJ CFTR (a gift from Dr. Ray Frizzell, University of Pittsburgh), Iscove media, fetal bovine serum, phosphate buffered saline (PBS)

Ca^{2+}, Mg^{2+}-free solution (UCSF Cell Culture Facility, San Francisco, CA), CFTR (S), CFTR (AS), P-gp (S), P-gp (AS), MRP1 (S), MRP1 (AS), MRP2 (S), MRP2 (AS), MRP3 (S), MRP3 (AS), OATP-A (S), OATP-A (AS), OATP-C (S), OATP-C (AS), OATP-D (S), OATP-D (AS), OATP-E (S), OATP-E (AS), OATP-8 (S) and OATP-8 (AS) primers (Gibco BRL Life Technologies, Grand Island, NY), Qiagen One-Step RT-PCR Kit (Qiagen, Valencia, CA), 2% E-gels (Invitrogen Life Technologies, Carlsbad, CA), X Systems centrifuge (Abbott Laboratories, Abbott Park, IL), UV transilluminator (Fisher Biotech, Pittsburgh, PA), Pipetman (Rainin, Woburn, MA), Fisher Vortex Genie 2 (Fisher Scientific, Santa Clara, CA), BioRad Power Pac 300 (BioRad, Hercules, CA), E-gel power base (Invitrogen Life Technologies, Carlsbad, CA), photo-documentation system (Fisher Biotech, Pittsburgh, PA), Black and White film (Polaroid, Cambridge, MA), ART RNase & DNase free tips (Molecular BioProduct, San Diego, CA), PCR Express (Thermo Hybaid, Ashford, Middlesex, United Kingdom), 0.2 ml PCR tubes (Ambion, Austin, TX), Fisher Minifuge (Fisher Scientific, Santa Clara, CA) and 50 bp DNA Ladder 1 μg/μl (Invitrogen Life Technologies, Carlsbad, CA) were utilized for semi-quantitative RT-PCR.

6.3.4.2 Primer design

We designed primers for the human *MDR1* gene in order to compare the expression level of *MDR1* between CFPAC-1 and CFPAC-1 pLJ CFTR cells. Table 6.4 lists the sequences of the primers for the *MDR1* gene. This primer pair produces a 285 bp segment. We compared the expression of the *CFTR* gene between CFPAC-1 and CFPAC-1 pLJ CFTR cells. For an internal control, we utilized the *18S* gene with the competimer technology from Ambion (Austin, Texas). The expected product of the *18S* gene is 489 bp. We also compared the expression of other transporter genes as negative controls (*MRP1, MRP2, MRP3, OATP-A, OATP-C, OATP-D, OATP-E* and *OATP-8*).

6.3.4.3 One-step semi-quantitative RT-PCR

CFPAC-1 and CFPAC-1 pLJ CFTR cells were grown in T-75 flasks in Iscove media. The cells were rinsed in PBS Ca^{2+}, Mg^{2+}-free solution and RNA isolation was done according to the protocol outlined in section 6.3.1. However, instead of performing the cDNA synthesis

Table 6.4 Primer sequences for human *MDR1, CFTR, MRP1, MRP2, MRP3, OATP-A, OATP-C, OATP-D, OATP-E* and *OATP-8* genes

Primer Name	Sequences	Expected Size (bp)
P-gp primer (S)	GCC TGG CAG CTG GAA GAC AAA TAC ACA AAA T	285
P-gp primer (AS)	AGA CAG CAG CTG ACA GTC CAA GAA CAG GAC T	
CFTR primer (S)	TCT TAC TGG GAA GAA TCA TAG CTT	305
CFTR primer (AS)	CGA AAT GTG CCA ATG CAA GTC C	
MRP1 primer (S)	CTG TTT TGT TTT CGG GTT CC	287
MRP1 primer (AS)	GAT GGT GGA CTG GAT GAG GT	
MRP2 primer (S)	CTG CCT CTT CAG AAT CTT AG	240
MRP2 primer (AS)	CCC AAG TTG CAG GCT GGC C	
MRP3 primer (S)	GAT ACG CTC GCC ACA GTC CTC	254
MRP3 primer (AS)	TCA GTT GCC GTG ATG TGG CTG	
OATP-A primer (S)	AAG AAG AGG TCA AGA AGG AAA AAT	660
OATP-A primer (AS)	GGA GCA TCA AGG AAC AGT CAG GTC	
OATP-C primer (S)	TGT CAT TGT CCT TTT ACC TAT TAT	195
OATP-C primer (AS)	TGT AAG TTA TTC CAT TGT TTC CAC	
OATP-D primer (S)	CTC AAA TCC TTC GCC TTC ATC CTG	128
OATP-D primer (AS)	AGG GTC AGA GTA GAG GCA AAG AAC	
OATP-E primer (S)	CAC GGC GGG CAC TCA GCA TTT CCT	240
OATP-E primer (AS)	CGA TCG GGT ATA AAA CAC ATT CTA	
OATP-8 primer (S)	ATG CAA ATC CTC AAG TGG TAT TAA AAA	368
OATP-8 primer (AS)	CTT TGT CTC CAC AGC TGT TGG TGG ACC	

separately from the PCR process, here we performed the cDNA and PCR in one step using the Qiagen OneStep RT-PCR Reaction Kit (Qiagen, Valencia, CA).

The protocol is as follows:

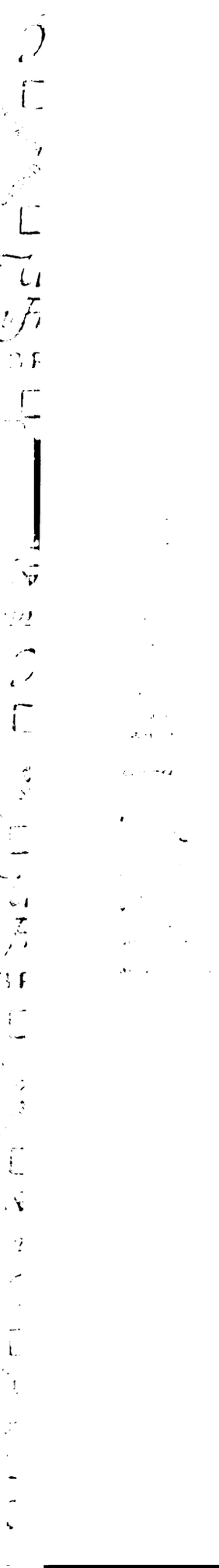

1. Preparation of RT-PCR reaction mix. Always prepare one extra reaction volume to account for pipetting loss. Table 6.5 lists the recipe for one reaction volume.

Table 6.5 RT-PCR reaction mix recipe for one reaction volume

Reagents	**Volume (μl)**	**Final Concentration**
Qiagen OneStep 5X buffer	10	1.25X
10 mM Qiagen OneStep dNTP Mix	2	0.5 mM
Qiagen OneStep Enzyme Mix	2	5% (v/v)
10 μM human P-gp primer (S)	3	0.75 μM
10 μM human P-gp primer (AS)	3	0.75 μM
Ambion 18S primer	0.5	1.25% (v/v)
Ambion 18S competimer	4.5	11.25% (v/v)
H_20	15	up to 40 μl
Total volume	40	

2. Aliquot 40 μl of solution from the master mix into a 0.2 ml PCR tube
3. Add 10 μl of 50 μg/ml RNA sample to each PCR tube
4. Vortex mix, briefly centrifuge and run the reactions sequentially in the PCR Express at:
   - 50°C for 30 min
   - 95°C for 15 min
   - 94°C for 1 min ┐
   - 59°C for 1 min │ 26 cycles
   - 72°C for 1 min ┘
   - 72°C for 15 min
5. Run the RT-PCR products on a 2% E-gel. Prerun the 2% E-gel at 66 V for 2 min with the comb on, remove the comb, load 12 μl H_2O into each well, load 10 μl PCR product into the well, load 20 μl of 50 fold-diluted 50 bp DNA ladder into one well, run at 66 V for 30 min, visualize the bands with a UV transilluminator and take a picture with the Polaroid camera.

6.3.5 Western blot

6.3.5.1 Materials

Kidneys from P-gp wild type and P-gp knockout mice (Taconic, Germantown, NY), CF wild type and ΔF508 CF mice (bred at UCSF Animal Care Facility, San Francisco, CA), CFPAC-1 (ATCC, Manassas, VA) and CFPAC-1 pLJ CFTR cells (a gift from Dr. Ray Frizzell, University of Pittsburgh), Laemmli sample buffer, protein assay dye reagent concentrate, dry milk, filter paper, nitrocellulose membrane, prestained SDS-PAGE broad range standard, SDS-PAGE gels, 10X Tris/Glycine/SDS running buffer, PVDF membranes (Bio-Rad, Hercules, CA), ECL reagents, Hyperfilm (Amersham, Piscataway, NJ), bovine serum albumin (Gibco BRL Life Technologies, Grand Island, NY), X Systems centrifuge (Abbott Laboratories, Abbott Park, IL), IEC Centra-8R centrifuge (IEC, Needham Heights, MA), Pellet pestle disposable with tubes (Kontes Glass Company, Vineland, NJ), Pipetman (Rainin, Woburn, MA), Fisher Vortex Genie 2 (Fisher Scientific, Santa Clara, CA), Complete protease inhibitor cocktail tablets (Boehringer Mannheim, Germany), rabbit mdr (Ab-1) antibody (Oncogene, Boston, MA), goat anti-rabbit IgG peroxidase-conjugated, Tween-20, Tris, KCl, EDTA, glycine, phenylmethanesulfonyl fluoride (PMSF), dithiothreitol (DTT), glycerol, methanol, NaCl, KH_2PO_4, K_2HPO_4 (Sigma, St. Louis, MO), QiaShredder (Qiagen, Valencia, CA) ECL detection reagent 1 and 2 (Amersham Pharmacia Biotech, Piscataway, NJ) and Kodak film developer (Eastman Kodak Company, Rochester, NY) were utilized for Western blot.

6.3.5.2 Western blot

Kidneys were homogenized in lysis buffer (Table 6.6) with the pellet pestle. The homogenates were centrifuged for 10 minutes at 2500 rpm (<6000 g) at 4°C. The supernatants were centrifuged for 15 minutes at 13,000 rpm (~12,000 g) at 4°C. The pellets were resuspended with storage buffer (Table 6.6). The protein concentrations were determined by BioRad assay with bovine serum albumin as the standard. All samples were diluted to the same concentration (4 μg/ml) with storage buffer. 100 μL of samples were mixed with 200 μL Laemmli sample buffer containing 5% β-mercaptoethanol (1:2) on the QiaShredder column and centrifuged for 30 s. Load 75 μL of the mixture (100 μg protein) onto SDS-PAGE gels.

The gels were run at 10 mA overnight. The gels were blotted to PVDF membranes for six hours at 150 mA. The membranes were incubated for one hour at room temperature with 5% dry milk solution in TBS (Table 6.6). After that the membranes were washed with TBS. The membranes were incubated for 90 minutes with 200-fold diluted polyclonal anti-P-gp antibody (mdr Ab-1). Then the membranes were washed several times with TTBS (Table 6.6) before incubating them for 30 minutes at room temperature with the secondary antibody (5000-fold diluted goat anti-rabbit IgG). The membranes were washed several times with TTBS and incubated with premix ECL reagent 1 & 2 for 1 min before developing the film.

Table 6.6 Recipes for Western blot solutions

Name of Solution	**Components**	**Amount**
Lysis buffer	100 mM Tris base	
	100 mM KCl	
	1 mM EDTA	
	2 mM PMSF	
	1X Complete Protease Inhibitor	
Storage buffer	100 mM $KHPO_4$ pH 7.4	
	1 mM EDTA	
	20%l Glycerol	
	1 mM DTT	
	2 mM PMSF	
	1X Complete Protease Inhibitor	
Blotting buffer (store at 4°C)	Tris base	3.03 g
	Glycine	14.4 g
	Methanol	200 ml
	distilled water	to make 1 L solution
Tris-buffered solution (TBS)	Tris base	4.87 g
	NaCl	58.44 g
	Concentrated HCl	to adjust pH to 7.4
	distilled water	to make 2 L solution
Tween-TBS (TTBS)	Tween-20	0.5 ml
	TBS	to make 1 L solution

6.4 Results

6.4.1 PCR efficiency tests

Figures 6.2, 6.3, 6.4 and 6.5 show the plots of $\log_{10}$ of cDNA concentration *vs.* C_T values for mdr1a, mdr1b, cftr and gapdh genes, respectively. The slopes of the lines are tabulated in Table 6.7. The results show that the PCR efficiency for all the genes is within the acceptable limit (± 10% of 100% efficiency).

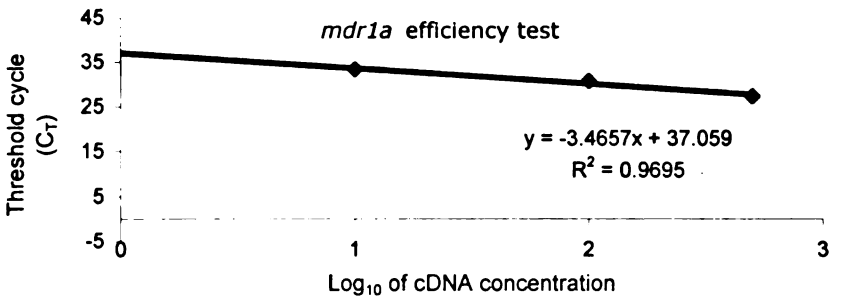

Figure 6.2 Plot of $\log_{10}$ cDNA concentration *vs.* C_T to determine *mdr1a* PCR efficiency.

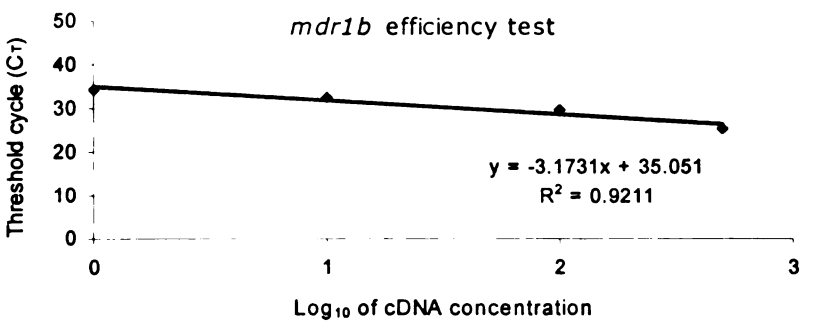

Figure 6.3 Plot of $\log_{10}$ cDNA concentration *vs.* C_T to determine *mdr1b* PCR efficiency

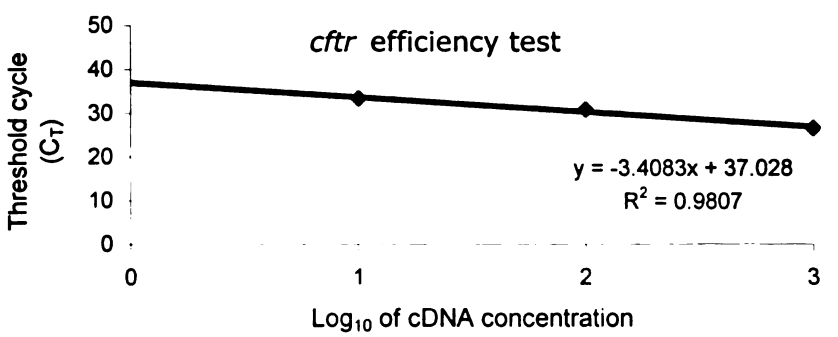

Figure 6.4 Plot of $\log_{10}$ cDNA concentration *vs.* C_T to determine *cftr* PCR efficiency

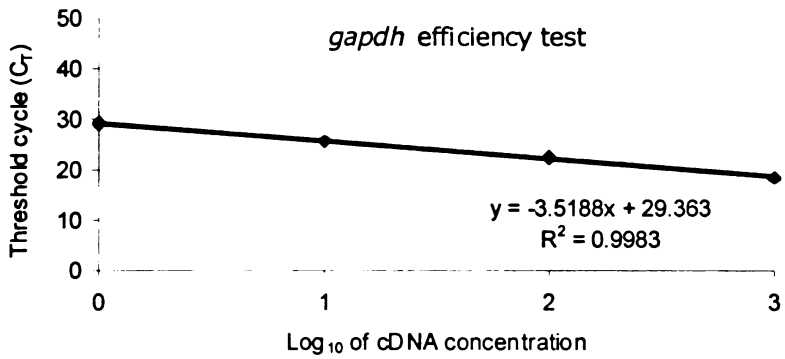

Figure 6.5 Plot of $\log_{10}$ cDNA concentration *vs.* C_T to determine *gapdh* PCR efficiency

Table 6.7 Results of PCR efficiency tests for *mdr1a, mdr1b, cftr* and *gapdh*

Genes	Slope	PCR Efficiency
mdr1a	3.466	94 %
mdr1b	3.173	107 %
cftr	3.408	97 %
gapdh	3.512	92 %

6.4.2 Reverse transcription linearity tests

Figures 6.6, 6.7, 6.8 and 6.9 show the plots of $\log_{10}$ of cDNA concentration *vs.* C_T values for *mdr1a, mdr1b, cftr* and *gapdh* genes, respectively. The slopes of the lines are tabulated in Table 6.8. The results show that the RT linearity tests for all the genes at the concentrations tested are within the acceptable limit (all are around 90 to 100 percent).

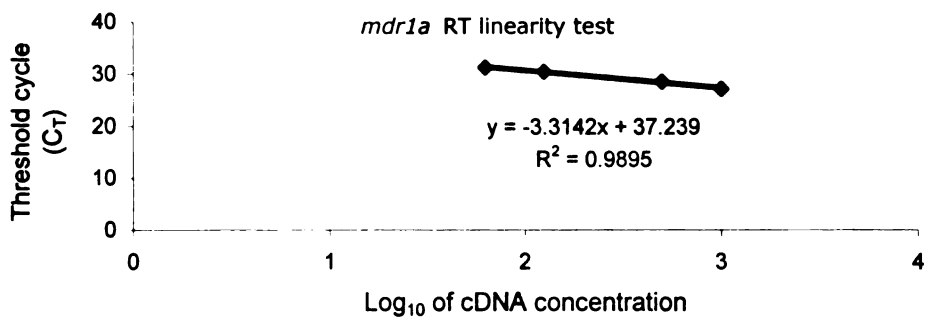

Figure 6.6 Plot of $\log_{10}$ cDNA concentration *vs.* C_T to test the linearity of *mdr1a* reverse transcription reaction.

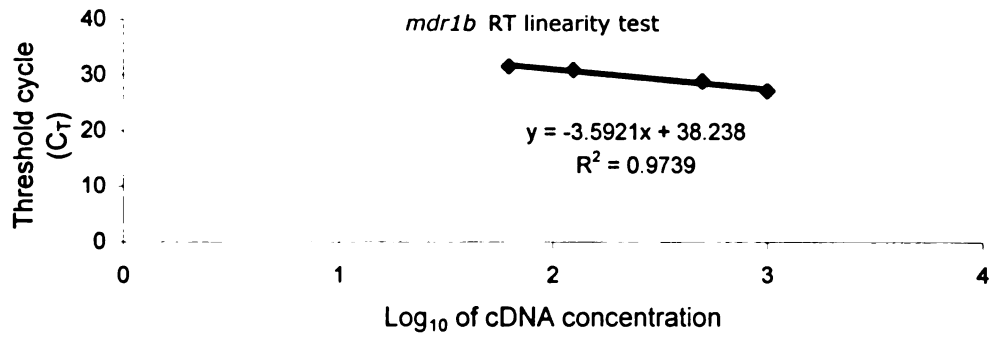

Figure 6.7 Plot of $\log_{10}$ cDNA concentration *vs.* C_T to test the linearity of *mdr1b* reverse transcription reaction.

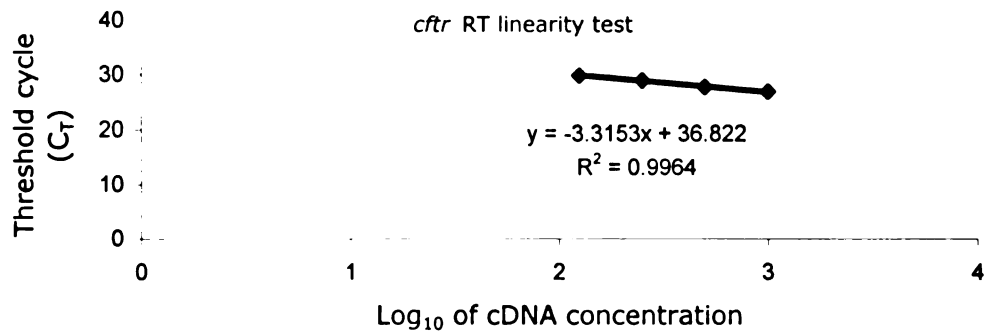

Figure 6.8 Plot of $\log_{10}$ cDNA concentration *vs.* C_T to test the linearity of *cftr* reverse transcription reaction.

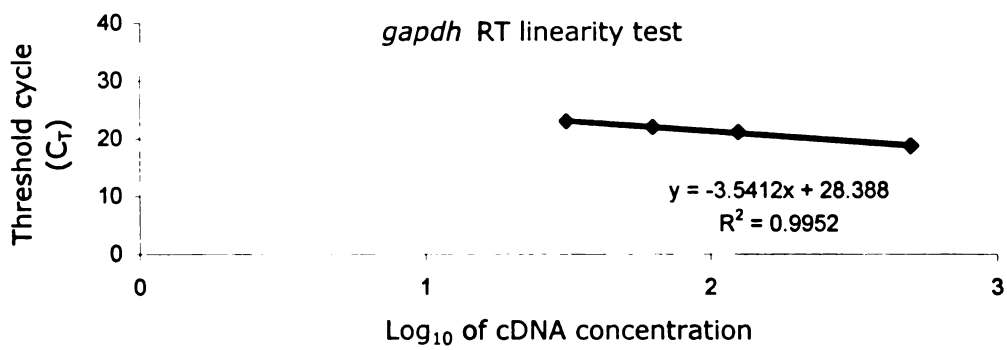

Figure 6.9 Plot of $\log_{10}$ cDNA concentration *vs.* C_T to test the linearity of *gapdh* reverse transcription reaction.

Table 6.8 Results of RT linearity tests for *mdr1a, mdr1b, cftr* and *gapdh*

Genes	Slope	RT Linearity
mdr1a	3.314	100 %
mdr1b	3.592	90 %
cftr	3.315	100 %
gapdh	3.541	90 %

6.4.3 *Mdr1a* and *mdr1b* expression in CF wild type and ΔF508 CF mice

Figure 6.10 shows the amplification plot of a real-time RT-PCR run of *mdr1a*. Each curve represents a sample. There are a total of twelve samples, six CF wild type and six ΔF508 CF mice kidney RNAs. For ease of comparison, the curves in Figure 6.10 are separated into two figures: Figure 6.11 shows the amplification plot of *mdr1a* in CF wild type while Figure 6.12 shows the amplification plot of *mdr1a* in ΔF508 CF mice.

The C_T values for all the samples are between 25 to 28 cycles. There is more variation in the C_T value in CF wild type mice compared to ΔF508 CF mice. The average C_T data for CF wild type and ΔF508 CF mice are tabulated in Table 6.9. The calculations show no difference in *mdr1a* expression in ΔF508 CF mice relative to wild type mice.

When the data are separated based on sex, the calculations reveal that *mdr1a* expression is significantly decreased (~60%) in ΔF508 CF female mice compared to CF wild type female mice (Table 6.10). On the other hand, there is a trend toward higher *mdr1a* expression (~50%) in ΔF508 CF male mice compared to CF wild male mice (Table 6.11). Table 6.12 shows that the expression of *mdr1a* is significantly higher in CF wild type female mice compared to CF wild type male mice (3-fold difference) while no difference is observed between female and male ΔF508 CF mice.

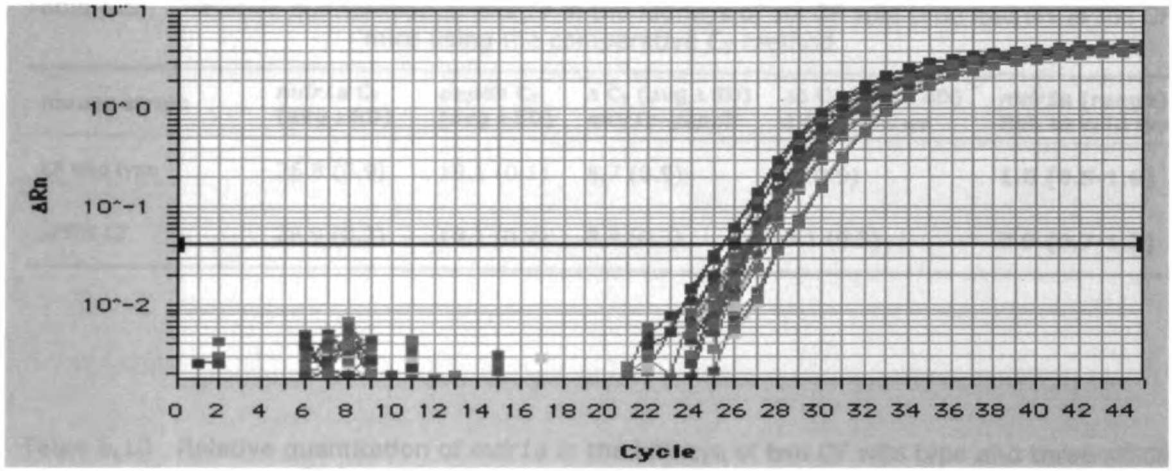

Figure 6.10 Amplification plot of *mdr1a* from six CF wild type and six ΔF508 CF mice kidney RNAs

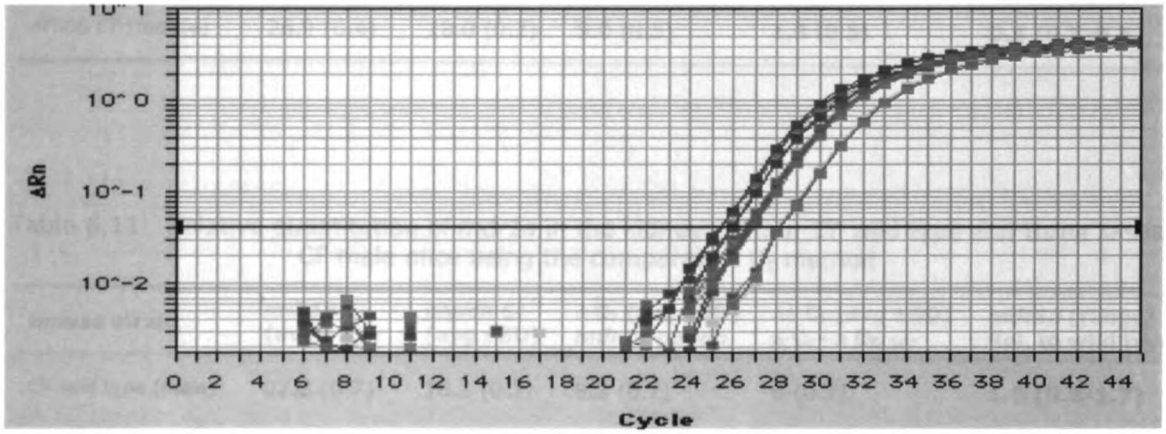

Figure 6.11 Amplification plot of *mdr1a* from six CF wild type mice kidney RNAs

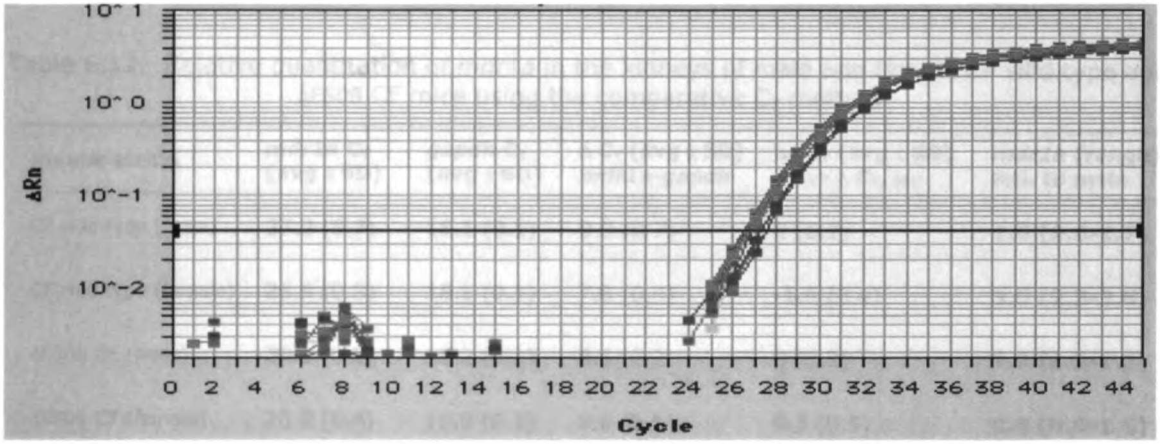

Figure 6.12 Amplification plot of *mdr1a* from six ΔF508 CF mice kidney RNAs

Table 6.9 Relative quantitation of *mdr1a* in the kidneys of six CF wild type and six ΔF508 CF mice using the comparative C_T method

mouse strain	***mdr1a*** **C_T (avg ± SD)**	***gapdh*** **C_T (avg ± SD)**	**Δ C_T (avg ± SD)** ***mdr1a-gapdh***	**ΔΔ C_T (avg ± SD)** **Δ C_T - Δ $C_{T,\ WT}$**	***mdr1a*** **(range) Rel. to wild type**
CF wild type	26.8 (0.9)	18.1 (0.1)	8.7 (0.9)	0 (0.9)	**1.0 (0.5-1.9)**
ΔF508 CF	26.9 (0.3)	18.1 (0.2)	8.8 (0.3)	0.1 (0.3)	**0.9 (0.7-1.2)**

Table 6.10 Relative quantitation of *mdr1a* in the kidneys of two CF wild type and three ΔF508 CF female mice using the comparative C_T method

mouse strain	***mdr1a*** **C_T (avg ± SD)**	***gapdh*** **C_T (avg ± SD)**	**Δ C_T (avg ± SD)** ***mdr1a-gapdh***	**ΔΔ C_T (avg ± SD)** **Δ C_T - Δ $C_{T,\ WT}$**	***mdr1a*** **(range) Rel. to wild type**
CF wild type (female)	25.9 (0.3)	18.2 (0.1)	7.6 (0.4)	0 (0.4)	**1.0 (0.8-1.3)**
ΔF508 CF (female)	26.9 (0.4)	18.0 (0.2)	9.0 (0.5)	1.3 (0.5)	**0.4 (0.3-0.5)**

Table 6.11 Relative quantitation of *mdr1a* in the kidneys of four CF wild type and three ΔF508 CF male mice using the comparative C_T method

mouse strain	***mdr1a*** **C_T (avg ± SD)**	***gapdh*** **C_T (avg ± SD)**	**Δ C_T (avg ± SD)** ***mdr1a-gapdh***	**ΔΔ C_T (avg ± SD)** **Δ C_T - Δ $C_{T,\ WT}$**	***mdr1a*** **(range) Rel. to wild type**
CF wild type (male)	27.2 (0.7)	18.1 (0.1)	9.2 (0.7)	0 (0.7)	**1.0 (0.6-1.7)**
ΔF508 CF (male)	26.8 (0.2)	18.2 (0.1)	8.6 (0.2)	-0.5 (0.2)	**1.5 (1.3-1.7)**

Table 6.12 Relative quantitation of *mdr1a* in the kidneys of male and female CF wild type and ΔF508 CF mice using the comparative C_T method

mouse strain	***mdr1a*** **C_T (avg ± SD)**	***gapdh*** **C_T (avg ± SD)**	**Δ C_T (avg ± SD)** ***mdr1a-gapdh***	**ΔΔ C_T (avg ± SD)** **Δ C_T - Δ $C_{T,\ WT}$**	***mdr1a*** **(range) Rel. to male**
CF wild type (male)	27.2 (0.7)	18.1 (0.1)	9.2 (0.7)	0 (0.7)	**1.0 (0.6-1.7)**
CF wild type (female)	25.9 (0.3)	18.2 (0.1)	7.6 (0.4)	-1.6 (0.4)	**3.0 (2.3-3.8)**
ΔF508 CF (male)	26.8 (0.2)	18.2 (0.1)	8.6 (0.2)	0 (0.2)	**1.0 (0.9-1.2)**
ΔF508 CF (female)	26.9 (0.4)	18.0 (0.2)	9.0 (0.5)	0.3 (0.5)	**0.8 (0.6-1.1)**

Figures 6.13 shows the amplification plot of a real-time RT-PCR run of *mdr1b*. Each curve represents a sample. There are a total of twelve samples, six CF wild type and six ΔF508 CF mice kidney RNAs. For ease of comparison, the curves in Figure 6.13 are separated into two figures: Figure 6.14 shows the amplification plot of *mdr1b* in CF wild type while Figure 6.15 shows the amplification plot of *mdr1b* in ΔF508 CF mice.

The C_T values for all the samples are between 23 to 28 cycles. There is more variation in the C_T value in CF wild type mice compared to ΔF508 CF mice. The average C_T data for CF wild type and ΔF508 CF mice are tabulated in Table 6.13. The calculations show a trend toward higher *mdr1b* expression (~80%) in ΔF508 CF mice relative to wild type mice.

When the data are separated based on sex, similar to what we observed for *mdr1a*, the calculations reveal that *mdr1b* expression is significantly decreased (~70%) in ΔF508 CF female mice compared to CF wild type female mice (Table 6.14). On the other hand, *mdr1b* expression is significantly increased (~360%) in ΔF508 CF male mice compared to CF wild male mice (Table 6.15). Table 6.16 shows that the expression of *mdr1b* is significantly higher in CF wild type female mice compared to CF wild type male mice (14-fold difference) while no difference is observed between female and male ΔF508 CF mice.

Figures 6.16, 6.17 and 6.18 show the amplification plot of *gapdh* in six CF wild type and six ΔF508 CF mice kidney RNAs. *Gapdh* is the internal control. As expected, there is not much variations in the C_T values for *gapdh*. The C_T values for *gapdh* were used in our calculations in Tables 6.9-6.16.

Figure 6.19 shows the results of Western blot of P-gp expression in six CF wild type and six ΔF508 CF mice kidneys. Western blot results agree with the RT-PCR experiments. P-gp expression is higher in CF wild type female mice (lanes 9 and 10) compared to CF wild type male mice (lanes 3-5, 11). P-gp expression appears higher in ΔF508 CF male mice (lanes 6-8) compared to CF wild type male mice (lanes 3-5, 11). P-gp expression is decreased in ΔF508 CF female mice (lanes 12-14) compared to CF wild type female mice (lanes 9 and 10).

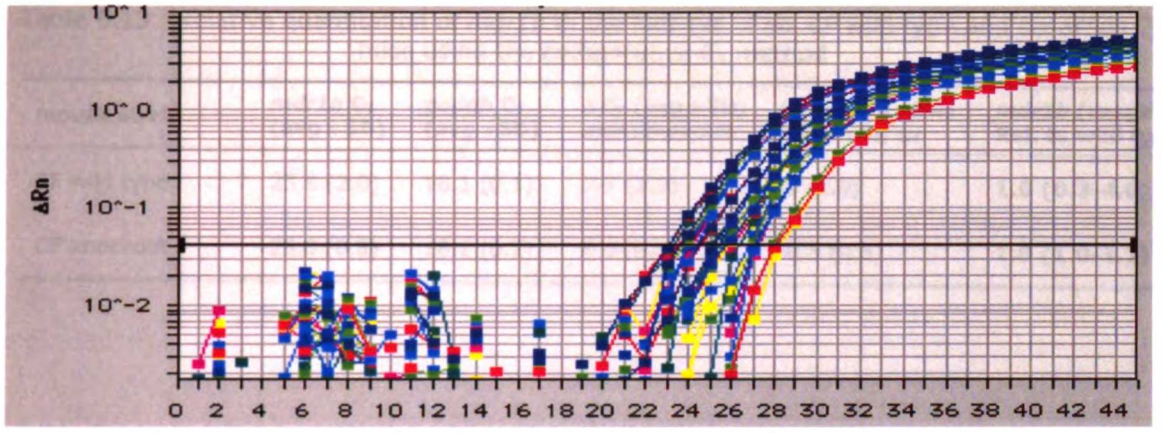

Figure 6.13 Amplification plot of *mdr1b* from six CF wild type and six ΔF508 CF mice kidney RNAs

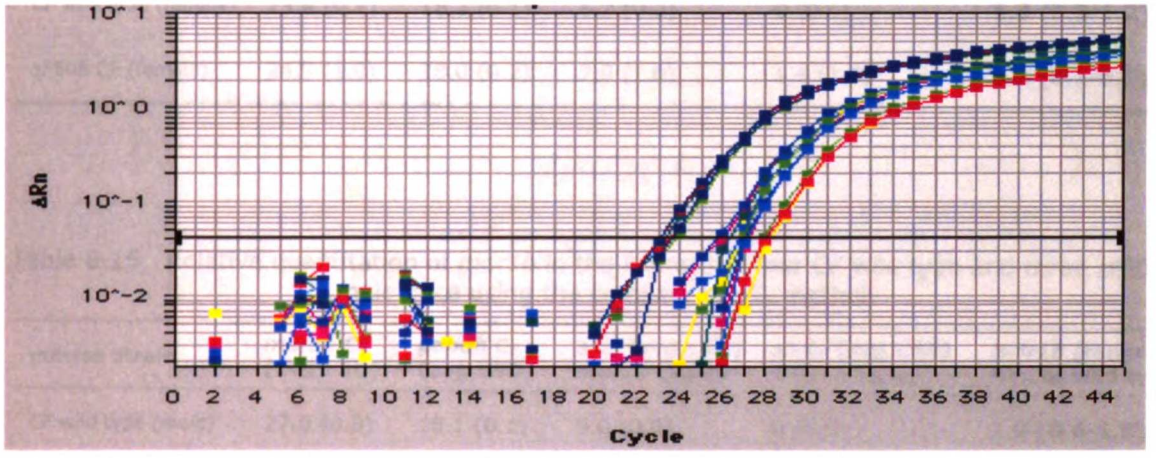

Figure 6.14 Amplification plot of *mdr1b* from six CF wild type mice kidney RNAs

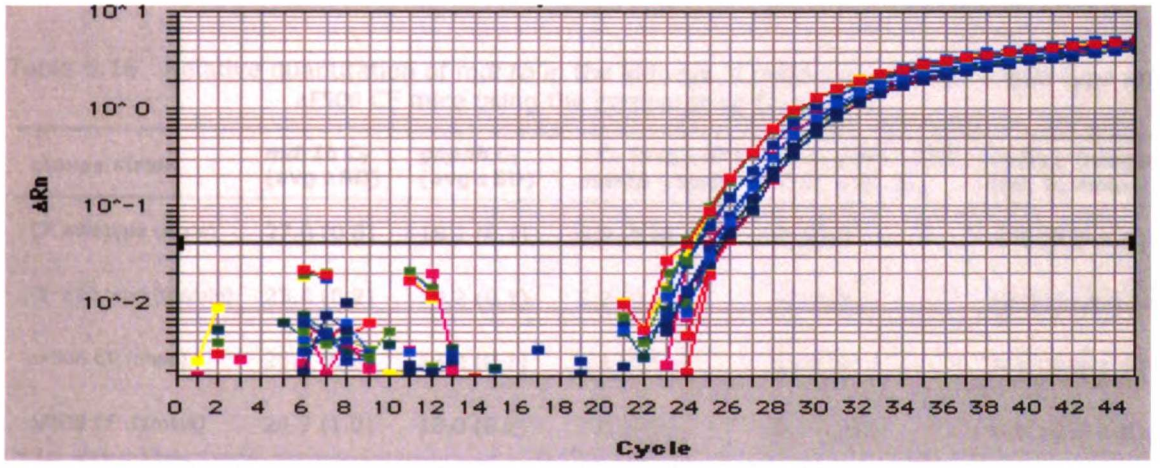

Figure 6.15 Amplification plot of *mdr1b* from six ΔF508 CF mice kidney RNAs

Table 6.13 Relative quantitation of *mdr1b* in the kidneys of six CF wild type and six ΔF508 CF mice using the comparative C_T method

mouse strain	*mdr1b* C_T (avg ± SD)	*gapdh* C_T (avg ± SD)	Δ C_T (avg ± SD) *mdr1b-gapdh*	ΔΔ C_T (avg ± SD) Δ C_T - Δ $C_{T,\ WT}$	*mdr1b* (range) Rel. to wild type
CF wild type	25.8 (2.0)	18.1 (0.1)	7.7 (2.0)	0 (2.0)	**1.0 (0.3-4.0)**
CF knockout	25.0 (0.8)	18.1 (0.2)	6.9 (0.8)	-0.8 (0.8)	**1.8 (1.0-3.2)**

Table 6.14 Relative quantitation of *mdr1b* in the kidneys of two CF wild type and three ΔF508 CF female mice using the comparative C_T method

mouse strain	*mdr1b* C_T (avg ± SD)	*gapdh* C_T (avg ± SD)	Δ C_T (avg ± SD) *mdr1b-gapdh*	ΔΔ C_T (avg ± SD) Δ C_T - Δ $C_{T,\ WT}$	*mdr1b* (range) Rel. to wild type
CF wild type (female)	23.4 (0.2)	18.2 (0.1)	5.2 (0.2)	0 (0.4)	**1.0 (0.9-1.2)**
ΔF508 CF (female)	24.9 (1.0)	18.0 (0.2)	7.0 (1.0)	1.8 (1.0)	**0.3 (0.1-0.6)**

Table 6.15 Relative quantitation of *mdr1b* in the kidneys of four CF wild type and three ΔF508 CF male mice using the comparative C_T method

mouse strain	*mdr1b* C_T (avg ± SD)	*gapdh* C_T (avg ± SD)	Δ C_T (avg ± SD) *mdr1b-gapdh*	ΔΔ C_T (avg ± SD) Δ C_T - Δ $C_{T,\ WT}$	*mdr1b* (range) Rel. to wild type
CF wild type (male)	27.0 (0.8)	18.1 (0.1)	9.0 (0.8)	0 (0.8)	**1.0 (0.6-1.8)**
ΔF508 CF (male)	25.0 (0.8)	18.2 (0.1)	6.8 (0.8)	-2.2 (0.8)	**4.6 (2.6-8.0)**

Table 6.16 Relative quantitation of m*dr1b* in the kidneys of male and female CF wild type and ΔF508 CF mice using the comparative C_T method

mouse strain	*mdr1b* C_T (avg ± SD)	*gapdh* C_T (avg ± SD)	Δ C_T (avg ± SD) *mdr1b-gapdh*	ΔΔ C_T (avg ± SD) Δ C_T - Δ $C_{T,\ WT}$	*mdr1b* (range) Rel. to male
CF wild type (male)	27.0 (0.8)	18.1 (0.1)	9.0 (0.8)	0 (0.8)	**1.0 (0.6-1.8)**
CF wild type (female)	23.4 (0.2)	18.2 (0.1)	5.2 (0.2)	-3.8 (0.2)	**14.0 (11.9-16.4)**
ΔF508 CF (male)	25.0 (0.8)	18.2 (0.1)	6.8 (0.8)	0 (0.3)	**1.0 (0.8-1.2)**
ΔF508 CF (female)	24.9 (1.0)	18.0 (0.2)	7.0 (1.0)	0.2 (1.0)	**0.9 (0.4-1.8)**

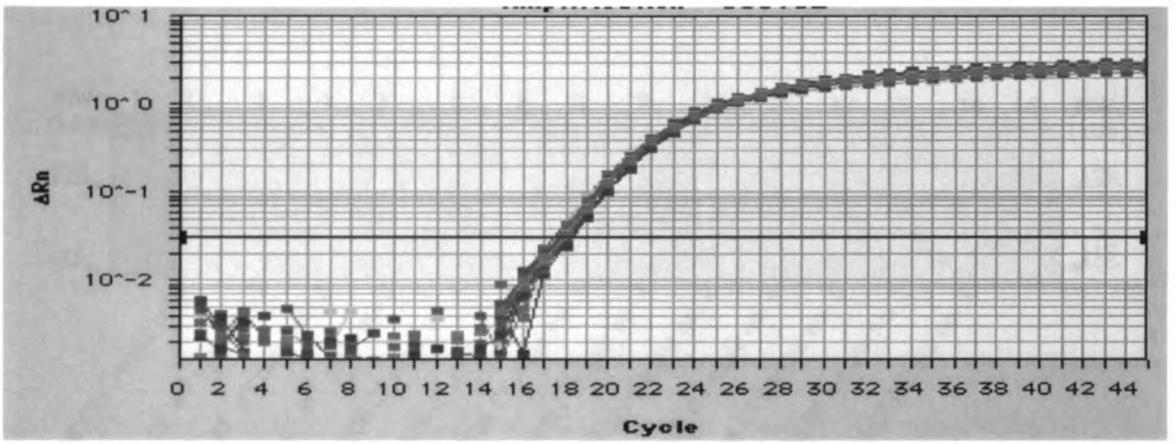

Figure 6.16 Amplification plot of *gapdh* from six CF wild type and six ΔF508 CF mice kidney RNAs

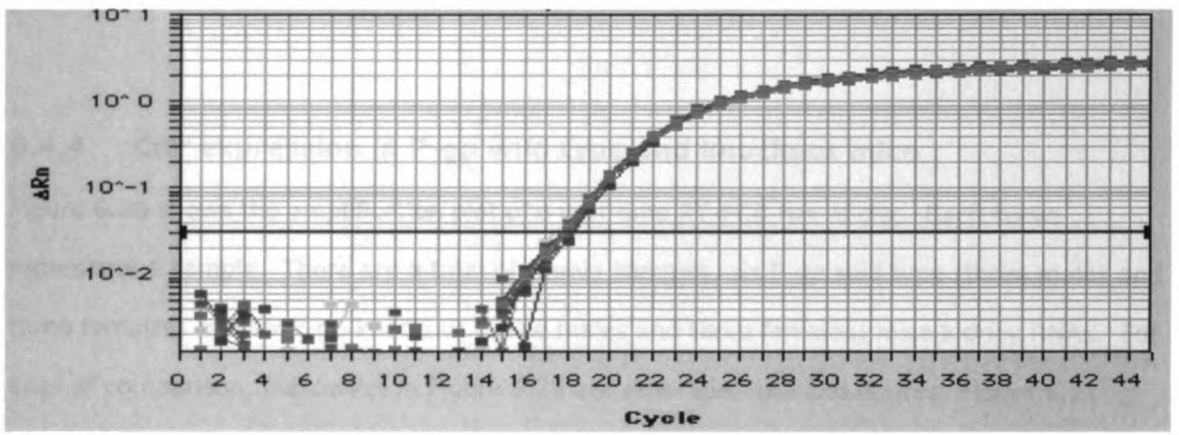

Figure 6.17 Amplification plot of *gapdh* from six CF wild type mice kidney RNAs

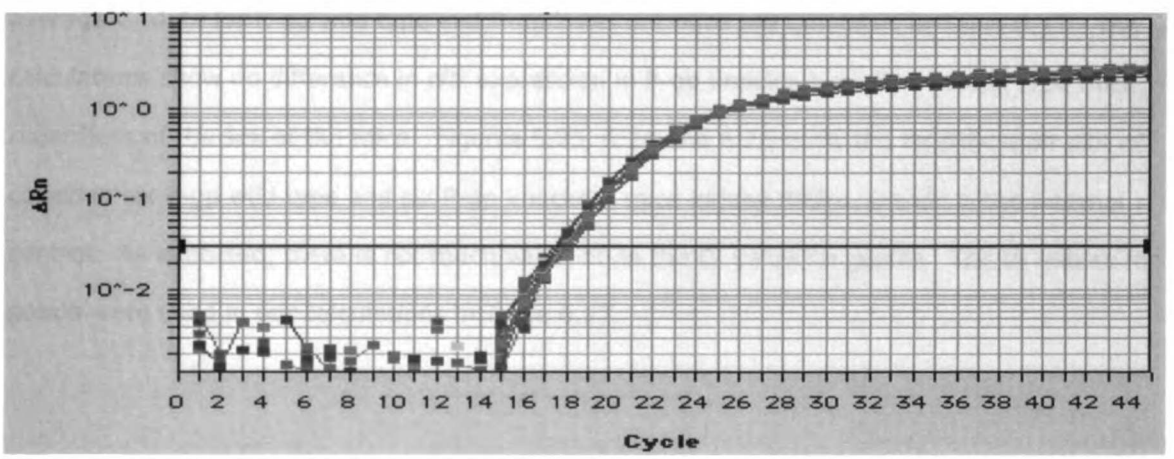

Figure 6.18 Amplification plot of *gapdh* from six CF ΔF508 mice kidney RNAs

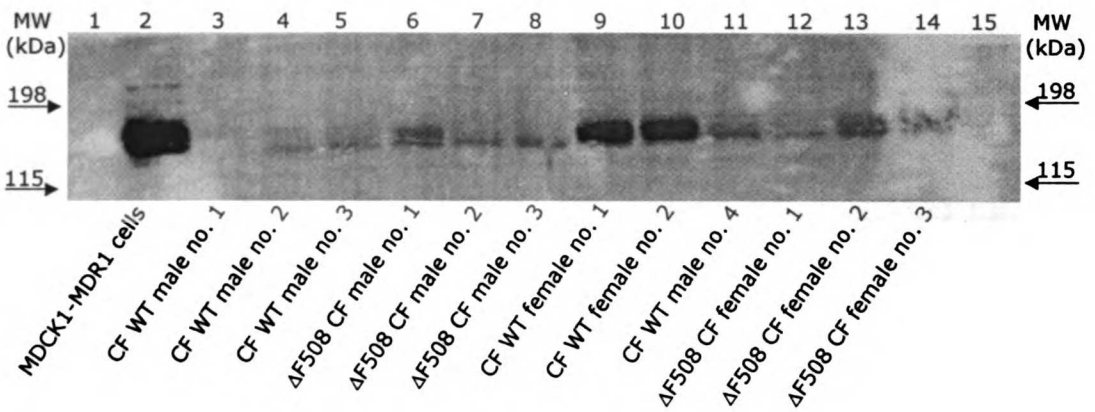

Figure 6.19 Western blot of P-gp in six CF wild type and six ΔF508 CF mice kidneys. The total protein loaded in each lane is 100 μg. MDCK1-MDR1 cells is our positive control. Lanes 1 and 15 were loaded with BioRad prestained SDS-PAGE broad range standard.

6.4.4 *Cftr* expression in P-gp wild type and knockout mice

Figure 6.20 shows the amplification plot of a real-time RT-PCR run of *cftr*. Each curve represents a sample. There are a total of twelve samples, six P-gp wild type (three males and three females) and six P-gp knockout (three males and three females) mice kidney RNAs. For ease of comparison, the curves in Figure 6.20 are separated into two figures: Figure 6.21 shows the amplification plot of *cftr* in P-gp wild type while Figure 6.22 shows the amplification plot of *cftr* in P-gp knockout mice. There is not much variation in the C_T value for *cftr* in P-gp wild type and P-gp knockout mice. The C_T value for all the samples is around 26 cycles. The average C_T data for P-gp wild type and P-gp knockout mice are tabulated in Table 6.17. The calculations show no difference in *cftr* expression in P-gp knockout relative to wild type mice, regardless of the sex of the mice. Figures 6.23, 6.24 and 6.25 show the amplification plot of *gapdh* in six P-gp wild type and six P-gp knockout mice kidney RNAs. *Gapdh* is the internal control. As expected, there is not much variation in the C_T value for *gapdh*. The C_T values for *gapdh* were used in our calculations in Table 6.17.

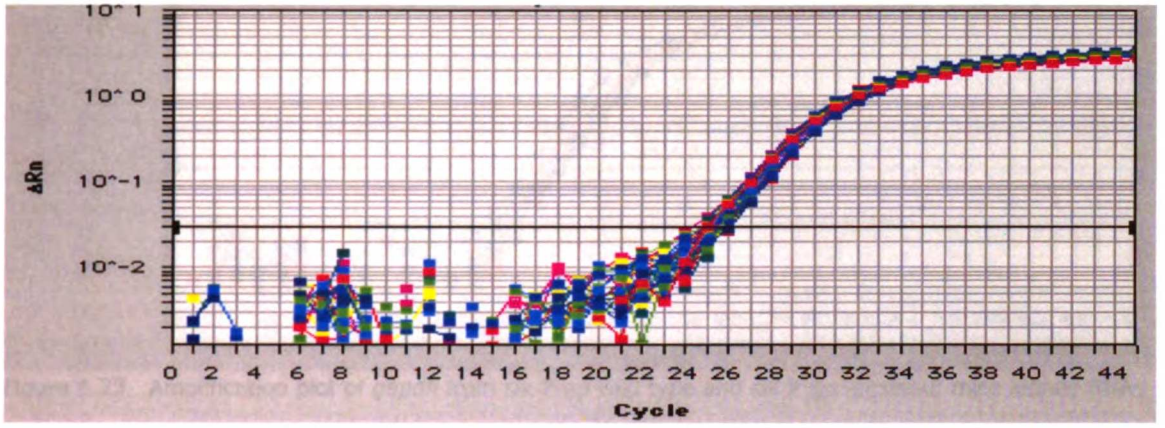

Figure 6.20 Amplification plot of *cftr* from six P-gp wild type and six P-gp knockout mice kidney RNAs

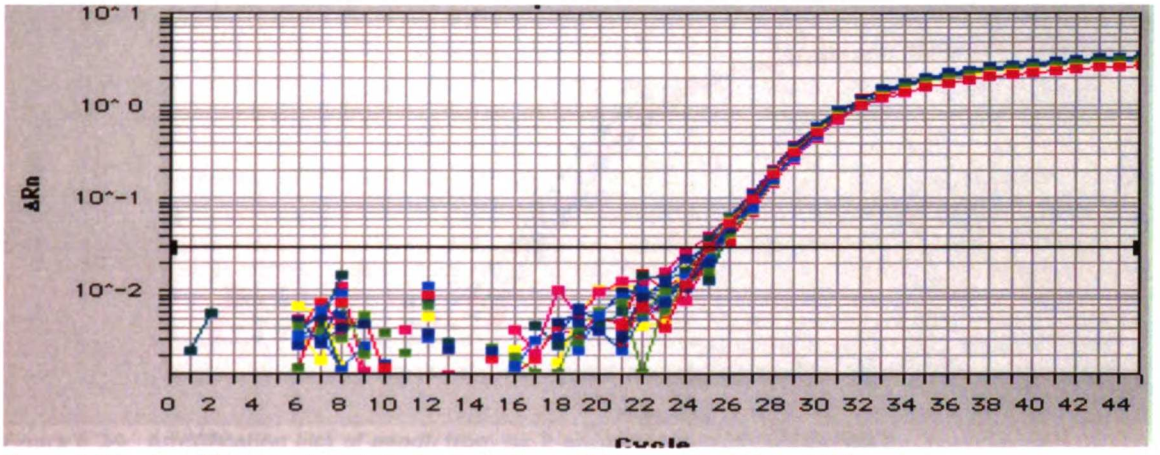

Figure 6.21 Amplification plot of *cftr* from six P-gp wild type mice kidney RNAs

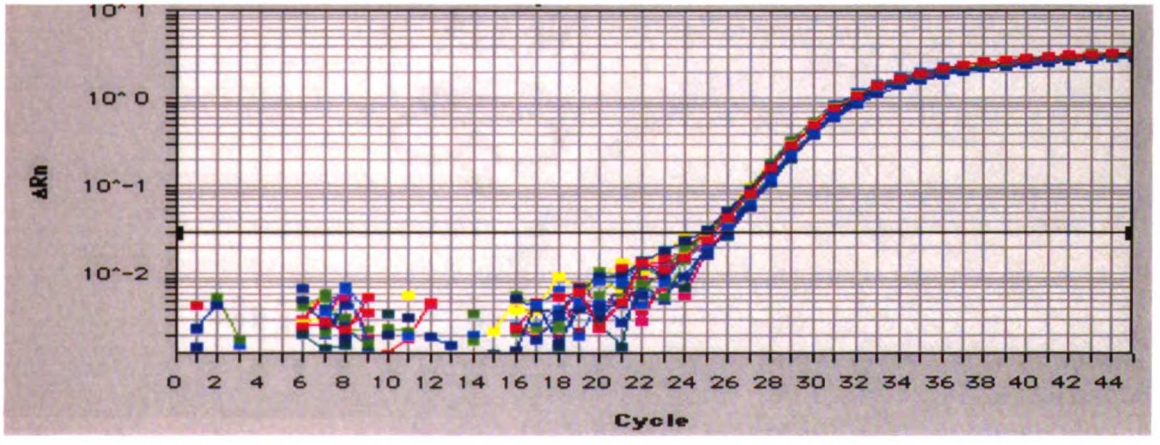

Figure 6.22 Amplification plot of *cftr* from six P-gp knockout mice kidney RNAs

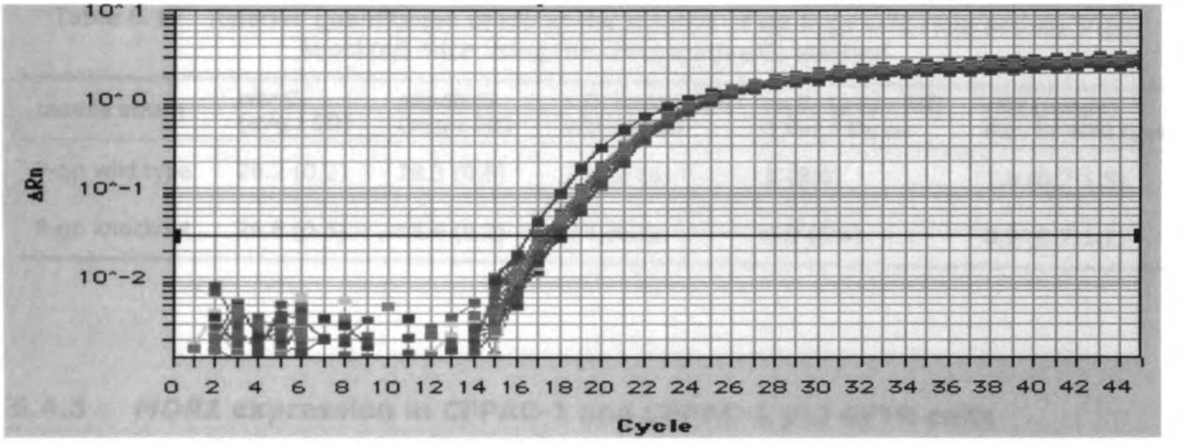

Figure 6.23 Amplification plot of *gapdh* from six P-gp wild type and six P-gp knockout mice kidney RNAs

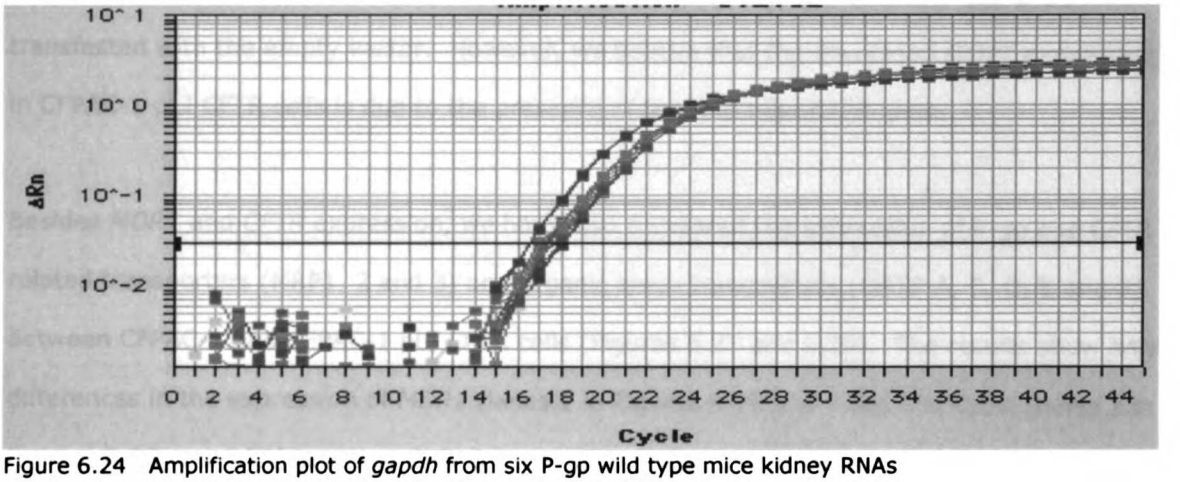

Figure 6.24 Amplification plot of *gapdh* from six P-gp wild type mice kidney RNAs

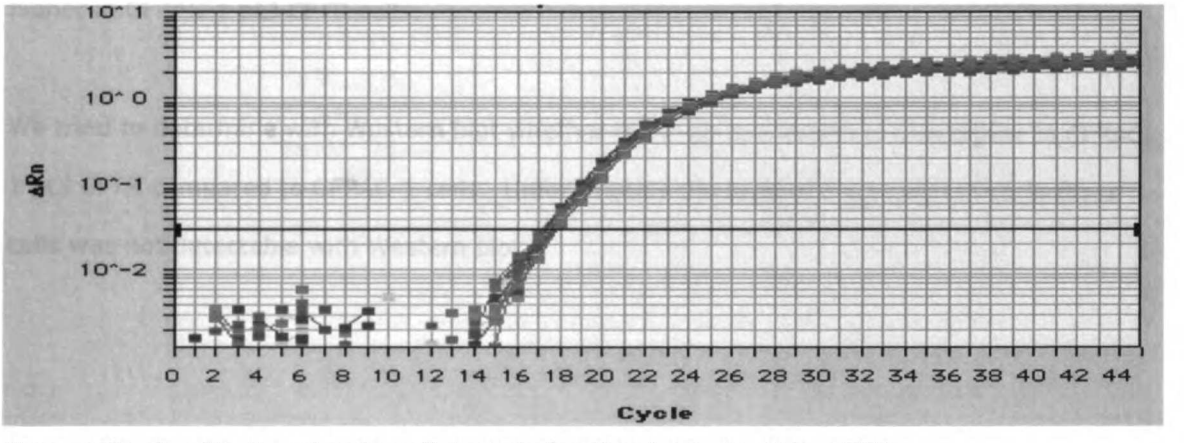

Figure 6.25 Amplification plot of *gapdh* from six P-gp knockout mice kidney RNAs

Table 6.17 Relative quantitation of *cftr* in the kidneys of six P-gp wild type and six P-gp knockout mice using the comparative C_T method

mouse strain	*cftr* C_T (avg ± SD)	*gapdh* C_T (avg ± SD)	Δ C_T (avg ± SD) *cftr-gapdh*	ΔΔ C_T (avg ± SD) Δ C_T - Δ $C_{T,\ WT}$	*cftr* (range) Rel. to wild type
P-gp wild type	26.2 (0.2)	18.3 (0.6)	7.9 (0.6)	0 (0.6)	1.0 (0.7-1.5)
P-gp knockout	26.6 (0.3)	18.4 (0.2)	8.1 (0.4)	0.2 (0.4)	0.9 (0.7-1.2)

6.4.5 *MDR1* expression in CFPAC-1 and CFPAC-1 pLJ CFTR cells

Figure 6.26 shows the results of semi-quantitative RT-PCR of *MDR1* in CFPAC-1 and CFPAC-1 pLJ CFTR cells. As expected from our hypothesis, there is a higher expression of *MDR1* mRNA in CFPAC-1 compared to CFPAC-1 pLJ CFTR cells. We do not have the control cell line transfected with the empty vector. However, we believe that the decreased *MDR1* expression in CFPAC-1 pLJ CFTR cells is due to the presence of the wild type *CFTR* gene.

Besides *MDR1* and *CFTR* expression, we have also compared the expression of P-gp and CFTR related transporters (MRP1, 2 and 3) and organic anion transporters (OATP-A, C, D, E and 8) between CFPAC-1 and CFPAC-1 pLJ CFTR cells (Figures 6.27 and 6.28). The results show only differences in the expression of *MDR1* (lanes 1 in Figures 6.27 and 6.28) and *CFTR* (lanes 2 in Figures 6.27 and 6.28) between CFPAC-1 and CFPAC-1 pLJ CFTR cells and no difference is observed with *MRP1, MRP2, MRP3, OATP-C, D, E* and *8*. Expression of *OATP-A* is not detected in these cells. Expression of *MDR1* is higher in CFPAC-1 cells while expression of *CFTR* is higher in CFPAC-1 pLJ CFTR cells.

We tried to determine with Western blot whether the P-gp expression is also higher in CFPAC-1 pLJ CFTR compared to CFPAC-1 cells. Unfortunately the level of P-gp expression in these cells was not detectable with Western blot.

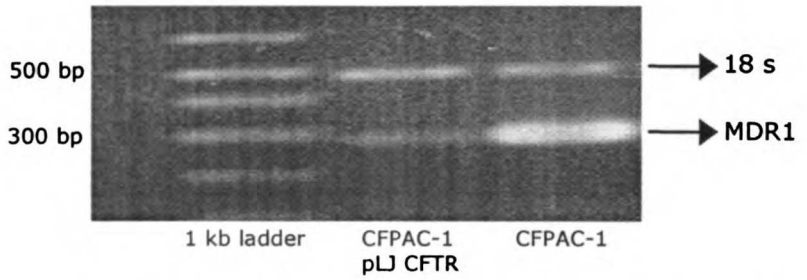

Figure 6.26 Comparison of *MDR1* mRNA expression between CFPAC-1 and CFPAC-1 pLJ CFTR cells.

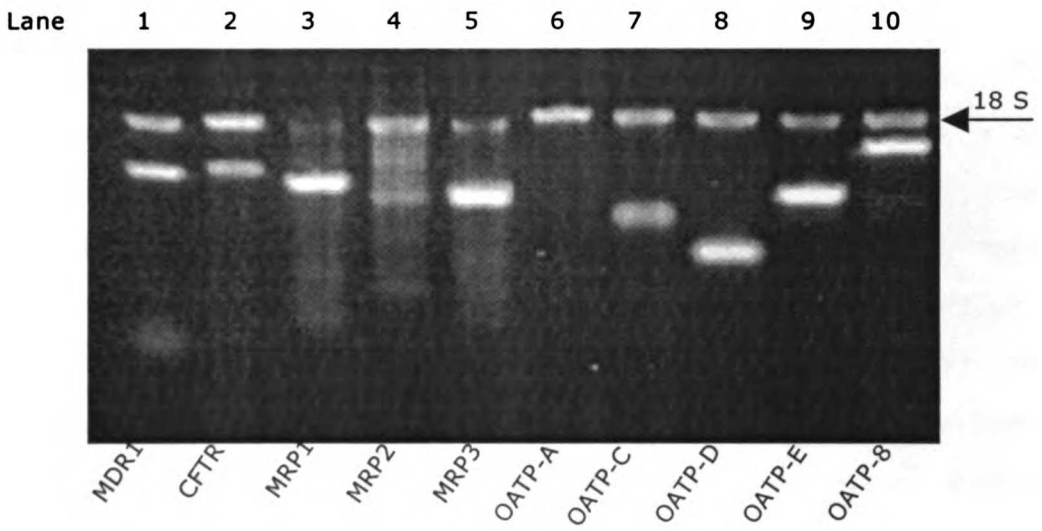

Figure 6.27 Expression of *MDR1, CFTR, MRP1, MRP2, MRP3, OATP-A, OATP-C, OATP-D, OATP-E* and *OATP-8* in CFPAC-1 cells.

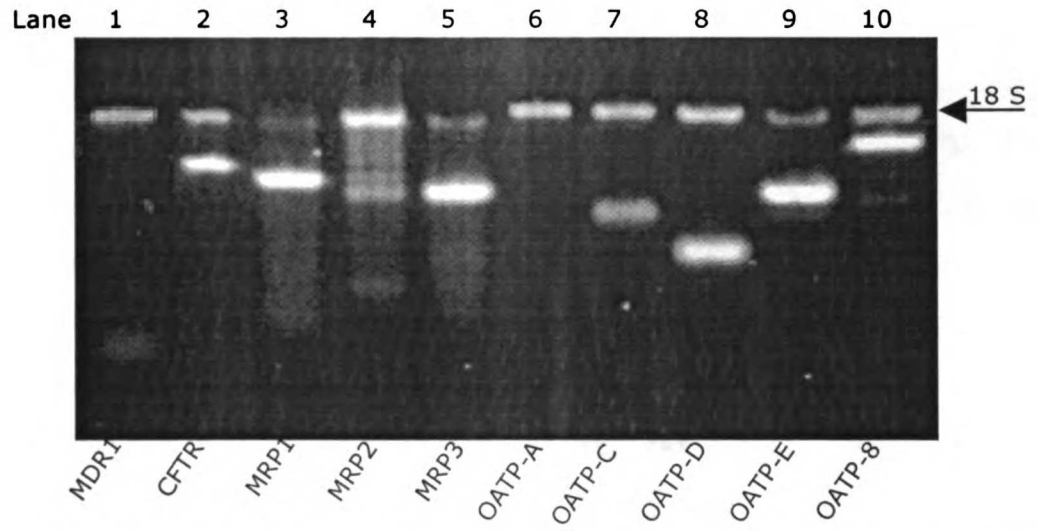

Figure 6.28 Expression of *MDR1, CFTR, MRP1, MRP2, MRP3, OATP-A, OATP-C, OATP-D, OATP-E* and *OATP-8* in CFPAC-1 pLJ CFTR cells.

6.5 Discussion and Conclusions

We hypothesize that P-gp expression is elevated in the kidneys of CF patients and this increase in P-gp expression is responsible for the enhanced renal clearance of some drugs observed in those patients. To test this hypothesis, we utilized a mouse model for cystic fibrosis, the ΔF508 CF mice. This mouse model exhibits similar intestinal but not the lung pathophysiology of CF patients.

We compared the expression of P-gp in the kidneys between CF wild type and the ΔF508 CF mice. Our results show that the expression of P-gp is subject to hormonal regulation. There is a sex-specific difference in P-gp expression. In wild type mice, P-gp expression is much higher in female than male mice. There is 3-fold higher *mdr1a* and 14-fold higher *mdr1b* expression in the kidneys of female than male mice. Our results agree with the reported higher *mdr1b* mRNA expression in the kidneys of female mice (285). To our knowledge, higher *mdr1a* mRNA expression in the kidneys of female mice has not been reported. Western blot results also show a significantly higher expression of P-gp in the kidneys of female wild type mice compared to male wild type mice. This higher expression of P-gp in the female mice is consistent with the reported finding of higher P-gp expression (~40%) in the livers of female rats (361). It is the opposite of the reported finding in humans (116). Men have a 2.5-fold higher expression of P-gp in their livers compared to women (116).

In ΔF508 CF mice, the sex-specific difference in P-gp expression is abolished. RT-PCR and Western blot results show a similar level of P-gp expression between male and female ΔF508 CF mice. However, there is a difference in P-gp expression between wild type and ΔF508 CF mice. Both *mdr1a* and *mdr1b* expression are decreased by approximately sixty and seventy percent, respectively, in female ΔF508 CF compared to female CF wild type mice. The Western blot results also show a decreased P-gp protein expression in female ΔF508 CF compared to female CF wild type mice. On the other hand, both *mdr1a* and *mdr1b* expression are increased by approximately fifty and three hundred sixty percent, respectively, in male ΔF508 CF compared to male CF wild type mice. The Western blot results also show a higher

expression of P-gp in male ΔF508 CF compared to male CF wild type mice, although the difference observed is smaller compared to the RT-PCR results.

The different effects of loss of *cftr* protein on P-gp expression in male and female ΔF508 CF mice could be due to a hormonal mechanism that leads to opposite effects in male and female mice. Our group has reported the sex effect of dexamethasone in rats (361). P-gp expression was increased and decreased by 500% and 60%, respectively, in the liver of male and female rats with dexamethasone (361). Jancis *et al.* (381) reported that estradiol regulated P-gp expression in rat pituitary tumor cells. Lee *et al.* (382) reported that estrogen and progesterone upregulated mouse *mdr* gene expressions. P-gp expression is also reported to be regulated by temporal and spatial mechanisms. P-gp expression is not detected in the fetus but it is detectable 1 month postnatally (381). P-gp is expressed differently in various tissues. *Mdr1a* is the predominant P-gp gene in mouse liver, intestine and brain tissues while *mdr1b* is the predominant P-gp gene in the kidneys, adrenal glands and in the uterus of pregnant mice (285). It would be interesting to see if other tissues beside kidneys exhibit the sex effect of P-gp expression due to defects in the *cftr* gene.

Trezise *et al.* (93) reported a 4-fold increase in *mdr1* expression in the intestines of neonatal and 3-4 week-old $Cftr^{tm1CAM}$ mice (a null knockout mice). They also reported a 3-fold decrease in *mdr1* expression in the intestines of 10-week-old $Cftr^{tm1CAM}$ mice. However, they did not report the sex of the mice used in their studies. Our results in the kidneys of adult ΔF508 CF mice show that, depending on the sex of the mice, P-gp expression might increase or decrease compared to the wild type mice. Further studies need to be performed to determine if neonatal and young ΔF508 CF mice also show a sex difference in P-gp expression in the kidneys.

We are interested in whether P-gp expression is elevated in CF patients due to defects in their *CFTR* gene. CFPAC-1 is a pancreas cell line from a male patient with the ΔF508 mutation and CFPAC-1 pLJ CFTR is the resulting cell line from CFPAC-1 cells transfected with wild type *CFTR* gene. We observe that in the presence of wild type *CFTR* gene, *MDR1* expression is decreased

while the expression of *MRP1, 2* and *3* and *OATP-C, D, E* and *8* were not changed. These results agree with the hypothesis that P-gp expression might be upregulated in the kidneys of CF patients due to defects in their *CFTR* gene. The exact mechanism of P-gp regulation by the *CFTR* gene is unknown. It could be related to the function of P-gp as the regulator of an unidentified cell-swelling activated chloride channel. Shumaker *et al.* (383) reported that the expression of NKCC1 (Na^+-K^+-Cl^- cotransporter) was increased two-fold in CFPAC-1 cells containing the wild type *CFTR* gene compared to CFPAC-1 cells. This is the opposite of the observed effect with P-gp.

Breuer *et al.* (94) and Trezise *et al.* (92) reported the inverse pattern of *CFTR* and *MDR1* regulation at the protein and mRNA levels, respectively. Increased *MDR1* expression is associated with decreased *CFTR* expression and vice versa. We investigated whether *cftr* expression is increased in the kidneys of P-gp knockout mice, where P-gp expression is absent. Our RT-PCR results show no difference in the expression of *cftr* between P-gp wild type and knockout mice, regardless of the sex of the mice. This result in the kidneys is consistent with the reported findings by Schinkel *et al.* (285) in the lung, jejunum, colon and liver of P-gp wild type and knockout mice. Our results indicate that the coordinate-regulation of P-gp and *CFTR* are not necessarily both ways. A defect in the *cftr* gene (the ΔF508 mutation) affects P-gp expression in the kidneys of ΔF508 CF mice while no change in *cftr* expression is observed between kidneys of P-gp wild type and knockout mice.

Trezise *et al.* (92) reported complementary expression of *cftr* and *mdr1* in the rat intestine and pancreas and in the uterus (a switch in predominantly *cftr* expression in the uterus of non-pregnant rats to predominantly *mdr1* expression in the uterus of pregnant rats). However, lack of complementary expressions of *CFTR* and *MDR1* genes was reported in human placenta (384). Both C *CFTR* and *MDR1* are expressed in syncytiotropoblast and cytotropoblast cells. Johannesson *et al.* (384) reported no variation in *cftr* and *mdr1* expression in the lung during pregnancy. These data show that coordinate-regulation of *CFTR* and *MDR1* expression is not consistent across various tissues.

To conclude, there is a higher basal P-gp expression in the kidneys of female compared to male wild type mice and P-gp expression is changed in ΔF508 CF mice compared to wild type mice. P-gp expression is decreased in female and increased in the kidneys of male ΔF508 CF mice, resulting in similar P-gp expression in male and female ΔF508 CF mice. Overall, there is a small net increase in P-gp expression in the kidneys of ΔF508 CF mice, agreeing with our hypothesis that P-gp expression might be upregulated in CF patients, which could be responsible for the observed higher renal clearance of drugs. It is not known whether the same phenomena also occurs in the human kidneys and other tissues. If human kidneys parallel mice kidneys and if P-gp plays a significant role in urinary excretion, we expect to see higher renal clearance of P-gp substrates in men *vs.* women and no difference is expected between male and female CF patients. We also expect to see lower and higher renal clearance in female and male CF patients, respectively, compared to healthy women and men.

Chapter 7

Summary and Future Directions

7.1 Summary

The overall goal of my thesis research was to determine if P-gp plays a role in enhancing the renal clearance of several drugs in CF patients. We hypothesized that the enhanced renal clearance of drugs observed in CF patients was due to increased P-gp expression in those patients, which in turn caused increased renal clearance of drugs that are substrates of P-gp. If this hypothesis was proven correct, we may adjust the dose given to CF patients based on whether or not the drug is a substrate of P-gp (Chapter 1).

Our hypothesis stated that enhanced renal clearance of some antibiotics observed in cystic fibrosis patients is due to elevated P-gp expression in those patients. Accordingly, antibiotics that showed enhanced renal clearance in CF patients should be substrates of P-gp while those that did not should not be substrates of P-gp. Therefore we determined if antibiotics that had a higher renal clearance in CF patients are indeed substrates of P-gp and whether those that did not, are not substrates of P-gp. This was achieved by running bidirectional transport studies using control and P-gp overexpressing cell lines grown in a monolayer. We tested *in vitro* whether dicloxacillin, trimethoprim, sulfamethoxazole, N4-acetylsulfamethoxazole, iothalamate, cefsulodin and ciprofloxacin are substrates of P-gp. Dicloxacillin, trimethoprim and ciprofloxacin showed enhanced active renal clearance while sulfamethoxazole, iothalamate and cefsulodin did not show enhanced active renal clearance in CF patients. We demonstrated with bidirectional transport and inhibition studies in MDCK1 and MDCK1-MDR1 cells that dicloxacillin, trimethoprim and ciprofloxacin are substrates of P-gp while sulfamethoxazole, N4-acetylsulfamethoxazole, iothalamate and cefsulodin are not substrates of P-gp. Our bidirectional transport studies showed that the B→A/A→B ratios in MDCK1-MDR1 cells for dicloxacillin, trimethoprim and ciprofloxacin were significantly greater than 1, with average

values of 20, 55 and 14, respectively, values that were very different from the ratios in MDCK1 cells (~1). Sulfamethoxazole, N4-acetylsulfamethoxazole, iothalamate and cefsulodin, on the other hand, showed no difference in B→A/A→B ratios (all ~1). This suggests that dicloxacillin, trimethoprim and ciprofloxacin are substrates of P-gp while sulfamethoxazole, N4-acetylsulfamethoxazole, iothalamate and cefsulodin are not. Inhibition studies with P-gp and non-P-gp inhibitors further reinforced this conclusion. P-gp inhibitors (e.g., cyclosporine, ketoconazole, vinblastine, GG918) decreased the B→A flux of dicloxacillin, trimethoprim and ciprofloxacin and increased the A→B flux of trimethoprim and ciprofloxacin in MDCK1-MDR1 cells, bringing the B→A/A→B ratios to about 1. We also discovered that ciprofloxacin, besides being a substrate of P-gp, is also a substrate of an unidentified absorptive transporter. This could partly explain the conflicting renal clearance values observed in CF patients. The renal clearance of ciprofloxacin may depend on the relative expression of P-gp and this transporter that works in the opposite direction of P-gp (Chapter 2).

The results from our first specific aim, the *in vitro* bidirectional transport studies, appeared to support the hypothesis that P-gp may be responsible for enhanced renal clearance in CF patients. Therefore, we proceeded with our second specific aim, where we performed *in vivo* pharmacokinetic studies to determine if the amount of P-gp expression affects the renal clearance values of antibiotics that are substrates of the P-gp. The results showed no correlation between P-gp expression and renal clearance values of the P-gp substrates, trimethoprim and ciprofloxacin, in mice (Chapter 4). Inhibition study results in rats with a P-gp inhibitor, GG918, agree with the data from P-gp knockout mice. GG918 had no effect on the disposition of trimethoprim and ciprofloxacin in rats (Chapter 5). These data suggest that P-gp does not play a role in the renal clearance of trimethoprim and ciprofloxacin in mice. However, it does not preclude the possibility that P-gp is important in the renal elimination of trimethoprim and ciprofloxacin in humans.

For our third specific aim, we investigated whether there is a difference in P-gp expression in the kidneys of CF wild type and ΔF508 CF mice and in the *cftr* expression in the kidneys of P-

gp wild type and knockout mice. In addition, we also compared the expression level of P-gp between CFPAC-1 and CFPAC-1 pLJ CFTR cells.

The results in the kidneys of CF wild type and ΔF508 CF mice showed that the expression of P-gp is subject to hormonal regulation. There is a sex-specific difference in P-gp expression. In wild type mice, P-gp expression was much higher in female than male mice. There was 3-fold higher *mdr1a* and 14-fold higher *mdr1b* expression in the kidneys of female compared to male mice. In ΔF508 CF mice, the sex-specific difference in P-gp expression was abolished. RT-PCR and Western blot results showed a similar level of P-gp expression between male and female ΔF508 CF mice. However, there was a difference in P-gp expression between wild type and ΔF508 CF mice. Both *mdr1a* and *mdr1b* expression were decreased by approximately 60% and 70%, respectively, in female ΔF508 CF compared to female CF wild type mice. This result was opposed to our hypothesis that P-gp expression might be increased in the kidneys of CF patients. On the other hand, both the *mdr1a* and *mdr1b* expression were increased by approximately 50% and 360%, respectively, in male ΔF508 CF compared to male CF wild type mice. The combined overall effect in the kidneys of male and female ΔF508 CF mice is a two-fold increase in *mdr1b* expression. This agrees with our hypothesis that P-gp expression might be increased in the kidneys of CF patients. The results in the kidneys of P-gp wild type and P-gp knockout mice showed no difference in the expression of *cftr* between P-gp wild type and P-gp knockout mice, regardless of the sex of the mice (Chapter 6).

The results in the CFPAC-1 and CFPAC-1 pLJ CFTR cells showed that in the presence of wild type *CFTR*, *MDR1* expression was significantly decreased while the expression of *MRP1, 2* and *3* and *OATP-C, D, E* and *8* were not changed. This result agrees with the hypothesis that P-gp expression might be upregulated in the kidneys of CF patients due to defects in their *CFTR* gene (Chapter 6).

7.2 Future Directions

The results of these studies do not conclusively show that P-gp is or is not responsible for the enhanced renal clearance of drugs observed in CF patients. The results of the *in vivo*

pharmacokinetic studies in mice showed no correlation between P-gp expression and renal clearance values of two P-gp substrates, trimethoprim and ciprofloxacin. However, this lack of correlation in mice does not necessarily mean that P-gp is not important in the renal clearance of trimethoprim and ciprofloxacin in humans. Species-differences are reported for P-gp.

In order to conclusively determine whether P-gp plays a role in enhancing the renal clearance of drugs in CF patients, a clinical study needs to be performed in CF patients with a specific P-gp inhibitor to determine if the P-gp inhibitor will decrease the observed enhanced renal clearance in those patients. This study is not currently feasible because there is no specific P-gp inhibitor yet approved by the FDA. Since in humans, trimethoprim, ciprofloxacin and dicloxacillin are extensively excreted unchanged, it would be possible to test the effects of a nonspecific inhibitor of P-gp, such as quinidine, on renal clearance of these drugs in CF patients.

Another possibility is to perform a clinical study in healthy volunteers with a drug that can induce P-gp expression in the kidneys to see if higher P-gp expression leads to higher renal clearance of drugs that are substrates of P-gp. The potential problem with this study is determining whether P-gp expression is induced since kidney biopsy is a very invasive procedure. If the renal clearance of P-gp substrates are higher after the induction study then we can assume that P-gp expression is elevated. However, if no change in renal clearance is observed, we cannot conclusively determine that P-gp is not important in the renal clearance without determining whether P-gp expression is changed. Another potential problem is the difficulty in observing the increase in renal clearance. The expected change with inhibition studies are more pronounced than induction studies.

Another study that could be performed is to compare the expression of P-gp in the kidneys of normal *vs.* CF patients to determine if P-gp expression is higher in CF patients. We observe that P-gp expression is decreased in the kidneys of female ΔF508 CF mice while it is increased in male ΔF508 compared to CF wild type mice. Unfortunately we do not have access to kidneys from human CF cadavers. It would be interesting to see if P-gp expression is indeed

higher in the kidneys of CF patients and whether there is a sex difference in the kidney expression of P-gp, as was observed in the kidneys of mice and the livers of rats and humans.

We hypothesize that P-gp expression is higher in CF patients due to defects in their *CFTR* gene. However, it is also possible that they might have higher expression of P-gp due to their repeated exposure to drugs. Due to their disease, CF patients take many antibiotics as well as pancreatic enzymes, vitamins and other drugs. It has been shown in tumor cells and in mice that chemotherapeutic agents can induce P-gp expression. For example, Gustafson and Long (385) reported that repeated exposure of female Balb/c mice to doxorubicin leads to ~20% increase in P-gp expression in the liver and kidney of these mice. Demeule *et al.* (386) reported that a single subcutaneous administration of cisplatin leads to greater than 200-300% increase in P-gp expression in rat renal brush border membrane and in crude membranes from liver and intestine. Cotrimazole, a combination of trimethoprim and sulfamethoxazole prescribed for *B. cepacia* treatment in CF patients, has been shown to activate PXR (Pregnane X Receptor). Activation of PXR induces the expression of P-gp (387). We could perform a study in mice to determine whether repeated exposure to antibiotics that are commonly taken by CF patients could induce P-gp expression in the kidneys of those mice.

In conclusion, the cause of the enhanced renal clearance of drugs in CF patients remains unknown. More research will need to be performed to answer the question and in determining whether P-gp could be responsible for the observed enhanced renal clearance in CF patients.

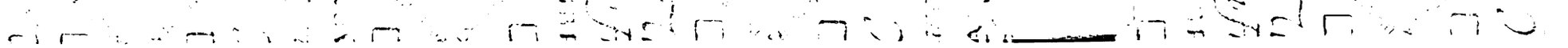

References

1. M. Welsh, B. Ramsey, F. Accurso, and G. Cutting. Cystic fibrosis. In C. Scriver, A. Beaudet, D. Valle, and W. Sly (eds.), *The Metabolic and Molecular Bases of Inherited Disease*, McGraw-Hill, New York, 2001, pp. 5121-88.
2. R. Busch. On the history of cystic fibrosis. *Acta Univ Carol [Med] (Praha)* **36**: 13-5 (1990).
3. G. Fanconi, E. Uehlinger, and C. Knauer. Das coeliakiesyndrom bei angeborener zysticher pankreasfibromatose und bronchiectasien. *Wiener Klin. Wochen.* **86**: 753 (1936).
4. P. M. Quinton. Physiological basis of cystic fibrosis: a historical perspective. *Physiol Rev* **79**: S3-S22 (1999).
5. D. Anderson. Cystic fibrosis of the pancreas and its relationship to celiac disease: Clinical and pathologic study. *Am J Dis Child* **56**: 344-99 (1938).
6. S. Farber. Some organic digestive disturbances in early life. *J Mich State Med Soc* **44**: 587-94 (1945).
7. D. H. Anderson and R. G. Hodges. Celiac Syndrome. V. Genetics of cystic fibrosis of the pancreas with a consideration of etiology. *Am J Dis Child* **72**: 62-80 (1946).
8. P. A. Di Sant 'Agnese, R. C. Darling, G. A. Perera, and E. Shea. Abnormal electrolyte composition of sweat in cystic fibrosis of the pancreas. *Pediatrics* **12**: 549-63 (1953).
9. B. Kerem, J. M. Rommens, J. A. Buchanan, D. Markiewicz, T. K. Cox, A. Chakravarti, M. Buchwald, and L. C. Tsui. Identification of the cystic fibrosis gene: genetic analysis. *Science* **245**: 1073-80 (1989).
10. J. R. Riordan, J. M. Rommens, B. Kerem, N. Alon, R. Rozmahel, Z. Grzelczak, J. Zielenski, S. Lok, N. Plavsic, J. L. Chou, M. L. Drumm, M. C. Iannuzzi, F. S. Collins, and L. C. Tsui. Identification of the cystic fibrosis gene: cloning and characterization of complementary DNA. *Science* **245**: 1066-73 (1989).
11. J. M. Rommens, M. C. Iannuzzi, B. Kerem, M. L. Drumm, G. Melmer, M. Dean, R. Rozmahel, J. L. Cole, D. Kennedy, N. Hidaka, M. Zsiga, M. Buchwald, J. R. Riordan, L.

C. Tsui, F. S. Collins, M. L. Drumm, B. Kerem, and M. C. Iannuzzi. Identification of the cystic fibrosis gene: chromosome walking and jumping. *Science* **245**: 1059-65 (1989).

12. http://www.gene.ucl.ac.uk/nomenclature/.

13. M. P. Anderson, R. J. Gregory, S. Thompson, D. W. Souza, S. Paul, R. C. Mulligan, A. E. Smith, and M. J. Welsh. Demonstration that CFTR is a chloride channel by alteration of its anion selectivity. *Science* **253**: 202-5 (1991).

14. M. P. Anderson, D. P. Rich, R. J. Gregory, A. E. Smith, and M. J. Welsh. Generation of cAMP-activated chloride currents by expression of CFTR. *Science* **251**: 679-82 (1991).

15. C. E. Bear, C. H. Li, N. Kartner, R. J. Bridges, T. J. Jensen, M. Ramjeesingh, and J. R. Riordan. Purification and functional reconstitution of the cystic fibrosis transmembrane conductance regulator (CFTR). *Cell* **68**: 809-18 (1992).

16. M. L. Drumm, D. J. Wilkinson, L. S. Smit, R. T. Worrell, T. V. Strong, R. A. Frizzell, D. C. Dawson, and F. S. Collins. Chloride conductance expressed by delta F508 and other mutant CFTRs in Xenopus oocytes. *Science* **254**: 1797-9 (1991).

17. N. Kartner, J. W. Hanrahan, T. J. Jensen, A. L. Naismith, S. Z. Sun, C. A. Ackerley, E. F. Reyes, L. C. Tsui, J. M. Rommens, C. E. Bear, and J. R. Riordan. Expression of the cystic fibrosis gene in non-epithelial invertebrate cells produces a regulated anion conductance. *Cell* **64**: 681-91 (1991).

18. J. A. Tabcharani, X. B. Chang, J. R. Riordan, and J. W. Hanrahan. Phosphorylation-regulated Cl- channel in CHO cells stably expressing the cystic fibrosis gene. *Nature* **352**: 628-31 (1991).

19. M. Mall, M. Bleich, J. Kuehr, M. Brandis, R. Greger, and K. Kunzelmann. CFTR-mediated inhibition of epithelial Na+ conductance in human colon is defective in cystic fibrosis. *Am J Physiol* **277**: G709-16 (1999).

20. M. Mall, A. Hipper, R. Greger, and K. Kunzelmann. Wild type but not deltaF508 CFTR inhibits Na+ conductance when coexpressed in Xenopus oocytes. *FEBS Lett* **381**: 47-52 (1996).

21. M. Mall, K. Kunzelmann, A. Hipper, A. E. Busch, and R. Greger. cAMP stimulation of CFTR-expressing Xenopus oocytes activates a chromanol-inhibitable K+ conductance. *Pflugers Arch* **432**: 516-22 (1996).

22. K. Kunzelmann and R. Schreiber. CFTR, a regulator of channels. *J Membr Biol* **168**: 1-8 (1999).

23. K. Kunzelmann, R. Schreiber, and A. Boucherot. Mechanisms of the inhibition of epithelial Na(+) channels by CFTR and purinergic stimulation. *Kidney Int* **60**: 455-61 (2001).

24. J. Konig, R. Schreiber, T. Voelcker, M. Mall, and K. Kunzelmann. The cystic fibrosis transmembrane conductance regulator (CFTR) inhibits ENaC through an increase in the intracellular Cl^- concentration. *EMBO Rep* **2**: 1047-51 (2001).

25. R. Greger. Role of CFTR in the colon. *Annu Rev Physiol* **62**: 467-91 (2000).

26. C. M. McNicholas, W. Wang, K. Ho, S. C. Hebert, and G. Giebisch. Regulation of ROMK1 K+ channel activity involves phosphorylation processes. *Proc Natl Acad Sci U S A* **91**: 8077-81 (1994).

27. R. Schreiber, R. Greger, R. Nitschke, and K. Kunzelmann. Cystic fibrosis transmembrane conductance regulator activates water conductance in Xenopus oocytes. *Pflugers Arch* **434**: 841-7 (1997).

28. R. Schreiber, R. Nitschke, R. Greger, and K. Kunzelmann. The cystic fibrosis transmembrane conductance regulator activates aquaporin 3 in airway epithelial cells. *J Biol Chem* **274**: 11811-6 (1999).

29. M. J. Stutts, B. C. Rossier, and R. C. Boucher. Cystic fibrosis transmembrane conductance regulator inverts protein kinase A-mediated regulation of epithelial sodium channel single channel kinetics. *J Biol Chem* **272**: 14037-40 (1997).

30. R. C. Boucher. Human airway ion transport. Part two. *Am J Respir Crit Care Med* **150**: 581-93 (1994).

31. J. D. Li, A. F. Dohrman, M. Gallup, S. Miyata, J. R. Gum, Y. S. Kim, J. A. Nadel, A. Prince, and C. B. Basbaum. Transcriptional activation of mucin by Pseudomonas aeruginosa lipopolysaccharide in the pathogenesis of cystic fibrosis lung disease. *Proc Natl Acad Sci U S A* **94**: 967-72 (1997).

32. J. J. Smith, S. M. Travis, E. P. Greenberg, and M. J. Welsh. Cystic fibrosis airway epithelia fail to kill bacteria because of abnormal airway surface fluid. *Cell* **85**: 229-36 (1996).

33. J. L. Burns, J. Emerson, J. R. Stapp, D. L. Yim, J. Krzewinski, L. Louden, B. W. Ramsey, and C. R. Clausen. Microbiology of sputum from patients at cystic fibrosis centers in the United States. *Clin Infect Dis* **27**: 158-63 (1998).

34. D. S. Armstrong, K. Grimwood, J. B. Carlin, R. Carzino, A. Olinsky, and P. D. Phelan. Bronchoalveolar lavage or oropharyngeal cultures to identify lower respiratory pathogens in infants with cystic fibrosis. *Pediatr Pulmonol* **21**: 267-75 (1996).

35. P. G. Noone and M. R. Knowles. Standard therapy of cystic fibrosis lung disease. In J.R. Yankaskas and M.R. Knowles (eds.), *Cystic Fibrosis in Adults*, Lippincott-Raven, Philadelphia, 1999, pp. 145.

36. L. Saiman, F. Mehar, W. W. Niu, H. C. Neu, K. J. Shaw, G. Miller, and A. Prince. Antibiotic susceptibility of multiply resistant Pseudomonas aeruginosa isolated from patients with cystic fibrosis, including candidates for transplantation. *Clin Infect Dis* **23**: 532-7 (1996).

37. A. Hamosh, T. M. King, B. J. Rosenstein, M. Corey, H. Levison, P. Durie, L. C. Tsui, I. McIntosh, M. Keston, D. J. Brock, M. Macek, Jr., D. Zemkova, H. Krasnicanova, V. Vavrova, M. Macek, Sr., N. Golder, M. J. Schwarz, M. Super, E. K. Watson, C. Williams, A. Bush, S. M. O'Mahoney, P. Humphries, M. A. DeArce, A. Reis, J. Burger, M. Stuhrmann, J. Schmidtke, U. Wulbrand, T. Dork, B. Tummler, and G. R. Cutting. Cystic fibrosis patients bearing both the common missense mutation Gly----Asp at codon 551 and the delta F508 mutation are clinically indistinguishable from delta F508 homozygotes, except for decreased risk of meconium ileus. *Am J Hum Genet* **51**: 245-50 (1992).

38. P. Kristidis, D. Bozon, M. Corey, D. Markiewicz, J. Rommens, L. C. Tsui, and P. Durie. Genetic determination of exocrine pancreatic function in cystic fibrosis. *Am J Hum Genet* **50**: 1178-84 (1992).

39. W. E. Highsmith, L. H. Burch, Z. Zhou, J. C. Olsen, T. E. Boat, A. Spock, J. D. Gorvoy, L. Quittel, K. J. Friedman, L. M. Silverman, R. C. Boucher, and M. R. Knowles. A novel mutation in the cystic fibrosis gene in patients with pulmonary disease but normal sweat chloride concentrations. *N Engl J Med* **331**: 974-80 (1994).

40. G. F. Vawter and H. Shwachman. Cystic fibrosis in adults: an autopsy study. *Pathol Annu* **14 Pt 2**: 357-82 (1979).

41. E. P. DiMagno, J. R. Malagelada, V. L. Go, and C. G. Moertel. Fate of orally ingested enzymes in pancreatic insufficiency. Comparison of two dosage schedules. *N Engl J Med* **296**: 1318-22 (1977).

42. P. M. Farrell, M. R. Kosorok, A. Laxova, G. Shen, R. E. Koscik, W. T. Bruns, M. Splaingard, and E. H. Mischler. Nutritional benefits of neonatal screening for cystic fibrosis. Wisconsin Cystic Fibrosis Neonatal Screening Study Group. *N Engl J Med* **337**: 963-9 (1997).

43. D. C. Wilson and P. B. Pencharz. Nutrition and cystic fibrosis. *Nutrition* **14**: 792-5 (1998).

44. R. J. Sokol. Fat-soluble vitamins and their importance in patients with cholestatic liver diseases. *Gastroenterol Clin North Am* **23**: 673-705 (1994).

45. R. J. Sokol, M. C. Reardon, F. J. Accurso, C. Stall, M. R. Narkewicz, S. H. Abman, and K. B. Hammond. Fat-soluble vitamins in infants identified by cystic fibrosis newborn screening. *Pediatr Pulmonol Suppl* **7**: 52-5 (1991).

46. S. Lanng. Diabetes mellitus in cystic fibrosis. *Eur J Gastroenterol Hepatol* **8**: 744-7 (1996).

47. S. Lanng, B. Thorsteinsson, J. Nerup, and C. Koch. Diabetes mellitus in cystic fibrosis: effect of insulin therapy on lung function and infections. *Acta Paediatr* **83**: 849-53 (1994).

48. S. Lanng, B. Thorsteinsson, C. Lund-Andersen, J. Nerup, P. O. Schiotz, and C. Koch. Diabetes mellitus in Danish cystic fibrosis patients: prevalence and late diabetic complications. *Acta Paediatr* **83**: 72-7 (1994).

49. S. Lanng, B. Thorsteinsson, F. Pociot, M. O. Marshall, H. O. Madsen, M. Schwartz, J. Nerup, and C. Koch. Diabetes mellitus in cystic fibrosis: genetic and immunological markers. *Acta Paediatr* **82**: 150-4 (1993).

50. S. Lanng, B. Thorsteinsson, J. Nerup, and C. Koch. Influence of the development of diabetes mellitus on clinical status in patients with cystic fibrosis. *Eur J Pediatr* **151**: 684-7 (1992).

51. E. Kerem, M. Corey, B. Kerem, P. Durie, L. C. Tsui, and H. Levison. Clinical and genetic comparisons of patients with cystic fibrosis, with or without meconium ileus. *J Pediatr* **114**: 767-73 (1989).

52. S. Rubinstein, R. Moss, and N. Lewiston. Constipation and meconium ileus equivalent in patients with cystic fibrosis. *Pediatrics* **78**: 473-9 (1986).

53. R. C. Stern, R. J. Izant, Jr., T. F. Boat, R. E. Wood, L. W. Matthews, and C. F. Doershuk. Treatment and prognosis of rectal prolapse in cystic fibrosis. *Gastroenterology* **82**: 707-10 (1982).

54. J. Bartman and B. H. Landing. Morphology of the sweat apparatus in cystic fibrosis. *Am J Clin Pathol* **45**: 455-9 (1966).

55. L. E. Gibson. Iontophoretic sweat test for cystic fibrosis: technical details. *Pediatrics* **39**: 465 (1967).

56. R. Rozmahel, M. Wilschanski, A. Matin, S. Plyte, M. Oliver, W. Auerbach, A. Moore, J. Forstner, P. Durie, J. Nadeau, C. Bear, and L. C. Tsui. Modulation of disease severity in cystic fibrosis transmembrane conductance regulator deficient mice by a secondary genetic factor. *Nat Genet* **12**: 280-7 (1996).

57. J. Zielenski, M. Corey, R. Rozmahel, D. Markiewicz, I. Aznarez, T. Casals, S. Larriba, B. Mercier, G. R. Cutting, A. Krebsova, M. Macek, Jr., E. Langfelder-Schwind, B. C. Marshall, J. DeCelie-Germana, M. Claustres, A. Palacio, J. Bal, A. Nowakowska, C. Ferec, X. Estivill, P. Durie, and L. C. Tsui. Detection of a cystic fibrosis modifier locus for meconium ileus on human chromosome 19q13. *Nat Genet* **22**: 128-9 (1999).

58. J. D. Acton and R. W. Wilmott. Phenotype of CF and the effects of possible modifier genes. *Paediatr Respir Rev* **2**: 332-9 (2001).

59. D. N. Sheppard and M. J. Welsh. Structure and function of the CFTR chloride channel. *Physiol Rev* **79**: S23-45 (1999).

60. J. W. Hanrahan, Z. Kone, C. J. Mathews, J. Luo, Y. Jia, and P. Linsdell. Patch-clamp studies of cystic fibrosis transmembrane conductance regulator chloride channel. *Methods Enzymol* **293**: 169-94 (1998).

61. D. C. Gadsby and A. C. Nairn. Control of CFTR channel gating by phosphorylation and nucleotide hydrolysis. *Physiol Rev* **79**: S77-S107 (1999).

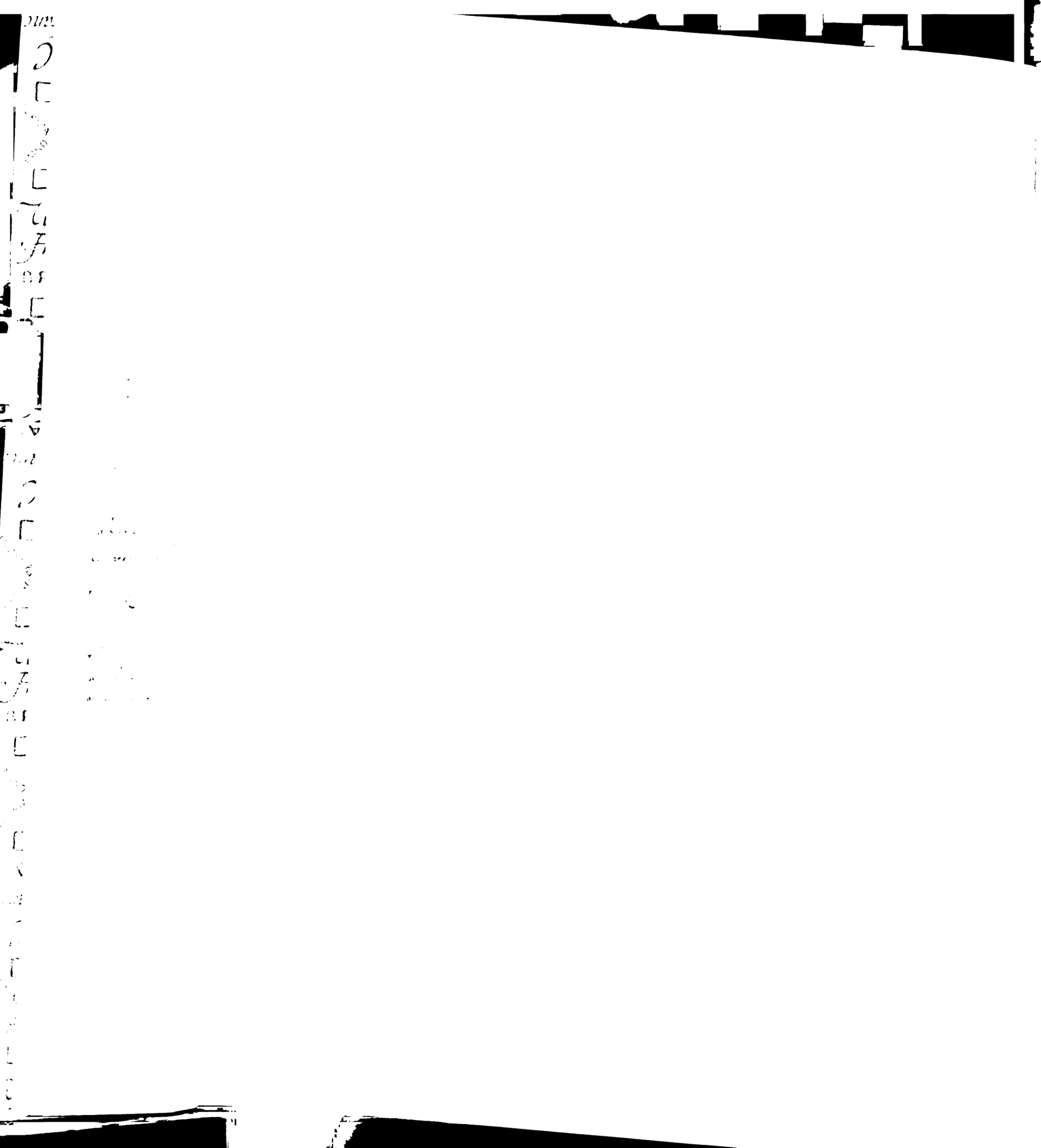

62. D. C. Dawson, S. S. Smith, and M. K. Mansoura. CFTR: mechanism of anion conduction. *Physiol Rev* **79**: S47-75 (1999).

63. www.genet.sickkids.on.ca/cftr/,

64. H. Cuppens, W. Lin, M. Jaspers, B. Costes, H. Teng, A. Vankeerberghen, M. Jorissen, G. Droogmans, I. Reynaert, M. Goossens, B. Nilius, and J. J. Cassiman. Polyvariant mutant cystic fibrosis transmembrane conductance regulator genes. The polymorphic (Tg)m locus explains the partial penetrance of the T5 polymorphism as a disease mutation. *J Clin Invest* **101**: 487-96 (1998).

65. T. Dork, B. Dworniczak, C. Aulehla-Scholz, D. Wieczorek, I. Bohm, A. Mayerova, H. H. Seydewitz, E. Nieschlag, D. Meschede, J. Horst, H. J. Pander, H. Sperling, F. Ratjen, E. Passarge, J. Schmidtke, and M. Stuhrmann. Distinct spectrum of CFTR gene mutations in congenital absence of vas deferens. *Hum Genet* **100**: 365-77 (1997).

66. D. Abeliovich, I. P. Lavon, I. Lerer, T. Cohen, C. Springer, A. Avital, and G. R. Cutting. Screening for five mutations detects 97% of cystic fibrosis (CF) chromosomes and predicts a carrier frequency of 1:29 in the Jewish Ashkenazi population. *Am J Hum Genet* **51**: 951-6 (1992).

67. T. Shoshani, A. Augarten, E. Gazit, N. Bashan, Y. Yahav, Y. Rivlin, A. Tal, H. Seret, L. Yaar, E. Kerem, and B. Kerem. Association of a nonsense mutation (W1282X), the most common mutation in the Ashkenazi Jewish cystic fibrosis patients in Israel, with presentation of severe disease. *Am J Hum Genet* **50**: 222-8 (1992).

68. S. H. Cheng, R. J. Gregory, J. Marshall, S. Paul, D. W. Souza, G. A. White, C. R. O'Riordan, and A. E. Smith. Defective intracellular transport and processing of CFTR is the molecular basis of most cystic fibrosis. *Cell* **63**: 827-34 (1990).

69. S. H. Cheng, S. L. Fang, J. Zabner, J. Marshall, S. Piraino, S. C. Schiavi, D. M. Jefferson, M. J. Welsh, and A. E. Smith. Functional activation of the cystic fibrosis trafficking mutant delta F508-CFTR by overexpression. *Am J Physiol* **268**: L615-24 (1995).

70. M. E. Egan, E. M. Schwiebert, and W. B. Guggino. Differential expression of ORCC and CFTR induced by low temperature in CF airway epithelial cells. *Am J Physiol* **268**: C243-51 (1995).

71. C. Li, M. Ramjeesingh, E. Reyes, T. Jensen, X. Chang, J. M. Rommens, and C. E. Bear. The cystic fibrosis mutation (delta F508) does not influence the chloride channel activity of CFTR. *Nat Genet* **3**: 311-6 (1993).

72. A. L. Brennan and D. M. Geddes. Cystic fibrosis. *Curr Opin Infect Dis* **15**: 175-82 (2002).

73. I. Crawford, P. C. Maloney, P. L. Zeitlin, W. B. Guggino, S. C. Hyde, H. Turley, K. C. Gatter, A. Harris, and C. F. Higgins. Immunocytochemical localization of the cystic fibrosis gene product CFTR. *Proc Natl Acad Sci U S A* **88**: 9262-6 (1991).

74. B. C. Trapnell, C. S. Chu, P. K. Paakko, T. C. Banks, K. Yoshimura, V. J. Ferrans, M. S. Chernick, and R. G. Crystal. Expression of the cystic fibrosis transmembrane conductance regulator gene in the respiratory tract of normal individuals and individuals with cystic fibrosis. *Proc Natl Acad Sci U S A* **88**: 6565-9 (1991).

75. A. E. Trezise and M. Buchwald. In vivo cell-specific expression of the cystic fibrosis transmembrane conductance regulator. *Nature* **353**: 434-7 (1991).

76. N. A. Ameen, T. Ardito, M. Kashgarian, and C. R. Marino. A unique subset of rat and human intestinal villus cells express the cystic fibrosis transmembrane conductance regulator. *Gastroenterology* **108**: 1016-23 (1995).

77. N. A. Ameen, B. Martensson, L. Bourguinon, C. Marino, J. Isenberg, and G. E. McLaughlin. CFTR channel insertion to the apical surface in rat duodenal villus epithelial cells is upregulated by VIP in vivo. *J Cell Sci* **112 (Pt 6)**: 887-94 (1999).

78. E. V. O'Loughlin, D. M. Hunt, T. E. Bostrom, D. Hunter, K. J. Gaskin, A. Gyory, and D. J. Cockayne. X-ray microanalysis of cell elements in normal and cystic fibrosis jejunum: evidence for chloride secretion in villi. *Gastroenterology* **110**: 411-8 (1996).

79. T. V. Strong, K. Boehm, and F. S. Collins. Localization of cystic fibrosis transmembrane conductance regulator mRNA in the human gastrointestinal tract by in situ hybridization. *J Clin Invest* **93**: 347-54 (1994).

80. P. Mylona, J. D. Glazier, S. L. Greenwood, M. K. Sides, and C. P. Sibley. Expression of the cystic fibrosis (CF) and multidrug resistance (MDR1) genes during development and differentiation in the human placenta. *Mol Hum Reprod* **2**: 693-8 (1996).

81. M. Johannesson, N. Bogdanovic, A. C. Nordqvist, L. Hjelte, and M. Schalling. Cystic fibrosis mRNA expression in rat brain: cerebral cortex and medial preoptic area. *Neuroreport* **8**: 535-9 (1997).

82. A. E. Mulberg, L. P. Resta, E. B. Wiedner, S. M. Altschuler, D. M. Jefferson, and D. L. Broussard. Expression and localization of the cystic fibrosis transmembrane conductance regulator mRNA and its protein in rat brain. *J Clin Invest* **96**: 646-52 (1995).

83. A. E. Mulberg, E. B. Wiedner, X. Bao, J. Marshall, D. M. Jefferson, and S. M. Altschuler. Cystic fibrosis transmembrane conductance regulator protein expression in brain. *Neuroreport* **5**: 1684-8 (1994).

84. A. E. Mulberg, R. T. Weyler, S. M. Altschuler, and T. M. Hyde. Cystic fibrosis transmembrane conductance regulator expression in human hypothalamus. *Neuroreport* **9**: 141-4 (1998).

85. M. M. Morales, T. P. Carroll, T. Morita, E. M. Schwiebert, O. Devuyst, P. D. Wilson, A. G. Lopes, B. A. Stanton, H. C. Dietz, G. R. Cutting, and W. B. Guggino. Both the wild type and a functional isoform of CFTR are expressed in kidney. *Am J Physiol* **270**: F1038-48 (1996).

86. M. M. Morales, M. A. Capella, and A. G. Lopes. Structure and function of the cystic fibrosis transmembrane conductance regulator. *Braz J Med Biol Res* **32**: 1021-8 (1999).

87. R. A. Donckerwolcke, R. van Diemen-Steenvoorde, J. van der Laag, H. A. Koomans, and W. H. Boer. Impaired diluting segment chloride reabsorption in patients with cystic fibrosis. *Child Nephrol Urol* **12**: 186-91 (1992).

88. P. Stenvinkel, L. Hjelte, G. Alvan, A. Hedman, E. Hultman, and B. Strandvik. Decreased renal clearance of sodium in cystic fibrosis. *Acta Paediatr Scand* **80**: 194-8 (1991).

89. Y. Okada, S. Oiki, M. Tominaga, M. Kubo, A. Miwa, T. Tominaga, T. Tsumura, and K. Ueda. Volume-sensitive Cl- channel in human epithelial cells: regulation by ATP and relation to P-glycoprotein. *Jpn J Physiol* **47 (Suppl 1)**: S19-20 (1997).

90. T. D. Bond, C. F. Higgins, and M. A. Valverde. P-glycoprotein and swelling-activated chloride channels. *Methods Enzymol* **292**: 359-70 (1998).

91. T. D. Bond, M. A. Valverde, and C. F. Higgins. Protein kinase C phosphorylation disengages human and mouse-1a P-glycoproteins from influencing the rate of activation of swelling-activated chloride currents. *J Physiol* **508 (Pt 2)**: 333-40 (1998).

92. A. E. Trezise, P. R. Romano, D. R. Gill, S. C. Hyde, F. V. Sepulveda, M. Buchwald, and C. F. Higgins. The multidrug resistance and cystic fibrosis genes have complementary patterns of epithelial expression. *EMBO J* **11**: 4291-303 (1992).

93. A. E. Trezise, R. Ratcliff, T. E. Hawkins, M. J. Evans, T. C. Freeman, P. R. Romano, C. F. Higgins, and W. H. Colledge. Co-ordinate regulation of the cystic fibrosis and multidrug resistance genes in cystic fibrosis knockout mice. *Hum Mol Genet* **6**: 527-37 (1997).

94. W. Breuer, I. N. Slotki, D. A. Ausiello, and I. Z. Cabantchik. Induction of multidrug resistance downregulates the expression of CFTR in colon epithelial cells. *Am J Physiol* **265**: C1711-5 (1993).

95. C. F. Higgins. ABC transporters: from microorganisms to man. *Annu Rev Cell Biol* **8**: 67-113 (1992).

96. M. M. Gottesman and S. V. Ambudkar. Overview: ABC transporters and human disease. *J Bioenerg Biomembr* **33**: 453-8 (2001).

97. R. L. Juliano and V. Ling. A surface glycoprotein modulating drug permeability in Chinese hamster ovary cell mutants. *Biochim Biophys Acta* **455**: 152-62 (1976).

98. J. A. Endicott and V. Ling. The biochemistry of P-glycoprotein-mediated multidrug resistance. *Annu Rev Biochem* **58**: 137-71 (1989).

99. P. Borst, A. H. Schinkel, J. J. Smit, E. Wagenaar, L. Van Deemter, A. J. Smith, E. W. Eijdems, F. Baas, and G. J. Zaman. Classical and novel forms of multidrug resistance and the physiological functions of P-glycoproteins in mammals. *Pharmacol Ther* **60**: 289-99 (1993).

100. M. M. Gottesman and I. Pastan. Biochemistry of multidrug resistance mediated by the multidrug transporter. *Annu Rev Biochem* **62**: 385-427 (1993).

101. U. A. Germann. P-glycoprotein--a mediator of multidrug resistance in tumour cells. *Eur J Cancer* **32A**: 927-44 (1996).

102. K. Ueda, D. P. Clark, C. J. Chen, I. B. Roninson, M. M. Gottesman, and I. Pastan. The human multidrug resistance (mdr1) gene. cDNA cloning and transcription initiation. *J Biol Chem* **262**: 505-8 (1987).

103. A. Fojo, R. Lebo, N. Shimizu, J. E. Chin, I. B. Roninson, G. T. Merlino, M. M. Gottesman, and I. Pastan. Localization of multidrug resistance-associated DNA sequences to human chromosome 7. *Somat Cell Mol Genet* **12**: 415-20 (1986).

104. C. R. Fairchild, S. P. Ivy, C. S. Kao-Shan, J. Whang-Peng, N. Rosen, M. A. Israel, P. W. Melera, K. H. Cowan, and M. E. Goldsmith. Isolation of amplified and overexpressed DNA sequences from adriamycin-resistant human breast cancer cells. *Cancer Res* **47**: 5141-8 (1987).

105. D. F. Callen, E. Baker, R. N. Simmers, R. Seshadri, and I. B. Roninson. Localization of the human multiple drug resistance gene, MDR1, to 7q21.1. *Hum Genet* **77**: 142-4 (1987).

106. C. J. Chen, D. Clark, K. Ueda, I. Pastan, M. M. Gottesman, and I. B. Roninson. Genomic organization of the human multidrug resistance (MDR1) gene and origin of P-glycoproteins. *J Biol Chem* **265**: 506-14 (1990).

107. I. B. Roninson, J. E. Chin, K. G. Choi, P. Gros, D. E. Housman, A. Fojo, D. W. Shen, M. M. Gottesman, and I. Pastan. Isolation of human mdr DNA sequences amplified in multidrug-resistant KB carcinoma cells. *Proc Natl Acad Sci U S A* **83**: 4538-42 (1986).

108. D. W. Shen, A. Fojo, J. E. Chin, I. B. Roninson, N. Richert, I. Pastan, and M. M. Gottesman. Human multidrug-resistant cell lines: increased mdr1 expression can precede gene amplification. *Science* **232**: 643-5 (1986).

109. D. W. Shen, A. Fojo, I. B. Roninson, J. E. Chin, R. Soffir, I. Pastan, and M. M. Gottesman. Multidrug resistance of DNA-mediated transformants is linked to transfer of the human mdr1 gene. *Mol Cell Biol* **6**: 4039-45 (1986).

110. P. Gros, J. Croop, I. Roninson, A. Varshavsky, and D. E. Housman. Isolation and characterization of DNA sequences amplified in multidrug-resistant hamster cells. *Proc Natl Acad Sci U S A* **83**: 337-41 (1986).

111. J. A. Silverman. Multidrug-resistance transporters. In G. Amidon and W. Sadée (eds.), *Membrane Transporters as Drug Targets*, Kluwer Academic/Plenum Publishers, New York, 1999, pp. 353-86.

112. P. Borst and A. H. Schinkel. Genetic dissection of the function of mammalian P-glycoproteins. *Trends Genet* **13**: 217-22 (1997).

113. S. E. Devine, A. Hussain, J. P. Davide, and P. W. Melera. Full length and alternatively spliced pgp1 transcripts in multidrug-resistant Chinese hamster lung cells. *J Biol Chem* **266**: 4545-55 (1991).

114. J. E. Chin, R. Soffir, K. E. Noonan, K. Choi, and I. B. Roninson. Structure and expression of the human MDR (P-glycoprotein) gene family. *Mol Cell Biol* **9**: 3808-20 (1989).

115. A. T. Fojo, K. Ueda, D. J. Slamon, D. G. Poplack, M. M. Gottesman, and I. Pastan. Expression of a multidrug-resistance gene in human tumors and tissues. *Proc Natl Acad Sci U S A* **84**: 265-9 (1987).

116. E. G. Schuetz, K. N. Furuya, and J. D. Schuetz. Interindividual variation in expression of P-glycoprotein in normal human liver and secondary hepatic neoplasms. *J Pharmacol Exp Ther* **275**: 1011-8 (1995).

117. C. Cordon-Cardo, J. P. O'Brien, D. Casals, L. Rittman-Grauer, J. L. Biedler, M. R. Melamed, and J. R. Bertino. Multidrug-resistance gene (P-glycoprotein) is expressed by endothelial cells at blood-brain barrier sites. *Proc Natl Acad Sci U S A* **86**: 695-8 (1989).

118. C. Cordon-Cardo, J. P. O'Brien, J. Boccia, D. Casals, J. R. Bertino, and M. R. Melamed. Expression of the multidrug resistance gene product (P-glycoprotein) in human normal and tumor tissues. *J Histochem Cytochem* **38**: 1277-87 (1990).

119. F. Thiebaut, T. Tsuruo, H. Hamada, M. M. Gottesman, I. Pastan, and M. C. Willingham. Cellular localization of the multidrug-resistance gene product P-glycoprotein in normal human tissues. *Proc Natl Acad Sci U S A* **84**: 7735-8 (1987).

120. I. Sugawara, I. Kataoka, Y. Morishita, H. Hamada, T. Tsuruo, S. Itoyama, and S. Mori. Tissue distribution of P-glycoprotein encoded by a multidrug-resistant gene as revealed by a monoclonal antibody, MRK 16. *Cancer Res* **48**: 1926-9 (1988).

121. G. Bradley, E. Georges, and V. Ling. Sex-dependent and independent expression of the P-glycoprotein isoforms in Chinese hamster. *J Cell Physiol* **145**: 398-408 (1990).

122. R. J. Arceci, J. M. Croop, S. B. Horwitz, and D. Housman. The gene encoding multidrug resistance is induced and expressed at high levels during pregnancy in the secretory epithelium of the uterus. *Proc Natl Acad Sci U S A* **85**: 4350-4 (1988).

123. P. M. Chaudhary, E. B. Mechetner, and I. B. Roninson. Expression and activity of the multidrug resistance P-glycoprotein in human peripheral blood lymphocytes. *Blood* **80**: 2735-9 (1992).

124. P. M. Chaudhary and I. B. Roninson. Expression and activity of P-glycoprotein, a multidrug efflux pump, in human hematopoietic stem cells. *Cell* **66**: 85-94 (1991).

125. S. Bremer, T. Hoof, M. Wilke, R. Busche, B. Scholte, J. R. Riordan, G. Maass, and B. Tummler. Quantitative expression patterns of multidrug-resistance P-glycoprotein (MDR1) and differentially spliced cystic-fibrosis transmembrane- conductance regulator mRNA transcripts in human epithelia. *Eur J Biochem* **206**: 137-49 (1992).

126. A. Andreana, S. Aggarwal, S. Gollapudi, D. Wien, T. Tsuruo, and S. Gupta. Abnormal expression of a 170-kilodalton P-glycoprotein encoded by MDR1 gene, a metabolically active efflux pump, in CD4+ and CD8+ T cells from patients with human immunodeficiency virus type 1 infection. *AIDS Res Hum Retroviruses* **12**: 1457-62 (1996).

127. J. Drach, S. Zhao, D. Drach, M. Korbling, H. Engel, and M. Andreeff. Expression of MDR1 by normal bone marrow cells and its implication for leukemic hematopoiesis. *Leuk Lymphoma* **16**: 419-24 (1995).

128. S. Kaczorowski, M. Ochocka, M. Kaczorowska, R. Aleksandrowicz, M. Matysiakl, and M. Karwacki. Is P-glycoprotein a sufficient marker for multidrug resistance in vivo? Immunohistochemical staining for P-glycoprotein in children and adult leukemia: correlation with clinical outcome. *Leuk Lymphoma* **20**: 143-52 (1995).

129. T. W. Loo and D. M. Clarke. Membrane topology of a cysteine-less mutant of human P-glycoprotein. *J Biol Chem* **270**: 843-8 (1995).

130. T. W. Loo and D. M. Clarke. Determining the structure and mechanism of the human multidrug resistance P-glycoprotein using cysteine-scanning mutagenesis and thiol-modification techniques. *Biochim Biophys Acta* **1461**: 315-25 (1999).

131. C. F. Higgins, R. Callaghan, K. J. Linton, M. F. Rosenberg, and R. C. Ford. Structure of the multidrug resistance P-glycoprotein. *Semin Cancer Biol* **8**: 135-42 (1997).

132. L. J. Goldstein, H. Galski, A. Fojo, M. Willingham, S. L. Lai, A. Gazdar, R. Pirker, A. Green, W. Crist, G. M. Brodeur, M. Lieber, J. Cossman, M. M. Gottesman, and I. Pastan. Expression of a multidrug resistance gene in human cancers. *J Natl Cancer Inst* **81**: 116-24 (1989).

133. J. R. Hammond, R. M. Johnstone, and P. Gros. Enhanced efflux of [3H]vinblastine from Chinese hamster ovary cells transfected with a full-length complementary DNA clone for the mdr1 gene. *Cancer Res* **49**: 3867-71 (1989).

134. B. C. Guild, R. C. Mulligan, P. Gros, and D. E. Housman. Retroviral transfer of a murine cDNA for multidrug resistance confers pleiotropic drug resistance to cells without prior drug selection. *Proc Natl Acad Sci U S A* **85**: 1595-9 (1988).

135. I. Pastan, M. M. Gottesman, K. Ueda, E. Lovelace, A. V. Rutherford, and M. C. Willingham. A retrovirus carrying an MDR1 cDNA confers multidrug resistance and polarized expression of P-glycoprotein in MDCK cells. *Proc Natl Acad Sci U S A* **85**: 4486-90 (1988).

136. K. Choi, T. O. Frommel, R. K. Stern, C. F. Perez, M. Kriegler, T. Tsuruo, and I. B. Roninson. Multidrug resistance after retroviral transfer of the human MDR1 gene correlates with P-glycoprotein density in the plasma membrane and is not affected by cytotoxic selection. *Proc Natl Acad Sci U S A* **88**: 7386-90 (1991).

137. V. J. Wacher, C. Y. Wu, and L. Z. Benet. Overlapping substrate specificities and tissue distribution of cytochrome P450 3A and P-glycoprotein: implications for drug delivery and activity in cancer chemotherapy. *Mol Carcinog* **13**: 129-34 (1995).

138. E. G. Schuetz, W. T. Beck, and J. D. Schuetz. Modulators and substrates of P-glycoprotein and cytochrome P4503A coordinately up-regulate these proteins in human colon carcinoma cells. *Mol Pharmacol* **49**: 311-8 (1996).

139. D. Kessel, T. C. Hall, and D. Roberts. Modes of uptake of methotrexate by normal and leukemic human leukocytes in vitro and their relation to drug response. *Cancer Res* **28**: 564-70 (1968).

140. K. Dano. Active outward transport of daunomycin in resistant Ehrlich ascites tumor cells. *Biochim Biophys Acta* **323**: 466-83 (1973).

141. T. Skovsgaard. Mechanism of cross-resistance between vincristine and daunorubicin in Ehrlich ascites tumor cells. *Cancer Res* **38**: 4722-7 (1978).

142. T. Skovsgaard. Mechanisms of resistance to daunorubicin in Ehrlich ascites tumor cells. *Cancer Res* **38**: 1785-91 (1978).

143. M. Inaba, H. Kobayashi, Y. Sakurai, and R. K. Johnson. Active efflux of daunorubicin and adriamycin in sensitive and resistant sublines of P388 leukemia. *Cancer Res* **39**: 2200-3 (1979).

144. A. Fojo, S. Akiyama, M. M. Gottesman, and I. Pastan. Reduced drug accumulation in multiply drug-resistant human KB carcinoma cell lines. *Cancer Res* **45**: 3002-7 (1985).

145. T. Tsuruo, H. Iida, S. Tsukagoshi, and Y. Sakurai. Overcoming of vincristine resistance in P388 leukemia in vivo and in vitro through enhanced cytotoxicity of vincristine and vinblastine by verapamil. *Cancer Res* **41**: 1967-72 (1981).

146. J. M. Ford. Experimental reversal of P-glycoprotein-mediated multidrug resistance by pharmacological chemosensitisers. *Eur J Cancer* **32A**: 991-1001 (1996).

147. J. M. Ford, E. P. Bruggemann, I. Pastan, M. M. Gottesman, and W. N. Hait. Cellular and biochemical characterization of thioxanthenes for reversal of multidrug resistance in human and murine cell lines. *Cancer Res* **50**: 1748-56 (1990).

148. J. M. Ford and W. N. Hait. Pharmacology of drugs that alter multidrug resistance in cancer. *Pharmacol Rev* **42**: 155-99 (1990).

149. B. L. Lum, G. A. Fisher, N. A. Brophy, A. M. Yahanda, K. M. Adler, S. Kaubisch, J. Halsey, and B. I. Sikic. Clinical trials of modulation of multidrug resistance. Pharmacokinetic and pharmacodynamic considerations. *Cancer* **72**: 3502-14 (1993).

150. W. D. Stein. Reversers of the multidrug resistance transporter P-glycoprotein. *Curr Opin Investig Drugs* **3**: 812-7 (2002).

151. A. M. Oza. Clinical development of P glycoprotein modulators in oncology. *Novartis Found Symp* **243**: 103-15; discussion 115-8, 180-5 (2002).

152. D. N. Tchamo, M. G. Dijoux-Franca, A. M. Mariotte, E. Tsamo, J. B. Daskiewicz, C. Bayet, D. Barron, G. Conseil, and A. Di Pietro. Prenylated xanthones as potential P-glycoprotein modulators. *Bioorg Med Chem Lett* **10**: 1343-5 (2000).

153. V. Nussler, R. Pelka-Fleisc, F. Gieseler, M. Hasmann, R. Loser, E. Gullis, O. Stotzer, H. Zwierzina, and W. Wilmanns. In vitro efficacy of known P-glycoprotein modulators compared to droloxifene E and Z: studies on a human T-cell leukemia cell line and their resistant variants. *Leuk Lymphoma* **31**: 589-97 (1998).

154. H. Tanabe, S. Tasaka, H. Ohmori, N. Gomi, Y. Sasaki, T. Machida, M. Iino, A. Kiue, S. Naito, and M. Kuwano. Newly synthesized dihydropyridine derivatives as modulators of P-glycoprotein-mediated multidrug resistance. *Bioorg Med Chem* **6**: 2219-27 (1998).

155. D. E. Burgio, M. P. Gosland, and P. J. McNamara. Effects of P-glycoprotein modulators on etoposide elimination and central nervous system distribution. *J Pharmacol Exp Ther* **287**: 911-7 (1998).

156. F. Bois, C. Beney, A. Boumendjel, A. M. Mariotte, G. Conseil, and A. Di Pietro. Halogenated chalcones with high-affinity binding to P-glycoprotein: potential modulators of multidrug resistance. *J Med Chem* **41**: 4161-4 (1998).

157. F. J. Sharom, P. Lu, R. Liu, and X. Yu. Linear and cyclic peptides as substrates and modulators of P-glycoprotein: peptide binding and effects on drug transport and accumulation. *Biochem J* **333 (Pt 3)**: 621-30 (1998).

158. S. Ayesh, Y. M. Shao, and W. D. Stein. Co-operative, competitive and non-competitive interactions between modulators of P-glycoprotein. *Biochim Biophys Acta* **1316**: 8-18 (1996).

159. W. T. Beck. Modulators of P-glycoprotein-associated multidrug resistance. *Cancer Treat Res* **57**: 151-70 (1991).

160. M. Ichikawa, A. Yoshimura, T. Furukawa, T. Sumizawa, and S. Akiyama. Modulators of the multidrug-transporter, P-glycoprotein, exist in the human plasma. *Biochem Biophys Res Commun* **166**: 74-80 (1990).

161. L. E. Shapiro and N. H. Shear. Drug interactions: Proteins, pumps, and P-450s. *J Am Acad Dermatol* **47**: 467-84; quiz 485-8 (2002).

162. L. Z. Benet and C. L. Cummins. The drug efflux-metabolism alliance: biochemical aspects. *Adv Drug Deliv Rev* **50 (Suppl 1)**: S3-11 (2001).

163. W. L. Chiou, S. M. Chung, T. C. Wu, and C. Ma. A comprehensive account on the role of efflux transporters in the gastrointestinal absorption of 13 commonly used substrate drugs in humans. *Int J Clin Pharmacol Ther* **39**: 93-101 (2001).

164. V. J. Wacher, L. Salphati, and L. Z. Benet. Active secretion and enterocytic drug metabolism barriers to drug absorption. *Adv Drug Deliv Rev* **46**: 89-102 (2001).

165. H. Suzuki and Y. Sugiyama. Role of metabolic enzymes and efflux transporters in the absorption of drugs from the small intestine. *Eur J Pharm Sci* **12**: 3-12 (2000).

166. M. F. Fromm. P-glycoprotein: a defense mechanism limiting oral bioavailability and CNS accumulation of drugs. *Int J Clin Pharmacol Ther* **38**: 69-74 (2000).

167. D. K. Yu. The contribution of P-glycoprotein to pharmacokinetic drug-drug interactions. *J Clin Pharmacol* **39**: 1203-11 (1999).

168. L. Z. Benet, T. Izumi, Y. Zhang, J. A. Silverman, and V. J. Wacher. Intestinal MDR transport proteins and P-450 enzymes as barriers to oral drug delivery. *J Control Release* **62**: 25-31 (1999).

169. Y. Tanigawara. Role of P-glycoprotein in drug disposition. *Ther Drug Monit* **22**: 137-40 (2000).

170. K. Ueda, N. Okamura, M. Hirai, Y. Tanigawara, T. Saeki, N. Kioka, T. Komano, and R. Hori. Human P-glycoprotein transports cortisol, aldosterone, and dexamethasone, but not progesterone. *J Biol Chem* **267**: 24248-52 (1992).

171. C. P. Yang, S. G. DePinho, L. M. Greenberger, R. J. Arceci, and S. B. Horwitz. Progesterone interacts with P-glycoprotein in multidrug-resistant cells and in the endometrium of gravid uterus. *J Biol Chem* **264**: 782-8 (1989).

172. C. G. Vanoye, A. F. Castro, T. Pourcher, L. Reuss, and G. A. Altenberg. Phosphorylation of P-glycoprotein by PKA and PKC modulates swelling- activated Cl- currents. *Am J Physiol* **276**: C370-8 (1999).

173. D. R. Gill, S. C. Hyde, C. F. Higgins, M. A. Valverde, G. M. Mintenig, and F. V. Sepulveda. Separation of drug transport and chloride channel functions of the human multidrug resistance P-glycoprotein. *Cell* **71**: 23-32 (1992).

174. M. A. Valverde, M. Diaz, F. V. Sepulveda, D. R. Gill, S. C. Hyde, and C. F. Higgins. Volume-regulated chloride channels associated with the human multidrug-resistance P-glycoprotein. *Nature* **355**: 830-3 (1992).

175. S. P. Hardy, H. R. Goodfellow, M. A. Valverde, D. R. Gill, V. Sepulveda, and C. F. Higgins. Protein kinase C-mediated phosphorylation of the human multidrug resistance P-glycoprotein regulates cell volume-activated chloride channels. *EMBO J* **14**: 68-75 (1995).

176. A. J. Vander. *Renal Physiology*. 4th ed. New York, McGraw-Hill, 1991

177. C. Lote. *Principles of Renal Physiology*. 4th ed. Kluwer Academic Publishers, 2000

178. S. V. Ambudkar, S. Dey, C. A. Hrycyna, M. Ramachandra, I. Pastan, and M. M. Gottesman. Biochemical, cellular, and pharmacological aspects of the multidrug transporter. *Annu Rev Pharmacol Toxicol* **39**: 361-98 (1999).

179. A. Seelig. How does P-glycoprotein recognize its substrates? *Int J Clin Pharmacol Ther* **36**: 50-4 (1998).

180. A. Seelig. A general pattern for substrate recognition by P-glycoprotein. *Eur J Biochem* **251**: 252-61 (1998).

181. R. Heidenhain and A. Neisser. Versuche über den vorgang der harnabsonderung. *Pflügers Arch ges Physiol* **9**: 1-6 (1874).

182. E. K. Marshall and J. L. Vickers. The mechanism of elimination of phenolsulphonphthalein by the kidney: A proof of secretion by the convoluted tubules. *Bull Johns Hopkins Hosp* **34**: 1-7 (1923).

183. B. R. Rennick. Renal excretion of drugs: tubular transport and metabolism. *Annu Rev Pharmacol* **12**: 141-56 (1972).

184. R. Bendayan. Renal drug transport: a review. *Pharmacotherapy* **16**: 971-85 (1996).

185. R. Masereeuw and F. G. Russel. Mechanisms and clinical implications of renal drug excretion. *Drug Metab Rev* **33**: 299-351 (2001).

186. A. Somogyi. Renal transport of drugs: specificity and molecular mechanisms. *Clin Exp Pharmacol Physiol* **23**: 986-9 (1996).

187. M. J. Dresser, M. K. Leabman, and K. M. Giacomini. Transporters involved in the elimination of drugs in the kidney: organic anion transporters and organic cation transporters. *J Pharm Sci* **90**: 397-421 (2001).

188. S. Ito. Drug secretion systems in renal tubular cells: functional models and molecular identity. *Pediatr Nephrol* **13**: 980-8 (1999).

189. E. Rey, J. M. Treluyer, and G. Pons. Drug disposition in cystic fibrosis. *Clin Pharmacokinet* **35**: 313-29 (1998).

190. D. J. Touw. Clinical pharmacokinetics of antimicrobial drugs in cystic fibrosis. *Pharm World Sci* **20**: 149-60 (1998).

191. M. Spino. Pharmacokinetics of drugs in cystic fibrosis. *Clin Rev Allergy* **9**: 169-210 (1991).

192. J. Prandota. Clinical pharmacology of antibiotics and other drugs in cystic fibrosis. *Drugs* **35**: 542-78 (1988).

193. R. de Groot and A. L. Smith. Antibiotic pharmacokinetics in cystic fibrosis. Differences and clinical significance. *Clin Pharmacokinet* **13**: 228-53 (1987).

194. F. Sörgel, M. Kinzig, C. Labisch, M. Hofmann, and U. Stephan. Pharmacokinetics of antibacterials in cystic fibrosis. In A. Bauernfeind, M.I. Marks, and B. Strandvik (eds.), *Cystic Fibrosis Pulmonary Infections: Lessons from Around the World*, Birkhäuser-Verlag, Basel, 1996, pp. 13-27.

195. W. J. Jusko, L. L. Mosovich, L. M. Gerbracht, M. E. Mattar, and S. J. Yaffe. Enhanced renal excretion of dicloxacillin in patients with cystic fibrosis. *Pediatrics* **56**: 1038-44 (1975).

196. A. Arvidsson, G. Alvan, and B. Strandvik. Difference in renal handling of cefsulodin between patients with cystic fibrosis and normal subjects. *Acta Paediatr Scand* **72**: 293-4 (1983).

197. M. Spino, R. P. Chai, A. F. Isles, J. J. Thiessen, A. Tesoro, R. Gold, and S. M. MacLeod. Cloxacillin absorption and disposition in cystic fibrosis. *J Pediatr* **105**: 829-35 (1984).

198. J. S. Leeder, M. Spino, A. F. Isles, A. M. Tesoro, R. Gold, and S. M. MacLeod. Ceftazidime disposition in acute and stable cystic fibrosis. *Clin Pharmacol Ther* **36**: 355-62 (1984).

199. J. Levy, A. L. Smith, J. R. Koup, J. Williams-Warren, and B. Ramsey. Disposition of tobramycin in patients with cystic fibrosis: a prospective controlled study. *J Pediatr* **105**: 117-24 (1984).

200. D. C. Knoppert, M. Spino, R. Beck, J. J. Thiessen, and S. M. MacLeod. Cystic fibrosis: enhanced theophylline metabolism may be linked to the disease. *Clin Pharmacol Ther* **44**: 254-64 (1988).

201. R. M. Hutabarat, J. D. Unadkat, C. Sahajwalla, S. McNamara, B. Ramsey, and A. L. Smith. Disposition of drugs in cystic fibrosis. I. Sulfamethoxazole and trimethoprim. *Clin Pharmacol Ther* **49**: 402-9 (1991).

202. J. P. Wang, J. D. Unadkat, S. McNamara, T. A. O'Sullivan, A. L. Smith, W. F. Trager, and B. Ramsey. Disposition of drugs in cystic fibrosis. VI. In vivo activity of cytochrome P450 isoforms involved in the metabolism of (R)-warfarin (including P450 3A4) is not enhanced in cystic fibrosis. *Clin Pharmacol Ther* **55**: 528-34 (1994).

203. A. Isles, M. Spino, E. Tabachnik, H. Levison, J. Thiessen, and S. MacLeod. Theophylline disposition in cystic fibrosis. *Am Rev Respir Dis* **127**: 417-21 (1983).

204. T. A. O'Sullivan, J. P. Wang, J. D. Unadkat, S. M. al-Habet, W. F. Trager, A. L. Smith, S. McNamara, and M. L. Aitken. Disposition of drugs in cystic fibrosis. V. In vivo CYP2C9 activity as probed by (S)-warfarin is not enhanced in cystic fibrosis. *Clin Pharmacol Ther* **54**: 323-8 (1993).

205. B. Strandvik, U. Berg, A. Kallner, and E. Kusoffsky. Effect on renal function of essential fatty acid supplementation in cystic fibrosis. *J Pediatr* **115**: 242-50 (1989).

206. A. Hedman, G. Alvan, B. Strandvik, and A. Arvidsson. Increased renal clearance of cefsulodin due to higher glomerular filtration rate in cystic fibrosis. *Clin Pharmacokinet* **18**: 168-75 (1990).

207. A. Hedman, Y. Adan-Abdi, G. Alvan, B. Strandvik, and A. Arvidsson. Influence of the glomerular filtration rate on renal clearance of ceftazidime in cystic fibrosis. *Clin Pharmacokinet* **15**: 57-65 (1988).

208. M. Aladjem, D. Lotan, H. Boichis, S. Orda, and D. Katznelson. Renal function in patients with cystic fibrosis. *Nephron* **34**: 84-6 (1983).

209. S. J. Yaffe, L. M. Gerbracht, L. L. Mosovich, M. E. Mattar, M. Danish, and W. J. Jusko. Pharmacokinetics of methicillin in patients with cystic fibrosis. *J Infect Dis* **135**: 828-31 (1977).

210. R. de Groot, B. D. Hack, A. Weber, D. Chaffin, B. Ramsey, and A. L. Smith. Pharmacokinetics of ticarcillin in patients with cystic fibrosis: a controlled prospective study. *Clin Pharmacol Ther* **47**: 73-8 (1990).

211. B. A. Hamelin, N. Moore, C. A. Knupp, M. Ruel, F. Vallee, and M. LeBel. Cefepime pharmacokinetics in cystic fibrosis. *Pharmacotherapy* **13**: 465-70 (1993).

212. M. Spino, R. P. Chai, A. F. Isles, J. W. Balfe, R. G. Brown, J. J. Thiessen, and S. M. MacLeod. Assessment of glomerular filtration rate and effective renal plasma flow in cystic fibrosis. *J Pediatr* **107**: 64-70 (1985).

213. U. Berg, E. Kusoffsky, and B. Strandvik. Renal function in cystic fibrosis with special reference to the renal sodium handling. *Acta Paediatr Scand* **71**: 833-8 (1982).

214. G. Marra, S. Tirelli, G. Cavanna, M. Amoretti, A. Giunta, A. C. Appiani, and B. M. Assael. Renal function in cystic fibrosis. Abstr. 365, Ped Res Meeting, 1984.

215. G. L. Kearns, B. C. Hilman, and J. T. Wilson. Dosing implications of altered gentamicin disposition in patients with cystic fibrosis. *J Pediatr* **100**: 312-8 (1982).

216. M. LeBel, M. G. Bergeron, F. Vallee, C. Fiset, G. Chasse, P. Bigonesse, and G. Rivard. Pharmacokinetics and pharmacodynamics of ciprofloxacin in cystic fibrosis patients. *Antimicrob Agents Chemother* **30**: 260-6 (1986).

217. R. L. Davis, J. R. Koup, J. Williams-Warren, A. Weber, L. Heggen, D. Stempel, and A. L. Smith. Pharmacokinetics of ciprofloxacin in cystic fibrosis. *Antimicrob Agents Chemother* **31**: 915-9 (1987).

218. M. D. Reed, R. C. Stern, C. M. Myers, T. S. Yamashita, and J. L. Blumer. Lack of unique ciprofloxacin pharmacokinetic characteristics in patients with cystic fibrosis. *J Clin Pharmacol* **28**: 691-9 (1988).

219. J. Mimeault, F. Vallee, R. Seelmann, F. Sorgel, M. Ruel, and M. LeBel. Altered disposition of fleroxacin in patients with cystic fibrosis. *Clin Pharmacol Ther* **47**: 618-28 (1990).

220. H. Michalsen and T. Bergan. Pharmacokinetics of netilmicin in children with and without cystic fibrosis. *Antimicrob Agents Chemother* **19**: 1029-31 (1981).

221. E. Autret, S. Marchand, M. Breteau, and B. Grenier. Pharmacokinetics of amikacin in cystic fibrosis: a study of bronchial diffusion. *Eur J Clin Pharmacol* **31**: 79-83 (1986).

222. A. A. Vinks. *Pharmacokinetics of Aztreonam after Single Dose Compared to Matched Controls and During Home Treatment by Continuous Infusion in Patients with Cystic Fibrosis*. University of Leiden, Thesis, 1996

223. E. Finkelstein and K. Hall. Aminoglycoside clearance in patients with cystic fibrosis. *J Pediatr* **94**: 163-4 (1979).

224. M. D. Reed, R. C. Stern, J. S. Bertino, Jr., C. M. Myers, T. S. Yamashita, and J. L. Blumer. Dosing implications of rapid elimination of trimethoprim-sulfamethoxazole in patients with cystic fibrosis. *J Pediatr* **104**: 303-7 (1984).

225. S. W. Bender, A. Dalhoff, P. M. Shah, R. Strehl, and H. G. Posselt. Ciprofloxacin pharmacokinetics in patients with cystic fibrosis. *Infection* **14**: 17-21 (1986).

226. G. L. Kearns, J. T. Wilson, and B. C. Hilman. Gentamicin pharmacokinetics in cystic fibrosis. *J Pediatr* **111**: 310-2 (1987).

227. C. E. Huls, R. A. Prince, D. K. Seilheimer, and J. A. Bosso. Pharmacokinetics of cefepime in cystic fibrosis patients. *Antimicrob Agents Chemother* **37**: 1414-6 (1993).

228. G. Alvan, B. Beermann, L. Hjelte, M. Lind, A. Lindholm, and B. Strandvik. Increased nonrenal clearance and increased diuretic efficiency of furosemide in cystic fibrosis. *Clin Pharmacol Ther* **44**: 436-41 (1988).

229. M. W. Konstan, C. L. Hoppel, B. L. Chai, and P. B. Davis. Ibuprofen in children with cystic fibrosis: pharmacokinetics and adverse effects. *J Pediatr* **118**: 956-64 (1991).

230. G. L. Kearns, G. B. Mallory, Jr., W. R. Crom, and W. E. Evans. Enhanced hepatic drug clearance in patients with cystic fibrosis. *J Pediatr* **117**: 972-9 (1990).

231. G. L. Kearns, W. R. Crom, K. H. Karlson, Jr., G. B. Mallory, Jr., and W. E. Evans. Hepatic drug clearance in patients with mild cystic fibrosis. *Clin Pharmacol Ther* **59**: 529-40 (1996).

232. B. A. Christensson, I. Nilsson-Ehle, B. Ljungberg, A. Lindblad, A. S. Malmborg, L. Hjelte, and B. Strandvik. Increased oral bioavailability of ciprofloxacin in cystic fibrosis patients. *Antimicrob Agents Chemother* **36**: 2512-7 (1992).

233. K. K. Tan, K. L. Hue, S. E. Strickland, A. K. Trull, R. L. Smyth, J. P. Scott, A. W. Kelman, B. Whiting, T. W. Higenbottam, and J. Wallwork. Altered pharmacokinetics of cyclosporin in heart-lung transplant recipients with cystic fibrosis. *Ther Drug Monit* **12**: 520-4 (1990).

234. V. T. Tsang, A. Johnston, F. Heritier, N. Leaver, M. E. Hodson, and M. Yacoub. Cyclosporin pharmacokinetics in heart-lung transplant recipients with cystic fibrosis. Effects of pancreatic enzymes and ranitidine. *Eur J Clin Pharmacol* **46**: 261-5 (1994).

235. G. Koren, Z. Weizman, G. Forstner, S. M. MacLeod, and P. R. Durie. Altered PABA pharmacokinetics in cystic fibrosis. Implications for bentiromide test. *Dig Dis Sci* **30**: 928-32 (1985).

236. L. Z. Benet, S. Øie, and J. B. Schwartz. Design and optimization of dosage regimens; pharmacokinetic data. In J.G. Hardman, L.E. Limbird, P.B. Molinoff, R.W. Ruddon, and A.G. Gilman (eds.), *Goodman & Gilman's The Pharmacological Basis of Therapeutics*, 9th ed, McGraw-Hill, New York, 1996, pp. 1707-1792.

237. J. P. Wang, J. D. Unadkat, S. M. al-Habet, T. A. O'Sullivan, J. Williams-Warren, A. L. Smith, and B. Ramsey. Disposition of drugs in cystic fibrosis. IV. Mechanisms for enhanced renal clearance of ticarcillin. *Clin Pharmacol Ther* **54**: 293-302 (1993).

238. J. Y. Lallemand, V. Stoven, J. P. Annereau, J. Boucher, S. Blanquet, J. Barthe, and G. Lenoir. Induction by antitumoral drugs of proteins that functionally complement CFTR: a novel therapy for cystic fibrosis? *Lancet* **350**: 711-2 (1997).

239. J. S. Handler, F. M. Perkins, and J. P. Johnson. Studies of renal cell function using cell culture techniques. *Am J Physiol* **238**: F1-9 (1980).

240. R. Chambers and R. T. Kempton. Indications of function of the chick mesonephros in tissue culture with phenol red. *J Cell Comp Physiol* **3**: 131-167 (1933).

241. M. Horio, K. V. Chin, S. J. Currier, S. Goldenberg, C. Williams, I. Pastan, M. M. Gottesman, and J. Handler. Transepithelial transport of drugs by the multidrug transporter in cultured Madin-Darby canine kidney cell epithelia. *J Biol Chem* **264**: 14880-4 (1989).

242. G. Wilson. Cell culture techniques for the study of drug transport. *Eur J Drug Metab Pharmacokinet* **15**: 159-63 (1990).

243. R. T. Borchardt, I. J. Hidalgo, K. M. Hillgren, and M. Hu. Pharmaceutical applications of cell culture: An overview. In G. Wilson, S.S. Davis, L. Illum, and A. Zweibaum (eds.), *Pharmaceutical Applications of Cell and Tissue Culture to Drug Transport*, Plenum, New York, 1991, pp. 1-14.

244. J. Karlsson, S. M. Kuo, J. Ziemniak, and P. Artursson. Transport of celiprolol across human intestinal epithelial (Caco-2) cells: mediation of secretion by multiple transporters including P- glycoprotein. *Br J Pharmacol* **110**: 1009-16 (1993).

245. N. M. Griffiths, B. H. Hirst, and N. L. Simmons. Active intestinal secretion of the fluoroquinolone antibacterials ciprofloxacin, norfloxacin and pefloxacin; a common secretory pathway? *J Pharmacol Exp Ther* **269**: 496-502 (1994).

246. K. I. Hosoya, K. J. Kim, and V. H. Lee. Age-dependent expression of P-glycoprotein gp170 in Caco-2 cell monolayers. *Pharm Res* **13**: 885-90 (1996).

247. M. E. Cavet, M. West, and N. L. Simmons. Fluoroquinolone (ciprofloxacin) secretion by human intestinal epithelial (Caco-2) cells. *Br J Pharmacol* **121**: 1567-78 (1997).

248. Y. Zhang and L. Z. Benet. Characterization of P-glycoprotein mediated transport of K02, a novel vinylsulfone peptidomimetic cysteine protease inhibitor, across MDR1-MDCK and Caco-2 cell monolayers. *Pharm Res* **15**: 1520-4 (1998).

249. S. D. Flanagan, C. L. Cummins, M. Susanto, X. Liu, L. H. Takahashi, and L. Z. Benet. Comparison of furosemide and vinblastine secretion from cell lines overexpressing multidrug resistance protein (P-glycoprotein) and multidrug resistance-associated proteins (MRP1 and MRP2). *Pharmacology* **64**: 126-34 (2002).

250. M. Susanto and L. Z. Benet. Can the enhanced renal clearance of antibiotics in cystic fibrosis patients be explained by P-glycoprotein transport? *Pharm Res* **19**: 457-62 (2002).

251. S. Lowes and N. L. Simmons. Multiple pathways for fluoroquinolone secretion by human intestinal epithelial (Caco-2) cells. *Br J Pharmacol* **135**: 1263-75 (2002).

252. B. Alberts, D. Bray, J. Lewis, M. Raff, K. Roberts, and J. Watson. *Molecular Biology of the Cell*, 3rd ed, Garland Publishing, Inc., New York, 1994.

253. K. M. Hillgren, A. Kato, and R. T. Borchardt. In vitro systems for studying intestinal drug absorption. *Med Res Rev* **15**: 83-109 (1995).

254. M. J. Lydon, T. W. Minett, and B. J. Tighe. Cellular interactions with synthetic polymer surfaces in culture. *Biomaterials* **6**: 396-402 (1985).

255. H. Yu and P. J. Sinko. Influence of the microporous substratum and hydrodynamics on resistances to drug transport in cell culture systems: calculation of intrinsic transport parameters. *J Pharm Sci* **86**: 1448-57 (1997).

256. R. S. Talhouk, R. L. Neiswander, and F. L. Schanbacher. Effect of substratum on growth, cell morphology and lactoferrin synthesis and secretion in bovine mammary cell culture. *Tissue Cell* **30**: 226-35 (1998).

257. H. Yu, T. J. Cook, and P. J. Sinko. Evidence for diminished functional expression of intestinal transporters in Caco-2 cell monolayers at high passages. *Pharm Res* **14**: 757-62 (1997).

258. D. S. Misfeldt, S. T. Hamamoto, and D. R. Pitelka. Transepithelial transport in cell culture. *Proc Natl Acad Sci U S A* **73**: 1212-6 (1976).

259. M. Cereijido, E. S. Robbins, W. J. Dolan, C. A. Rotunno, and D. D. Sabatini. Polarized monolayers formed by epithelial cells on a permeable and translucent support. *J Cell Biol* **77**: 853-80 (1978).

260. J. S. Handler. Use of cultured epithelia to study transport and its regulation. *J Exp Biol* **106**: 55-69 (1983).

261. S. P. Cole and R. G. Deeley. Multidrug resistance associated with overexpression of MRP. *Cancer Treat Res* **87**: 39-62 (1996).

262. R. Evers, G. J. Zaman, L. van Deemter, H. Jansen, J. Calafat, L. C. Oomen, R. P. Oude Elferink, P. Borst, and A. H. Schinkel. Basolateral localization and export activity of the human multidrug resistance-associated protein in polarized pig kidney cells. *J Clin Invest* **97**: 1211-8 (1996).

263. R. Evers, M. de Haas, R. Sparidans, J. Beijnen, P. R. Wielinga, J. Lankelma, and P. Borst. Vinblastine and sulfinpyrazone export by the multidrug resistance protein MRP2 is associated with glutathione export. *Br J Cancer* **83**: 375-83 (2000).

264. Y. Tanigawara, N. Okamura, M. Hirai, M. Yasuhara, K. Ueda, N. Kioka, T. Komano, and R. Hori. Transport of digoxin by human P-glycoprotein expressed in a porcine kidney epithelial cell line (LLC-PK1). *J Pharmacol Exp Ther* **263**: 840-5 (1992).

265. E. Bakos, R. Evers, G. Szakacs, G. E. Tusnady, E. Welker, K. Szabo, M. de Haas, L. van Deemter, P. Borst, A. Varadi, and B. Sarkadi. Functional multidrug resistance protein (MRP1) lacking the N-terminal transmembrane domain. *J Biol Chem* **273**: 32167-75 (1998).

266. R. Evers, M. Kool, L. van Deemter, H. Janssen, J. Calafat, L. C. Oomen, C. C. Paulusma, R. P. Oude Elferink, F. Baas, A. H. Schinkel, and P. Borst. Drug export activity of the human canalicular multispecific organic anion transporter in polarized kidney MDCK cells expressing cMOAT (MRP2) cDNA. *J Clin Invest* **101**: 1310-9 (1998).

267. Y. Cui, J. Konig, J. K. Buchholz, H. Spring, I. Leier, and D. Keppler. Drug resistance and ATP-dependent conjugate transport mediated by the apical multidrug resistance protein, MRP2, permanently expressed in human and canine cells. *Mol Pharmacol* **55**: 929-37 (1999).

268. Z. S. Chen, T. Kawabe, M. Ono, S. Aoki, T. Sumizawa, T. Furukawa, T. Uchiumi, M. Wada, M. Kuwano, and S. I. Akiyama. Effect of multidrug resistance-reversing agents on transporting activity of human canalicular multispecific organic anion transporter. *Mol Pharmacol* **56**: 1219-28 (1999).

269. R. N. Hull, W. R. Cherry, and G. W. Weaver. The origin and characteristics of a pig kidney cell strain, LLC-PK. *In Vitro* **12**: 670-7 (1976).

270. S. H. Madin and N. B. Darby. *As Catalogued in: American Type Culture Collection Catalogue of Strains II.* 1st ed. Rockville, Maryland, American Type Culture Collection, 1975

271. J. C. Richardson, V. Scalera, and N. L. Simmons. Identification of two strains of MDCK cells which resemble separate nephron tubule segments. *Biochim Biophys Acta* **673**: 26-36 (1981).

272. J. D. Valentich. Morphological similarities between the dog kidney cell line MDCK and the mammalian cortical collecting tubule. *Ann N Y Acad Sci* **372**: 384-405 (1981).

273. N. L. Simmons. Cultured monolayers of MDCK cells: a novel model system for the study of epithelial development and function. *Gen Pharmacol* **13**: 287-91 (1982).

274. F. Jehl, P. Birckel, and H. Monteil. Hospital routine analysis of penicillins, third-generation cephalosporins and aztreonam by conventional and high-speed high-performance liquid chromatography. *J Chromatogr* **413**: 109-19 (1987).

275. I. A. de Lannoy and M. Silverman. The MDR1 gene product, P-glycoprotein, mediates the transport of the cardiac glycoside, digoxin. *Biochem Biophys Res Commun* **189**: 551-7 (1992).

276. N. Okamura, M. Hirai, Y. Tanigawara, K. Tanaka, M. Yasuhara, K. Ueda, T. Komano, and R. Hori. Digoxin-cyclosporin A interaction: modulation of the multidrug transporter P-glycoprotein in the kidney. *J Pharmacol Exp Ther* **266**: 1614-9 (1993).

277. S. Ito, G. Koren, P. A. Harper, and M. Silverman. Energy-dependent transport of digoxin across renal tubular cell monolayers (LLC-PK1). *Can J Physiol Pharmacol* **71**: 40-7 (1993).

278. R. Hori, N. Okamura, T. Aiba, and Y. Tanigawara. Role of P-glycoprotein in renal tubular secretion of digoxin in the isolated perfused rat kidney. *J Pharmacol Exp Ther* **266**: 1620-5 (1993).

279. M. E. Cavet, M. West, and N. L. Simmons. Transport and epithelial secretion of the cardiac glycoside, digoxin, by human intestinal epithelial (Caco-2) cells. *Br J Pharmacol* **118**: 1389-96 (1996).

280. M. de Bruin, K. Miyake, T. Litman, R. Robey, and S. E. Bates. Reversal of resistance by GF120918 in cell lines expressing the ABC half-transporter, MXR. *Cancer Lett* **146**: 117-26 (1999).

281. M. Yamazaki, W. E. Neway, T. Ohe, I. Chen, J. F. Rowe, J. H. Hochman, M. Chiba, and J. H. Lin. In vitro substrate identification studies for p-glycoprotein-mediated transport: species difference and predictability of in vivo results. *J Pharmacol Exp Ther* **296**: 723-35 (2001).

282. A. H. Schinkel, E. Wagenaar, L. van Deemter, C. A. Mol, and P. Borst. Absence of the mdr1a P-glycoprotein in mice affects tissue distribution and pharmacokinetics of dexamethasone, digoxin, and cyclosporin A. *J Clin Invest* **96**: 1698-705 (1995).

283. A. H. Schinkel, C. A. Mol, E. Wagenaar, L. van Deemter, J. J. Smit, and P. Borst. Multidrug resistance and the role of P-glycoprotein knockout mice. *Eur J Cancer* **31A**: 1295-8 (1995).

284. A. H. Schinkel, U. Mayer, E. Wagenaar, C. A. Mol, L. van Deemter, J. J. Smit, M. A. van der Valk, A. C. Voordouw, H. Spits, O. van Tellingen, J. M. Zijlmans, W. E. Fibbe, and P. Borst. Normal viability and altered pharmacokinetics in mice lacking mdr1-type (drug-transporting) P-glycoproteins. *Proc Natl Acad Sci U S A* **94**: 4028-33. (1997).

285. A. H. Schinkel, U. Mayer, E. Wagenaar, C. A. Mol, L. van Deemter, J. J. Smit, M. A. van der Valk, A. C. Voordouw, H. Spits, O. van Tellingen, J. M. Zijlmans, W. E. Fibbe, and P. Borst. Normal viability and altered pharmacokinetics in mice lacking mdr1-type (drug-transporting) P-glycoproteins. *Proc Natl Acad Sci U S A* **94**: 4028-33 (1997).

286. A. H. Schinkel. Pharmacological insights from P-glycoprotein knockout mice. *Int J Clin Pharmacol Ther* **36**: 9-13 (1998).

287. J. N. Snouwaert, K. K. Brigman, A. M. Latour, N. N. Malouf, R. C. Boucher, O. Smithies, and B. H. Koller. An animal model for cystic fibrosis made by gene targeting. *Science* **257**: 1083-8 (1992).

288. J. R. Dorin, P. Dickinson, E. W. Alton, S. N. Smith, D. M. Geddes, B. J. Stevenson, W. L. Kimber, S. Fleming, A. R. Clarke, M. L. Hooper, L. Anderson, R. S. P. Beddington, and D. J. Porteous. Cystic fibrosis in the mouse by targeted insertional mutagenesis. *Nature* **359**: 211-5 (1992).

289. R. Ratcliff, M. J. Evans, A. W. Cuthbert, L. J. MacVinish, D. Foster, J. R. Anderson, and W. H. Colledge. Production of a severe cystic fibrosis mutation in mice by gene targeting. *Nat Genet* **4**: 35-41 (1993).

290. W. K. O'Neal, P. Hasty, P. B. McCray, Jr., B. Casey, J. Rivera-Perez, M. J. Welsh, A. L. Beaudet, and A. Bradley. A severe phenotype in mice with a duplication of exon 3 in the cystic fibrosis locus. *Hum Mol Genet* **2**: 1561-9 (1993).

291. P. Hasty, W. K. O'Neal, K. Q. Liu, A. P. Morris, Z. Bebok, G. B. Shumyatsky, T. Jilling, E. J. Sorscher, A. Bradley, and A. L. Beaudet. Severe phenotype in mice with termination mutation in exon 2 of cystic fibrosis gene. *Somat Cell Mol Genet* **21**: 177-87 (1995).

292. B. G. Zeiher, E. Eichwald, J. Zabner, J. J. Smith, A. P. Puga, P. B. McCray, Jr., M. R. Capecchi, M. J. Welsh, and K. R. Thomas. A mouse model for the delta F508 allele of cystic fibrosis. *J Clin Invest* **96**: 2051-64 (1995).

293. J. H. van Doorninck, P. J. French, E. Verbeek, R. H. Peters, H. Morreau, J. Bijman, and B. J. Scholte. A mouse model for the cystic fibrosis delta F508 mutation. *EMBO J* **14**: 4403-11 (1995).

294. W. H. Colledge, B. S. Abella, K. W. Southern, R. Ratcliff, C. Jiang, S. H. Cheng, L. J. MacVinish, J. R. Anderson, A. W. Cuthbert, and M. J. Evans. Generation and characterization of a delta F508 cystic fibrosis mouse model. *Nat Genet* **10**: 445-52 (1995).

295. S. J. Delaney, E. W. Alton, S. N. Smith, D. P. Lunn, R. Farley, P. K. Lovelock, S. A. Thomson, D. A. Hume, D. Lamb, D. J. Porteous, J. R. Dorin, and B. J. Wainwright. Cystic fibrosis mice carrying the missense mutation G551D replicate human genotype-phenotype correlations. *EMBO J* **15**: 955-63 (1996).

296. M. McKenney, B. Auerbach, G. Timmel, K. Hoffman, P. Wong, D. Lau, and N. Hahn, eds. *The UCSF Animal Care and Use Training Manual*, 1st ed, Regents of the University of California, San Francisco, 1996.

297. J. G. Fox, B. J. Cohen, and F. M. Loew, eds. *Laboratory Animal Medicine*, Academic Press, Orlando, 1984.

298. H. L. Foster, J. D. Small, and J. G. Fox, eds. *The Mouse in Biomedical Research*, Academic Press, New York, 1983.

299. B. R. Grubb and R. C. Boucher. Pathophysiology of gene-targeted mouse models for cystic fibrosis. *Physiol Rev* **79**: S193-214 (1999).

300. L. Zhou, C. R. Dey, S. E. Wert, M. D. DuVall, R. A. Frizzell, and J. A. Whitsett. Correction of lethal intestinal defect in a mouse model of cystic fibrosis by human CFTR. *Science* **266**: 1705-8 (1994).

301. C. K. Arquitt, C. Boyd, and J. T. Wright. Cystic fibrosis transmembrane regulator gene (CFTR) is associated with abnormal enamel formation. *J Dent Res* **81**: 492-6 (2002).

302. J. T. Wright, K. I. Hall, and B. R. Grubb. Enamel mineral composition of normal and cystic fibrosis transgenic mice. *Adv Dent Res* **10**: 270-4; discussion 275. (1996).

303. L. R. Gawenis, P. Spencer, L. S. Hillman, M. C. Harline, J. S. Morris, and L. L. Clarke. Mineral content of calcified tissues in cystic fibrosis mice. *Biol Trace Elem Res* **83**: 69-81 (2001).

304. Y. Miyazaki, H. Sakai, Y. Shibata, M. Shibata, S. Mataki, and Y. Kato. Expression and localization of ferritin mRNA in ameloblasts of rat incisor. *Arch Oral Biol* **43**: 367-78 (1998).

305. A. Halse and K. A. Selvig. Incorporation of iron in rat incisor enamel. *Scand J Dent Res* **82**: 47-56 (1974).

306. P. F. Heap, B. K. Berkovitz, M. S. Gillett, and D. W. Thompson. An analytical ultrastructural study of the iron-rich surface layer in rat-incisor enamel. *Arch Oral Biol* **28**: 195-200 (1983).

307. P. Borst and A. H. Schinkel. What have we learnt thus far from mice with disrupted P-glycoprotein genes? *Eur J Cancer* **32A**: 985-90 (1996).

308. A. H. Schinkel, E. Wagenaar, C. A. Mol, and L. van Deemter. P-glycoprotein in the blood-brain barrier of mice influences the brain penetration and pharmacological activity of many drugs. *J Clin Invest* **97**: 2517-24 (1996).

309. J. J. Smit, A. H. Schinkel, R. P. Oude Elferink, A. K. Groen, E. Wagenaar, L. van Deemter, C. A. Mol, R. Ottenhoff, N. M. van der Lugt, M. A. van Roon, M. A. van der Valk, G. J. A. Offerhaus, A. J. M. Berns, and P. Borst. Homozygous disruption of the murine mdr2 P-glycoprotein gene leads to a complete absence of phospholipid from bile and to liver disease. *Cell* **75**: 451-62 (1993).

310. T. R. Pippert and D. R. Umbenhauer. The subpopulation of CF-1 mice deficient in P-glycoprotein contains a murine retroviral insertion in the mdr1a gene. *J Biochem Mol Toxicol* **15**: 83-9 (2001).

311. D. R. Umbenhauer, G. R. Lankas, T. R. Pippert, L. D. Wise, M. E. Cartwright, S. J. Hall, and C. M. Beare. Identification of a P-glycoprotein-deficient subpopulation in the CF-1

mouse strain using a restriction fragment length polymorphism. *Toxicol Appl Pharmacol* **146**: 88-94 (1997).

312. G. Y. Kwei, R. F. Alvaro, Q. Chen, H. J. Jenkins, C. E. Hop, C. A. Keohane, V. T. Ly, J. R. Strauss, R. W. Wang, Z. Wang, T. R. Pippert, and D. R. Umbenhauer. Disposition of ivermectin and cyclosporin A in CF-1 mice deficient in mdr1a P-glycoprotein. *Drug Metab Dispos* **27**: 581-7 (1999).

313. G. R. Lankas, M. E. Cartwright, and D. Umbenhauer. P-glycoprotein deficiency in a subpopulation of CF-1 mice enhances avermectin-induced neurotoxicity. *Toxicol Appl Pharmacol* **143**: 357-65 (1997).

314. A. H. Schinkel, J. J. Smit, O. van Tellingen, J. H. Beijnen, E. Wagenaar, L. van Deemter, C. A. Mol, M. A. van der Valk, E. C. Robanus-Maandag, H. P. te Riele, A. J. M. Berns, and P. Borst. Disruption of the mouse mdr1a P-glycoprotein gene leads to a deficiency in the blood-brain barrier and to increased sensitivity to drugs. *Cell* **77**: 491-502 (1994).

315. R. Garret and C. Grisham. *Biochemistry*, Saunders College Publishing, Orlando, 1995.

316. L. L. Clarke, L. R. Gawenis, C. L. Franklin, and M. C. Harline. Increased survival of CFTR knockout mice with an oral osmotic laxative. *Lab Anim Sci* **46**: 612-8 (1996).

317. B. Davies and T. Morris. Physiological parameters in laboratory animals and humans. *Pharm Res* **10**: 1093-5 (1993).

318. W. Petri Jr. Antimicrobial agents: sulfonamides, trimethoprim-sulfamethoxazole, quinolones, and agents for urinary tract infections. In J.G. Hardman, L.E. Limbird, and A.G. Gilman (eds.), *Goodman & Gilman's The Pharmacological Basis of Therapeutics*, 10th ed, McGraw-Hill, New York, 2001, pp. 1171-88.

319. T. B. Vree, A. J. van der Ven, C. P. Verwey-van Wissen, E. W. van Ewijk-Beneken Kolmer, A. E. Swolfs, P. M. van Galen, and H. Amatdjais-Groenen. Isolation, identification and determination of sulfamethoxazole and its known metabolites in human plasma and urine by high-performance liquid chromatography. *J Chromatogr B Biomed Appl* **658**: 327-40 (1994).

320. *The Merck Index*. 12th ed, Merck & CO., Inc., New Jersey, 1996.

321. C. W. Sigel and D. A. Brent. Identification of trimethoprim 3-oxide as a new urinary metabolite of trimethoprim in man. *J Pharm Sci* **62**: 694-5 (1973).

322. M. LeBel. Ciprofloxacin: chemistry, mechanism of action, resistance, antimicrobial spectrum, pharmacokinetics, clinical trials, and adverse reactions. *Pharmacotherapy* **8**: 3-33 (1988).

323. P. Nielsen and L. Dalgaard. A sulphate metabolite of trimethoprim in goats and pigs. *Xenobiotica* **8**: 657-64 (1978).

324. P. Nielsen and F. Rasmussen. Elimination of trimethoprim in swine: comparison of results obtained by three analytical methods. *Acta Pharmacol Toxicol (Copenh)* **37**: 309-16 (1975).

325. P. Nielsen and F. Rasmussen. Trimethoprim and sulphadoxine in swine. Half-lives, volume of distribution and tissue concentrations. *Zentralbl Veterinarmed A* **22**: 564-71 (1975).

326. P. Nielsen and F. Rasmussen. Half-life and renal excretion of trimethoprim in swine. *Acta Pharmacol Toxicol (Copenh)* **36**: 123-31 (1975).

327. P. Nielsen and F. Rasmussen. Concentrations of trimethoprim and sulphadoxine in tissues from goats and a cow. *Acta Vet Scand* **16**: 405-10 (1975).

328. S. A. Kaplan, R. E. Weinfeld, S. Cotler, C. W. Abruzzo, and K. Alexander. Pharmacokinetic profile of trimethoprim in dog and man. *J Pharm Sci* **59**: 358-63 (1970).

329. H. Yamaguchi, I. Yano, H. Saito, and K. Inui. Pharmacokinetic role of P-glycoprotein in oral bioavailability and intestinal secretion of grepafloxacin in vivo. *J Pharmacol Exp Ther* **300**: 1063-9 (2002).

330. F. G. King and R. L. Dedrick. Pharmacokinetic model for 2-amino-1,3,4-thiadiazole in mouse, dog, and monkey. *Cancer Treat Rep* **63**: 1939-47 (1979).

331. M. Garty and A. Hurwitz. Tolerance to morphine effects on renal disposition of xenobiotics in mice. *J Pharmacol Exp Ther* **239**: 346-50 (1986).

332. A. Hurwitz. Narcotic effects on phenol red disposition in mice. *J Pharmacol Exp Ther* **216**: 90-4 (1981).

333. R. J. Griep and W. B. Nelp. Mechanism of excretion of radioiodinated sodium iothalamate. *Radiology* **93**: 807-11 (1969).

334. M. D. Blaufox and A. Cohen. Single-injection clearances of iothalamate-131-I in the rat. *Am J Physiol* **218**: 542-4 (1970).

335. B. Pihl. The single injection technique for determination of renal clearance. V. A comparison with the continuous infusion technique in the dog and in man. *Scand J Urol Nephrol* **8**: 147-54 (1974).

336. J. A. Gagnon, R. W. Schrier, T. P. Weis, W. Kokotis, and L. U. Mailloux. Clearance of iothalamate-125 I as a measure of glomerular filtration rate in the dog. *J Appl Physiol* **30**: 774-8 (1971).

337. M. Rehling, J. Frokiaer, E. U. Poulsen, J. Marqversen, B. V. Nielsen, and T. Bacher. 99mTc-MAG3 kinetics in the normal pig. A comparison to 131I-OIH and 125I-iothalamate after single injection and during continuous infusion. *Clin Physiol* **15**: 57-71 (1995).

338. R. B. Kim, M. F. Fromm, C. Wandel, B. Leake, A. J. Wood, D. M. Roden, and G. R. Wilkinson. The drug transporter P-glycoprotein limits oral absorption and brain entry of HIV-1 protease inhibitors. *J Clin Invest* **101**: 289-94 (1998).

339. A. E. Kim, J. M. Dintaman, D. S. Waddell, and J. A. Silverman. Saquinavir, an HIV protease inhibitor, is transported by P-glycoprotein. *J Pharmacol Exp Ther* **286**: 1439-45 (1998).

340. J. Alsenz, H. Steffen, and R. Alex. Active apical secretory efflux of the HIV protease inhibitors saquinavir and ritonavir in Caco-2 cell monolayers. *Pharm Res* **15**: 423-8 (1998).

341. M. T. Huisman, J. W. Smit, H. R. Wiltshire, R. M. Hoetelmans, J. H. Beijnen, and A. H. Schinkel. P-glycoprotein limits oral availability, brain, and fetal penetration of saquinavir even with high doses of ritonavir. *Mol Pharmacol* **59**: 806-13 (2001).

342. J. Savolainen, J. E. Edwards, M. E. Morgan, P. J. McNamara, and B. D. Anderson. Effects of a P-glycoprotein inhibitor on brain and plasma concentrations of anti-human immunodeficiency virus drugs administered in combination in rats. *Drug Metab Dispos* **30**: 479-82 (2002).

343. J. van Asperen, O. van Tellingen, A. H. Schinkel, and J. H. Beijnen. Comparative pharmacokinetics of vinblastine after a 96-hour continuous infusion in wild-type mice and mice lacking mdr1a P-glycoprotein. *J Pharmacol Exp Ther* **289**: 329-33 (1999).

344. A. Leusch, A. Volz, G. Muller, A. Wagner, A. Sauer, A. Greischel, and W. Roth. Altered drug disposition of the platelet activating factor antagonist apafant in mdr1a knockout mice. *Eur J Pharm Sci* **16**: 119-28 (2002).

345. S. Desrayaud, E. C. De Lange, M. Lemaire, A. Bruelisauer, A. G. De Boer, and D. D. Breimer. Effect of the Mdr1a P-glycoprotein gene disruption on the tissue distribution of SDZ PSC 833, a multidrug resistance-reversing agent, in mice. *J Pharmacol Exp Ther* **285**: 438-43 (1998).

346. U. I. Schwarz, T. Gramatte, J. Krappweis, R. Oertel, and W. Kirch. P-glycoprotein inhibitor erythromycin increases oral bioavailability of talinolol in humans. *Int J Clin Pharmacol Ther* **38**: 161-7 (2000).

347. U. I. Schwarz, T. Gramatte, J. Krappweis, A. Berndt, R. Oertel, O. von Richter, and W. Kirch. Unexpected effect of verapamil on oral bioavailability of the beta-blocker talinolol in humans. *Clin Pharmacol Ther* **65**: 283-90 (1999).

348. R. A. Boyd, R. H. Stern, B. H. Stewart, X. Wu, E. L. Reyner, E. A. Zegarac, E. J. Randinitis, and L. Whitfield. Atorvastatin coadministration may increase digoxin concentrations by inhibition of intestinal P-glycoprotein-mediated secretion. *J Clin Pharmacol* **40**: 91-8 (2000).

349. S. Song, H. Suzuki, R. Kawai, and Y. Sugiyama. Effect of PSC 833, a P-glycoprotein modulator, on the disposition of vincristine and digoxin in rats. *Drug Metab Dispos* **27**: 689-94 (1999).

350. U. Mayer, E. Wagenaar, B. Dorobek, J. H. Beijnen, P. Borst, and A. H. Schinkel. Full blockade of intestinal P-glycoprotein and extensive inhibition of blood-brain barrier P-glycoprotein by oral treatment of mice with PSC833. *J Clin Invest* **100**: 2430-6 (1997).

351. Y. Kurata, I. Ieiri, M. Kimura, T. Morita, S. Irie, A. Urae, S. Ohdo, H. Ohtani, Y. Sawada, S. Higuchi, and K. Otsubo. Role of human MDR1 gene polymorphism in

bioavailability and interaction of digoxin, a substrate of P-glycoprotein. *Clin Pharmacol Ther* **72**: 209-19 (2002).

352. J. M. Kovarik, L. Rigaudy, M. Guerret, C. Gerbeau, and K. L. Rost. Longitudinal assessment of a P-glycoprotein-mediated drug interaction of valspodar on digoxin. *Clin Pharmacol Ther* **66**: 391-400 (1999).

353. K. M. Jalava, J. Partanen, and P. J. Neuvonen. Itraconazole decreases renal clearance of digoxin. *Ther Drug Monit* **19**: 609-13 (1997).

354. M. Kawahara, A. Sakata, T. Miyashita, I. Tamai, and A. Tsuji. Physiologically based pharmacokinetics of digoxin in mdr1a knockout mice. *J Pharm Sci* **88**: 1281-7 (1999).

355. U. Mayer, E. Wagenaar, J. H. Beijnen, J. W. Smit, D. K. Meijer, J. van Asperen, P. Borst, and A. H. Schinkel. Substantial excretion of digoxin via the intestinal mucosa and prevention of long-term digoxin accumulation in the brain by the mdr 1a P-glycoprotein. *Br J Pharmacol* **119**: 1038-44 (1996).

356. I. A. de Lannoy, R. S. Mandin, and M. Silverman. Renal secretion of vinblastine, vincristine and colchicine in vivo. *J Pharmacol Exp Ther* **268**: 388-95 (1994).

357. S. Tsuruoka, K. I. Sugimoto, A. Fujimura, M. Imai, Y. Asano, and S. Muto. P-glycoprotein-mediated drug secretion in mouse proximal tubule perfused in vitro. *J Am Soc Nephrol* **12**: 177-81 (2001).

358. U. Jaehde, F. Sorgel, A. Reiter, G. Sigl, K. G. Naber, and W. Schunack. Effect of probenecid on the distribution and elimination of ciprofloxacin in humans. *Clin Pharmacol Ther* **58**: 532-41 (1995).

359. D. Jung, M. H. AbdelHameed, J. Hunter, P. Teitelbaum, A. Dorr, and K. Griffy. The pharmacokinetics and safety profile of oral ganciclovir in combination with trimethoprim in HIV- and CMV-seropositive patients. *Br J Clin Pharmacol* **47**: 255-9 (1999).

360. N. R. Srinivas, C. A. Knupp, B. Batteiger, R. A. Smith, and R. H. Barbhaiya. A pharmacokinetic interaction study of didanosine coadministered with trimethoprim and/or sulphamethoxazole in HIV seropositive asymptomatic male patients. *Br J Clin Pharmacol* **41**: 207-15 (1996).

361. L. Salphati and L. Z. Benet. Modulation of P-glycoprotein expression by cytochrome P450 3A inducers in male and female rat livers. *Biochem Pharmacol* **55**: 387-95 (1998).

362. R. A. McLellan, R. K. Drobitch, M. Monshouwer, and K. W. Renton. Fluoroquinolone antibiotics inhibit cytochrome P450-mediated microsomal drug metabolism in rat and human. *Drug Metab Dispos* **24**: 1134-8 (1996).

363. K. Naora, Y. Katagiri, N. Ichikawa, M. Hayashibara, and K. Iwamoto. A possible reduction in the renal clearance of ciprofloxacin by fenbufen in rats. *J Pharm Pharmacol* **42**: 704-7 (1990).

364. K. I. al-Khamis, L. K. Jim, S. A. Bawazir, L. F. Ashour, N. el-Sayed, and Y. M. el-Sayed. Effect of famotidine on ciprofloxacin pharmacokinetics after single intravenous and oral doses in rats. *J Clin Pharm Ther* **19**: 335-9 (1994).

365. F. Sorgel, K. G. Naber, U. Jaehde, A. Reiter, R. Seelmann, and G. Sigl. Gastrointestinal secretion of ciprofloxacin. Evaluation of the charcoal model for investigations in healthy volunteers. *Am J Med* **87**: 62S-65S (1989).

366. R. W. Rohwedder, T. Bergan, S. B. Thorsteinsson, and H. Scholl. Transintestinal elimination of ciprofloxacin. *Diagn Microbiol Infect Dis* **13**: 127-33 (1990).

367. T. Bergan, A. Dalhoff, and R. Rohwedder. Pharmacokinetics of ciprofloxacin. *Infection* **16 (Suppl 1)**: S3-13 (1988).

368. T. Bergan, S. B. Thorsteinsson, R. Rohwedder, and H. Scholl. Elimination of ciprofloxacin and three major metabolites and consequences of reduced renal function. *Chemotherapy* **35**: 393-405 (1989).

369. S. Dautrey, K. Felice, A. Petiet, B. Lacour, C. Carbon, and R. Farinotti. Active intestinal elimination of ciprofloxacin in rats: modulation by different substrates. *Br J Pharmacol* **127**: 1728-34 (1999).

370. S. Dautrey, L. Rabbaa, D. Laouari, B. Lacour, C. Carbon, and R. Farinotti. Influence of renal failure on intestinal clearance of ciprofloxacin in rats. *Antimicrob Agents Chemother* **43**: 678-80 (1999).

371. B. Nouaille-Degorce, C. Veau, S. Dautrey, M. Tod, D. Laouari, C. Carbon, and R. Farinotti. Influence of renal failure on ciprofloxacin pharmacokinetics in rats. *Antimicrob Agents Chemother* **42**: 289-92 (1998).

372. S. Dautrey, L. Rabbaa, A. Petiet, C. Carbon, and R. Farinotti. Comparison of models for studying the intestinal elimination of ciprofloxacin in the rat. *Drugs* **49 (Suppl 2)**: 310-1 (1995).

373. E. Rubinstein, S. Dautrey, R. Farinoti, L. St Julien, J. Ramon, and C. Carbon. Intestinal elimination of sparfloxacin, fleroxacin, and ciprofloxacin in rats. *Antimicrob Agents Chemother* **39**: 99-102 (1995).

374. E. Rubinstein, L. St Julien, J. Ramon, S. Dautrey, R. Farinotti, J. F. Huneau, and C. Carbon. The intestinal elimination of ciprofloxacin in the rat. *J Infect Dis* **169**: 218-21 (1994).

375. M. M. Malingre, J. H. Beijnen, H. Rosing, F. J. Koopman, R. C. Jewell, E. M. Paul, W. W. Ten Bokkel Huinink, and J. H. Schellens. Co-administration of GF120918 significantly increases the systemic exposure to oral paclitaxel in cancer patients. *Br J Cancer* **84**: 42-7 (2001).

376. H. A. Bardelmeijer, J. H. Beijnen, K. R. Brouwer, H. Rosing, W. J. Nooijen, J. H. Schellens, and O. van Tellingen. Increased oral bioavailability of paclitaxel by GF120918 in mice through selective modulation of P-glycoprotein. *Clin Cancer Res* **6**: 4416-21 (2000).

377. F. Hyafil, C. Vergely, P. Du Vignaud, and T. Grand-Perret. In vitro and in vivo reversal of multidrug resistance by GF120918, an acridonecarboxamide derivative. *Cancer Res* **53**: 4595-602 (1993).

378. M. L. Drumm, H. A. Pope, W. H. Cliff, J. M. Rommens, S. A. Marvin, L. C. Tsui, F. S. Collins, R. A. Frizzell, and J. M. Wilson. Correction of the cystic fibrosis defect in vitro by retrovirus- mediated gene transfer. *Cell* **62**: 1227-33 (1990).

379. D. G. Ginzinger. Gene quantification using real-time quantitative PCR: an emerging technology hits the mainstream. *Exp Hematol* **30**: 503-12 (2002).

380. www.appliedbiosystems.com.

381. E. M. Jancis, R. Carbone, K. J. Loechner, and P. S. Dannies. Estradiol induction of rhodamine 123 efflux and the multidrug resistance pump in rat pituitary tumor cells. *Mol Pharmacol* **43**: 51-6 (1993).

382. G. Y. Lee, J. M. Croop, and E. Anderson. Multidrug resistance gene expression correlates with progesterone production in dehydroepiandrosterone-induced polycystic and equine chorionic gonadotropin-stimulated ovaries of prepubertal rats. *Biol Reprod* **58**: 330-7 (1998).

383. H. Shumaker and M. Soleimani. CFTR upregulates the expression of the basolateral Na(+)-K(+)-2Cl(-) cotransporter in cultured pancreatic duct cells. *Am J Physiol* **277**: C1100-10 (1999).

384. M. Johannesson, A. C. Nordqvist, N. Bogdanovic, L. Hjelte, and M. Schalling. Polymorphic expression of multidrug resistance mRNA in lung parenchyma of nonpregnant and pregnant rats: a comparison to cystic fibrosis mRNA expression. *Biochem Biophys Res Commun* **239**: 606-11 (1997).

385. D. L. Gustafson and M. E. Long. Alterations in P-glycoprotein expression in mouse tissues by doxorubicin: implications for pharmacokinetics in multiple dosing regimens. *Chem Biol Interact* **138**: 43-57 (2001).

386. M. Demeule, M. Brossard, and R. Beliveau. Cisplatin induces renal expression of P-glycoprotein and canalicular multispecific organic anion transporter. *Am J Physiol* **277**: F832-40 (1999).

387. S. A. Kliewer, B. Goodwin, and T. M. Willson. The nuclear pregnane X receptor: a key regulator of xenobiotic metabolism. *Endocr Rev* **23**: 687-702 (2002).

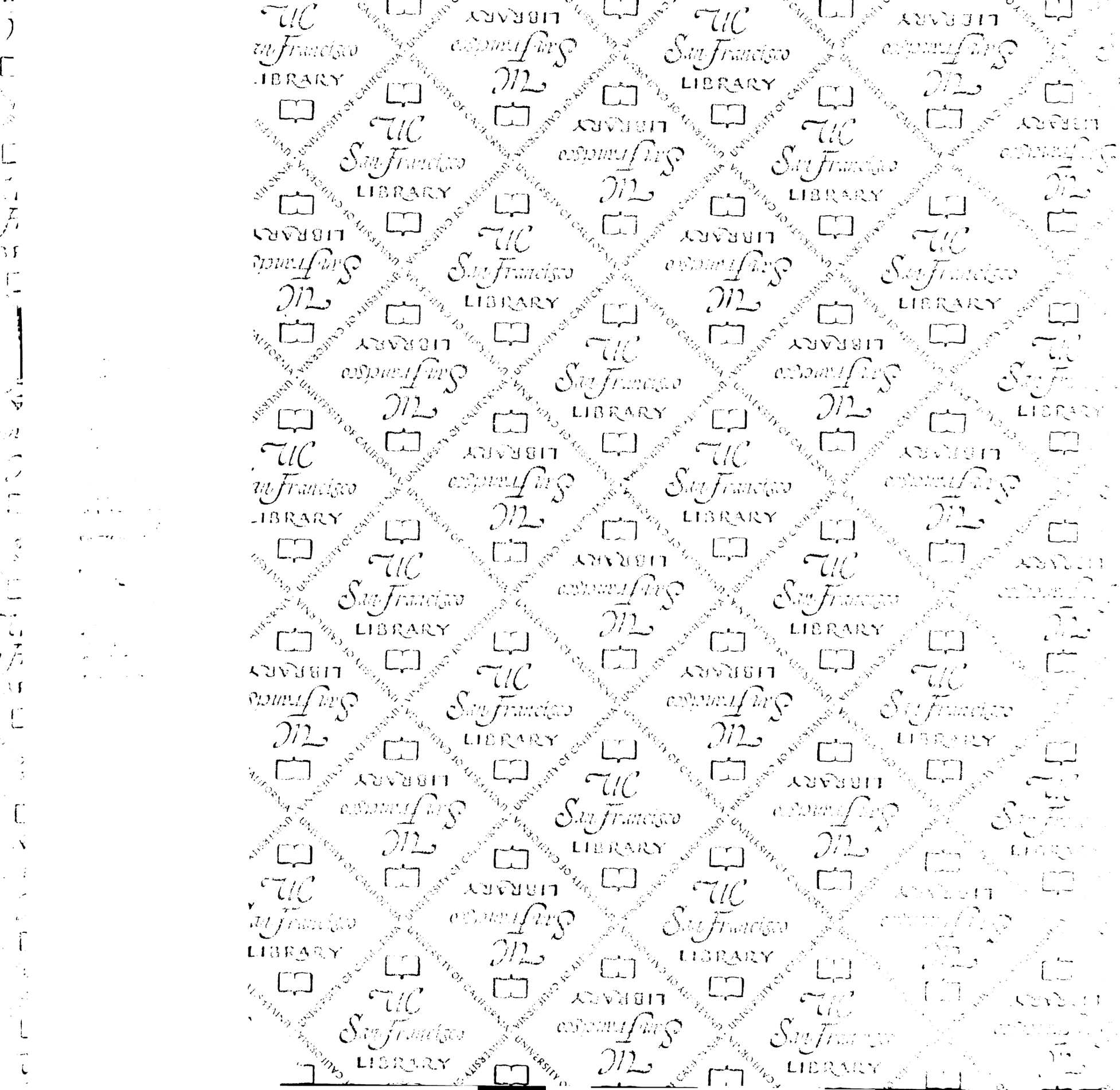
UC
San Francisco
LIBRARY
UNIVERSITY OF CALIFORNIA